

School of Medicine

Divisions of Rheumatology, Orthopaedics and Dermatology

PhD Thesis

An in vivo feasibility study investigating the fixation of osteotomised rabbit tibia using a bioresorbable composite plate and a comparison of the effects of the bioresorbable plate and a metal plate on intact bone

Assad Qureshi (4153623)

Abstract

Background: Modern fracture management uses surgically implanted metal plates to fix fractured bones to restore pre-injury anatomy. Following healing, the plate may have to be removed requiring a second operation. Reactive thinning of the bone beneath the metal plate (stress shielding) can increase the theoretical risk of re-fracture once the plate is removed. Bioresorbable plates offer the possibility of reduced stress shielding due to plate degradation causing a progressive reduction in mechanical properties and obviating the need for a second operation to remove the plate.

Aim: To determine the feasibility of using a novel bioresorbable composite plate to fix an in vivo osteotomised bone in an animal model. Following the failure of this experiment, the study aimed to determine the in vivo effects of the composite plate on intact bone in comparison to a conventional steel plate. A secondary aim was to determine the in vitro mechanical properties of both types of plate compared to bone.

Methods: A reproducible in vivo osteotomy technique was developed using a rabbit tibia model and fixed with the composite plate. Following the failure of this experiment, subsequent in vivo experiments compared the effects of the composite plate with a metal plate on intact bone. Twenty-five rabbits underwent surgical application of the composite plate to the intact right tibia. In parallel, 25 rabbits underwent surgical application of the metal plate to the right tibia. In each study arm, groups of five rabbits were sacrificed at 5 sequential time points - 2, 6, 12, 26 and 52 weeks. At sacrifice, the right plated tibia and the left unplated bone, which acted as a control, were retrieved. The outcomes assessed included structural changes (radiographs, Micro CT, electron microscopy); mechanical changes (flexural testing) and histological changes (paraffin slides). In vitro mechanical tests investigated the mechanical properties of different plate designs, intact bone and osteotomised bone.

Results: The single in vivo osteotomy experiment resulted in composite plate failure within a few hours of implantation. No further in vivo osteotomy experiments were conducted. The intact bone experiments demonstrated new bone growth around both types of plate, but greater bone loss occurred beneath the steel plated bones compared with the composite plated bones as the duration of implantation increased. The relative augmentation in mechanical characteristics when comparing the plated with control bones reduced to a greater extent in the metal plated bones compared with the composite plated bones. Few inflammatory cells were seen in both types of implanted bone at the surveyed time points. In vitro studies demonstrated reduced mechanical properties in the degraded composite plates compared with polymer and metal plates.

Conclusion: The mechanical properties of the composite plate are insufficient to enable application as a fracture fixation device. Improved outcomes in terms of bone preservation when comparing the composite plate with the steel plate in an in vivo intact bone model reflect differences in the mechanical properties of the two types of plate.

Contents

Abstract 2

Acknowledgements 7

Chapter 1 Introduction 8

1.1 Bone structure and fracture healing 8

1.1.1 The mechanical properties of bone 8

1.1.2 The adaptive nature of bone 9

1.1.3 The biomechanics of fracture healing 11

1.1.4 Fracture treatment – aims and strategies 14

1.1.5 Fracture management and the principles of internal fixation 15

1.2 The influence of rigid fixation on bone adaptation 18

1.2.1 Structural changes in plated bones 18

1.2.2 The biomechanics of plated bones 20

1.2.3 Time dependent effects of internal fixation on bone 22

1.2.4 Bone-implant interfaces and transmission of stress shielding 23

1.2.5 The effect of fixation stiffness on bone healing 25

1.2.6 The mechanical paradox of internal fixation and the need for resorbable technologies 27

1.3 Biomaterials and biodegradation 28

1.3.1 Bioresorbable materials 28

1.3.2 Degradation mechanisms of synthetic polymers 30

1.3.3 Factors influencing the degradation of aliphatic polyesters 31

1.3.4 Biocompatibility of bioresorbable implants 33

1.3.5 The mechanical properties of resorbable implants 35

1.3.6 Bioresorbable implants in orthopaedics 36

1.4 Bioresorbable composites as fracture fixation devices 39

1.5 Aim and objectives 41

Chapter 2 Methods 43

2.1 Plate design 43

2.2 Selection of the animal model 44

2.3 In vivo plating of osteotomised rabbit tibia 46

2.3.1 Trial experimentation 46

2.3.2 Preparation before implantation 49

2.3.3 Theatre setup and anaesthesia during experimentation 49

2.3.4 Osteotomy and plating experiment 51

2.4 Study comparing the effects of the composite plate with the metal plate on intact bone 54
2.5 Selection of sample size 56
2.6 Surgical implantation of composite and metal plates to intact tibiae 59
2.6.1 Radiography of plated and control bones 61
2.6.2 Recovery and Housing following surgery 62
2.7 Assessment of outcomes in experimental implantations in intact tibiae 63
2.7.1 Scheme of outcomes assessment 63
2.7.2 Retrievals 64
2.7.3 Perfusion fixation 65
2.7.4 Dissection and radiographs 66
2.7.5 Mechanical testing of in vivo plated and control bones 71
2.7.6 Mechanical testing of in vitro samples 74
2.7.7 Micro Computed Tomographic Imaging 75
2.7.8 Histology 77
2.7.9 Resin embedding 79
2.7.10 Scanning Electron Microscopy analysis 81
2.7.11 Paraffin embedding and histological staining 82
2.7.12 Giemsa staining 84
2.7.13 Tartrate-resistant Acid Phosphatase (TRAP) staining 85
2.7.14 Slide analysis 86
2.8 Statistical analysis of normalised outcomes 88
Chapter 3 Results 93
3.1 In vivo plating of osteotomised rabbit tibia 93
3.2 In vivo plating of intact rabbit tibiae with the composite and metal plates 97
3.3 Imaging 99
3.3.1 Relative plate position at surgery and at retrieval 99
3.3.2 Radiographic assessment of retrieved plated and control bones 101
3.3.3 Radiographic assessment of cortical thickness 105
3.3.4 Micro Computed Tomography Imaging 108
3.3.4.1 Structural changes in the composite plate 108
3.3.4.2 Structural changes in composite plated bones 108

3.3.4.3 Micro CT cortical thickness measurements 112
3.3.4.4 Micro CT cortical area measurements 114
3.3.4.5 Micro CT bone area measurements 117
3.4 Scanning electron microscopy of resin embedded sections 120
3.4.1 Reproducibility of bone blocks corresponding to the plate periphery and plate mid-section 120
3.4.2 Structural bone changes in composite plated bones 121
3.4.3 Structural changes in the composite plate over time 124
3.4.4 Structural bone changes in metal plated bones 125
3.4.5 Cortical thickness and cross sectional bone area measurements 129
3.4.5.1 Cortical thickness measurements in composite and metal plated groups 130
3.4.5.2 Cortical area measurements in composite and metal plated groups 134
3.5 Mechanical testing of in vitro and in vivo specimens 139
3.5.1 In vitro testing of cadaveric bones and plates 139
3.5.2 Fracture morphology of in vivo plated specimens and controls 146
3.5.3 Correlation between mechanical properties of control bones and host characteristics 148
3.5.4 Ultimate load of in vivo plated specimens 149
3.5.5 Flexural stiffness of in vivo plated specimens 153
3.6 Results Paraffin embedded histology 157
3.6.1 Inflammatory response in Composite plated specimens and controls 157
3.6.3 Structural bone changes in the plated bones 160
Chapter 4 Discussion 166
4.1 Structural changes in the plated bones 166
4.1.1 Plain radiographic assessment 167
4.1.2 Cross sectional analysis using Micro CT and Scanning Electron Microscopy (SEM) 168
4.2 The effects of plating on the mechanical properties of the plated bones 176
4.3 The time dependent effects of plate application 180
4.4 The influence of remaining growth on structural bone changes in plated bones 185
4.5 Transitional mechanical properties of the composite plate 187

4.6 Non-mechanical effects of plating on bone structural changes. 189
4.7 Critical analysis of experimental design 192
4.7.1 Selection of animal model 192
4.7.2 Selection of plate location and reproducible placement 194
4.7.3 Selection of plate geometry 194
4.7.4 Selection of time points 195
4.7.5 Selection of controls, sample size and statistics 196
4.7.6 Surgical complications.....202
4.7.7 Selection of screws 203
4.7.8 Mechanical testing conditions 203
4.7.9 Selection of outcome measures 205
4.7.10 Sampling errors 206
4.7.11 Processing artefacts.....207
4.7.12 Observer bias 209
4.8 Creating a model to explain the structural and mechanical behaviour of plated bones 210
4.9 Extrapolating the current findings to human studies..... 216
4.10 Bioresorbable composites as fracture fixation devices – current limitations and future developments 218
4.10.1 Theorised effects of the composite plate on soft tissue inflammation and infection 218
4.10.2 Bone forming potential of phosphate glass fibre composites 219
4.10.3 Stress shielding and bioresorbable composite fixation devices.....221
4.10.4 Composite plate failure following fixation of in vivo osteotomy 222
4.10.5 Future developments in composite plate design 228
4.11 Conclusion 232
References.....233

Acknowledgements

Above all, I would like to thank God in whose remembrance, I endeavored to remain grateful through both the best and the most difficult of times when completing this period of study. God be praised.

I cannot thank my supervisors enough for their continued support, direction and above all, patience whilst I struggled with balancing my daily work life, family and completing my thesis. Brigitte Scammell, Ifty Ahmed and Chris Rudd laid much of the groundwork before I was involved in the project by gaining home office approval for the studies to be undertaken, successfully obtaining sufficient funding for a project of this scope in addition to bringing their practical experience of in vivo animal and engineering studies. Richard Pearson assisted greatly in his supervision of the histology experiments and imparting his vast knowledge on the subtle technical aspects of processing histological specimens into slides. I am deeply indebted to them all for their tireless support and guidance.

Many of the experiments I conducted would not have been possible without the expertise and time of a diverse cadre of academic and technical support staff. I would especially like to thank the following individuals for their notable contributions. Colin Scotchford and Andrew Parsons for their sustained and enthusiastic support throughout the course of the project. Dawn-Marie Walker in the research design service for her extensive input in planning the patient and surgeon questionnaire studies. Neil, Mark, Ian and Donna for facilitating the animal experiments and helping with the husbandry, surgery and the wellbeing of the animals frequently beyond the call of duty. Jeni Luckett for giving up much of her time to undertake the Micro CT scanning and assisting in the analysis. Martin Roe for his technical advice, guidance and time in helping process the samples for electron microscopy. Dr Andrea Venn for assisting with the statistical analysis and reviewing the findings.

I would like to thank both of the BMedSci students who contributed greatly to this project – Ahmad and Wojciech. Special praise must go to all of my colleagues in the Division of Orthopaedic and Accident Surgery who helped me on occasions too numerous to detail.

Finally, I would like to thank my family for their patience, understanding and steadfast support as well as overlooking my shortcomings as both a husband and a father during the years it took to complete this work. The fundamental and most important truth of being able to get thus far is that I was never alone. Thank you Mariam and Shareen Qureshi.

Chapter 1 Introduction

1.1 Bone structure and fracture healing

1.1.1 The mechanical properties of bone

Bone is a very complex biological material which serves several diverse functions within the human body and has the innate capacity for healing[1]. Its principle function is to impart rigidity to the skeleton to resist deformation in response to the imposition of physiological loads induced by movement and locomotion[2]. Consequently, bone must be sufficiently strong enough to withstand repetitive loading cycles of fluctuating magnitude and frequency whilst optimising size on a strength by weight basis[1] and maintaining a low metabolic cost. Human bone is able to maintain mechanical properties enabling load bearing whilst retaining an ability to remodel to permit growth and adaptation by utilising a composite structure.

A composite is an amalgamation of two different materials to produce a structure with improved properties compared to its constituent materials. Bone is a composite, consisting of an organic phase chiefly composed of collagen fibres and proteoglycan ground substance, and a mineral phase of hydroxyapatite crystals[3]. Individual collagen fibres form fibrils interspersed with mineral deposits layered in sheets known as lamellae. The arrangement of these lamellae gives rise to the two characteristic types of bone found in the mature skeleton – cortical bone and cancellous bone. Bone demonstrates structural optimization with respect to its mechanical environment[4]. Although, the fundamental shape of a bone appears to be genetically determined[5], its lamellar architecture is designed to resist deformation induced by its mechanical environment[6]. The shafts of the lower limb long bones contain densely packed lamellae aligned to the longitudinal axis so as to offer maximum resistance to compressive loads when an upright posture is assumed. In bones where the imposed force profile is more complex, the lamellae adopt a three dimensional spatial arrangement of interconnecting trabeculae so as to minimize stresses within the bone. This can be seen in the trabecular architecture of the human femoral neck where the

alignment of the trabeculae resists compressive forces but also the bending moment brought about by having a femoral head offset from the shaft[7-9]. Repetitive loading cycles can induce failure through fatigue as microscopic cracks accumulate over time and eventually coalesce to cause fracture manifesting as a complete discontinuity extending across a previously intact bone.

Bone like articular cartilage and tendon, demonstrates strain or loading rate dependent mechanical behaviour known as viscoelasticity. Strength usually defines the ultimate load a structure can withstand prior to failure and is expressed in the SI unit Pascals (Pa) or force per unit area (N/m^2). Stiffness defines the magnitude of deformation of a structure when it is loaded[1]. Bone demonstrates complex mechanical behaviour due to these parameters of strength and stiffness being influenced by the rate of loading. As the frequency and magnitude of loading increase, so too does the bone's strength and stiffness making it more resistant to failure. When this property is exhausted, failure occurs resulting in fracture. Loading to failure results in this macroscopic disruption. However, failure may also occur at a microscopic level as a result of stress concentration at structural defects leading to localized stresses in excess of the tolerance of the bone. The loads required for microscopic failure are on a far smaller scale than those required for complete fracture. However, the number and size of these defects increases over time as a result of repetitive physiological loading[2] eventually resulting in a complete fracture. This failure through mechanical fatigue is inevitable unless the bone can counteract the progressive accumulation of these defects[10]. The composite structure does confer some resistance to fatigue. Microscopic cracks are insulated from each other by intervening collagen fibres thus inhibiting crack propagation[11]. However, eventual failure through accumulation of multiple defects can only be prevented if bone has the ability to renew itself and heal such defects before they reach a critical size.

1.1.2 The adaptive nature of bone

Biological systems are not inert and must be able to adapt and react to environmental change to ensure survival. In the context of bone, adaptation must occur to enable growth as well as to accommodate a constantly fluctuating mechanical environment.[12].

Bone must be able to resist excessive forces as well as fatigue failure through repetitive loading. This is achieved through the continual ordered renewal of bone to ensure structural optimization with respect to size, geometry and microstructure. This renewal continues throughout the life of the host and is vital to growth, adaptation to extreme mechanical environments, preventing the accumulation of microscopic defects and restitution of normal structure at the end of the healing process.

To understand how bone adapts, the effects of different mechanical environments can be considered. If a bone is mechanically isolated such that no external forces act on it, no deformation of its microarchitecture occurs. Deformation under loading underpins the concept of strain. Strain is defined as the change in length upon imposition of a fixed load as a proportion of the original length in the unloaded state[2]. Although dimensionless, strain is frequently expressed as a percentage. The mechanically isolated bone exhibits minimal deformation and therefore low strain. Each bone demonstrates homeostasis with respect to a specific strain distribution[2]. Therefore, if the strain level reduces below the range for that bone, bone volume is reduced thus increasing the strain. Clinically, immobilizing a limb in plaster leads to cortical bone thinning referred to as disuse osteoporosis which can be observed on conventional radiographs[13, 14]. Eventually a new equilibrium is reached where no further loss of bone occurs[13]. This minimum mass of bone in the absence of any functional stimulus is most likely genetically determined[2]. Bone seeks to maintain its mechanical properties through preferential bone loss in specific regions of the bone. Consequently, in long bones we observe endosteal resorption and incomplete refilling of secondary osteons[2]. Although the cortex is consequently thinner, the second and polar moments of inertia are optimized for the given bone volume of bone by retaining the outer circumferential diameter. These mechanical parameters quantitatively define the distribution of the cross sectional area relative to the neutral axis in structures subjected to bending and torsion respectively. Endosteal resorption in contrast to periosteal resorption maintains these values in a higher range by maintaining the outer diameter of the bone. This provides the bone with greater resistance to bending and torsion.

The sensing mechanism of bone with respect to its mechanical environment allows the converse phenomenon to occur. The radiographic changes seen in disuse osteoporosis

after limb immobilization can be seen to reverse with remobilization[15]. The increased forces generate excessive strain and deformation of the bone which is countered by increasing bone mass. This augmentation is directed by structural optimization with selective augmentation of lamellae resisting the specific force profiles imposed. In long bones, cortical thickening of the shaft occurs whereas in trabecular bone, trabecular thickening and increased connectivity occurs. Thus, the physical stimulus for adaptation in bone appears to be related to the level of deformation or strain. It is likely that the size of the deviation of the strain distribution from normal, in terms of the magnitude and frequency of the strain wave form, govern this behaviour[16]. The specific sensing apparatus and its coupling to the mechanisms of bone remodelling are still subject to speculation and ongoing investigation[2].

1.1.3 The biomechanics of fracture healing

The capacity to heal damage is intrinsic to bone. A fracture is a mechanical failure of bone resulting in a discontinuity. Bone healing occurs as a continual process whereby the tissue formed within the fracture gap undergoes progressive substitution, accruing improved mechanical properties as the tissue is successively replaced[17]. Once the fracture is bridged, function can be restored. Restoration of overall bone integrity continues as internal remodelling seeks to restore the normal Haversian architecture long after union is achieved. The process of fracture healing is critically dependent on the mechanical conditions at the fracture site. These processes are dichotomized into one of two types of healing depending on the mechanical environment. Direct healing occurs by direct progression to the final stage of bony restitution without the formation of callus[18]. In contrast, indirect healing takes place through the formation of intermediary tissues at the fracture site. The type of healing is a function of stability at the fracture site[19]. A stable fracture is defined as a fracture that does not visibly displace under imposition of a physiological load. Absolute stability at the fracture site implies a complete absence of motion upon imposition of a physiological load[20]. In these circumstances, direct healing is enabled. Relative stability implies that the anatomy of the fractured bone is maintained in an acceptable position but limited

motion is permitted at the fracture site. This prompts callus formation and indirect healing.

Perren's strain theory explains how fracture healing is influenced by and, in turn, influences the mechanical environment[21, 22]. Initially, the fracture site is filled with tissues exhibiting low stiffness. Therefore, for a given load, greater strain or deformation occurs. Resorption of the fractured bone ends increases the area of the intervening fracture gap thereby attenuating the tissue strain in the intervening gap[23]. The theory predicts that different biological tissues develop once the environmental strain conditions permit their existence[20]. Early on, granulation tissue develops at the fracture site as it is not very stiff and has a 100% strain tolerance. The formation of granulation tissue increases stiffness and reduces strain in the fracture gap permitting the formation of stiffer tissues with reduced strain tolerance. Cartilage forms within the soft callus which is progressively replaced by woven bone bridging the two bone ends. Intact bone has a strain tolerance of 2% and permits minimal deformation without fracture[1]. This seismic leap in tissue strain tolerance is achieved through progressive substitution of soft callus by hard callus and ultimately bone. The process is assisted by the production of a greater amount of soft callus than that required to bridge the bone ends with much of this generated from the periosteum[24]. The volume and distribution of this callus confers added stiffness with respect to increasing the second and polar moments of inertia. This vastly reduces the strain and may represent the dominant influence of indirect healing enabling progressive tissue substitution as predicted by Perren's theory[21] (Figure 1.1). The transduction mechanisms of mechanical stimuli influencing the type of healing have yet to be fully elucidated[20].

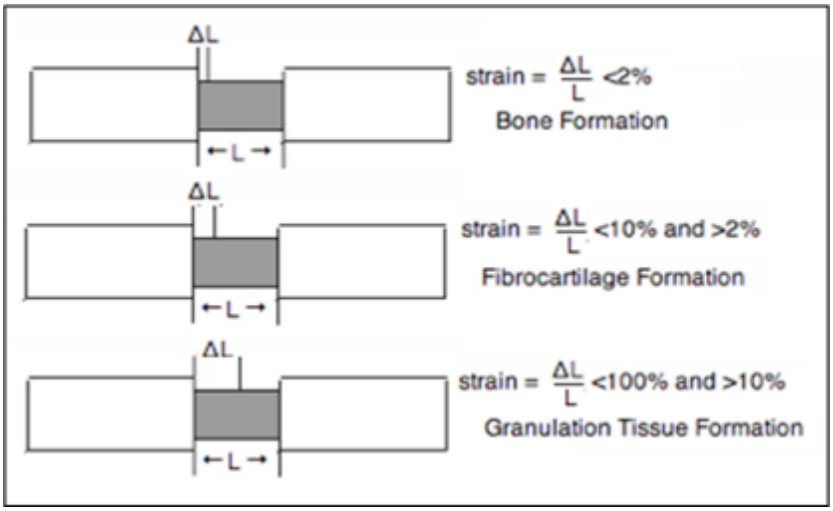


Figure 1.1 A diagram demonstrating how different strain conditions in the fracture gap dictate the type of tissue which forms. The strain is dictated by the change which occurs in the length of the gap (ΔL) as a function of the length of the gap (L). Each type of tissue has a specific strain tolerance which favours its formation thereby creating an environment of progressive substitution where granulation tissue is replaced by fibrocartilage which is replaced by bone. Diagram adapted from Gitajn and Rodriguez[25] (2011)

The achievement of direct healing has several pre-requisites that can only be enabled through internal fixation of the fracture with a rigid implant[20]. Anatomical reduction with inter-fragmentary compression is mandatory to achieve direct apposition of the fractured bone ends. Absolute stability allows the fractured bone to directly remodel without the requirement of intermediary tissues to create the requisite stiffness in the mechanical environment. In direct bone healing, no bone resorption or callus formation is observed[17]. Small gaps are bridged by direct secretion of osteoid. Cutting cones formed of osteoclasts advance directly across the fracture site where the bone is in contact enabling direct osteonal remodelling to occur. The result is restitution of the bone's original architecture without the requirement of preceding callus formation. Internal fixation using plate and screw constructs is a reliable means of achieving this[1]. In contrast, certain fracture fixation systems such as intramedullary devices rely upon creating sufficient micro motion to stimulate callus formation.

1.1.4 Fracture treatment – aims and strategies

The principal aim of fracture treatment is to achieve function analogous to the pre-injury state[20]. Historically, most fractures have been treated by immobilization in a splint or plaster cast. The bone is immobilized in acceptable alignment providing some pain relief while creating sufficient stability to enable indirect healing to occur. Cast immobilisation is still routinely employed in modern fracture management to treat a large proportion of fractures. However, it does have its limitations in specific clinical scenarios.

Immobilisation has deleterious effects on biological tissues whose homeostasis is dependent on physiological loading. Disuse osteoporosis occurs in immobilized bones[15]. Non-osseous structures are equally vulnerable. Muscle unit inactivity induces muscular atrophy and weakness. The porous permeable matrix of articular cartilage relies on the transudation of fluid through its proteoglycan matrix created by force transmission during loading to maintain chondrocyte nutrition and matrix turnover[26]. The absence of motion within the fluid phase leads to structural alterations which in the long term may predispose to chondropathy[27]. Joints are bridged by tendons and ligaments designed to resist joint deformation and enable force transmission without attenuation during movement. In the absence of loading, intra-substance changes lead to stiffening and formation of contractures within involved joints[1]. Many of these changes are reversed by remobilization. Restitution occurs as a function of time with successful rehabilitation requiring an equivalent if not greater length of time to that of immobilization. A large proportion of fractures continue to be managed by cast immobilisation due to the eventual re-establishment of normal structure and function[28-30]. However, certain patient populations such as the elderly are less able to cope with prolonged immobilization where extra-skeletal sequelae such as venous thrombosis and pulmonary stasis confer significant morbidity[31].

It is very difficult to eliminate motion at the fracture site through external splintage which necessitates indirect healing by formation of callus. External callus is beneficial in the shaft of long bones where increased cross sectional area properties are better able to resist bending and torsion while the bone remodels[20]. However, in joint

surfaces unwanted callus can distort the morphology of bearing surfaces creating articular incongruity causing chondropathy and arthritis[32]. External splints work favourably for controlling rotation and alignment in long bones but cannot directly control intra-articular displacement.

1.1.5 Fracture management and the principles of internal fixation

The limitations of cast immobilisation acted as an impetus to the development and successive refinement of modern fracture management techniques. The fundamental ethos is to restore function to the affected parts as rapidly as possible while avoiding the musculoskeletal morbidity associated with immobilization[1, 33]. Rigid internal fixation with metal plates is a well-established method of achieving this due to the extensive work of the AO foundation (Arbeitsgemeinschaft für Osteosynthesefragen; The Association for the study of internal fixation problems, Switzerland)[34]. Plate fixation stabilizes the fracture site by application of a rigid metal lag screw or a compression plate which is attached to the underlying bone by screws[1]. This enables direct apposition of the fractured bone ends and confers absolute stability fulfilling the biomechanical environmental requirements for direct bone healing[20]. The plate's purpose is not to permanently replace the broken bone but to provide immediate stability enabling transmission of light functional loads and early functional rehabilitation without risking fracture displacement. However, the benefits must be offset against the risks of complications.

Surgical plate application requires anatomical access to the bone which risks inadvertent trauma to neighbouring structures such as nerves, muscles and tendons, all of which are crucial to the successful rehabilitation of the injured limb. Fracture healing is dependent on the preservation of the blood supply to the fracture site and this may be impeded by the surgical insult in addition to the precipitating trauma[20]. The establishment of absolute stability requires fixation devices to have sufficient stiffness to ensure that the combined bone-implant construct is rigid enough to resist displacement of the bone ends until fracture healing is complete. The need for rigid plates is necessitated by evidence that most plates currently used cannot achieve more than a third of the strength of the intact bone[35]. No plate in current use is strong enough

to withstand the expected physiological loads without excessive deformation of the plate[36]. Historically, thicker plates or double plating techniques have been advocated[37, 38] to prevent implant failure before healing has occurred.

The fundamental requirement of materials used to manufacture fracture fixation systems is biocompatibility. Biocompatible materials can be broadly categorized as bioinert, porous, bioactive and bioresorbable. Most conventional plate systems are bioinert due to their lack of soft tissue reaction and ease of removal if required. Metallic alloys, such as stainless steel additionally offer excellent resistance to corrosion as well as cost effectiveness. Although they have superior mechanical characteristics compared with cortical bone, mechanical theory predicts that if the implant is relatively stiffer compared with the bone it may lead to reduced strains in the underlying bone. Predictably, the adaptive nature of bone will lead to a consequent decreased bone mass in this region. This phenomena is commonly referred to as stress shielding or stress protection[20]. Stress shielding can be considered as a reduction in the normal functional stimulus to part of the bone and is commonly seen in conjunction with plate fixation[39]. Stress shielding occurs if two or more components with different moduli of elasticity form one mechanical system. When loaded, the component with the higher modulus, bears more of the load thus "shielding" the other component from external mechanical influences. In the context of fixation devices, if the implant is significantly stiffer than the bone, strains within the latter decrease leading to loss of bone to restore strain equilibrium. Observations of cortical thinning after application of rigid plates (Figure 1.2) and re-fracture after their removal[40-42] have supported this theoretical prediction prompting extensive study in to the influence of these fracture fixation devices on the underlying bone's structure and biomechanics.

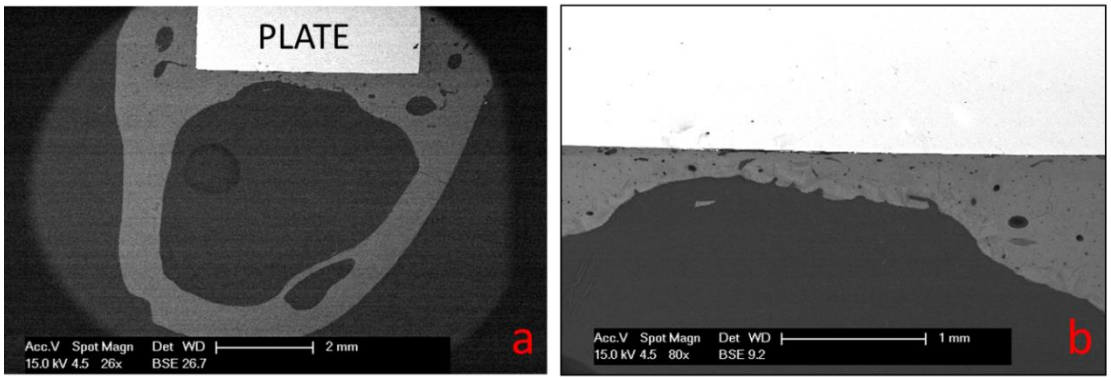


Figure 1.2 Scanning electron micrograph images of a cross section of a steel plated rabbit tibia bone one year following surgery at (a) 26x mag and (b) 80x mag taken from the current study. There is marked thinning of the cortical bone beneath the plate suggestive of stress shielding.

1.2 The influence of rigid fixation on bone adaptation

1.2.1 Structural changes in plated bones

Previous studies have noted localized cortical osteopenia or loss of bone beneath rigid metal plates[43, 44]. Concerns exist regarding the risk of re-fracture especially if the plate is removed. Experimental studies have investigated the changes occurring in bone beneath rigid plates in animal models[45-48]. Initial studies determined the effects of plating in osteotomised bones where the bone was experimentally fractured and then fixed with a plate-screw construct. Plated bones demonstrated a reduction in bone density beneath the plate, an effect which could be reversed by removing the plate. However, as these bones had fractures which were healing, the new bone formed may have offset that lost due to stress shielding. It was clear that to better understand the adaptive changes in bone beneath plates, experimental studies would need to assess the effects of plating in intact bones.

Terjesen et al[49] experimentally applied rigid plates to intact rabbit tibia and found increased cortical porosity which could not be explained by any remodelling influence of fracture healing. The porosity increased with the duration of plate implantation suggesting a persistent mechanical effect as a cause rather than a discrete insult arising at the time of surgery. A similar study by Moyen et al[50] in a canine femur model also demonstrated increased porosity beneath a rigid metal plate. In these dogs, the opposite femur was plated with a flexible plate with reduced stiffness which theoretically produced less stress shielding due to a reduction in the relative difference in elastic moduli between plate and bone. However, the extent of intra-cortical porosity was similar for both plates and did not appear to be related to the duration of implantation. Similarly, removal of the plate did not lead to a change in the porosity. Other studies similarly reported no difference in the extent of porosity with attachment of plates of different stiffness[51 52]or failed to demonstrate a difference in porosity in plated and unplated regions of the same bone[53-55]. Changes in the blood supply to bone have an important effect on bone remodelling[56]. Plate application has been shown to significantly hamper the periosteal blood supply[57] and a correlation has been observed between the width of contact of the plate and intra cortical porosity

suggesting blood flow disruption as an important contributory factor [58]. If stress protection in plated bone does occur, there must be structural changes other than alterations in porosity.

Morphological changes in bone that may occur in stress shielding include a change in density through increased porosity or a change in the bone's overall geometry. The most consistent finding in several studies of plated long bones has been a reduction in cortical thickness beneath the plate[47, 50, 51, 53, 55, 59] . In all but one of these studies, resorption principally occurred endosteally thereby maintaining the outer diameter of the bone and minimizing impairment to the bone's mechanical characteristics. However, the study by Uhthoff et al[47] suggested that periosteal bone resorption occurred leading to a reduced outer diameter. One study failed to demonstrate a change in cortical thickness with plating [60] while others have suggested that the stress shielding morphological changes relate to bone density rather than spatial characteristics such as cortical thickness[49, 61]. It has been speculated that the discordant findings regarding changes in cortical thickness induced by plating may reflect differences in the animal models and bones studied[49, 59].

Despite controversy regarding the distinct morphological changes accompanying stress shielding, the hypothesis that altering the stiffness of the plate will alter the response of the underlying bone has been explored in several studies. To eliminate the possibility of different experimental models influencing the stress shielding response observed, experiments have been undertaken where plates of similar geometry but different mechanical properties have been implanted in the paired long bones of the same animal[50, 53 51]. In all of these studies, the stiffer plate induced greater bone loss in the underlying cortex when measuring skeletal mass[50], bone mass[53] or cortical thickness[51].

These findings would suggest that fracture fixation systems with reduced bone-plate construct stiffness should lead to reduced stress shielding in comparison to stiffer fixation systems. This was explored by comparing the bone loss from stress shielding in rigid plate fixation with that induced by a less stiff construct of external fixation on the intact rabbit tibia[62]. The results demonstrated that the morphological changes in the externally fixated bones were less pronounced compared with the metal plated

bones. The cumulative evidence supports a dose dependent effect between fixation stiffness and the adaptive changes seen in the underlying bone despite controversy regarding the morphology of these changes.

1.2.2 The biomechanics of plated bones

In an attempt to further characterize how stress shielding affects plated bones, investigators turned to biomechanical testing of plated bones to assess their mechanical characteristics. The biomechanical properties of bone relate to its geometry, mass, chemical composition and the mode of mechanical testing. Most investigators employ a flexural bending test[49] or a torsional test[63] to ascertain the ultimate bending load in addition to flexural stiffness or torsional stiffness respectively.

The relationship between mechanical properties, such as ultimate bending strength and stiffness on one hand, and mineral content of bone on the other is well established[64]. Measurement of residual bone strains in plated human tibiae demonstrated reduced strains under steel plates compared with less rigid titanium plates[65, 66]. Animal models have been used to investigate the effect of stress shielding induced by plates of different rigidity on the mechanical properties of the bone following plate removal. Cochran demonstrated a mean axial strain reduction of 45% in the underlying cortex in metal plated dog femora[67]. Gautier et al[68] found that axial bending strains were significantly reduced in the cortex underlying a steel plate compared with the unplated bone in sheep tibiae in vivo. This reduction was more marked with a steel plate compared with a titanium plate. Having demonstrated differences in mechanical properties of plated and unplated bones, difficulties arise in correlating these changes with structural changes associated with plating. Comparison of structural changes in plated and unplated bones in different animals creates a significant confounding factor due to individual differences in limb geometry between different sized animals of the same species.

This variation can be excluded from the experimental model by plating paired bones in the same animal using different plates or leaving one side undisturbed as a control.

There is ample evidence demonstrating symmetry of mechanical characteristics in paired bones in various animal models to support the validity of this study design[53, 62, 69-71]. Thus, paired bone studies provide an effective experimental model in which to determine the effect of varying plate design or biomechanical testing parameters. Retrieved bone-plate specimens from mechanical testing can be examined to determine the structural changes accompanying altered biomechanical properties. This enables correlation between the porosity and cortical thinning seen beneath plates with the attenuation in mechanical properties.

Tonino studied the effects of two plates of different rigidity on the bending strength of plated dog femora[53]. They found a 30% reduction in the ultimate load to failure in the steel plated bones compared to the plastic plated bones after plate removal. This was attributed to observed differences in both porosity and cortical thinning. Akeson et al[51] investigated the effects of a graphite fibre plate and a stiffer vitallium plate on adult dog femora. The bones with stiffer plates demonstrated relatively greater cortical thinning with a lower ultimate bending load and energy absorption to failure. These two mechanical properties relate to structural characteristics implying a difference in the bony architecture. However, testing revealed no difference in the material properties of the bone; the ultimate bending strength and elastic modulus, between the two plated bones. They concluded that the material properties of the bone were similar in both plated specimens and that the difference in mechanical characteristics related to differences in the structural or geometric properties of the bone such as cortical thickness. Terjessen[49] demonstrated reduced bending strength and elastic modulus in plated rabbit tibia bones which he related to differences in bone mineral density rather than geometric differences. Although, controversy exists as to whether the altered mechanical properties in plated bones are due to changes in the material or structural properties of the bone, numerous studies support a stress shielding effect on the mechanical characteristics of plated bones. Both torsional and compression testing have demonstrated reduced strength of plated bones compared to the opposite control bone[54, 63, 71, 72].

1.2.3 Time dependent effects of internal fixation on bone

Bone adaptation beneath metal plates occurs as a function of time. Previous studies have investigated the relationship between duration of plate implantation and the magnitude of the underlying stress shielding response. Several animal studies have demonstrated progressive structural changes and reductions in mechanical strength in the plated bone as the duration of plating increases[50, 53, 55]. Moyen et al[50] demonstrated that these changes progressed up to 9 months in plated dog femora. Akeson et al[51] demonstrated progressive differences in dog bone atrophy between two types of plates studied at 9 and 12 months post implantation. In rabbits, one study demonstrated that progressive changes occur in the bone underlying the plate up to 36 weeks[63] whereas another study suggested that the stress shielding effect is progressive up to 12 weeks and then an equilibrium state is achieved[49]. The temporal effects of rigid fixation have also been explored in humans. A study reporting the computed tomography findings in femora plated after trauma demonstrated a mean 11% reduction in cortical density[61]. However, this change in density was unaffected by the length of time the plate had been in situ and the magnitude of the stress protection response was unchanged beyond one to two years. The timing of this equilibrium in plated bone is unclear but is most likely a function of the relative sizes and mechanical properties of the plates and underlying bones[49].

Establishing the optimum timing for removal of plates raises the question of whether the stress shielding response has a linear relationship with the duration of plate implantation. Bone changes early on may not demonstrate significance[49]. Paavolainen et al[63] investigated the torsional characteristics of plated intact rabbit tibia at regular intervals over 36 weeks after plating. After 12 weeks there was a steady decline in mechanical characteristics due to stress shielding. The results would suggest that a window exists between union being achieved and the deleterious effects of stress shielding. The optimal timing for plate removal is subject to debate. Some studies have suggested that this may be undertaken as early as 8 to 9 weeks[73, 74]. In contrast, Hayes et al[75] found the bending strength of healed canine tibia plated with a stainless steel plate peaked at 20 weeks. Extrapolating the findings of animal studies to clinical fracture treatment is complex[76]. Current guidelines regarding the timing of removal of

forearm plates are based on allowing adequate time for bony healing rather than the prevention of stress shielding[77]. Some authors recommend a fewer number of plate removals to avoid the risk of re-fracture once the protective implant has been removed[78].

The restitution of bone anatomy and physiology requires restoration of the normal mechanical environment. In the context of fractured diaphyseal bones treated with rigid internal fixation, this can only be achieved once the plate and its mechanical influence are removed[79, 80]. Studies have demonstrated reversal of bone changes induced by rigid plate fixation following plate removal. In studies of plated dog femora, both Moyen et al[50] and Uhthoff et al[47] demonstrated near complete recovery three months after removal. In plated rabbit tibia, Laftman et al[71] observed recovery to take half the time in which the progressive deterioration in mechanical properties of the plated bone occurred. It is clear that the recovery response, analogous to the induced stress shielding response, does not assume a linear relationship with time. The mechanisms underlying the disparity between the time required for the stress shielding to become manifest and the time taken for recovery is unclear. The treatment of a diaphyseal bone fracture by rigid plating should not be regarded as complete until a certain recovery period has elapsed after plate removal whose magnitude is probably less than the duration of plate fixation[71].

1.2.4 Bone-implant interfaces and transmission of stress shielding

Although contrary to the adaptive nature of bone, some studies have suggested that restitution of normal bone anatomy eventually occurs with the implant in situ[81-83]. This may reflect progressive attenuation in force transmission between the bone and plate with the passage of time. The stress shielding response is proportional to the rigidity of the fixation which in turn reflects the extent of mechanical coupling between the plate and bone[84]. This is influenced by the number of screws, plate geometry and screw hole location. If load transmission is optimal between plate and bone then maximum

stress shielding occurs in the bone in the immediate vicinity of the plate and diminishes as we move away from the plate[47, 51, 52, 54, 83, 85].

Although implant induced stress shielding leads to a reduction in bone, ancillary effects of surgical implantation also occur which may offset this bone loss. Subperiosteal new bone formation is readily observed around the periphery of plates[56]. The space created between the stripped periosteal layer and the underlying bone surface acts as a potential bone formation compartment. Therefore, plates with a smaller contact footprint elicit increased new bone formation[56].

A study investigated the change in long bone structural properties during the first 8 weeks of plate implantation demonstrated new bone formation to predominate at the sites of fixation with a reduction in flexural strength of the mid plated region of the bone[52]. They theorized that these two phenomena were related. Where increased new bone formation was evident near the screw tips, there was a corresponding reduction in the flexural strength of the middle of the plated bone. The study compared this effect in bones plated with metal plates and bones plated with plastic plates. The metal plated bones demonstrated greater augmentation in mechanical properties with the presence of the plate but increased loss of mechanical strength in the midsection of the bone once the plate was removed compared to the plastic plated bones. In the metal plated bones, greater bone formation was observed at the periphery of the plate and endosteally around the screws. Although, the presence of screw holes in the diaphysis of a bone confers detriment to the mechanical characteristics of the bone, this effect is short lived. Recovery of strength occurs within 8 weeks due to endosteal bone formation around screws[86]. The inversely related phenomenon of weakening of the midplated section of the bone and new bone formation at the sites of attachment reflects the non-uniform stress transmission across the bone plate interface. Studies suggest that the outer most screws are chiefly responsible for the transmission of stress from plate to bone as evidenced by proximal and distal bone hypertrophy at these sites[87, 88]. Very minor differences in screw tightness or plate placement on bone may cause significant differences in the underlying bone strain distribution and ensuing stress shielding[52]. The cumulative evidence suggests that the greater the stiffness of the plate and the rigidity of fixation, the greater the bone formation at the sites of stress transfer and the greater the extent of weakening through stress shielding in the bone

under the centre of the plate[52, 89]. The interface properties of implants permitting bony in-growth have been studied using metal plates with porous surfaces[84, 90]. These plates are associated with greater stress shielding compared with conventional plate designs due to optimization of stress transfer at the bone plate interface.

1.2.5 The effect of fixation stiffness on bone healing

Successive studies into the effects of plating on intact bones have yielded significant insight into the factors influencing the stress shielding response. In parallel with these studies, research has been conducted into the influence of plates of different stiffness on bone healing. Terjessen and Apalset[76] looked at plate fixation in rabbit tibiae fixed with steel and plastic plates of varying stiffness and found that the amount of periosteal callus was inversely related to the stiffness of the applied plates. Evaluation of mechanical properties of the retrieved specimens revealed a trend towards lower stiffness in the tibiae in which stiffer plates had been used. Similar studies[91-93] have demonstrated a similar inverse relationship between plate stiffness on one hand and callus formation and mechanical properties of the bone on the other. Analysis of the type of healing reveals that less stiff plates are associated with abundant callus formation due to the micro motion permitted by reduced stiffness. Although the mechanical properties of formed callus are a function of its volume, the quality in terms of density of the callus assumes equal importance[76]. A study[93] has suggested that callus "quality" is also a function of the mechanical environment and augments bone material properties independent of volume. This is supported by observations of fractures experimentally created in healed bone occurring through the "old" bone compared to the newly deposited bone[56]. Finite element studies have explored the effects of callus development at the fracture site on stress distribution in plated fractures[94]. Initially, the neutral axis is located in the middle of the plate due to the load bearing cross section at the fracture interface consisting of the plate alone. As callus develops at the fracture site, the neutral axis shifts outwards towards the bone plate interface. At this point the callus assists the plate in taking on some compressive stress. As the callus volume progressively increases and matures, the neutral axis

moves towards the centre of the bone restoring pre-injury in vivo bone strains and minimising stress shielding.

Fracture healing occurs through time dependent processes which vary according to the type of healing. Although the experience of some investigators has been that the initial phase of bone healing advances faster with rigid fixation, it is very difficult to judge clinically whether or not a fracture plated to achieve compression of the bone ends has healed[95]. Direct osteonal remodelling in direct bone healing is a far slower process compared with indirect healing through callus formation. Completion of direct healing is not a clinically detectable event. On this basis, the AO group revised their original recommendation concerning time for plate removal from 12 months[79] to 18 months[96] to minimize the risk of re-fracture. Re-fracture rates up to 1.5%[97] have been reported with re-fracture occurring up to two years after removal of the plate. A study of the re-fracture rate of forearm bones after plate removal[77] demonstrated no re-fractures to occur if plate removal was undertaken after 40 weeks from implantation. To achieve their aim, plates must have sufficient rigidity to support the healing bone throughout the healing process. If the plate is removed too early re-fracture may occur due to inadequate healing. However, late removal also carries a re-fracture risk due to bone loss induced by a profound stress shielding response. The benefits of flexible plate designs that minimize stress shielding and encourage bone healing through callus formation must be offset against the risks of displacement during the healing process due to implant failure or progressive ductile deformation. Reducing the stiffness of a plate to equalize stresses between implant and bone risks introducing motion at the fracture site thus favouring healing by callus formation. As long as fracture displacement is restricted to within acceptable limits dictated by the location and configuration of the fracture, callus formation should favour faster healing with minimal deformity. However, if the plate's mechanical properties are unable to tolerate physiological loading, then there is a risk of re-displacement at the fracture site due to ductile or complete implant failure. Terjessen and Apalset investigated the effects of several different plates with varying stiffness[76] on plating simulated fractures in rabbit tibiae. In three of the ten bones where the least stiff plate was used, fracture of the implant and re-displacement of the bone ends occurred.

1.2.6 The mechanical paradox of internal fixation and the need for resorbable technologies

The results of several studies demonstrate the practical difficulties in achieving the requisite balance between early rigid fixation to prevent displacement of the bone ends whilst minimising the stiffness of the combined bone plate construct to reduce stress shielding. The conflicting demands of achieving differing mechanical conditions at different stages of healing presents a significant challenge. Early on, adequate stiffness is required to prevent fracture re-displacement and implant failure. However, once union is achieved, reduced plate stiffness is required to minimize the effects of stress shielding. A plate capable of exhibiting transitional mechanical properties is desirable to meet the mechanical demands during both phases of the fracture healing process[98]. Biologically degradable materials offer the possibility of designing internal fixation plates with the requisite stiffness early on in fracture healing. Later degradation and a consequent loss of mechanical properties leads to increased stress transfer to the underlying bone minimising stress shielding changes[99]. The additional theoretical benefit is that there is no need to remove a plate due to its fully resorbable capacity thereby avoiding the morbidity, potential complications and additional costs of a second operation[99].

1.3 Biomaterials and biodegradation

1.3.1 Bioresorbable materials

Biomaterials are materials of natural or manmade origin that are used to direct, supplement, or replace the functions of tissues of the human body[100]. Their increasing use in modern healthcare has been fuelled by advances in synthetic materials, sterilization methods and surgical techniques. Common modern orthopaedic applications include joint replacement, fracture fixation and bone regeneration strategies[101]. Biomaterials with the capacity for in vivo degradation are denoted as having *biodegradable*, *bioabsorbable* or *bioresorbable* characteristics[100]. Although these terms are often used interchangeably, they have specific definitions with respect to the type of degradation. *Bioabsorbable* and *biodegradable* implants specifically refer to implants which principally degrade due to direct cellular activity and dissolution respectively. In the context of fracture fixation systems, neither scenario is desirable. Cellular processes accelerate degradation and have the potential to elicit chronic inflammatory responses. The degradation kinetics of dissolvable implants negates their use in fracture fixation systems where retention of mechanical characteristic is integral to success. *Bioresorbable* materials have the ability to degrade in vivo in to products capable of "resorption" by entering general metabolic pathways[102]. In the context of fracture fixation devices, plates made of cortical bone would appear to be the most effective bioresorbable implant. However, the rapid in vivo resorption and consequent loss of mechanical properties restricts their employment in fracture fixation[98]. Attention has been focused on the development of synthetic bioresorbable polymers to fulfil this purpose.

Over the last 40 years, biodegradable polymers have been safely used in many musculoskeletal clinical applications[101]. Most currently available bioresorbable polymers are derived from esters of aliphatic acids[103, 104]. Poly α-hydroxy acids are bioresorbable polyesters derived from α-hydroxy acids (HO-CHR-COOH) such as glycolic and lactic acids. The simplest linear polyester, polyglycolic acid (PGA) is relatively hydrophobic contributing to its rapid degradation. Esters of polylactic acid (PLA) exhibit slower degradation rates with improved mechanical properties in terms

of strength and toughness[105]. Their inclusion in many developing technologies has been encouraged by prior regulatory approval of devices composed of PGA or PLA on the basis of proven efficacy and safety[102, 105]. Other synthetic polymers of interest include the polymers of amino acids and ortho esters. Although they demonstrate inferior mechanical characteristics compared with PLA and PGA, these polymers offer the potential for therapeutic applications of controlled drug delivery and direct effects through mimicking extracellular proteins found in the human body[100].

The biocompatibility and bioresorbability of PLA polymers are well established. Wide ranges of physical, thermal, mechanical and biological properties can be engineered through modifying the chemistry of the polymer chain. PLA demonstrates chirality allowing different isomers to exist – PLLA and PDLA[105]. The homopolymer of the L-lactide isomer (PLLA) exhibits high tensile strength (50-70 MPa) and low deformation (≈4%), and consequently has a high modulus (3 GPa) that makes it suitable for load bearing applications such as fracture fixation[105]. PLLA is partially crystallisable with a melting temperature of 175-178°C and has the longest degradation time of the aliphatic ester polymer group. While PGA may fully degrade in vitro in three months, PLLA may take several years to break down[106-108] (see Table 1.1). Composites formed from different polymers exhibit varying degradation characteristics.

Table 1.1 Time to complete absorption and loss of mechanical properties for various bioresorbable materials and composites (PGA – poly glycolic acid; SR – self reinforced PGA composite, P (D/L) LA – PLA composite of D and L isomers; PLLA – Poly –L lactic acid; SR PLLA – self reinforced PLLA composite) (Table adapted from Kontakis et al[109]).

Material	Complete absorption time	Mechanical properties loss time
PGA	4-7 weeks[110]	36 weeks[111]
SR PGA composite	6-12 months[112]	1 month[101]
PLA/PGA composite (80:20)	1-2 years[113]	6-8 weeks[113]
P(D/L)LA composite (70:30)	2-3 years[101, 113]	18-36 weeks[113]
PLLA	>5 years[108, 114, 115]	
SR PLLA composite	5-6 years[101]	36 weeks[116] (reduction to cortical bone levels

1.3.2 Degradation mechanisms of synthetic polymers

Polymer degradation is defined as the deterioration in the functionality of the polymeric material caused by a change in its physical and/or chemical properties[117]. Appreciation of a specific polymer's degradation characteristics is required in order to achieve kinetic alignment between the processes of implant degradation and host tissue regeneration. In the context of fractures, stability at the fracture site must be maintained until union has been achieved whilst maintaining a degradation rate which favours load transmission to the regenerating bone. Both the degradation characteristics and mechanical properties of a resorbable implant are important. Satisfactory balancing of the two parallel, dynamic systems, i.e. degradation of the implant and regeneration of the bone, can prevent early fracture re-displacement and later stress shielding.

There has been extensive study into the factors influencing the in vitro and in vivo degradation characteristics of aliphatic polyesters (see Table 1.2). Variable degradation rates of synthetic polymers reflect differences in implant geometry, material composition, in vivo location and chosen animal model between different studies[118-120]. From a manufacturing perspective, the degradation profile is influenced by the method of manufacture, crystal size, pore size and the geometry of the implant[101]. In vitro studies have been shown to be a good model for simulating in vivo degradation. The most widely adopted in vitro model is that of degradation in pH 6.9-7.4 phosphate buffer solution at 37°C[121].

Table 1.2 Factors influencing implant degradation[101]

Implant factors	Composite factors	Manufacturing factors	Environmental factors
Chemical composition	Composite constituent polymers	Sterilisation	Implantation site
Molecular weight	Co-polymer ratio	Storage	Tissue type
Steroisomerism	Fibre:matrix volume ratio		Mechanical stresses
Volume:surface ratio	Fibre orientation		
Porosity			
Predominant degradation mechanism (enzymatic vs hydrolysis)			

The chief mechanism by which aliphatic polyesters degrade in vivo is by hydrolysis of the hydrolytically unstable backbone of the polyester molecule and to a lesser extent through non-specific enzymatic action, the main route of final elimination being respiration[122, 123]. Hydrolytic degradation of implants is rarely uniform. Two mechanisms of erosion have been identified[124]. Surface erosion causes degradation at the implant host tissue interface. The implant thins but retains its gross integrity predicting a linear relationship between implant degradation and mechanical characteristics. Conversely, in bulk erosion, sample dimensions remain relatively constant as the implant degrades from within due to the ingress of water into its structure. Once a critical threshold is reached, complete structural failure occurs with a dramatic reduction in mechanical properties.

1.3.3 Factors influencing the degradation of aliphatic polyesters

The relative susceptibility to surface and bulk degradation is a function of the crystallinity of the polymer. Crystalline regions resist the permeation of water and bulk degradation while amorphous regions are more susceptible[105]. Amorphous PLA can

take 2 to 3 years to resorb but in its highly crystalline form, PLA may take up to 5 years to degrade completely[105]. Increasing the molecular weight of the polymer favours crystallization and reduces the number of acidic end groups which can take part in reactions[105]. The surface to volume ratio and porosity also determine hydration at the implant-tissue interface. Although reducing the porosity may seem desirable to minimize hydration, this also restricts the flow of catalytic degradation products away from the implant into the surrounding media. In vitro studies have demonstrated faster degradation in buffered solutions due to increased removal of degradation products through neutralization of the end groups[125]. Alkaline conditions contribute to greater bulk degradation than acidic environments due to the increased neutralization of acidic products enabling their removal which in turn drives local reactions forward.

In the in vivo setting, additional degradation effects can occur[126]. Surface hydration damage may be accentuated by chemical erosion mediated by biological macromolecules, such as blood and extracellular proteins, adhering to the external surface[126]. These proteins and acidic degradation products act as chemo-tactic stimuli for leukocyte and macrophage migration. These cells are unable to ingest these particles by the process of phagocytosis and respond by releasing enzymes and oxidative agents[122]. Macrophages have the ability to form an enclosed environment around the implant before releasing their enzymatic contents. Over time, several macrophages may merge to form a foreign body giant cell capable of phagocytosing larger particles with greater chemical destruction. This process is mediated by lymphocyte derived cytokines and is important in the chronic changes occurring in response to slowly degrading implants. The immune response to bioresorbable implants can be modulated by impregnating the implant with an antibody against lymphocyte derived cytokines known to activate macrophages[127].

Fibrous encapsulation is an innate response towards implanted biomaterials[126]. In the context of fracture fixation systems, this may be beneficial as fibrous capsules are relatively acellular and avascular. This inert status prevents host cell invasion into the implant thereby slowing down its degradation. Conversely, the escape of acidic products may also be hindered contributing to autocatalytic degradation mechanisms. The formation and thickness of the fibrous capsule has been shown to be influenced by the polymer surface groups, polymer fibre diameter and porosity[126].

In vivo effects also include thermal and mechanical effects on implants[126]. The in vivo temperature of 37°C may contribute to direct degradation as well as optimising catalysis of enzymatic processes. The site of implantation is also important. Bioresorption in the medullary canal of rabbits has been shown to be greater than intramuscular or subcutaneous implantations[128]. Fracture fixation systems bear mechanical stresses such as loading, shear and friction, all of which have been shown to accelerate the in vivo degradation of biomaterials[129].

The degradation of synthetic polymers is critically dependent on their manufacture, fabrication, sterilisation and storage conditions[130]. Gamma irradiation is the mainstay sterilisation technique due to its relatively low chemical reactivity[105]. However, studies have demonstrated chain scission in PLA and PGA polymers leading to reduced molecular weight and faster degradation[130]. Research continues into methods of sterilization which are safe as well as being environmentally and implant friendly such as supercritical carbon dioxide processing[130]. Packaging of implants in inert gas or vacuum environments is essential to maximize shelf life by preventing oxidization. Prevention of moisture infiltration can be achieved through the use of desiccators maintained under vacuum in sub ambient temperatures[105].

1.3.4 Biocompatibility of bioresorbable implants

The in vivo biocompatibility of resorbable implants manufactured from PLA has been extensively investigated in animal studies and has not demonstrated any toxic or teratogenic effects[131]. Although one study has reported sarcomatous change associated with a PLA implant in rats, other studies have not reported tumorgenicity[132, 133]. Although, in vitro human lymphocyte cultures have not demonstrated an immune response to PGA, complement activation has been reported in serum samples from patients with osteochondritis desiccans of the knee treated with PLA pins[134]. The results of clinical studies significantly differ to animal studies. Histological evaluation reveals that bioresorbable implants elicit a non-specific foreign-body type of tissue

response[99] but macroscopic inflammatory foreign body reactions are conspicuously absent in animal experiments[106, 135].

In clinical studies, soft tissue inflammatory reactions to bioresorbable implants occur more frequently. Histological assessment reveals a non-specific foreign body type reaction to polymeric debris particles with numerous mononuclear phagocytes and multinucleated foreign body giant cells[136-141]. This histologic response persists even in the absence of macroscopic inflammation. Although some studies have not observed clinically evident soft tissue reactions in association with PLA implants[99, 142], the reported incidence of soft tissue reactions ranges from 2% to 46.7%[99]. The highest reaction rates have been observed in regions with scant soft tissue cover such as in the wrist and carpal fractures[138, 143]. The ability of a tissue bed to clear polymeric debris is a function of its perfusion capacity[131] and significantly higher incidences of adverse tissue reactions have been reported in regions of poor vascularity such as scaphoid non unions[143]. Large volume implants with subcutaneous locations are associated with soft tissue reaction rates as high as 47.4%[144]. Although one study suggested a correlation between polymer volume and frequency of secondary bacterial infection[145], two large clinical series have not demonstrated a difference in the rate of soft tissue reactions related to the volume of the implant[136, 146]. Implant geometry also has an effect with screws demonstrating a higher incidence of reaction compared with pins or rods[99].

Soft tissue reactions typically occur after a latent period following implantation. PLA implants manifest soft tissue reactions much later than PGA implants reflecting their slower degradation[99]. Typical reactions occur 8 to 16 weeks post implantation[136, 147]. Prolonged latencies have been observed with PLA implants with reactions reported in the literature up to 4 to 5 years after the original operation[108, 146, 148]. Currently, there is limited evidence regarding the long term incidence of foreign body reactions to resorbable implants[99].

The soft tissue response to bioresorbable implants varies immensely from minor mechanical irritation of overlying soft tissues to peri-implant osteolysis and formation of sinuses discharging polymeric debris[146]. The typical natural history is the emergence of a painful, erythematous lump at the site of implantation[99]. Left untreated, the lump eventually bursts forming a sinus with discharge of polymeric debris. These

sinuses are usually sterile unless they become secondarily infected and may continue to discharge for up to 6 months[99]. Surgical debridement is usually mandatory for early resolution. Where implants have been used in close proximity to joints, sterile effusions have been observed[140, 149-151]. Radiographic assessment of soft tissue reactions accompanying intra-osseous implants reveal osteolytic lesions in up to 50% of patients[103, 152]. Resolution may take up to a year and is occasionally incomplete. Bioabsorbable pins inserted via joint surfaces may cause osteolysis with long term adverse sequelae[153].

1.3.5 The mechanical properties of resorbable implants

Bioresorbable devices made of aliphatic esters have been used in the internal fixation of fractures, osteotomies and arthrodeses in addition to treating ligament and meniscal avulsions[101]. The chief concern is their ability to retain sufficient mechanical properties from the time of implantation up to the point that bony union is achieved[154]. PLA and related polymers demonstrate inferior mechanical properties compared to stainless steel which limits their inclusion in high load bearing fracture fixation systems (see Table 1.3).

Table 1.3 Mechanical properties of different types of bioresorbable materials, bone and steel. *(PGA – poly glycolic acid; PLA – poly lactic acid; SR PGA – self reinforced PGA composite; PLLA – Poly –L lactic acid; SR PLLA – self reinforced PLLA composite).*

Material	Tensile strength	Flexural strength	Flexural modulus
PGA	57 MPa[155]		
PLLA	11-72 MPa[119]		
PLA		45 - 145 MPa[116]	
SR PGA composite		195 - 400 MPa[112]	
PGA matrix PLA fibre composite		250 MPa[156]	
SR PLLA composite		250 - 300 MPa[112, 116]	
Cancellous bone	1 – 20 MPa[157, 158]		0.1 – 4.5 GPa[158]
Cortical bone	53 – 135 MPa[159]		12 – 17 GPa[159]
Stainless steel 316L		280 MPa[101]	200 GPa[101]

The tensile yield strength for PLLA varies between 11-72MPA whilst the flexural strength lies somewhere between 45 and 145 MPA[119]. Optimisation of mechanical characteristics is required prior to implantation due to the early loss of strength after implantation[131]. In vivo studies have demonstrated that one half of the initial bending and shear strength is lost within two weeks in PGA implants and within 12 weeks in PLLA implants[131]. The mechanical properties of aliphatic polyesters can be improved by creating a composite consisting of a polymer matrix reinforced by polymer fibres. This arrangement confers a 5-8 fold improvement in strength. However, overall stiffness or resistance to deformation only improves to a smaller extent[45, 156, 160, 161]. Composites composed of PGA matrix reinforced with PLA fibres have been shown to have a flexural strength of 250 MPa which approaches that of steel (280MPa)[156]. However, these polymer composites retain a low flexural modulus (1.6 - 27GPa) when compared with stainless steel (200 GPa)[162]. Although the loads to failure are comparable in bending, the polymer composites deform to a greater extent when loaded compared with steel. This deformation without failure may be useful to promote healing through callus formation but the excess ductility may lead to healing with an angular deformity[131]. The fixation characteristics of bioresorbable polymer implants have been the subject of several animal studies[101]. Studies have demonstrated that bioresorbable rods can be made strong enough for intramedullary nailing of femoral diaphyseal osteotomies in the dog, rabbit and cat[163-165].

1.3.6 Bioresorbable implants in orthopaedics

Most commercial bioresorbable implant systems in clinical use are composed of polymer screws and rods, rather than plates, which are usually applied in areas of low stress[166]. Applications include the fixation of small articular fragments, reattachment of bony insertions of tendons and in maxillofacial surgery[154]. PGA screws have been used to fix tibial condylar split depression type fractures[167] as well as fractures of the talus and calcaneum[168, 169]. Elbow fractures where resorbable screw or pin fixation is feasible include radial head, capitellum, condylar and olecranon fractures[170, 171]. Due to the low loads involved, resorbable implants have also been used to fix hand

fractures[143, 172, 173] and treat scaphoid delayed union and non union[143, 174]. Paediatric physeal and small fragment fractures have been successfully treated using bioresorbable implants[131]. They have also been applied outside of trauma in hallux valgus surgery[142], foot osteotomies[142], shoulder instability surgery[175] and repair of bucket handle tears of the meniscus.[176] The current evidence would suggest that bioresorbable implants are less suited to replacing internal fixation implants such as nails, screws and plates while potentially having a limited role for fixing small articular fractures and in special need areas such as maxillofacial surgery[154].

Bioresorbable plates have found a clinical role in the treatment of mandibular fixation of fractures and osteotomies due to the light loading demands in this anatomical region[101]. Bioresorbable implants are generally not recommended for use without external support in sites of high mechanical stress[166, 177]. Widespread applications have been reported but have principally been undertaken in specialist centres[131]. Bostman *et al* reported the use of intramedullary PGA rods to fix fractures in both the upper and lower limb[131] but their application was restricted to specific fracture locations and configurations. A large scale prospective study has been conducted into the use of resorbable devices for fracture fixation in a single centre undertaking a high volume of operations. They reported the results of 319 operations performed in 318 patients using PLLA and PGA[170] implants to fix 41 olecranon fractures and 259 ankle fractures. Assessment, although subjective, revealed good or excellent results in more than 90% of patients.

Numerous studies have investigated the use of resorbable implants to fix ankle fractures[178, 179]. Although favourable outcomes have been reported up to 18 months post implantation[180], there is a high incidence of soft tissue problems associated with plating of the fibula[144]. Two comparative studies of bioresorbable ankle fracture fixation using PLA screws suggested that they were safe and effective[178, 181]. Ahl et al[182] conducted motion analysis of ankle fractures treated with conventional stainless steel fixation compared with those treated with bioresorbable implants. Despite similar clinical results, the bioresorbable group demonstrated greater abnormal motion in the ankle mortise reflecting inferior fixation stiffness compared with steel fixation.

Two bioresorbable distal radial plate systems are commercially available. These include the Inion OTPS biodegradable distal radius plate[183] (Inion Oy, Tampere, Finland) made of L-poly-lactic acid (PLA)/D,L-PLA polymers with trimethylene carbonate and the Reunite bioresorbable distal radius plate[184, 185] (Reunite, Biomet Inc, Warsaw, IN) made of a co-polymer of L lactic acid and glycolic acid. Distal radial fractures lend themselves to resorbable fixation devices due to the relatively low functional loads and post-operative cast immobilisation being acceptable to patients. They also offer the theoretical advantage of avoiding the need for a second operation for removal. However, a cadaveric biomechanical study demonstrated early failure on cyclical loading in a commercially available bioresorbable plate compared with established titanium plate designs[183]. Gangopadhyay et al[184] reported successful results from plating of unstable distal radial fractures using a bioresorbable plate in twenty eight patients. However, a randomised controlled trial of bioresorbable plates versus metallic plates to treat distal radius fractures demonstrated a significant re-operation rate associated with the bioresorbable implants[185]. Mechanical failure and re-displacement occurred in six out of the 19 fractures treated with a bioresorbable plate. Three patients demonstrated evidence of soft tissue inflammation with one developing a persistent sinus requiring surgical intervention.

1.4 Bioresorbable composites as fracture fixation devices

Non-reinforced PLA and PLLA plates and screws are initially too weak to permit early mobilization and have a tendency towards sudden brittle failure[186]. This has generated interest in composite bioresorbable materials which could theoretically overcome these limitations in mechanical properties. Studies of ceramic reinforced polymers demonstrated rapid loss of strength in vivo negating their use in fracture fixation devices[187]. Development of self-reinforced composites with polymer fibres reinforcing a polymer matrix has resulted in some improvements in mechanical properties[156, 160] but have not lessened concerns regarding polymer degradation associated soft tissue reactions. Developments in bioactive glass manufacture have led to success in creating bioactive glass fibres[188] with a very high initial modulus and bending strength compared to polymer fibres while retaining the ability to degrade in vivo. Cytocompatibility tests have demonstrated in vitro biocompatibility with human osteoblast and osteosarcoma cell lines[189, 190]. Early fibre designs demonstrated rapid degradation leading to an early loss of the reinforcement mechanical effect. More durable glass fibre formulations were sought with the emphasis firmly placed on their biocompatibility[191]. The properties of these fibres can be tailored by modifying their composition[192]. The chemical composition of phosphate glass fibres is close to that of normal bone leading to speculation that ions released during degradation may exert bioactive effects on the healing process. The mechanical and degradation properties of the glass fibre-polymer composites can be modified by altering the relative volume fractions of polymer and glass fibres as well as the spacial arrangement and orientation of the fibres within the matrix. PLA composites reinforced with P40 phosphate based glass fibres have shown retention of their mechanical properties for much longer periods than previously investigated composites produced using P50 fibres[193]. Studies have demonstrated improved mechanical properties of strength and stiffness in uni-directional composites in which the fibres are parallel to the long axis of the plate compared to random mat arrangements[194].

A fracture fixation plate was developed with a composite structure consisting of phosphate glass fibres reinforcing a PLA polymer matrix[195]. The plate has been

designed to enable in vivo experimentation in an animal model. The fibres were produced from a quaternary phosphate based glass ($50P_2O_5$-$40CaO$-$5Na_2O$-$5Fe_2O_3$) to reinforce a conventional PLA polymer matrix. In vitro studies investigated the effects of screw holes and gamma sterilization on mechanical properties of these composite plates with varying fibre layup and volume fraction[195]. The flexural mechanical properties were improved by increasing the volume fraction and utilization of thinner unidirectional fibres. The measured flexural moduli of these plates ranged from 4 GPa to 24GPa which compared well with similar measurements in cortical bone. There was minimal attenuation in the flexural strength characteristics when comparing sterilized with unsterilized plates. Degradation studies in physiological saline demonstrated attenuation in mechanical properties after 30 days which was within the expected time frame for fracture union in experimental animal models.

The biocompatibility and degradation profile of this composite plate in vivo have not been evaluated. The retention of mechanical characteristics is dependent on the in vivo rate of degradation and it is important to establish if the composite plate could maintain its structural integrity to enable fracture union in an animal model. Plating studies in an intact bone model could assess the potential stress shielding effects of the composite plate and how these compared to a similarly dimensioned steel plate. If the composite plate could maintain sufficient mechanical properties to permit healing with favourable effects on the underlying bone, subsequent in vivo studies could investigate the outcomes from plating an experimentally created osteotomy in the same animal model. Parallel studies using a steel plate to fix the osteotomy could enable a comparison of the type of healing and the strength of the callus formed at various time points for the two types of plated bone.

1.5 Aim and objectives

The aim of the current study was to investigate the in vivo effects of a novel bio-resorbable fracture fixation plate manufactured from a phosphate glass fibre reinforced PLA composite. The feasibility of using this plate as a fracture fixation device and its biocompatibility were experimentally investigated in an animal model. Following the failure of the composite plate to fix an in vivo osteotomised bone, parallel in vivo studies in the same animal model were conducted comparing the effects of the composite plate with a similar sized stainless steel plate on intact bone. In vitro mechanical tests were conducted to determine the properties of the composite plate compared with different types of plate and bone.

The objectives of the study were

1. To determine the feasibility of fixing an in vivo osteotomised animal bone model with the composite plate to enable anatomical healing of the osteotomy.

2. To compare the in vivo effects of the composite plate with a metal plate on adaptive structural changes in an intact rabbit tibia model at five different time points following implantation (2, 6, 12, 26 and 52 weeks).

3. To compare the in vivo effects of the composite plate with a metal plate on the mechanical properties of a plated intact rabbit tibia model at the five time points following implantation.

4. To compare the in vitro mechanical properties of the composite plate before and after degradation with the metal plate, poly-lactic acid plate, intact bone and osteotomised bone.

5. To compare the in vivo clinical and histological inflammatory response to the composite and metal plates at three time points of implantation – 2, 6 and 12 weeks.

Chapter 2 Methods

2.1 Plate design

The plate geometry in the current study was based on dimensions used in a previous in vivo study in which plates were applied to the rabbit tibia[85] (Figure 2.1). The plate design was based on these dimensions of 45mm length and 5mm width. However, in this study the 316L stainless steel plate was only 1mm thick. To optimise the mechanical properties of the composite plate, the plate thickness for the composite plate was doubled to 2mm (Figure 2.1b). To avoid differences in geometry, the 316L stainless steel plate used in the parallel experiments was similarly dimensioned (Figure 2.1c). The method of composite plate manufacture has been described in a previous study based on optimisation of mechanical and degradation properties[195]. PLA sheets, produced from heating PLA pellets, were sandwiched alternately with three unidirectional fibre mats and placed in 2mm thick moulds. The composite was formed by heating to 210°C for 15 minutes, compressed at 38bar for 15 minutes and then cooled under continuous pressure. The laminated composite was sectioned into plates measuring 45mm length and 5mm width using a scroll saw. The fibre volume fraction of these plates was experimentally determined as 47±3% in a previous study[195].

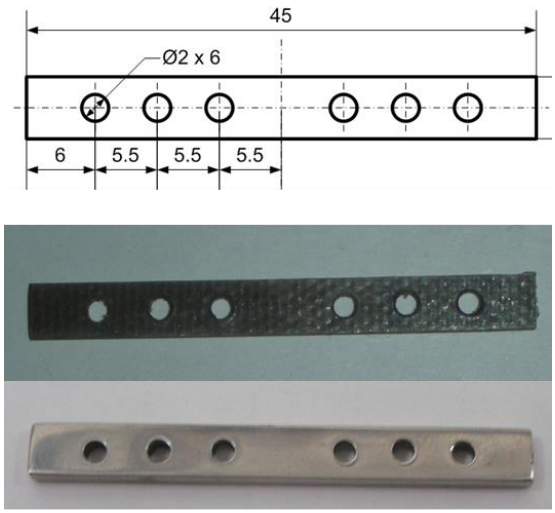


Figure 2.1 Plates used in experiments. (a) Schematic for plate design based on previous plating studies in rabbits[49]. Two mm thick composite (b) and steel (c) plates based on this schematic used in the current experiment

2.2 Selection of the animal model

An application for a Home Office project licence was completed during initial study design. The licence application detailed the estimated number and species of the animals to be experimented upon, the severity of the intervention, the likely adverse effects and the fate of the animals at the end of the study. Humane end points were established regarding the extent of distress or suffering the animals were permitted to endure within the study. Breach of these would necessitate euthanasia of the involved animals.

The Project Licence for the current study was granted prior to the appointment of a research fellow who would undertake the experimentation. Since its approval, it was amended to incorporate additions to the study design after review of the study protocol. Although the project licence application was submitted by the chief investigator, the author performed an in depth review and expansion of the protocol to elaborate on the desired scientific objectives, improve the robustness of experimental design through inclusion of additional outcome measures and a further study arm investigating the same outcomes in the metal plated group.

Personal licences were sought for the chief investigator supervising the experiments and the author, who performed the experiments. The four compulsory training modules were completed as part of the Home Office Licence Training Course in November 2010 at the University of Cambridge. The personal licence holder was responsible for the animals on which the procedures were performed, maintaining the primary record keeping of the conduct of the study and ensuring adherence to the project protocol. A competency log was maintained to ensure competency in undertaking the surgical experiments. Risk assessments were completed for all procedures undertaken. The use of a radiation source for radiographic assessment was approved by the Radiation Protection Officer. All of the experiments, in line with Home Office recommendations, were conducted in a dedicated scientific establishment with standardised laboratory animal resources, enabling availability, transport, housing and husbandry of the animals.

The selection of an appropriate animal model in the current study was sought from the existing literature. The current study utilised a rabbit animal model due to the popularity and extensive use of this animal model to assess the influence of plating on intact bone[49, 59, 63, 71, 76, 196, 197]. Other considerations included the ability to manufacture an appropriately sized plate from the composite material, ease of husbandry, availability and cost. The tibia was chosen as the site of application of the bioresorbable composite plate based upon these previous studies[49, 59, 63, 71, 76, 196, 197]. Tibial plating studies in rabbits have reported methodologies for assessing structural properties of intact plated bones[49, 63], fracture union following plated of experimentally created osteotomies[76, 196, 197] and reproducible methodologies for flexural[49] and torsional[63] mechanical testing.

The New Zealand White rabbit strain was chosen as it is the most commonly used strain in laboratory experimentation[198]. Due to extensive inbreeding, the strain demonstrates greater phenotype homogeneity when compared with cat or dog strains enabling reduced sample sizes to accommodate inter-animal differences. Exclusively female rabbits were used to negate the influence of inter-gender variation and enable group housing to improve husbandry over the study period. The rabbits were skeletally immature at the time of surgery as evidenced by open growth plates on radiographs taken immediately post operatively.

2.3 In vivo plating of osteotomised rabbit tibia

2.3.1 Trial experimentation

To refine the experimental technique, trial experiments were conducted on cadaveric tibia retrieved from wild type rabbits. The trial experiments enabled a reproducible method of plate application to the medial tibial cortex utilising a medial approach. The rabbit fibula fuses with the tibia at the latter bone's mid-point (see Figure 2.2). Analysis of multiple cadaveric specimens revealed symmetry in the location of this tibio-fibular junction in the paired tibia bones. Placement of the proximal end of the plate at the level of the inferior aspect of the tibial tuberosity achieved reproducible placement of the plate mid-section at the level of the tibio-fibular junction. In the sagittal plane, the plate was centred on the tibia both proximally and distally (Figure 2.2).

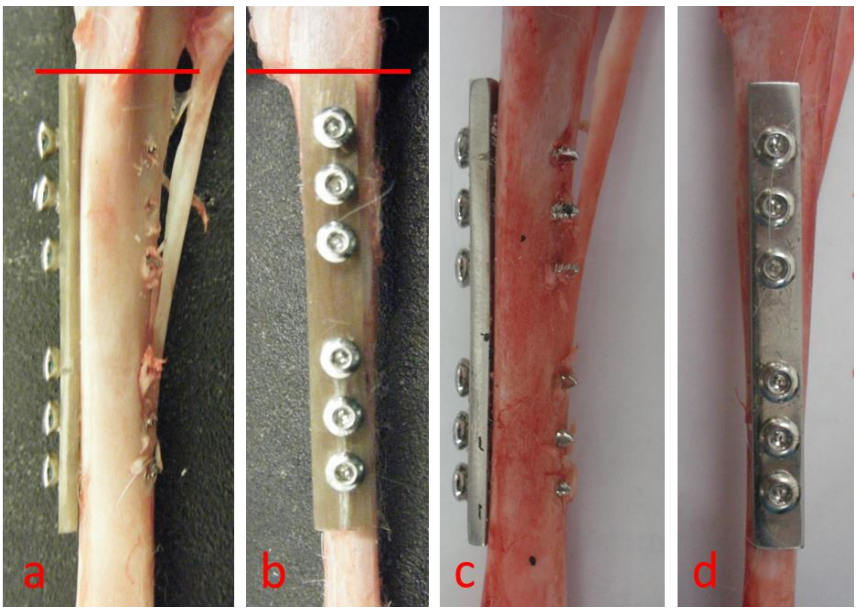


Figure 2.2 Photographs of a composite and metal plated cadaveric tibia in antero-posterior (AP) (b, d) and sagittal (a, c) planes. The fibula fuses with the tibia at the level of the central region of the plate. The plates have been placed with the proximal tip in line with the inferior aspect of the tibial tuberosity (red lines – a,b).

Trial experimentation with tibias retrieved from 20 week old New Zealand White rabbits confirmed that 2mm diameter screws of 12mm length were appropriate to achieve satisfactory bi-cortical fixation of the plate to the medial aspect of the tibia. Practical difficulties arose in drilling screw holes to enable the composite plate to be attached to the bone. The diameter of the plate screw holes was 2mm and the drill bit diameter was 1.8mm. Drilling through the metal plate is an established technique to correctly position the screws. However, attempts to drill through the composite plate caused damage to the plate due to the tight clearance. A jig was therefore developed to achieve correct placement of the screw holes. The jig was manufactured from surgical stainless steel to the same dimensions and screw-hole locations as the composite plate (see Figure 2.3). However, to ensure perpendicular trajectories of the screw holes, the jig screw-hole diameter was reduced to 1.9mm to achieve a tighter clearance. To avoid jig displacement while drilling, a concave jig-bone interface geometry was adopted to accommodate the tibia curvature. The risk of jig displacement was also reduced through the use of 1.7mm diameter wires to secure the jig through the drilled screw holes. The jig was tested on cadaveric tibias to ensure that it would accommodate the expected variation in tibia geometry between different sized rabbits.

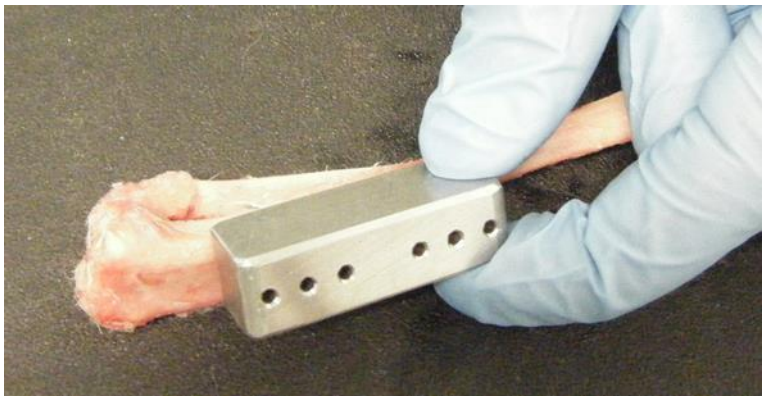


Figure 2.3 Photograph of jig held against the intended site of plate attachment on the medial cortex.

The current study sought to determine the feasibility of using the composite plate to fix an experimentally created fracture in the in vivo rabbit tibia animal model. To improve reproducibility of the model, an osteotomy technique was used instead of fracturing the bone. Trial experiments with a fine oscillating saw demonstrated that sawing the bone removed a 1mm thick section of the bone. A new jig was designed to allow drilling the screw holes for the composite plate before performing the osteotomy between the central two screw holes. Use of the jig enabled compression of the bone ends when the osteotomised tibia was plated using the composite plate (Figure 2.4). A third jig was designed enabling a saw cut to be made perpendicular to the bone at the level of the mid-section of the plate. This jig was essentially the previous jig divided in two which allowed the flat surface of the blade to make an osteotomy directly midway between the central two screw holes in the composite plate (6mm from the third screw hole). Trial experiments with the new jigs demonstrated reproducible closure of the osteotomy gap on cadaveric tibiae (Figure 2.4c).

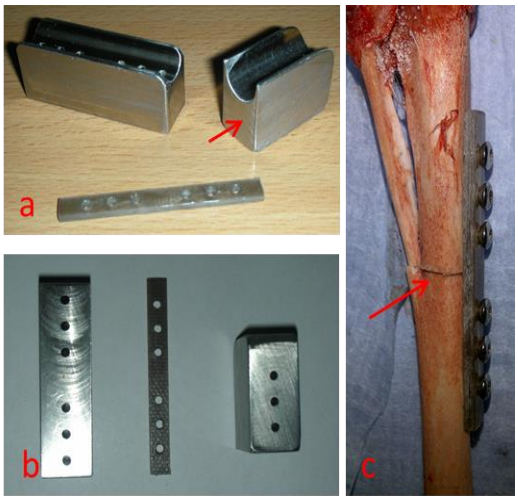


Figure 2.4 Photographs demonstrating the osteotomy jigs. (a) Osteotomy jigs and composite plate. The curved surface of the jig improved apposition of the jig to the bone. The smaller jig was placed over the proximal three screw holes and secured with wires. The saw was passed along the flat face (red arrow) to create the osteotomy at a fixed distance between the central two screw holes. (b) View of the jigs and the composite plate from above demonstrating location of holes enabling screw holes to be drilled to close 2 mm gap created by saw. (c) Trial cadaveric tibia plated with composite plate using the jigs demonstrating satisfactory closure of the osteotomy site.

2.3.2 Preparation before implantation

The rabbits were procured from an approved domestic supplier with membership of the Laboratory Animal Breeders Association (LABA) who were able to supply specific pathogen free animals. The animals were acclimatised in the Biomedical Sciences Unit for at least 1 week before surgery as per Home Office recommendations. Peri-operative care involved an inter-disciplinary approach to optimise the ethical and welfare aspects of the animals involved. The peri-operative protocol was developed with the team which was made up of the surgeon (author), animal technicians, the named animal care and welfare officer (NACWO), and the named veterinary surgeon (NVS). Pre-operative checks were carried out on all of the rabbits prior to surgery to establish normal activity, coat appearance, oral cavity and faecal pellets. All animals were weighed to confirm appropriate weight gain since the date of arrival. The animals had three unique identifiers – a skin marking with a 4 character alpha-numeric code, implanted microchip transponders encoding a unique 8 character code that could be read with a remote device and an animal specific study ID number. This was essential to avoid mis-identification during group housing. The right leg of each rabbit was shaved the day before surgery.

2.3.3 Theatre setup and anaesthesia during experimentation

The surgical implantation experiments were conducted in a dedicated theatre using an aseptic technique (see Figure 2.5a). Personal protective equipment consisted of surgical gowns, gloves, masks and a lead apron for radiation protection when taking radiographs. The premedication and initial anaesthetic gas administration were undertaken in an anaesthetic room adjoining the theatre. The anaesthetic protocol was developed in consultation with the NACWO and the NVS. The NACWO conducted the anaesthesia during all of the surgical experiments. Induction of anaesthesia was achieved through administration of an intramuscular agent and maintained through inhalation of a volatile agent. The rabbits received an intramuscular injection of Medetomidine (0.16ml/kg) 20 minutes prior to the beginning of the procedure. Medetomidine (Trade name Domitor ^{TM}) is an alpha-2

adrenergic agonist and has sedative and muscle relaxation effects. The rabbits were provided with oxygen through a face mask. Once sedated, isoflurane was introduced incrementally to the inhaled gas up to a concentration of 2.5% (flow rate of 1.5l/min). An antiemetic (Metaclopramide 0.1ml/kg), was administered intramuscularly. Enrofloxacin, a fluroquinone antibiotic, was administered subcutaneously. The rabbit was transferred to the operating table and the anaesthesia was maintained with 3.5% inhaled isoflurane in oxygen (2l/min). Pain relief was provided with subcutaneous bolus administration of Carprofen, a non steriodal anti-inflammatory drug with potent analgesic effects, and Buprenorphine (0.02 mg/kg), an opioid analgesic.

In the first few cases, it was noted that the rabbits emitted a vocal response when the tibia was first drilled. This was not accompanied by a visible return to consciousness and no further vocal response was observed during the drilling of subsequent holes. This finding was discussed with the NVS who speculated that the depth of anaesthesia could be influenced by diminished respiration induced by the muscle relaxation effect of the Medetomidine. Following this, we reversed the Medetomidine once the animal was maintained on gaseous agents, immediately prior to making the incision, using a synthetic alpha-2 adrenergic antagonist (Atipamezole 0.12ml/kg). Immediately prior to the drilling of the first screw hole the concentration of inhaled isoflurane was increased from 3.5% to 4%. Following this modification to the anaesthetic regime, the vocalisation response was not observed.



Figure 2.5 (a) Theatre setup showing operating table, anaesthetic equipment at head end and overhead lights. (b) X-ray equipment consisting of emitting device (green) suspended from gantry and black processing cassette directly beneath.

2.3.4 Osteotomy and plating experiment

The rabbits were positioned in right lateral recumbency on a heated mat on the operating table. The leg was prepared with 70% alcoholic chlorhexidene. Sterile drapes were used to isolate the leg above the knee from the ankle in the sterile field. The animals were monitored while anaesthetised by inspection of the quality of respiration, heart rate, degree of muscle relaxation and eye position.

Surface anatomical landmarks were identified and the incision marked with a pen. The tibial tuberosity, calcaneal tuberosity and subcutaneous medial border of the tibia were readily palpable. Before incising the skin, the depth of anaesthesia was assessed by observing the response to a toe pinch. A longitudinal incision was made from the inferior aspect of the tibial tuberosity to above the ankle (see Figure 2.6). The incision was made slightly away from the site of plate application to avoid the thin skin overlying the medial tibia surface.

The periosteum overlying the bone was incised and stripped away using blunt dissection. The muscles in the posterior and lateral compartments were retracted to preserve the posterior neurovascular structures. The jig was placed on the medial

aspect of the tibia and was correctly positioned when the proximal edge of the jig was in line with the inferior border of the tibial tuberosity.

The surgical steps are shown in Figure 2.6. The medial aspect of the tibia was exposed. The jig was applied to drill all 6 screw holes for the plate. Soft tissue retractors were placed circumferentially around the bone at the proposed osteotomy site corresponding to the mid-section of the plate. The jig was secured through passage of wires through each of the screw holes as they were drilled. Once all the screw holes were drilled the jig was substituted for the second jig enabling the osteotomy to be performed. A fine pneumatically powered saw blade (46/25x6.0x0.6/0.4mm) was used to make a single perpendicular cut completely through the bone. The composite plate was then applied and secured with the use of wires in the screw holes. The wires were sequentially replaced by screws to fix the osteotomy. The wound was washed with saline and closed. Anteroposterior (AP) and lateral radiographs were taken while under anaesthesia to confirm satisfactory plate placement and bi-cortical screw fixation. The animal was recovered in theatre and monitored hourly following surgery.

Three hours following surgery the rabbit was found to be lame. Radiographs demonstrated complete plate failure. Following discussion with the research group, no further osteotomy experiments were undertaken.

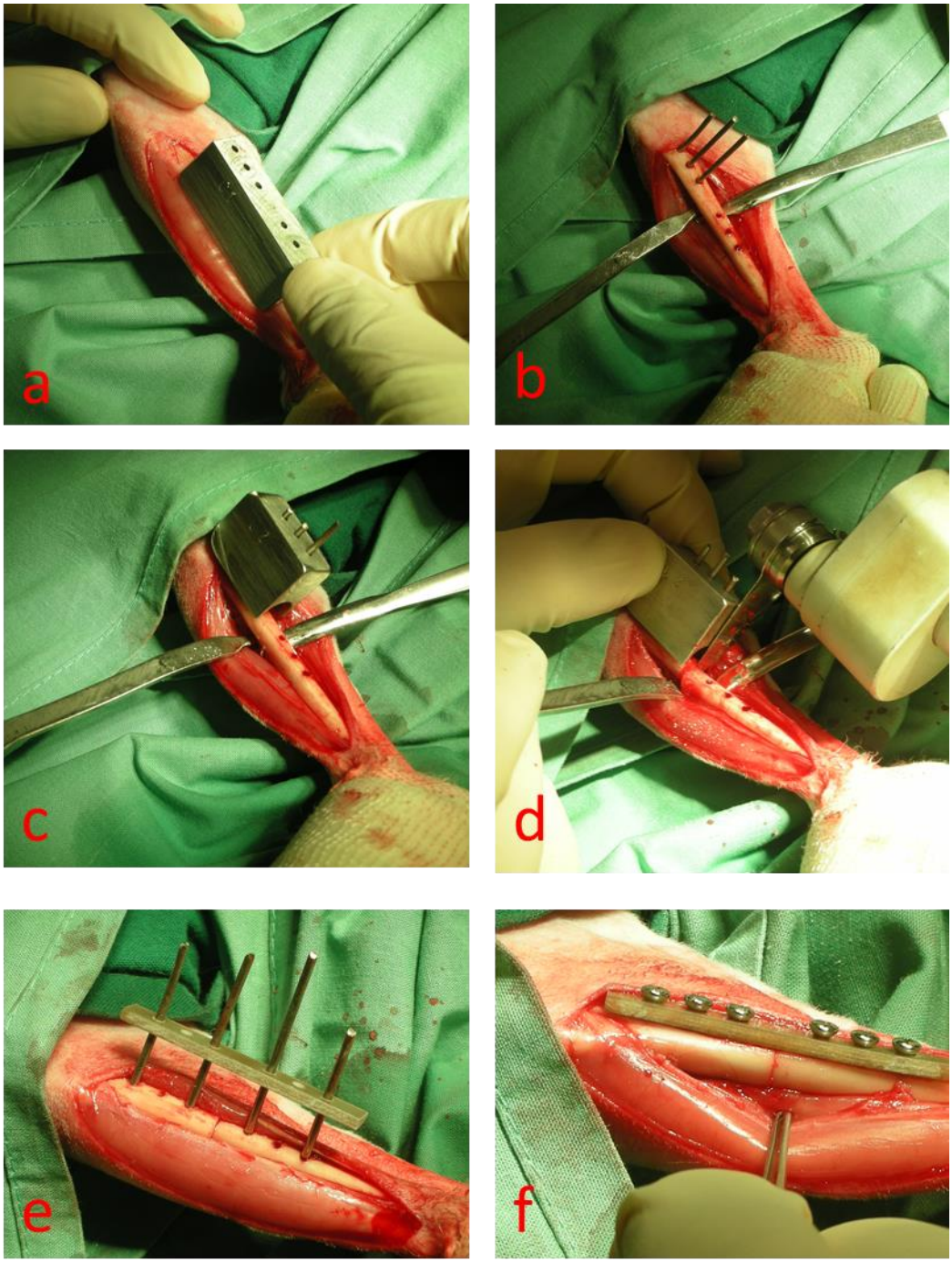


Figure 2.6 Surgical steps in composite plating of osteotomised tibia. (a) Application of osteotomy jig to site drill holes. (b) Wires placed in proximal three drill holes. (c) Osteotomy jig for saw cut placed on to the bone and secured with wires. Retractors passed around bone at planned osteotomy site to protect surrounding soft tissue structures. (d) Osteotomy made with mechanical saw. (e) Wires placed in to screw holes and composite plate applied to the bone. (f) Successful plate application demonstrating gap closure at the osteotomy site.

2.4 Study comparing the effects of the composite plate with the metal plate on intact bone

In parallel with the experiments investigating composite plate fixation in an in vivo osteotomised rabbit tibia model, experiments were planned to determine the effects of the composite plate on intact bone. The aim of this set of experiments was to establish the biocompatibility of the composite plate in an in vivo setting and also to determine the stress shielding effects of the plate on intact bone without the superimposed effects of fracture biology in the osteotomised animal model. Following failure of the osteotomy experiments, the aim of the study was to compare the in vivo effects of the composite plate on intact bone with a similarly dimensioned steel plate. Outcomes investigated included changes in the bone beneath the plate and the mechanical properties of the plated bones. Further in vitro experiments were conducted to determine the mechanical properties of the composite plate, before and after degradation, in comparison to a polylactic acid polymer plate, the metal plate used and intact and osteotomised cadaveric bones.

The revised study design investigated the influence of the composite plate on the underlying bone in comparison with a similar sized metal plate. Thus, there were two arms to the study comparing the two types of plate. The study sample baseline characteristics were similar for the two arms of the study (Table 2.1).

	Composite plate	**Metal plate**
Number of rabbits	25	25
Species	New Zealand White	New Zealand White
Gender	Female	Female
Mean age at time of surgery	14 weeks (12-16 weeks)	14 weeks (12 – 16 weeks)
Mean weight at time of surgery	2750g (2381-3321g)	2680g (2475-2922g)

Table 2.1 Table showing study sample characteristics for the two arms of the study investigating the two types of plate.

Each arm of the study utilised a paired study design to improve the assessment of outcomes. In the paired study design, the contralateral limb of the animal acted as an experimental control. Thus at the time of sacrifice, the left un-plated tibia was also harvested to enable measurements on an experimental control. This study design minimised the influence of different animal weights, bone sizes and geometries acting as potential confounding factors when comparing the two types of plate. By normalising each measured outcome in the plated bone relative to its respective control bone, more meaningful comparisons could be made between the two types of plate with respect to structural changes in the underlying bone. This approach was supported by experimental findings demonstrating symmetry of mechanical properties of paired long bones such as the tibia in a rabbit animal model[69-71, 85]. This obviated the use of a separate control group of un-operated animals in keeping with the "reduced numbers" ethos of animal experimentation.

2.5 Selection of sample size

All animal studies must endeavour to use the smallest possible sample size to answer the research question. When investigating outcomes whose characteristics are a function of time, the sample size is dependent on whether experiments are conducted in series or parallel. The current study investigated how the duration of implantation influenced the inflammatory response and stress shielding changes in the bone. The outcome measures included assessing the structural and mechanical properties of the plated bones necessitating post sacrifice retrieval. This was in contrast to longitudinal studies where in vivo assessments enable observation of the same group of animals at successive time points without sacrifice. Thus, the current study utilised a parallel study design to investigate the influence of increasing durations of implantation in different groups of animals.

The time points of sacrifice were based on the intended outcomes of interest and the previous literature investigating the effects of plate application in this animal model. The current study investigated the degradation of the implant, the host inflammatory response, stress shielding changes related to the duration of implantation as well as establishing findings at comparative time points for the study investigating fracture healing of the plated rabbit tibia osteotomy. Five time points of retrieval were chosen relative to the time of implantation – 2 weeks, 6 weeks, 12 weeks, 26 weeks and 52 weeks.

In the current study it was necessary to establish that the plate had retained its structural integrity up to the point we would have expected an experimentally created fracture to heal. In the rabbit tibia model, most plated fractures have united by 4 weeks[76, 196, 197]. Accommodating potential delays in union by factoring a threefold increase in the time taken for union to occur suggested a time span of 12 weeks by which we could reasonably expect all fractures to have healed. The time point of 12 weeks was selected to assess implant degradation by the time the fracture would have healed. The in vitro studies of the composite plate's degradation suggested that the mechanical properties of the composite plate attenuated rapidly within the first week after which they plateaued[195]. To capture this potential phenomenon *in vivo*, a

2 week time point was selected to assess the plate degradation once this deterioration had occurred. This time point also served as a useful temporal point for later comparative analysis with the plated osteotomy model as it represented the mid-point in the healing process from the time of osteotomy to the time of expected union[199]. The previous study on which the plate geometry was based suggested that an equilibrium state of bone adaptation was achieved at 12 weeks in the steel plated bones[49]. As the relative stiffness of this steel plate and the current composite plate were unknown, we could not predict whether an equilibrium state might occur earlier necessitating an intermediary time point between implantation and 12 weeks. The selection of a 6 week time point would enable the study of the relative rates of progression of the evolving stress shielding response towards equilibrium in both plated samples. In the current study, the evaluation of long term outcomes was restricted by the funding stream. The protocol submitted with the project grant application intended to investigate outcomes up to 1 year post implantation by which time an experimentally created fracture in this model would have remodelled. The selection of a 26 week time point served as an intermediate time point between expected union and complete remodelling at 52 weeks.

This is the first study investigating the in vivo effects of this bioresorbable plate and therefore the magnitude of any relative effect size in the measured outcomes when comparing the two plates was unknown. Consequently, a sample size calculation could not be undertaken. Resource equations were used to calculate the sample size[200]. A resource equation targets an error for degrees of freedom between 10 and 20 for exploratory experiments where power analysis is not practical or feasible. In our study, we intended to establish 5 time points of sacrifice. If we propose 5 animals per time point of sacrifice, the calculation for the error in degrees of freedom is shown below:

Total proposed sample size (n) = 5 rabbits x 5 time points = 25
Total sample size degrees of freedom (n – 1) = 25 – 1 = 24
Total number of time points (t) = 5
Time dependant degrees of freedom (t-1) = 5 – 1 = 4
Error in degrees of freedom = (n-1) – (t-1) = 24 – 4 = 20

Thus, the calculated error was equivalent to 20 corresponding to the minimum sample size achievable with an estimated error between the boundaries of 10 and 20. By consensus opinion, the error size of 20 was regarded as appropriate for the current study design. Following statistical analysis of the outcomes, a post-hoc analysis of sample size was undertaken to determine the minimum sample size required to detect the observed differences in outcomes when comparing the metal and composite plated groups.

2.6 Surgical implantation of composite and metal plates to intact tibiae

The same peri-operative and anaesthetic protocol was used as the osteotomised bone experiments. Surface anatomical landmarks were identified and the incision marked with a pen. Before incising the skin, the depth of anaesthesia was assessed by observing the response to a toe pinch. A longitudinal incision was made from the inferior aspect of the tibial tuberosity to above the ankle (see Figure 2.7). The incision was made slightly away from the site of plate application to avoid the thin skin overlying the medial tibia surface.

The periosteum overlying the bone was incised and stripped away using blunt dissection. The muscles in the posterior and lateral compartments were retracted to preserve the posterior neurovascular structures. In the composite plate experiments, the jig was placed on the medial aspect of the tibia and was correctly positioned when the proximal edge of the jig was in line with the inferior border of the tibial tuberosity.

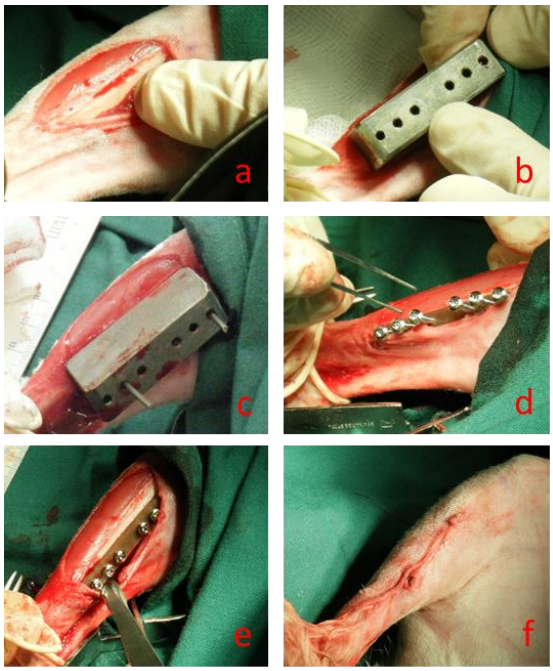


Figure 2.7 Surgical steps in the composite plate implantation experiments. The medial aspect of the tibia was exposed (a) and the jig sited (b). The jig was used to drill the screw holes and was secured in place with wires passing through the holes (c). The composite plate was applied and the screws inserted (d) and tightened (e). The skin was closed (f).

The most proximal screw hole was drilled first and a wire was placed through the jig in to the screw hole to anchor the jig. The jig was pivoted on this wire to ensure that the most distal screw hole was centred on the bone. This screw hole was drilled and a second wire was used to secure the jig (Figure 2.7c). The intervening screw holes were sequentially drilled in the order – 2nd, 5th, 3rd and finally the 4th screw hole. Two additional wires were used to secure the jig through the 2nd and 4th screw holes as the holes were sequentially drilled. The jig and wires were removed and the bone thoroughly irrigated with 0.9% saline solution to remove the bone debris. The wires were then reinserted in to their previous screw-hole locations and the composite plate was lowered on to the bone by passage of the wires through their respective screw holes. Once the plate was sitting flush with the bone, the wires were sequentially replaced by stainless steel screws inserted in the same order that the holes were drilled (Figures 2.7d,e). The appropriate torque for satisfactory screw placement was judged manually by the operating surgeon.

The metal plate experiments did not require the jig as the screw holes could be drilled through the plate. The plate location was analogous to the composite plate experiments. The surgical steps are shown in Figure 2.8.

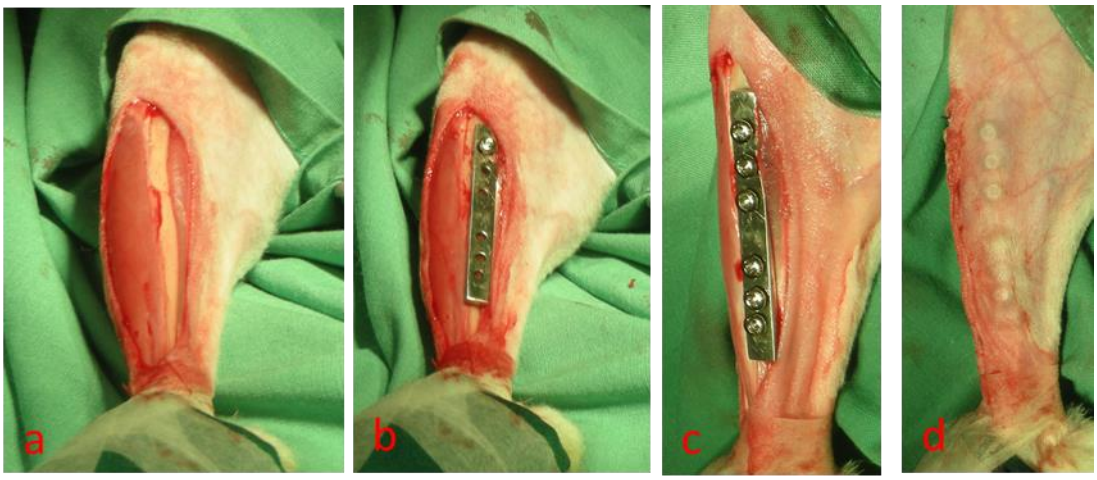


Figure 2.8 Surgical steps in metal plate implantation experiments. The medial aspect of the tibia was exposed (a) and the plate applied. The first screw hole was drilled and screw inserted (b). The remaining screw holes were filled (c) and the skin closed (d).

Once plate fixation was achieved, the wound was washed with 0.9% saline solution. The skin was sutured using a continuous subcuticular Poliglecaprone 25 undyed monofilament suture (Monocryl, Ethicon Ltd). After insertion of the first screw, the concentration of inhaled isoflurane was reduced to 3.5% and once the incision was closed this was further reduced to 2% to ensure gentle recovery at the end of surgery.

2.6.1 Radiography of plated and control bones

Intra-operative radiographs were performed while the rabbit was still under anaesthesia (see Figure 2.5b) to confirm satisfactory plate fixation. Images were taken in two orthogonal planes – frontal plane (AP view) and the sagittal plane (Lateral view) (Figure 2.9). The rabbit was positioned in lateral recumbency. Tapes were tied around the ankles. To minimise superimposition of the opposite leg, traction was applied to the operated leg while the opposite leg was abducted and pulled caudally. The operated leg was secured to the cassette with radiolucent tape enabling the lateral radiograph to be taken (see Figure 2.9b). The rabbit was then positioned in dorsal recumbency and traction applied to the operated leg to extend the knee. The leg was secured while the AP radiograph was taken (Figure 2.9a).

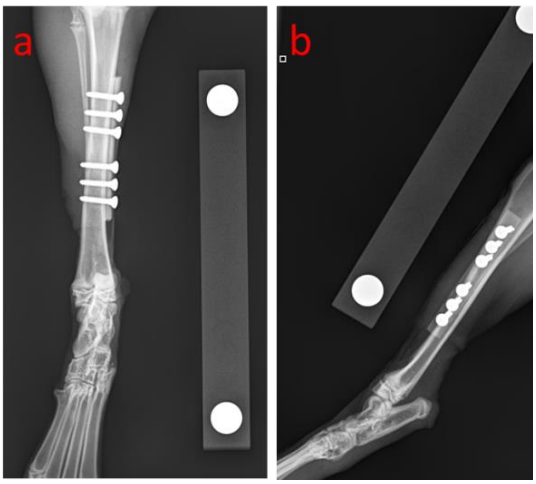


Figure 2.9 AP (a) and Lateral (b) radiographic views of the right leg showing the composite plate attached to the medial aspect of the tibia with stainless steel screws. The calibration guide measured 100mm between the two radio-opaque spheres.

The x-ray beam was centred using the laser marker and the area was collimated to 8” by 6”. The radiographic parameters were a film focal distance of 75cm, current 7.0mAs and potential difference of 52kVP. A 100mm radio-opaque calibration guide was placed adjacent to the leg to enable calibration of measured distances on the radiographs. The cassettes were digitally processed (AGFA PACS) ensuring that the image LGM value was between 2 and 2.22 indicating appropriate light-dark balance.

2.6.2 Recovery and Housing following surgery

Once satisfactory radiographs were obtained, the inhaled concentration of isoflurane was gradually reduced and the mask removed. The animal was relocated to a cage for recovery and periodically monitored. Once the rabbit was able to demonstrate maintenance of a satisfactory sternal position they were relocated to their respective group cages. Postoperative antibiotics were administered for three days and pain relieving medications for one week.

Initially, a single experiment was undertaken and the animal observed for 24 hours to detect any early complications before a further two experimental implantations were undertaken. The three animals were observed for two weeks prior to continuing the experiments to identify potential early failures and monitor responses. Once the safety of the technique had been established, five implantation experiments were completed each week until the completion of the experiments. This number was based on the maximum achievable throughput with respect to the available rabbit housing during the course of the study. The animals were monitored daily for general health and weight gain until the date of sacrifice. Initially, all animals were housed individually for one week postoperatively before being transferred to floor pens.

2.7 Assessment of outcomes in experimental implantations in intact tibiae

2.7.1 Scheme of outcomes assessment

At each time point of sacrifice, 5 rabbits were sacrificed giving rise to 5 pairs of tibiae- the right composite plated tibia and the left un-plated control tibia. The scheme of outcomes assessment for each of these 5 rabbits is shown in Figure 2.10. All of the retrieved tibiae underwent radiographic assessment as well as Micro Computed Tomographic (Micro CT) imaging. Practical difficulties arose in conducting mechanical testing and histology on the retrieved specimens. Mechanical testing was a destructive process making it difficult to histologically assess the specimens post testing. Similarly, perfusion fixation of the bones with 10% neutral buffered formalin as part of the histological processing affects the mechanical properties of bones[201]. A compromise was sought. Out of the three rabbits destined for mechanical testing, one rabbit's tibia was retrieved after mechanical testing and post fixed in 10% neutral buffered formalin to enable subsequent histological processing. This enabled a sample size of n= 3 for both mechanical testing and histological assessment.

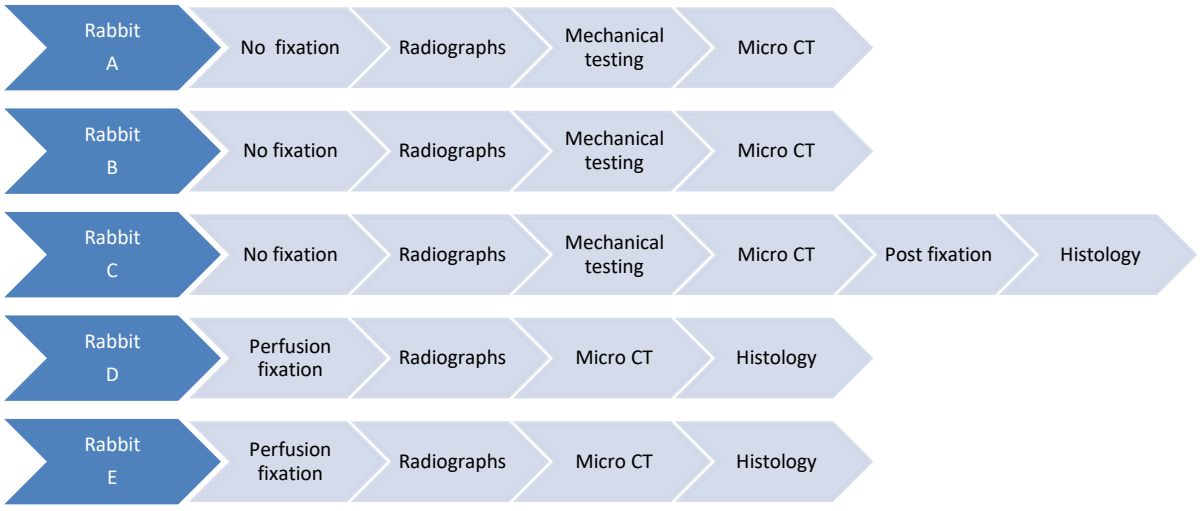


Figure 2.10 Schedule of outcomes assessment in composite plated experiments for the five rabbits (A-E) at each time point. All rabbits underwent imaging with radiographs and Micro CT. One rabbit (C) was utilised for both mechanical testing and histological assessment.

In the metal plated experiments, Micro CT assessment was not feasible due to artefacts generated by the metal plate obscuring the surrounding cortex. With the exception of the omission of Micro CT, the scheme of outcomes assessment was analogous between the two arms of the study comparing the two types of plate (Figure 2.11).

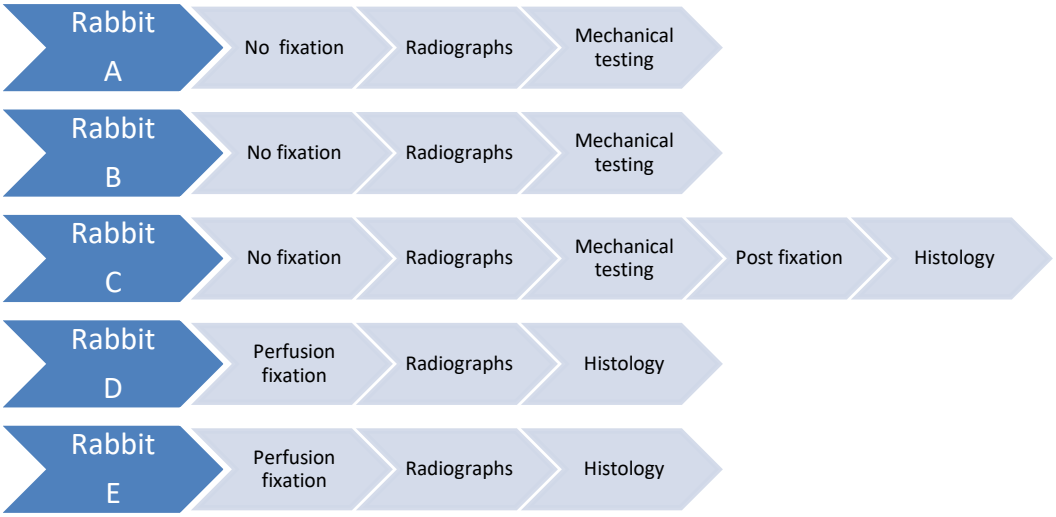


Figure 2.11 Schedule of outcomes assessment in metal plated experiments for the five rabbits (A-E) at each time point. One rabbit (C) was utilised for both mechanical testing and histological assessment.

2.7.2 Retrievals

At the time of retrieval, the rabbit identity was confirmed by checking the identifiers against the cage label and log of operations. The rabbit was weighed and transferred to a procedure room for euthanasia through terminal anaesthesia by intravenous administration of 10-15ml of pentobarbital. The rabbits destined for histological assessment were subsequently perfusion fixed while the rabbits intended for mechanical testing were processed for retrieval of the plated and control tibiae.

2.7.3 Perfusion fixation

Two of the five rabbits at each time point underwent perfusion fixation at the time of sacrifice to improve the quality of histological processing. In a third animal, in which the tibiae were retrieved following mechanical testing, post fixation was performed prior to histological processing.

First, the perfusion machine was flushed with saline and then primed with 10% neutral buffered formalin (NBF). Two anatomical sites of perfusion fixation were used during the course of the study – intra-cardiac administration and descending aorta cannulation[202].

The rabbit was placed in dorsal recumbency and a midline skin incision was extended from the xiphoid to the pubis. The linea alba corresponding to the midline of the abdominal musculature was elevated and divided under tension. Large Belfour retractors and swabs were used to retract the abdominal organs and expose the large vessels. The main artery, the aorta, and the main vein of the lower limbs, the vena cava, were isolated and clamped below the level of the diaphragm. An 18G intravenous catheter was placed in the aorta enabling flow of 10% NBF into the lower extremities circulation. The vena cava was perforated to enable the blood to escape. The rate of aorta perfusion was steadily increased to 100ml/min and a total of 800ml were perfused[202]. Evidence of tissue penetration included fine tremor, increasing rigidity and increasing transparency of the blood escaping from the vena cava.

This methodology demonstrated poor reproducibility and technical difficulties in cannulating the small vessels in five out of the first ten cases. Bones from these rabbits underwent prolonged post fixation in NBF to ensure satisfactory fixation prior to further processing.

Subsequently, intra-cardiac perfusion was used. Under terminal anaesthesia, the skin was incised in the midline from the umbilicus to the sternal notch. The sternum and

costal cartilages were divided on the left to expose the heart (see Figure 2.12). The perfusion needle was introduced into the left ventricle and directed cephalad into the aorta. The aorta was clamped externally to secure the perfusion needle. A stab incision was made in the right side of the heart to enable the blood to escape. The heart was perfused with 10% NBF at a rate of 100ml/min with a total perfusion volume of 1600ml to accommodate perfusion of the entire rabbit via this route. This technique proved successful on each occasion.

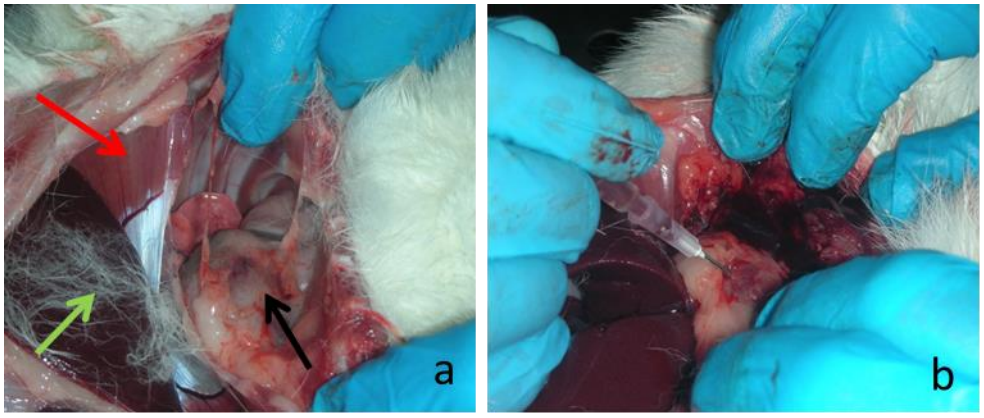


Figure 2.12 Photographs showing surgical exposure for intra-cardiac perfusion fixation. (a) The diaphragm has been split (red arrow) and the liver retracted (green arrow) to improve access to the heart (black arrow). The needle was inserted into the left side of the heart (b) and connected to the perfusion machine.

2.7.4 Dissection and radiographs

The technique for retrieval was similar in both tibias and in specimens destined for both histology and mechanical testing. The leg was disarticulated at the knee and ankle joints. Radiographs were then taken of both legs in AP and Lateral planes in their un-dissected state to characterise changes in the plated bones without disruption of the soft tissue envelope and after soft tissue removal (Figure 2.13).

The following measurements were taken from the radiographs (see Figure 2.14).

1. Length of plated bone and control bones (mm)
2. Distance of plate tip from proximal aspect of plated bone (mm)
3. Thickness of cortex beneath plate mid-section (mm)
4. Thickness of cortex at same level in control bone (mm)

The length of the plated tibia and the distance from the proximal tip of the tibia to the proximal tip of the plate were measured for both the composite plated and metal plated samples. This enabled the calculation of a Plate Location Index (PLI) at surgery and at retrieval using the below equation.

$$\text{Plate Location Index (PLI)} = \frac{Distance\ from\ tip\ of\ bone\ to\ tip\ of\ plate\ (mm)}{Total\ bone\ length\ (mm)} \text{ x } 100$$

Comparison of the plate location index between different plated bones enabled assessment of the reproducibility of the surgical technique in terms of plate placement relative to the bone between different experiments.

To enable comparison of the cortical thickness changes in the plated bones between different groups of animals, a normalised outcome measure (normalised cortical thickness) was calculated expressing the plated bone cortical thickness as a percentage of the same measurement in the respective control bone. This was calculated using the following equation.

$$\text{Normalised Cortical Thickness (NCT)} = \frac{Plated\ bone\ cortical\ thickness\ (mm)}{Control\ bone\ cortical\ thickness\ (mm)} \text{ x } 100$$

The NCT outcomes exist as percentage functions with values greater than 100 indicating that the cortical thickness was greater in the plated bone compared with the control bone.

In the right plated leg, photographs were taken of the surgical site to note any soft tissue inflammation (Figure 2.15a). Using sharp dissection, the tibias with attached fibula bones were stripped of their overlying soft tissues. In the plated specimens destined for histological characterisation, the soft tissues overlying the plate were

preserved to minimise disruption to any new bone formation and to aid specimen orientation during processing (Figure 2.15d). In the specimens destined for mechanical testing, preservation of the soft tissues interfered with alignment in the testing machine necessitating their removal (Figure 2.15c). The plated and control tibiae were photographed to note any structural changes (Figure 2.15c,d). The tibias destined for histological assessment were placed in NBF for post retrieval fixation in a volume ratio of 1:10. The tibias destined for mechanical testing underwent flexural strength testing on the same day of retrieval.

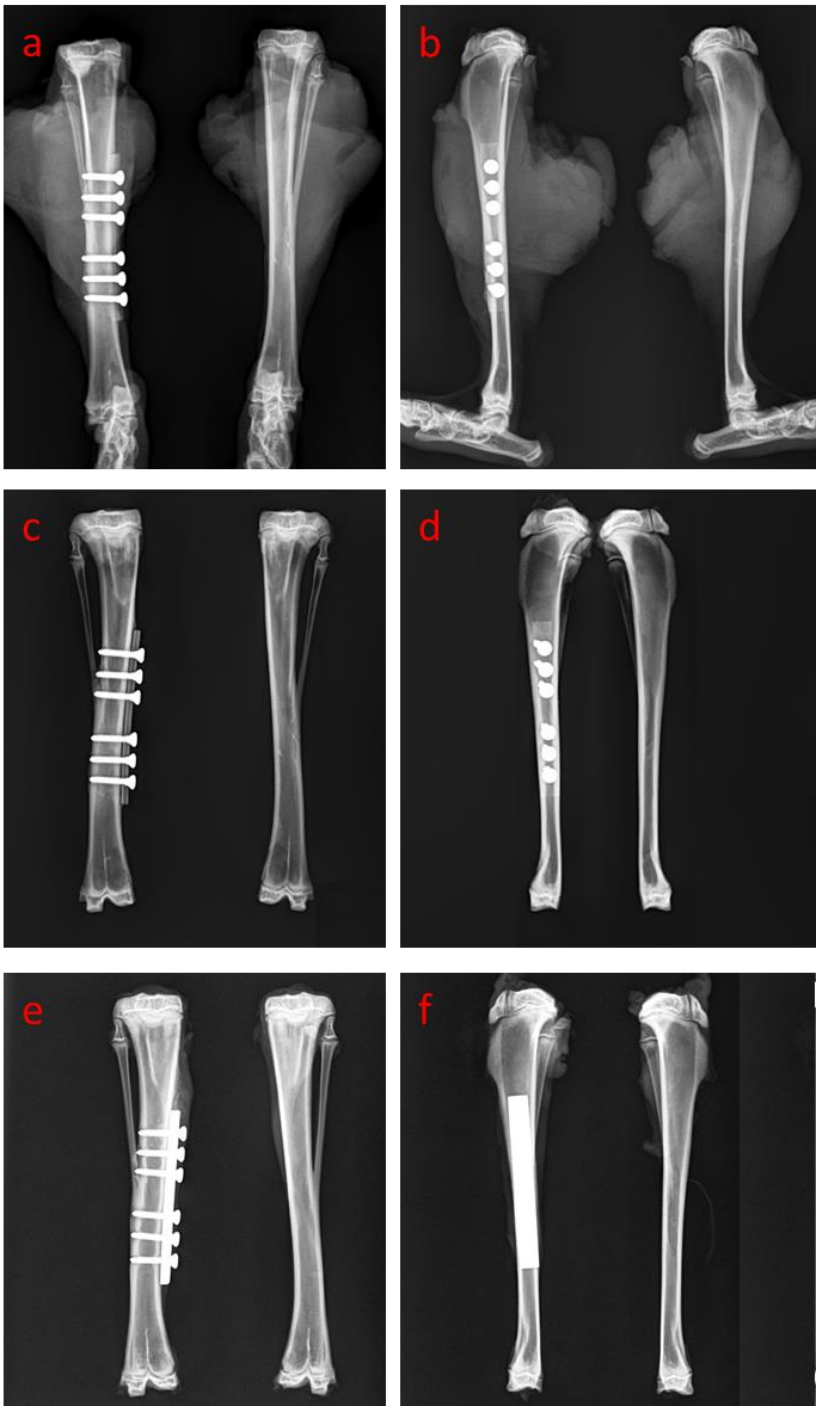


Figure 2.13 (a-d)AP and Lateral radiographs of a right composite plated tibia and left control tibia sacrificed at 2 weeks. AP (a) and Lateral (b) radiographs with overlying soft tissue envelope intact. AP (c) and Lateral (d) radiographs of the same specimens stripped of soft tissues. AP (e) and Lateral (f) radiographs of a right metal plated tibia and left control tibia sacrificed at 2 weeks stripped of soft tissues.

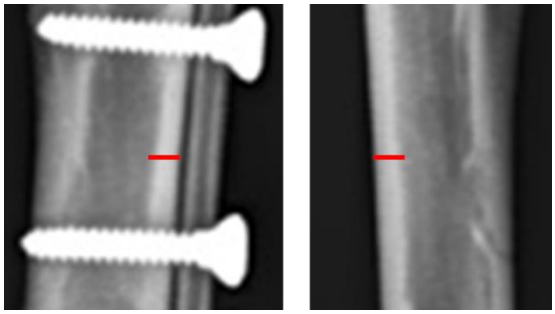


Figure 2.14 Magnified radiographic images of AP views of a composite plated bone and respective control bone at 2 weeks. The thickness of the cortex was measured beneath the middle of the plate and in the same location in the opposite control bone (red).

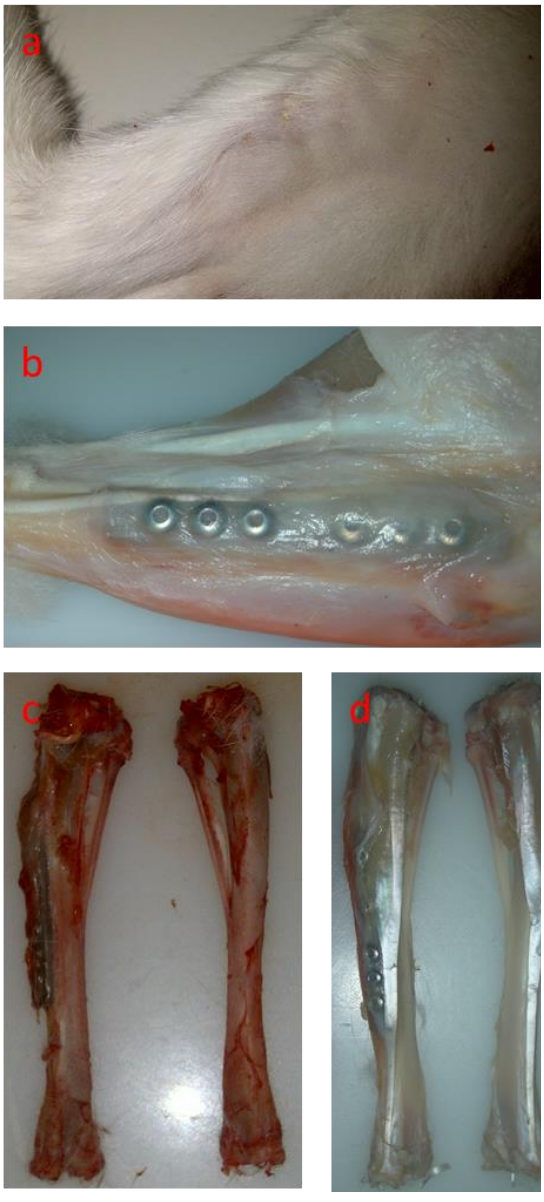


Figure 2.15 (a) Right operated leg demonstrating complete healing of incision at 2 weeks. (b) Skin removed revealing soft tissues overlying composite plate in same specimen. (c)Composite plated and control tibiae destined for mechanical testing with all overlying soft tissues removed. (d) Composite plated and control tibiae destined for histological processing with retention of soft tissues overlying plate.

2.7.5 Mechanical testing of in vivo plated and control bones

The plated and control bones were wrapped in moist saline soaked gauze following retrieval and during mechanical testing. Flexural testing of the bone specimens was undertaken using a servohydraulic testing machine (Instron 5960 system, Instron, MA, USA) capable of delivering variable axial loads at specified strain rates. Preliminary testing of cadaveric tibia taken from rabbits weighing 2 to 3.5 kg had demonstrated satisfactory testing with a load cell of 5 kN.

Based on a previous study[49], a three point bending test was used with the plated bone oriented so that the plate rested on the inferior rollers and was stressed perpendicular to its long axis (Figure 2.16).

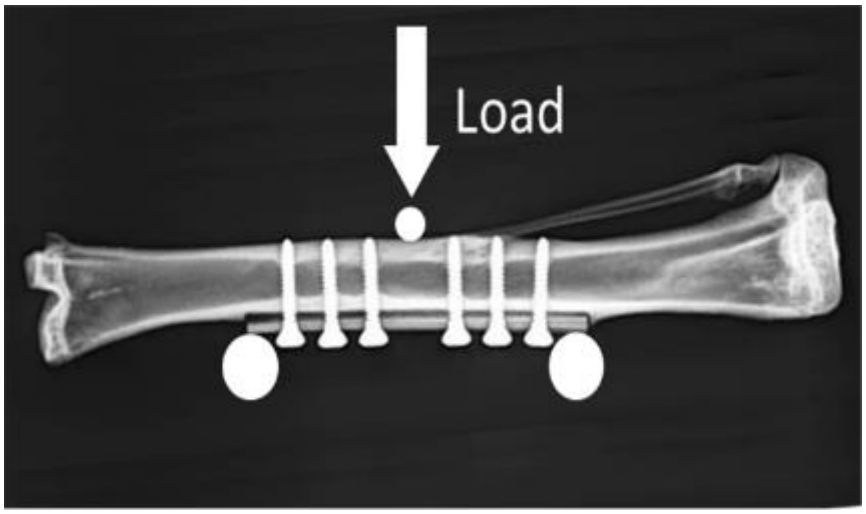


Figure 2.16 Diagram demonstrating orientation of plated tibia during the three point bending test. The plate rested on the inferior rollers (40mm span) and three point bending was introduced by downward displacement of the central roller (5mm/min rate).

The three point bending imparted a tensile stress on the plate and medial cortex while placing the lateral cortex under compressive stress. The span distance between the inferior two rollers was 40mm which enabled force transmission to the plate rather than the screw heads. To ensure that the control bone was stressed by the rollers in the same sites as the plated bone, the distance of the mid-section of the

plate from the tibial tuberosity was measured prior to testing. This was used to determine the positioning of the central superior roller relative to the tibial tuberosity in the control bones during mechanical testing. A fixed displacement rate of 5mm/min of the central roller relative to the inferior rollers was chosen based on a previous study[49].

During preliminary testing, the fibula demonstrated failure independent of the tibia and caused rotation of the entire specimen due to the fibula's eccentric location relative to the tibia. As the roller descended, pressure on the fibula caused rotation of the bone along its long axis affecting the measured strain values. To remove these effects the fibula was excised prior to testing in both plated and control bones. A notched central roller was used to prevent rotation during force application.

Both right plated and left control tibiae were tested to complete failure. The specimens retrieved from testing were photographed in two planes corresponding to the AP and lateral radiographic projections. The fracture configuration was characterised by the nature of the fracture (spiral, oblique, and transverse), location (relationship to screw holes) and the extent of comminution (defined as the number of pieces). Plate failure was judged in terms of the mode of failure – ductile or brittle depending on the extent of plastic deformation, location of failure (relationship to screw holes) and the number of fragments.

Measured data during testing included the axial loading force (Newtons) and the displacement of the central roller measured at 10msec intervals. This data was used to construct load-displacement curves (Figure 2.17). The ultimate load (N) was calculated as the maximum load to failure which was derived from the peak of the curve. To determine the flexural stiffness (N/sec) of the specimen, a tangent was constructed along the linear elastic region of the curve. The gradient of this tangent was calculated to determine the flexural stiffness.

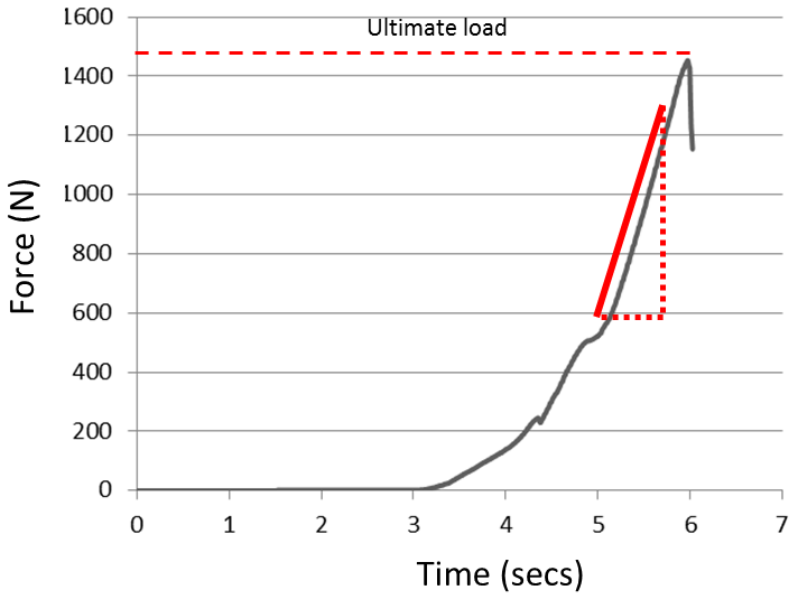


Figure 2.17 Load – displacement curve for a left control tibia retrieved at 52 weeks. The ultimate load was measured at the peak of the curve when failure occurred. The flexural stiffness of the bone (N/sec) was calculated from the gradient of a tangent constructed along the linear part of the curve.

The measured outcomes of ultimate load and flexural stiffness for the plated bones were normalised relative to the same outcomes in the respective control bones to enable statistical analysis of different groups using the below equations.

$$\text{Normalised Ultimate Load (NUL)} = \frac{Plated\ bone\ ultimate\ load\ (N)}{Control\ bone\ ultimate\ load\ (N)} \text{ x } 100$$

$$\text{Normalised Flexural Stiffness (NFS)} = \frac{Plated\ bone\ flexural\ stiffness(N/mm)}{Control\ bone\ flexural\ sstiffness\ (N/mm)} \text{ x } 100$$

These normalised outcomes exist as percentage functions with values greater than 100 indicating that the measured parameter is greater in the plated bone than in the control bone.

2.7.6 Mechanical testing of in vitro samples

Following early failure of the composite plate when used to fix the experimentally created osteotomy, in vitro experiments were undertaken to evaluate the relative mechanical properties of the composite plates, metal plates and the rabbit tibia. To determine the independent mechanical properties of the plates and the tibiae alone, different plate and cadaveric tibiae specimens were subjected to flexural testing (see Table 2.2). The mechanical properties of the composite plate and a similarly dimensioned plate made from PLA polymer alone were compared during testing. To investigate the potential effects of in vivo degradation on the two types of plate, samples of both plates underwent in vitro degradation in physiological saline at 37°C for 6 weeks. These samples were then mechanically tested to determine the effects of *in vitro* degradation on their mechanical properties. To aid comparison with the *in vivo* experiments, the metal plates were also tested in isolation.

Five groups of cadaveric bone specimens harvested from New Zealand White rabbits were tested as part of the *in vitro* tests (Table 2.2). In four cadaveric tibiae, the fibula bone was detached and the tibiae and fibula bones were tested individually to determine their mechanical properties. Three cadaveric tibiae had screw holes drilled using the custom made jig from the *in vivo* study. The screw holes were filled with metal screws used in the in vivo experiments to determine the influence of screws in the absence of a plate on the bones' mechanical properties. Two groups consisting of three cadaveric tibiae were plated with the composite and metal plates respectively and mechanically tested. This was undertaken to investigate the effect of plate application on the bone-plate construct's combined mechanical characteristics immediately following surgery before any structural bone changes could occur. The orientation of the specimens, span length between rollers and the displacement rate were the same as for the *in vivo* plated and control bones. The ultimate load to failure and the flexural stiffness were calculated from the load-displacement curves in the same manner.

Specimen	Number of samples
Composite plate	8
Composite plate – degraded*	3
PLA polymer plate	3
PLA polymer plate – degraded*	3
Metal plate	3
Fibula	4
Bone	4
Bone + screw holes	3
Bone + composite plate	3
Bone + metal plate	3

Table 2.2 Table showing numbers and types of plates and tibiae (bone) mechanically tested under the same testing conditions as the in vivo plated and control bones.*The degraded composite and PLA plates were degraded in physiological saline at 37 degrees for 6 weeks[117].

2.7.7 Micro Computed Tomographic Imaging

The composite plated bones and their respective controls were scanned using micro computed tomography (Micro CT) to quantitatively analyse cross sectional structural changes in these specimens. Early scans demonstrated significant artefact from the presence of the metal screws. This precluded the use of this imaging modality to assess the metal plated specimens. In the composite specimens, the screws had to be removed to enable analysis. The Micro CT analysis was conducted after mechanical testing in the specimens destined for mechanical testing. Analysis of retrieved specimens demonstrated bone growth over the screws which would have to be excised if the screws were to be removed prior to mechanical testing. The removal of this newly formed bone and the need for subsequent screw reinsertion prior to mechanical testing would likely influence the results of mechanical testing.

The images from the Micro CT analysis were saved as Dicom files and analysed using a dedicated program (ImageJ[203] , U. S. National Institutes of Health, Bethesda, Maryland, USA). Axial image slices were generated as a stack of images and viewed in ImageJ with the image resolution varying from a voxel thickness of 0.213mm to 0.06 mm. The lower resolution enabled axial images of the whole bone whereas the higher resolution permitted analysis of the shorter mid plate region. Two levels were

chosen for structural measurements in the composite plated bones and their respective control bones. Level 1 corresponded to the plate periphery and the axial image was selected mid-way between the 1st and 2nd screw holes in the composite plate. The distance of this axial slice from the tip of the bone enabled appropriate selection of the corresponding axial image in the control bone to generate comparative measurements. The Level 2 axial image was selected as the axial slice through the middle of the plate equidistant between the central two screws.

Three geometric parameters were measured on each axial slice – (a) the cortical thickness; (b) the cortical bone area and (c) the cross sectional bone area. The cortical thickness was measured as the bone thickness perpendicular to the plate under the mid-point of the plate on the axial image (Figure 2.18a) and on the corresponding axial slice in the control bone (Figure 2.18b). The cortical bone area was measured as the area of bone in a 2mm x 4mm rectangular region of interest lying parallel to and centred immediately beneath the plate (Figure 2.18c) and in an equivalent region in the control bone. The cross sectional bone area was measured as the total bone area of the on the selected axial image for the composite (Figure 2.18d) and the control bones. Bone area was measured by selecting the appropriate region of interest and using an automated thresholding tool (BoneJ)[204] to isolate the bone from the plate and surrounding soft tissues.

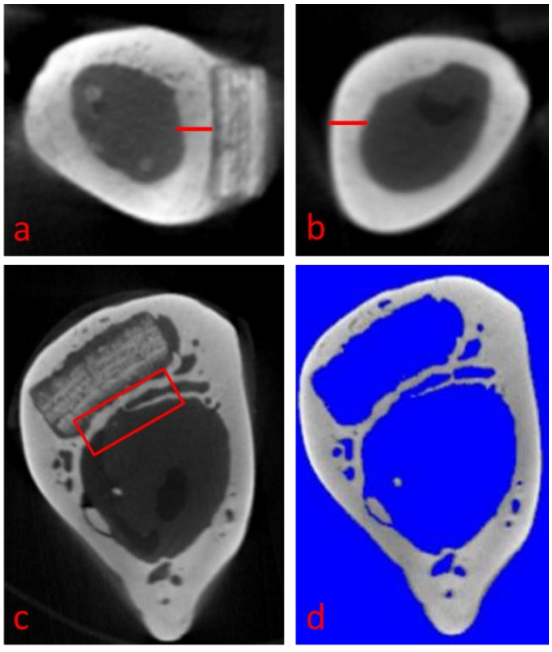


Figure 2.18 Micro CT images and measurements. Axial image slices were taken of both the composite plated bone (a) and control bone (b) to measure the cortical thickness (red) (composite plated and control bone level 1 images at 2 weeks). (c) The cortical bone area was measured in a 2cm x 4cm rectangular region of interest beneath the plate. The axial image was thresholded (d) to remove the plate silhouette and any soft tissue to enable calculation of the total bone cross sectional area (composite plated bone level 2 section at 26 weeks).

To enable direct comparison of these geometric parameters from the three pairs of bones retrieved from each time point, normalised outcome measures were derived. As before, these normalised outcomes were calculated by expressing each outcome in the plated bone as a percentage of the same measurement in the respective control bone. These normalised values were calculated for each of the measurements at the two levels. The equations for deriving these three normalised outcomes are shown below.

$$\text{Normalised Cortical Thickness (NCT)} = \frac{Plated\ bone\ cortical\ thickness\ (mm)}{Control\ bone\ cortical\ thickness\ (mm)} \times 100$$

$$\text{Normalised Cortical Area (NCA)} = \frac{Plated\ bone\ cortical\ area\ (mm2)}{Control\ bone\ cortical\ area\ (mm2)} \times 100$$

$$\text{Normalised Bone Area (NBA)} = \frac{Plated\ bone\ cross\ section\ area\ (mm2)}{Control\ bone\ cross\ section\ area\ (mm2)} \times 100$$

2.7.8 Histology

All of the retrieved composite plated and metal plated bones and their respective controls were fixed in 10% neutral buffered formalin (NBF) for a minimum of 12 weeks. To enable a sample size of n=3 at each of the time points, the plated and control bones from one of the rabbits used for mechanical testing were retrieved and fixed in NBF for a minimum of 16 weeks. Increased fixation time was required as the samples retrieved from mechanical testing had not undergone prior perfusion fixation at the time of retrieval.

Each composite and metal plated tibia was cut in to blocks using a diamond circular saw. All of the blocks were approximately 5mm thick and generated from transverse sections at specific levels (see Figure 2.19). Three blocks were taken per bone to sample different regions in the plated section of the bone. From each bone, two blocks corresponding to Level 1 and Level 2 were destined for resin embedding and analysis with scanning electron microscopy (SEM) (Figure 2.19). These two levels

corresponded to the same named levels in the Micro CT experiments. The level 1 block corresponded to the plate periphery and was sampled between the first and second screws. The level 2 block corresponded to the plate mid-section and was taken from the plated region between the central two screws. A further block was taken adjacent to this for paraffin embedding and characterisation of inflammatory changes. In the metal plated bones and their controls, this block was only taken from the rabbits at the earlier three time points of 2, 6 and 12 weeks. In the composite plated bones and their controls, these blocks were taken from rabbits at every time point. The sectioned bone and the thickness of each block were measured. These measurements were used to generate analogous blocks from the respective control bone in terms of location and thickness.

To determine the magnitude of any potential sampling error between the location of these bone blocks in the plated and control bones, the distance from the tip of the bone to each bone block was measured. To enable comparison of the sampling location between different animals, the distance of the bone block from the tip of the bone was expressed as a percentage function of the total bone length using the below equation.

$$\text{Distance index (DI)} = \frac{Distance\ from\ tip\ of\ bone\ to\ bone\ block\ (mm)}{Total\ bone\ length\ (mm)} \times 100$$

Each of the blocks was photographed to enable specimen identification and aid orientation during processing. Each block was placed in a labelled cassette and fixed in NBF for a further two weeks.

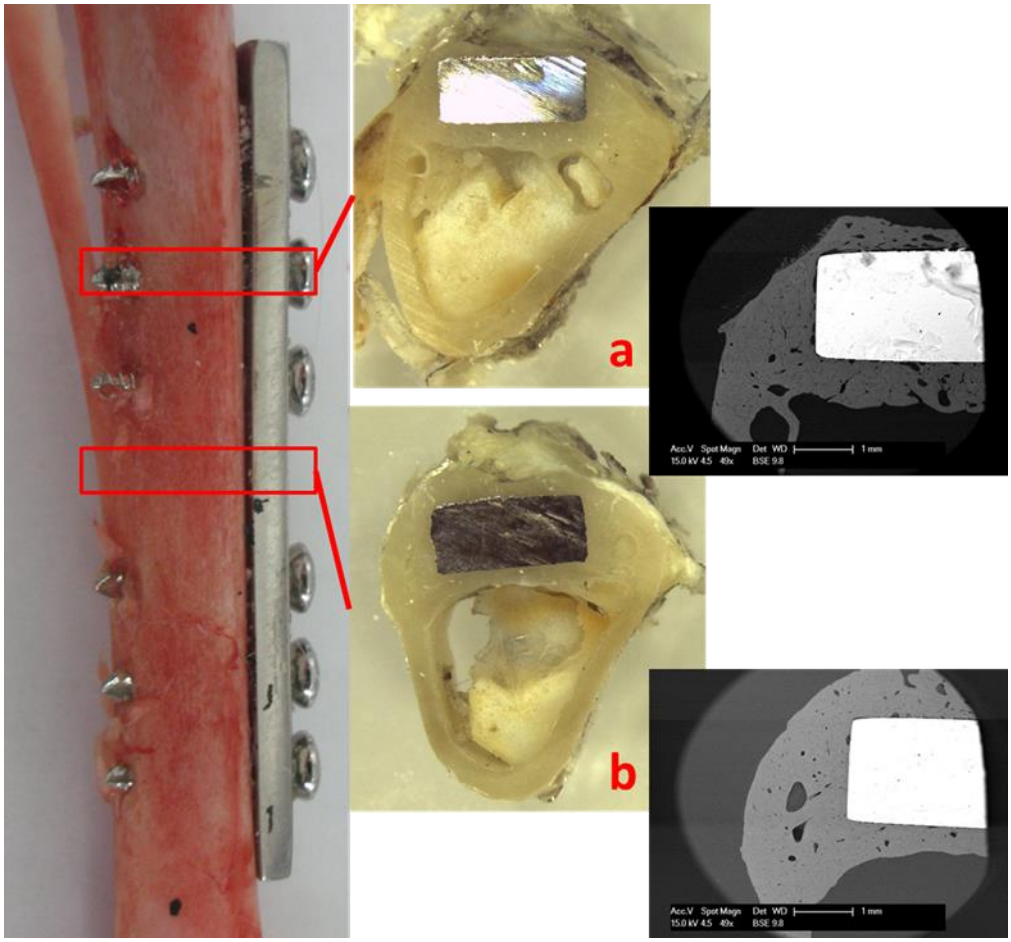


Figure 2.19 Cadaveric tibia (left) with attached metal plate demonstrating bone block location corresponding to level 1 (top - plate periphery) and level 2 (bottom - plate mid-section). Photographs (obj x10) of bone blocks from level 1(a) and level 2(b) are shown for a metal plated bone retrieved at 52 weeks (specimen 52MD) with inset scanning electron microscopy images of the prepared sections (obj x80).

2.7.9 Resin embedding

The steps undertaken to prepare the blocks for SEM analysis are outlined below in Figure 2.20. The blocks were embedded in Technovit 7100 resin prior to surface preparation and carbon coating. Technovit 7100 was selected due to its setting time, handling characteristics and sectioning properties.

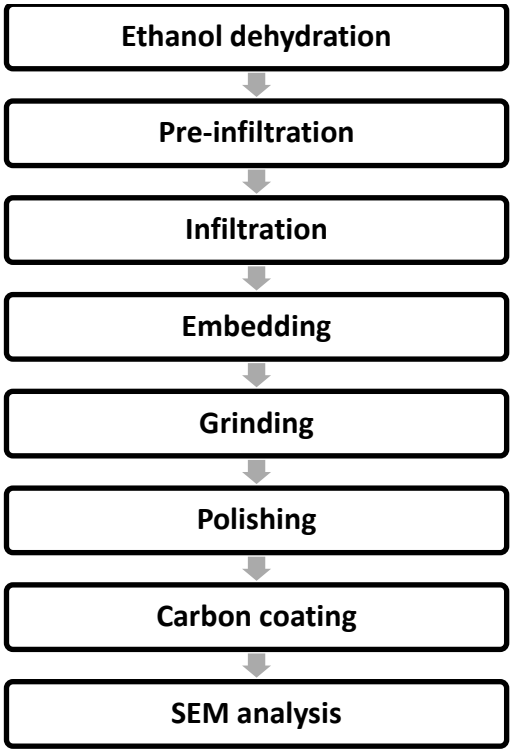


Figure 2.20 Steps in processing of level 1 and 2 blocks for SEM analysis.

The blocks were stored in cassettes and sequentially dehydrated in an increasing concentration of ethanol in a 1:10 ratio of specimen to solution (Table 2.3). Each block was transferred to a labelled vial. Pre-infiltration solution was made up from equal volumes of Technovit 7100 base solution and 100% ethanol. In a ventilated environment, four to five ml of solution was pipetted into each vial and the vials transferred to a rotator for 48 hours. Infiltration solution was prepared from dissolving 1g of Hardener 1 in 100ml of Technovit base solution. The blocks were transferred to new vials each filled with 4-5 ml of infiltration solution and placed on a rotator for a further 48 hours.

Ethanol concentration	Duration
70% ethanol	24 hours
90% ethanol	24 hours
100% ethanol	72 hours
100% ethanol	48 hours

Table 2.3 Dehydration protocol for level 1 and 2 blocks prior to resin embedding.

Once infiltrated, the blocks were transferred to their respective moulds. Photographs of the specimens were used to aid orientation and identify the corresponding cortices in the control specimens. Resin solution was prepared by mixing 45 ml of infiltration solution with 3ml of Hardener 2. The moulds were filled with resin solution, covered with stubs and left to polymerise over 48 hours in a ventilated environment. The embedded blocks were mounted on stubs and ground using SiC paper – 800 grit and then 1200 grit, to expose the surface of the specimen. The blocks were then polished using a soft cloth with 6um diamond paste followed by 1um diamond paste. The polished blocks were then carbon coated under vacuum.

2.7.10 Scanning Electron Microscopy analysis

The specimens were analysed using an XL30 scanning electron microscope. The instrument settings are shown in Table 2.4.

Parameter	Setting
Mode	Backscatter
Beam energy	15Kv
Spot size	4.0-4.7
Working distance	10cm
Contrast	90-98
Brightness	15-30

Table 2.4 Instrument settings for XL30 Scanning Electron Microscope.

Two geometric parameters were measured at each level analogous to the measurements in the Micro CT experiments– (a) the cortical thickness and the (b) cortical bone area beneath the plate. The cortical thickness was measured as the bone thickness perpendicular to the plate under the mid-point of the plate on the SEM image (Figure 2.21a). The cortical bone area was measured as the area of bone in a 2mm x 4mm rectangular region of interest lying parallel to and centred immediately beneath the plate (Figure 2.21b). Normalised outcomes were calculated from these two measurements in the plated and control bones analogous to similar normalisation of the datasets from the MicroCT experiments. The Normalised Cortical Thickness (NCT) was calculated from the cortical thickness measurements and the Normalised

Cortical Area (NCA) from the cortical area measurements in the plated and control bones using the below equations.

$$\text{Normalised Cortical Thickness (NCT)} = \frac{Plated\ bone\ cortical\ thickness\ (mm)}{Control\ bone\ cortical\ thickness\ (mm)} \times 100$$

$$\text{Normalised Cortical Area (NCA)} = \frac{Plated\ bone\ cortical\ area\ (mm2)}{Control\ bone\ cortical\ area\ (mm2)} \times 100$$

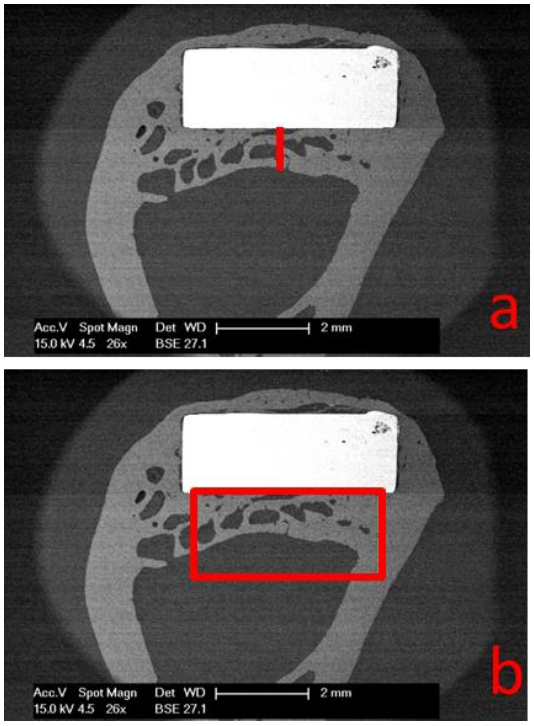


Figure 2.21 Measurement of cortical thickness and bone area beneath the plate (metal plated tibia at 52 weeks, obj x 26). (a) Cortical thickness was measured by constructing a perpendicular line (red) to the midpoint of the plate cross section. (b) The bone area beneath the plate was measured by constructing a 2mm x 4mm region of interest (red box) directly abutting and parallel to the plate under-surface and centred on the mid-point of the plate cross section. This region of interest was thresholded to highlight bone alone and the bone area was measured.

2.7.11 Paraffin embedding and histological staining

The plate mid-section blocks from the composite and metal plated bones and their respective control bones were decalcified in ethylene-di-nitrilo-tetra-acetic acid (EDTA) solution for six to eight weeks. Successful decalcification was confirmed with radiography (see Figure 2.22). Prior to embedding, both the composite and

metal plates were removed from their respective blocks to enable further processing. The composite plates would have degraded during processing causing artefacts and were thus removed by immersion in chloroform for one hour. Retention of the metal plates would not permit sectioning on the microtome necessitating their removal. The blocks were dehydrated and embedded in paraffin wax using a Citadel Tissue Processor with a carousel arrangement of sequential immersion in different solutions (Table 2.5).

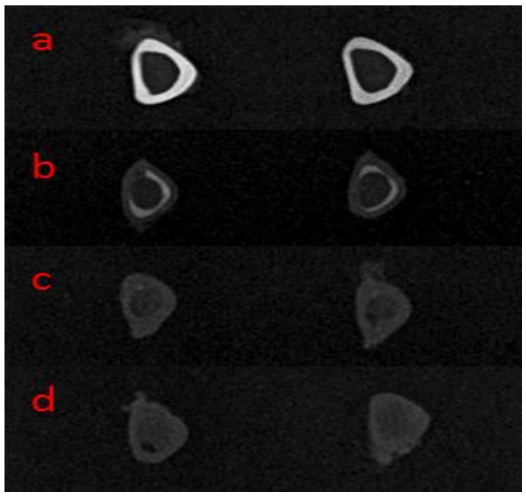


Figure 2.22 Radiographs of trial tibial blocks decalcified for (a) 0 weeks, (b) 2 weeks, (c) 4 weeks and (d) 6 weeks. Radiodensity reflecting calcium content progressively attenuated with complete decalcification at 6 weeks.

Order	Solution	Duration (minutes)
1	Water	1
2	Water	1
3	50% Ethanol	180
4	70% Ethanol	180
5	90% Ethanol	180
6	100% Ethanol	180
7	100% Ethanol	180
8	Xylene and 100% ethanol (ratio 1:1)	180
9	Xylene	120
10	Xylene	120
11	Paraffin wax	150
12	Paraffin wax	150

Table 2.5 Block dehydration and paraffin wax embedding protocol

The embedded blocks were sectioned at a thickness of 5 micrometers using a microtome (HM 325, MICROM). The sectioned paraffin ribbons were floated in a 35°C water bath, mounted on to slides (Surgipath®, Leica) and dried on a hot plate for 12 hours. Xylene was used to remove the wax. The slides were rehydrated in decreasing concentrations of ethanol (see Table 2.6) and stored in deionised water until staining.

Order	Solution	Duration (minutes)
1	Xylene	7
2	Fresh xylene	7
3	100% Ethanol	2
4	100% Ethanol	2
5	50% Ethanol	2

Table 2.6 Slide rehydration protocol

Two commercially available stains were used to characterise inflammatory changes and bone structural changes. The stained slides were then sequentially dehydrated (Table 2.7) and mounted with coverslips using DPX mountant.

Order	Solution	Duration
1	Deionised water	30 seconds
2	50% Ethanol	30 seconds
3	100% Ethanol	30 seconds
4	100% Ethanol	30 seconds
5	Xylene	2 minutes

Table 2.7 Slide dehydration protocol

2.7.12 Giemsa staining

The Romanowsky based Giemsa stain contains methylene blue which highlights basophilic structures such as the nuclei in varied hues of blue while the eosin counterstains acidophilic structures orange-red. Neutrophilic elements are stained by both producing a pink coloration. The staining steps are shown in Table 2.8.

Order	Solution	Duration
1	Giemsa azure eosin methylene blue solution	15 minutes
2	0.1 % acetic acid	10 seconds
3	Deionised water	10 seconds

Table 2.8 Giemsa staining protocol

2.7.13 Tartrate-resistant Acid Phosphatase (TRAP) staining

This stain is directed at osteoclastic acid phosphatase activity. It works on the basis of the Naphthol AS-BI phosphoric acid (NABPA) acting as a substrate which is hydrolysed by acid phosphatases. Hydrolysis of the NABPA induces coupling with the chromogen (Fast garnet GBC salt) which precipitates as a maroon coloration at the sites of acid phosphatase activity. Selective acid phosphatase activity is highlighted by tartaric acid mediated inhibition of all subtypes with the exception of isoenzyme 5 of acid phosphatases. This isoenzyme is predominantly found in osteoclasts which defines the specificity of the staining. Osteoclastic activity acts as a phenotypic marker of bone remodelling. The components of the stain (Table 2.9) were stirred for 30 seconds and then filtered (Whatman No 1 filter). The filtrate was warmed to 37°C and the slides were incubated in the stain in darkness for 60 minutes. They were then rinsed in deionised water for 3 minutes followed by immersion in acid haematoxylin for 3 minutes. Once dry, the slides were mounted with coverslips.

Reagents	Volume (ml)
Deionised water, (pre-heated to 37°C)	44.0
Acetate solution	2.0
Naphthol AS-BI phosphoric acid	2.0
Tartrate solution	2.0

Table 2.9 Trap stain reagent composition

2.7.14 Slide analysis

The stained slides were analysed using a Leica DM4000 B LED light microscope and Surveyor Software (Objective Imaging). Giemsa stained slides were inspected for inflammatory cells with morphology characteristic of neutrophils and macrophages. Characterisation was aided by referencing a histology atlas. Upon staining, neutrophils demonstrate lobulated nuclei with light pink cytoplasm (Figure 2.23). Macrophages are typically larger cells which stain less intensely with a pale greyish blue cytoplasm (Figure 2.23). The relative numbers of these cell types were quantified for a specific region of interest. In the plated tibiae, this was the interface tissue between the plate and outer cortical bone (Figure 2.24). In the control bones, the equivalent region was the overlying periosteum on the medial cortex. The depth of the region of interest was three cell layers thick from the outer periosteal surface.

Method development of the TRAP staining protocol demonstrated acid phosphatase activity occurring diffusely in the vicinity of clusters of cells rather than within specific cells (see Figure 2.25). The maroon staining was not reproducible on staining different slides from the same block. However, the TRAP stained slides demonstrated satisfactory visualisation of the osteonal architecture of the bone. These slides were used to qualitatively assess the structural changes occurring in the plated bones.

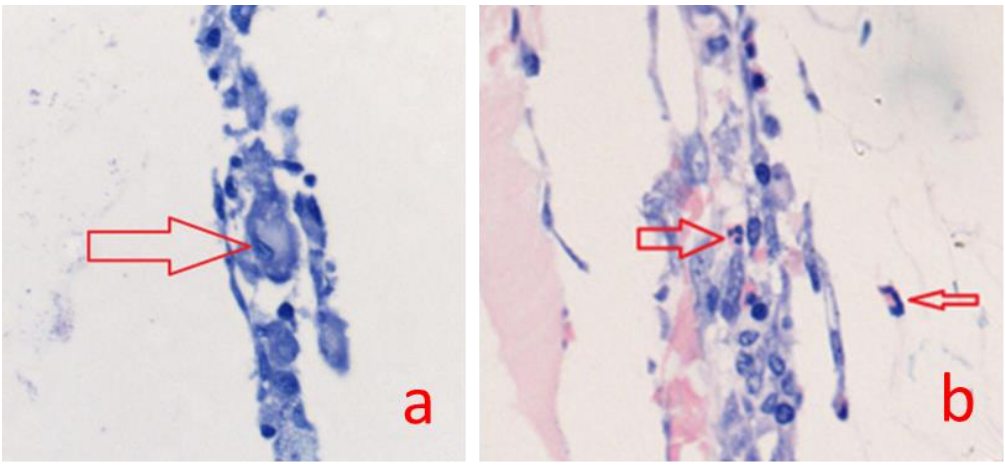


Figure 2.23 Photomicrographs demonstrating cells with morphological characteristics of a macrophage (a) and neutrophils (b) with Giemsa staining (composite plated sample interface tissue, retrieved after 2 weeks, obj.x40).

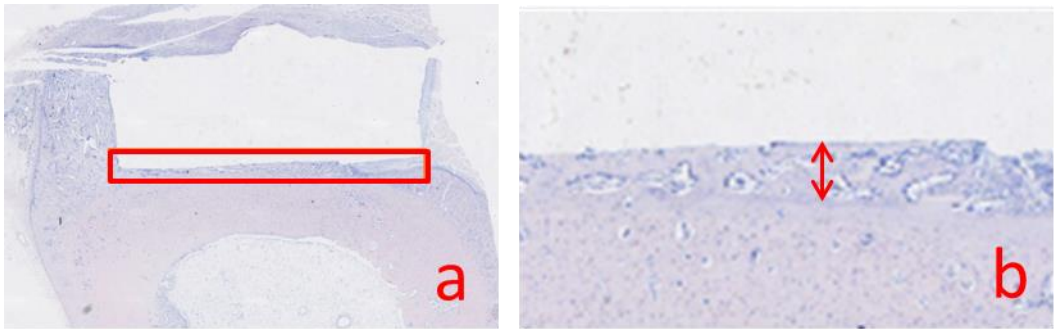


Figure 2.24 Region of interest (ROI) for inflammatory cell quantification. (a) Photomicrograph at low magnification highlighting ROI (red box) between composite plate and bone. (b) Photomicrograph at higher magnification demonstrating interface tissue (red arrow) between outer cortical bone and site of plate (Giemsa stain, metal plated right tibia retrieved at 6 weeks).

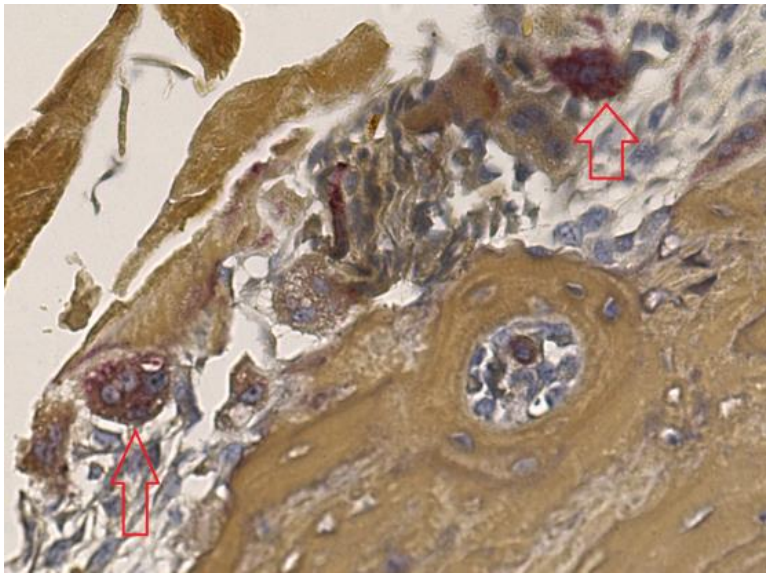


Figure 2.25 Photomicrograph demonstrating pockets of TRAP activity around cell clusters from a composite plated tibia retrieved at 6 weeks (TRAP stain, obj x 40).

2.8 Statistical analysis of normalised outcomes

The study design sought to compare the outcomes of the composite plated samples with the metal plated samples at each time point in the experiments. To enable comparison of different sized animals in these two study groups, normalisation of each outcome variable was performed by expressing the absolute value for each outcome for a plated bone as a relative percentage of the opposite control bone in the same animal. These normalised outcomes for each experiment comparing the two types of plate are shown in Table 2.10. Although the analysis was primarily comparing the two types of plate with respect to the outcomes, other variables of interest were included in the statistical analysis. The duration of implantation was included as a variable to investigate the stress shielding changes in the plated bone as a function of time. In the Micro CT and SEM experiments, cortical thickness and area were measured in two distinct regions. Normalised values of cortical thickness and cortical area were derived at the plate periphery (level 1) and the plate mid-section (level 2) enabling statistical analysis of theorised differences in the stress shielding response along the plated region of bone.

Each measured normalised outcome had at least two independent variables or factors of interest requiring investigation (Table 2.10). In all analyses, the factors of interest included the type of plate, the duration of implantation and, in the Micro CT and SEM experiments, the level of sampling. These three factors were categorical variables and the various categories for each variable are shown in Table 2.11. All of the calculated normalised outcomes were expressed as percentages and were thus continuous variables. To investigate the influence of these factors on the outcomes, analysis of variance tests (ANOVA) were undertaken after discussion with a Biomedical Statistician from the Research Design Service (University of Nottingham). In three of the experiments (plain radiographs, Micro CT and mechanical testing), there were only two factors of interest and a two way ANOVA test was undertaken. The two way ANOVA was used to determine if an interaction effect existed between the two factors on the normalised outcomes. Taking the example of the normalised cortical thickness (NCT) in the radiography experiments, it was important to determine: (a) whether the normalised cortical thickness was

higher in the composite plated bones compared with the metal plated bones; and (b) whether the normalised cortical thickness for the two types of plate differed at each of the timepoints i.e. did an interaction effect exist between these two factors. A statistically significant interaction effect would suggest that the two types of plates demonstrated different effects on the normalised cortical thickness at different durations of implantation. In the Micro CT experiments, outcomes were not measured in the metal plate group. Consequently, the type of plate could not be included as a factor in this analysis. The two way ANOVA investigated the duration of implantation and the sampling location as the two factors. Similarly, in the mechanical testing experiments, the level of sampling was not a factor in the experiment design. The two way ANOVA analysis investigated the influence of the type of plate and the duration of implantation as factors influencing the outcomes of mechanical testing.

In the SEM experiments there were three factors under investigation - the type of plate, the level of sampling and the duration of implantation. Therefore, a three way ANOVA (analysis of variance) was undertaken to assess whether there was a statistically significant interaction effect between the three factors on the normalised outcomes. The level of significance was set at $p<0.05$. All statistical analysis was undertaken using dedicated statistical software (IBM SPSS Statistics, version 24. Armonk, NY:IBM Corp).

Factor (independent variable)	Categories
Type of plate	• Composite plate • Metal plate
Duration of implantation	• 2 weeks • 6 weeks • 12 weeks • 26 weeks • 52 weeks
Sampling location	• Level 1 – plate periphery • Level 2 – plate centre

Table 2.11. Table showing the three factors (independent variables) and their respective categories

Experiment	Outcomes (Dependent variables)	Factors (independent variables)	Statistical tests
Plain radiographs	• Normalised Cortical thickness (NCT)	• Type of plate • Duration of implantation	• Two way ANOVA – NCT
MicroCT	• Normalised Cortical Thickness (NCT) • Normalised Cortical Area NCA) • Normalised Bone Area (NBA)	• Duration of implantation • Level of sampling	• Two way ANOVA- NCT • Two way ANOVA – NCA • Two way ANOVA - NBA
Scanning electron microscopy (SEM)	• Normalised Cortical Thickness (NCT) • Normalised Cortical Area (NCA)	• Type of plate • Duration of implantation • Level of sampling	• Three way ANOVA – NCT • Three way ANOVA - NCA
Mechanical testing	• Normalised Ultimate Strength (NUS) • Normalised Flexural Stiffness (NFS)	• Type of plate • Duration of implantation	• Two way ANOVA – NUS • Two way ANOVA - NFS

Table 2.10. Table showing the Outcomes (dependent variables) for each set of experiments, the corresponding Factors (independent variables) under investigation and the statistical tests used. The normalised outcomes were derived by expressing the experimental measurements as a percentage function of the same variable in the opposite control bone. The factors were the independent variables of interest that were investigated to determine their effect on the outcomes. Analysis of variance (ANOVA) tests were undertaken to assess the influence of these variables on the outcomes. In experiments where there were two dependent variables (radiographs, MicroCT and mechanical testing), two way analysis of variance testing was performed. In the scanning electron microscopy experiments, there were three factors requiring three way analysis of variance testing.

There are 6 assumptions that need to be satisfied before undertaking ANOVA analysis. Three of the assumptions were satisfied by the study design -(1) The dependent variables were measured on a continuous scale; (2) The factors or independent variables under investigation were categorical variables and (3) there was independence of observations when grouping the outcomes for each factor i.e. each measurement of an outcome did not occur in more than one group. Once the outcomes were measured and analysed, analysis of the residuals was undertaken to test the remaining three assumptions of the ANOVA test. These assumptions are that in each cell of the study design there should be no significant outliers (4); the dependent variables should be approximately normally distributed (5) and that the variance of each dependent variable should be equal (6).

Outliers were assessed by inspection of boxplots of each cell in the study design. It was anticipated that the boxplots would not reveal any outliers due to the limited sample size for each type of plate at each time point of investigation. Normality was assessed for each cell of the study design using Shapiro-Wilk's normality test ($p>0.05$). Due to the small sample size in each cell of the study design, it was anticipated that normality testing would show that the data in some cells was not normally distributed. After discussion with the statistician, it was decided to conduct the ANOVA irrespective of this result, as the measured variables could be assumed to be normally distributed in a large enough sample size and ANOVA tests are considered fairly "robust" to deviations from normality[205]. Homogeneity of variances between different cells in the same study design was assessed using Levene's test ($p>0.05$). If the assumption of homogeneity of variances was violated, the analysis was still undertaken if there was normality of the data sets and the ratio of the largest group variance to the smallest group variance was less than 3 as the ANOVA can be considered "robust" to heterogeneity of variances in these circumstances[206].

In each ANOVA test, analysis was conducted to see if there was a statistically significant interaction effect between the factors. If no significant interaction effect was detected, simple main effects and pairwise comparisons were performed to determine if there was a statistically significant effect of the independent variables when comparing different cells in the ANOVA design. When multiple pairwise

comparisons were undertaken, p values were adjusted with a Bonferroni correction to detect statistical significance.

The current study design did not enable a sample size calculation before undertaking the experiments as the relative difference in outcomes when comparing the composite group to the metal group were unknown. Post hoc sample size calculations were undertaken using the means and standard deviations of the normalised outcome measures for the two groups. The sample size calculations were based on achieving statistical significance when comparing the observed outcomes in the two plate groups. The specific outcomes and four group comparisons used in the sample size calculations are shown in Table 2.12. The time point for comparison was selected as 52 weeks as theorised progressive changes in the mechanical and structural properties of the plated bones would be most manifest at the final time point. In the scanning electron microscopy experiments, the theorised stress shielding changes in bone would be most manifest in the plate mid-section (level 2) compared with the plate periphery (level 1) and outcomes at this level were used for the sample calculation. Calculations were based on a yielding a sample size with 80% power and significance set at 5% using dedicated software (IBM SPSS Sample Power 3.0. Armonk, NY:IBM Corp).

Experiment	Outcome measure	Group 1	Group 2
Scanning electron microscopy	Normalised cortical thickness (NCT)	Composite plated group NCT – level 2 (52 weeks)	Metal plated group NCT – level 2 (52 weeks)
Scanning electron microscopy	Normalised cortical area (NCA)	Composite plate group NCA – level 2 (52 weeks)	Metal plated group NCA – level 2 (52 weeks)
Mechanical Testing	Normalised ultimate load (NUL)	Composite plated group NUL (52 weeks)	Metal plated group NUL (52 weeks)
Mechanical testing	Normalised flexural stiffness (NFS)	Composite plated group NFS (52 weeks)	Metal plated group NFS (52 weeks)

Table 2.12. Table showing group comparisons for the four post hoc sample size calculations undertaken following data collection. Calculations were undertaken comparing the normalised outcomes from the composite and metal plated groups at 52 weeks.

Chapter 3 Results

3.1 In vivo plating of osteotomised rabbit tibia

Three hours after the completion of the experiment, the rabbit was found to be lame. Examination of the rabbit revealed a flail right leg. A radiograph confirmed plate failure through the third screw hole of the plate (Figure 3.1). In view of the short time to failure, the decision was made to discontinue further experiments in the osteotomy model using the composite plate. The animal was humanely euthanased by an overdose of intravenous phenobarbitol.

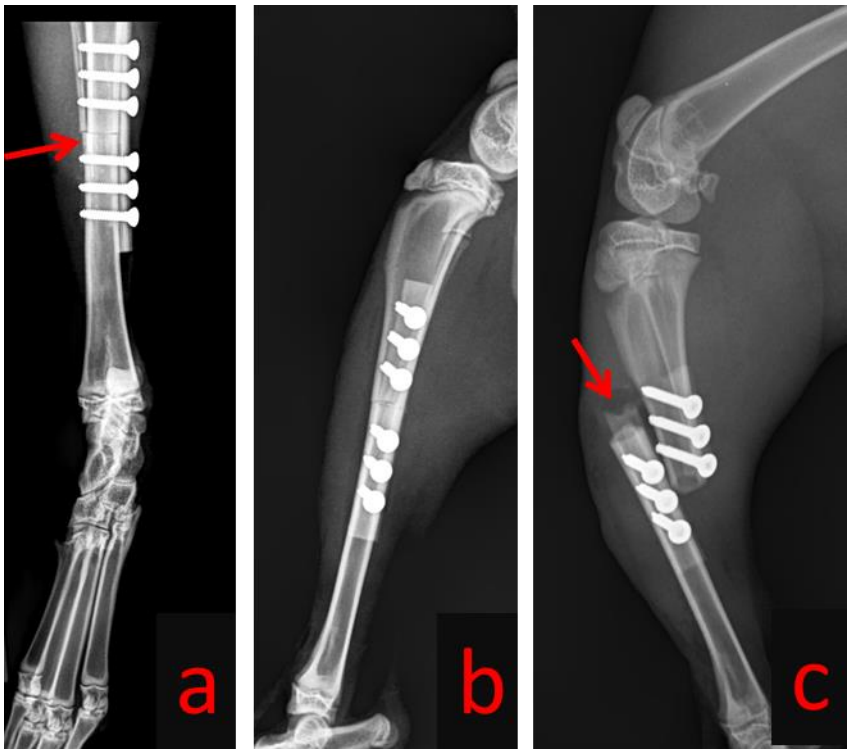


Figure 3.1 Radiographs of osteotomised tibia fixed with the composite plate. AP (a) and lateral (b) views showing satisfactory bone contact at the osteotomy site (arrow) and alignment following plate fixation. (c) Lateral radiograph showing complete plate failure at the third screw hole in the plate (arrow) with marked angulation and shortening.

Post mortem retrieval of the plated bone demonstrated plate failure at the third screw hole which was nearest the osteotomy site (Figures 3.1c). The fracture ends of the plate demonstrated significant plastic deformation indicating a ductile mode of failure. Scanning electron microscopy of the retrieved plate demonstrated exposed phosphate glass fibres at the fractured ends with plate surface damage caused by the screw head (Figure 3.2). Longitudinal cross-sectional analysis of the plate (Figure 3.3) demonstrated delamination along the centre of the plate which extended away from the site of failure. In the centre of the plate, the unidirectional fibres were clearly defined indicating poor fibre-matrix bonding.

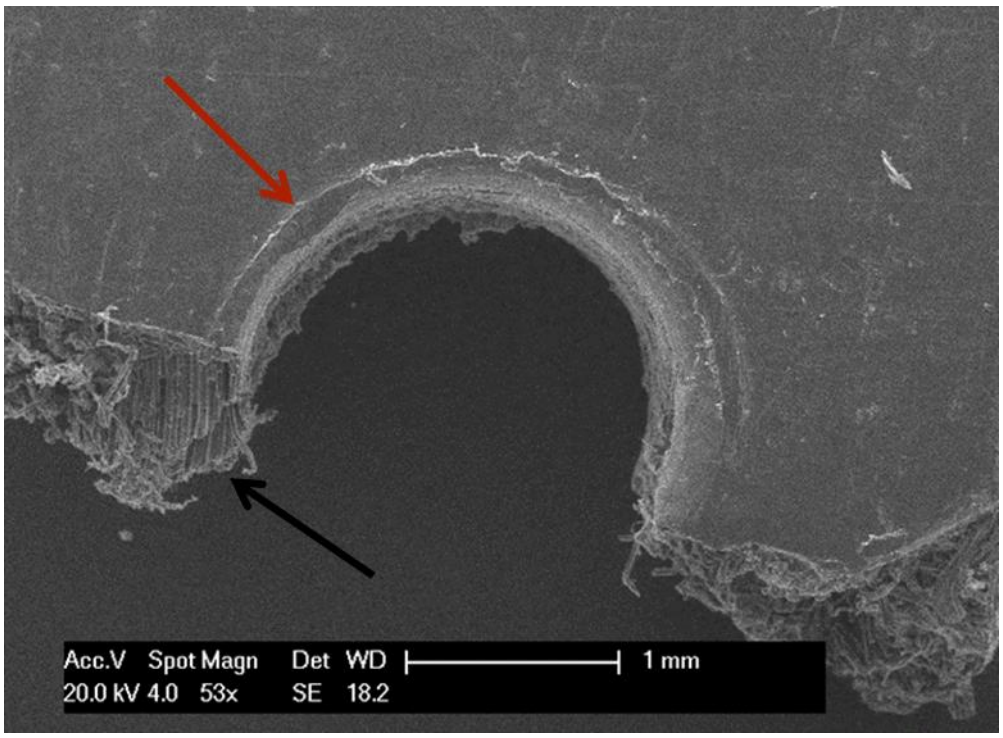


Figure 3.2. Scanning electron micrograph (obj x53) of the retrieved fractured plate from the osteotomy experiment showing the failure occurring at the screw hole. There was surface damage from the screw head (red arrow). The fractured end demonstrated well defined fibres suggesting fibre pull out and failure at the fibre-matrix interface (black arrow).

The theorised mode of failure based on the microscopy findings is that axial loading in the direction of the long axis of the plate resulted in buckling and delamination between the regions rich in matrix and phosphate glass fibres causing localised transition interfaces between regions with different mechanical properties. This

delamination can be seen in the centre of the plate on the microscopy images and extended to the fractured plate end. The separation of the composite layers occurring in the centre of the plate suggesting impaired strength of the fibre-matrix interface in the central region of the plate. The composite plate was manufactured by laying up the unidirectional fibre mats and PLA sheets and consolidating the laminate in a heated compressed mould. Poor fibre-matrix interactions in the centre of the plate indicate insufficient "wet-out" of these fibres leading to poor resistance of fibre-matrix interface to delamination. An important material property of metals is that they are isotropic i.e. the material mechanical properties remain unchanged irrespective of the direction of mechanical testing. In contrast, the laminar structure of the current plate created highly anisotropic mechanical properties. Although the longitudinal fibre arrangement may resist bending, the microscopy analysis demonstrated that axial loading caused relative shear between the longitudinal fibres leading to structural failure.

The diameter of the screw hole was 2 mm and the plate width was 5mm. Therefore, the cross sectional area between screw holes was $10mm^2$ while at the screw hole was $6mm^2$. Axial loading of the composite plated osteotomised bone would lead to plastic deformation and resulting delamination in the region of the plate closest to the osteotomy. The reduced cross sectional area at the screw hole and the delamination across the centre of the plate resulted in failure at this site.

The analysis of the retrieved failed composite plate from this experiment demonstrated significantly impaired mechanical properties of the fibre-matrix interface rather than direct failure of the composite material. Further in vitro experiments were conducted to investigate the mechanical properties of degraded and undegraded composite plates in comparison to PLA plates before and after degradation. This critical deficiency in the plate design leading to its early failure in the sole osteotomy experiment indicated that the current plate design could not be used as a fracture fixation device. Therefore, the study aims were revised to focus subsequent experiments on comparing the effects of the composite plate with respect to a metal plate on intact bone.



Figure 3.3. Stitched together scanning electron micrographs (obj x27) of the longitudinal cross section of the retrieved fractured plate from the osteotomy experiment. A clear interface is visible between the matrix rich region and the unidirectional fibre layers (red arrow). Individual unidirectional fibres are visible indicating poor wet out of the central fibres. There is a longitudinal split between the unidirectional fibres in this central region extending to the fractured end indicating poor fibre-matrix interface strength causing progressive delamination leading to failure.

3.2 In vivo plating of intact rabbit tibiae with the composite and metal plates

There were no intra-operative complications in any of the experiments where the composite and metal plates were applied to the intact tibia in the two arms of the comparative study. All rabbits demonstrated satisfactory weight gain post procedure. An animal monitoring log was completed daily for the first 2 weeks by the personal licence holder. Within a few hours of surgery, all rabbits were ambulating within their cages. Within a week, all rabbits were demonstrating weight bearing on their hind legs alone. It was difficult to judge the weight bearing status in the operated limb. However, within 4 weeks, the gait pattern of the operated rabbits was visually indistinguishable from the un-operated rabbits. Review of all post-operative radiographs confirmed satisfactory implantation of the composite plate (Figure 3.4).

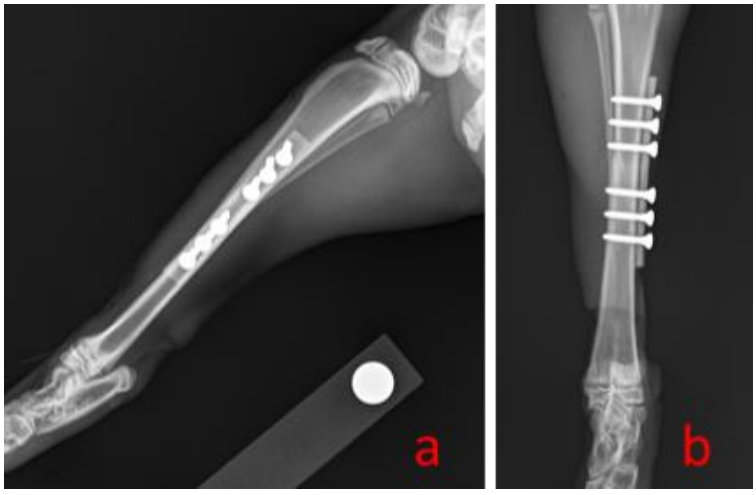


Figure 3.4 Post-operative radiographs of a composite plated tibia – (a) lateral radiograph, (b) AP radiograph

There were no infectious complications following surgery in any of the operated rabbits. Three rabbits sustained fractures within two weeks following surgery – two rabbits in the composite group and one rabbit in the metal group. In two of these rabbits (Figure 3.5), the fracture occurred close to the last screw hole at the narrowest region of the tibia bone. In the remaining rabbit, the fracture occurred in the pelvis on the operated side (Figure 3.6a). All of these rabbits were replaced in the experiments. One rabbit sustained a fracture of the heel bone prior to surgery (Figure 3.6b).



Figure 3.5 (a) Retrieved metal plated tibia and control bone demonstrating fracture close to the last screw. (b,c) AP and lateral radiographs demonstrating similar fracture pattern in a composite plated tibia. Both fractures occurred within two weeks of surgery.

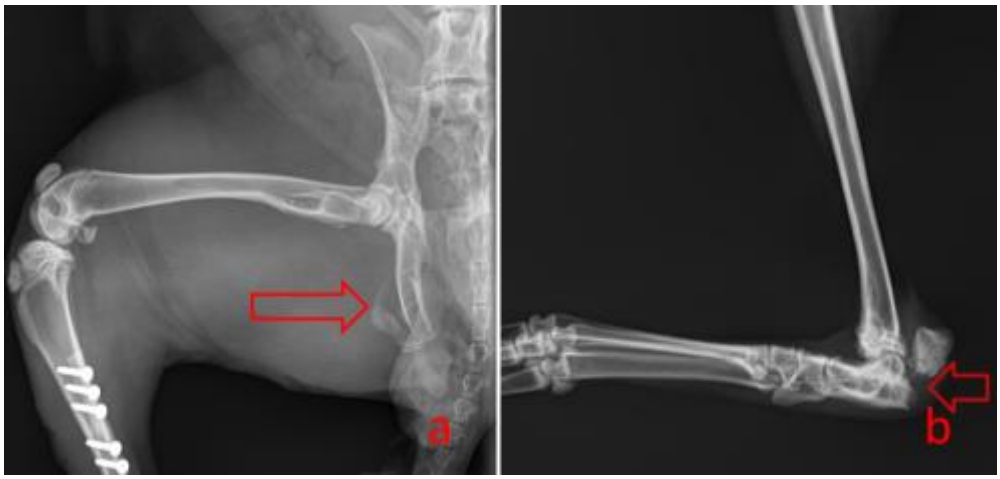


Figure 3.6 (a) AP radiograph showing fracture of the ischial tuberosity in the pelvis (red arrow) in a rabbit in the composite group. (b) Lateral radiograph of a heel fracture (red arrow) in an unoperated rabbit.

At the scheduled time points of sacrifice, the correct rabbits were identified using the three unique identifiers. The rabbits were euthanased by administering an overdose of intravenous anaesthetic. This was undertaken by an animal technician with a current personal licence for this procedure.

3.3 Imaging

3.3.1 Relative plate position at surgery and at retrieval

The mean tibia length increased from 101.6 mm at surgery to 109.2mm at 12 weeks (Table 3.1). There was no further increase at the subsequent time points suggesting that longitudinal bone growth slowed after 12 weeks. Radiographic evaluation revealed the proximal and distal tibia growth plates to be open at 2 and 6 weeks. There was radiographic evidence of progressive growth plate fusion from 12 weeks onwards (see Figure 3.7). The mean Plate Location Index (PLI) at the time of surgery was comparable for the different time point groups suggesting reproducibility of plate location during implantation. Comparing the mean PLI at surgery with the PLI at each of the time-points of sacrifice demonstrated a progressive increase indicating relative plate migration (Table 3.1). The mean PLI percentage increase between surgery and time of sacrifice was 0.56% at 2 weeks and increased to 3.89% at 52 weeks. Relative to the time of surgery, the mean change in the PLI was 3.89% compared with an increase in mean tibial length of 7.28% over the 52 week study period. This disparity may be explained by differential growth at the proximal and distal growth plates in the tibial bone leading to a change in the relative position of the plate with growth. The mean PLI at sacrifice did not change after 12 weeks in keeping with the cessation of growth. The mean PLI at sacrifice at each of the time points demonstrated small standard deviations indicating that the extent of plate migration was consistent among all plated bones at that time point. This supported the reproducibility of sampling based on pre-determined locations relative to the plate when comparing plated tibiae from different animals at the same time points of sacrifice.

Duration of implantation	Mean plated tibia length at surgery (mm) (±SD)	Mean distance from tip of tibia to plate at surgery (mm) (±SD)	Mean PLI - surgery (%)(±SD)	Mean plated tibia length at sacrifice (mm) (±SD)	Mean distance from tip of tibia to plate at sacrifice (mm) (±SD)	Mean PLI - sacrifice (%) (±SD)	Mean PLI change* (%) (±SD)
2 weeks	101.4 ± 3.4	25.4 ± 4.2	25 ± 4.1	105.2 ± 3	27.1 ± 3.7	25.8 ± 3.5	0.6 ± 1.2
6 weeks	101.3 ± 2.4	23.7 ± 3.4	23.4 ± 3.2	107.4 ± 3.7	28.1 ± 4.2	26.2 ± 3.6	2.7 ± 1.2
12 weeks	102.4 ± 2.5	25.4 ± 4.3	24.8 ± 4	109.2 ± 2.2	30.9 ± 4	28.3 ± 3.7	3.2 ± 1.1
26 weeks	102.4 ± 2.1	25.8 ± 1.7	25.3 ± 1.8	110 ± 3.8	31.2 ± 2.8	28.3 ± 2.1	2.8 ± 2.1
52 weeks	100.8 ± 2	23.6 ± 3.6	23.4 ± 3.5	109 ± 2.3	30.7 ± 2.4	28.2 ± 2.6	3.9 ± 1

Table 3.1 Mean plated tibia measurements and Plate Location Index (PLI) measurements post-surgery and at retrieval for each of the durations of implantation. *The mean PLI change expresses the mean PLI at sacrifice as a percentage of the mean PLI at surgery.

3.3.2 Radiographic assessment of retrieved plated and control bones

The radiographs of the retrieved composite plated specimens were compared with the opposite control bones at each of the time points (Figures 3.7 and 3.8). At 2 weeks there was no obvious structural change in the plated bone compared with the control bone. At the intermediate time points of 6 and 12 weeks there was evidence of bone formation at the superior and inferior tips of the plate when viewed on the lateral radiograph (see Figure 3.7b) as well as around the screws. At 26 weeks, two out of three samples demonstrated visible bone growth over the plate with thinning of the cortex beneath the plate (see Figure 3.8d). In the 52 week samples, there was no visible bone growth over the plate but the cortex beneath the plate was thinner and less distinct compared with samples from earlier time points (see Figure 3.8e).

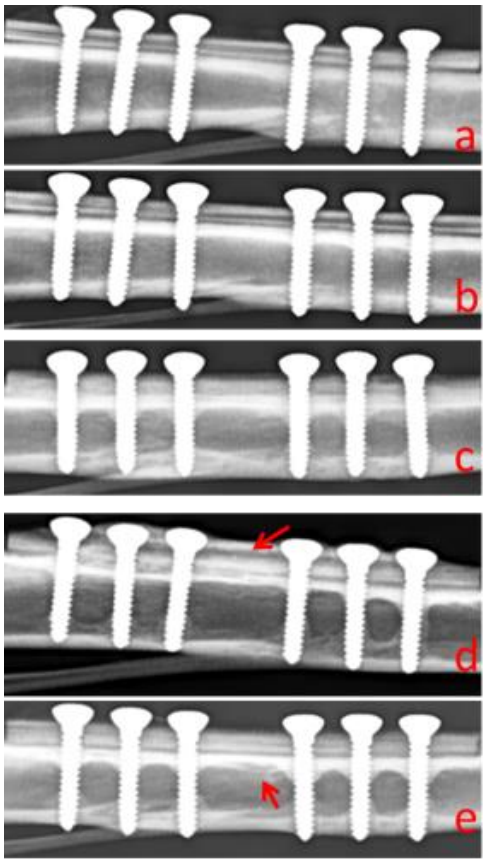


Figure 3.8 Plain radiographs demonstrating cortical changes beneath plate in composite plated specimens at 2 weeks – sample 2B (a), 6 weeks – sample 6A(b), 12 weeks – sample 12A(c), 26 weeks - sample 26B (d) and 52 weeks – sample 52C(e). In the 12, 26 and 52 week samples, there was bone formation around the screws. In the 26 week sample (d) there is new bone overlying the plate (red arrow). The cortex beneath the plate was also thinner compared with the previous samples. In the 52 week sample, there was a lucency in the cortex directly beneath the mid plate region suggesting bone resorption (red arrow).

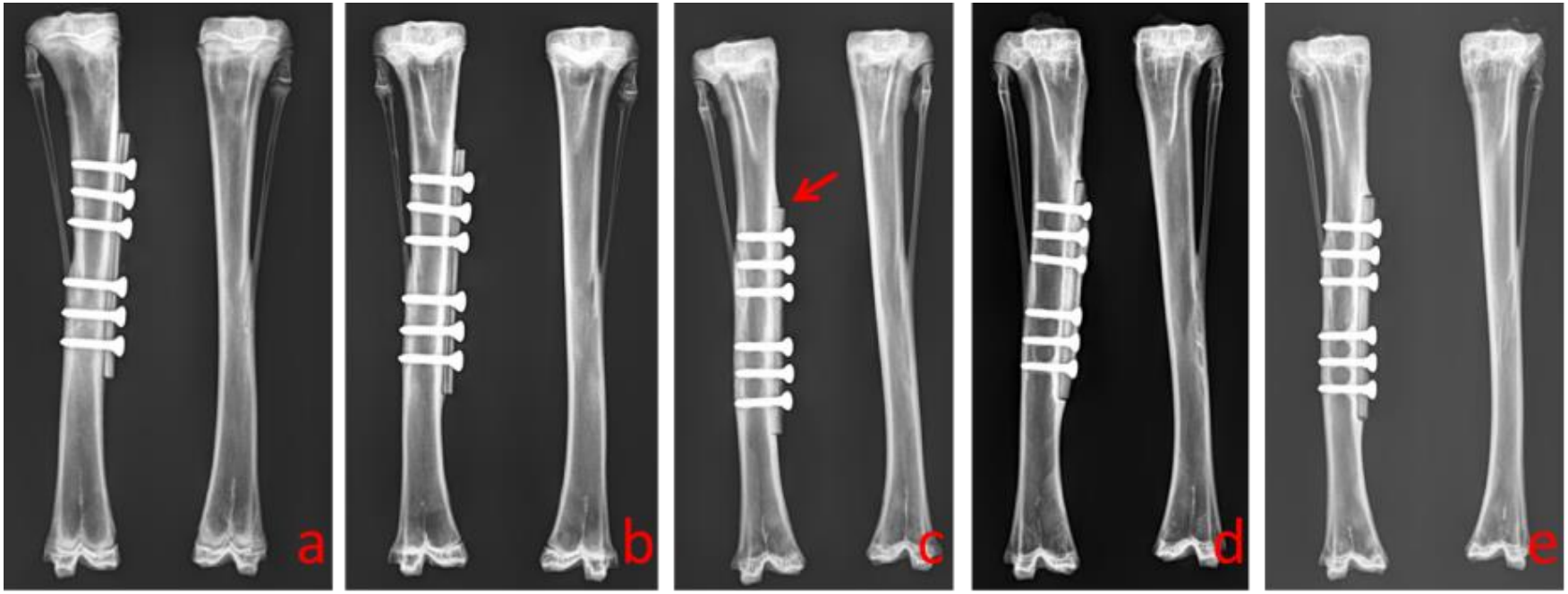


Figure 3.7 Plain radiographs of composite plated and respective control bones retrieved at each of the time points of sacrifice – (a) 2 weeks – sample 2B, (b) 6 weeks – sample 6A, (c) 12 weeks – sample 12A, (d) 26 weeks - sample 26B and (e) 52 weeks – sample 52C. There was evidence of progressive bone formation around the ends of the plate from 12 weeks onwards (red arrow). The composite plated bone at 26 weeks demonstrated a layer of bone overlying the plate. The growth plates at the ends of the bone show clear marginal radiolucency indicating that they are open at 2 and 6 weeks. From 12 weeks onwards, there was evidence of progressive fusion of both the proximal and distal growth plates.

The radiographs of the retrieved metal plated specimens were compared with the opposite control bones at each of the time points (Figures 3.9 and 3.10). Similar bone formation was observed at the plate ends from 2 weeks onwards (Figure 3.10a-e). The cortex between the central two screws corresponding to the mid-plate region demonstrated progressive thinning and was less distinct at 26 and 52 weeks (Figure 3.9d, e). Concurrently, there was bone formation around the outer screws at the plate periphery at these later time points (Figure 3.9c, d).

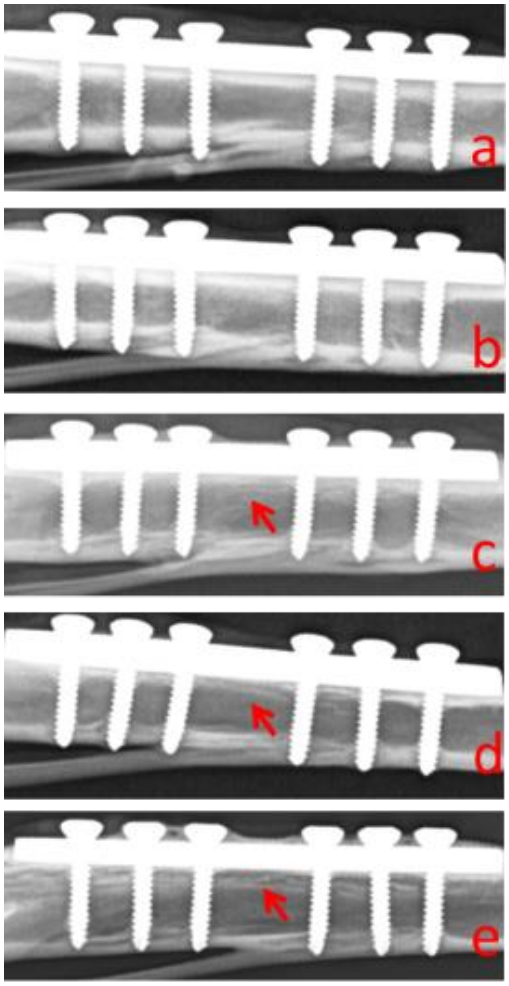


Figure 3.9 Plain radiographs demonstrating cortical changes beneath the plate in the metal plated specimens at 2 weeks – sample 2MC (a), 6 weeks – sample 6MB(b), 12 weeks – sample 12MD(c), 26 weeks - sample 26MD (d) and 52 weeks – sample 52MA(e). In the 2 and 6 week samples (a, b) the cortex was clearly defined beneath the plate. At 12 and 26 weeks (c, d), bone could be seen around the outermost screws but the cortex between the central two screws was less distinct (red arrows). At 26 and 52 weeks (d, e) the cortex beneath the plate between the central two screws (red arrows) was less distinct compared with earlier time points suggesting cortical thinning.

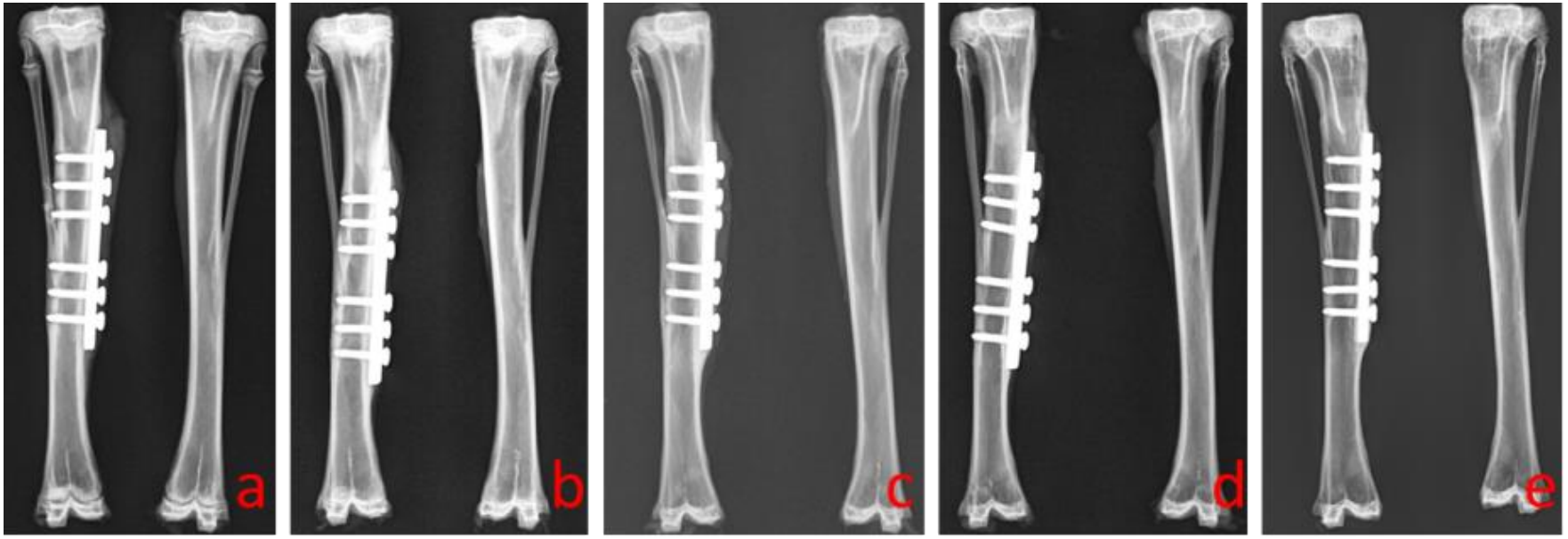


Figure 3.10 Plain radiographs of metal plated and respective control bones retrieved at each of the time points of sacrifice –(a) 2 weeks – sample 2MC, (b)6 weeks – sample 6MB, (c) 12 weeks – sample 12MD, (d) 26 weeks - sample 26MD and (e) 52 weeks – sample 52MA. There was progressive bone growth around the ends of the plate. The cortex beneath the plate between the central two screws became less distinct at the later time points.

3.3.3 Radiographic assessment of cortical thickness

The mid plate cortical thickness measurements in the composite plated and respective control bones and the normalised cortical thickness (NCT) at each of the time points are shown in Table 3.2 and depicted as a bar chart in Figure 3.11. Relative to the control bones, the mean NCT in the composite plated bones decreased from 106% at 2 weeks to 84.8% at 52 weeks. There was no obvious change in the mean NCT of the composite plated bones when comparing the samples at 26 weeks (85.2%) with those at 52 weeks (84.8%). This suggested that the cortical thinning remained unchanged after 26 weeks.

Table 3.2 Radiographic measurements of mean cortical thickness in the mid plate section in the composite plated and respective control bones at each time point. *The normalised cortical thickness (NCT) was calculated by expressing the plated cortical thickness as a percentage of the control cortical thickness.

Duration of implantation (weeks)	**Mean composite plated cortical thickness (mm) (±SD)**	**Mean control cortical thickness (mm) (±SD)**	***Mean Normalised Cortical Thickness (%) (±SD)**
2 weeks	1.5 ± 0.2	1.4 ± 0.2	106 ± 13.2
6 weeks	1.4 ± 0	1.4 ±0.1	100.3 ± 5
12 weeks	1.3 ± 0.2	1.4 ± 0.1	92 ± 14.2
26 weeks	1.2 ± 0.2	1.5 ± 0.1	85.2 ± 8.5
52 weeks	1.1 ± 0.3	1.3 ± 0.1	84.8 ± 16.7

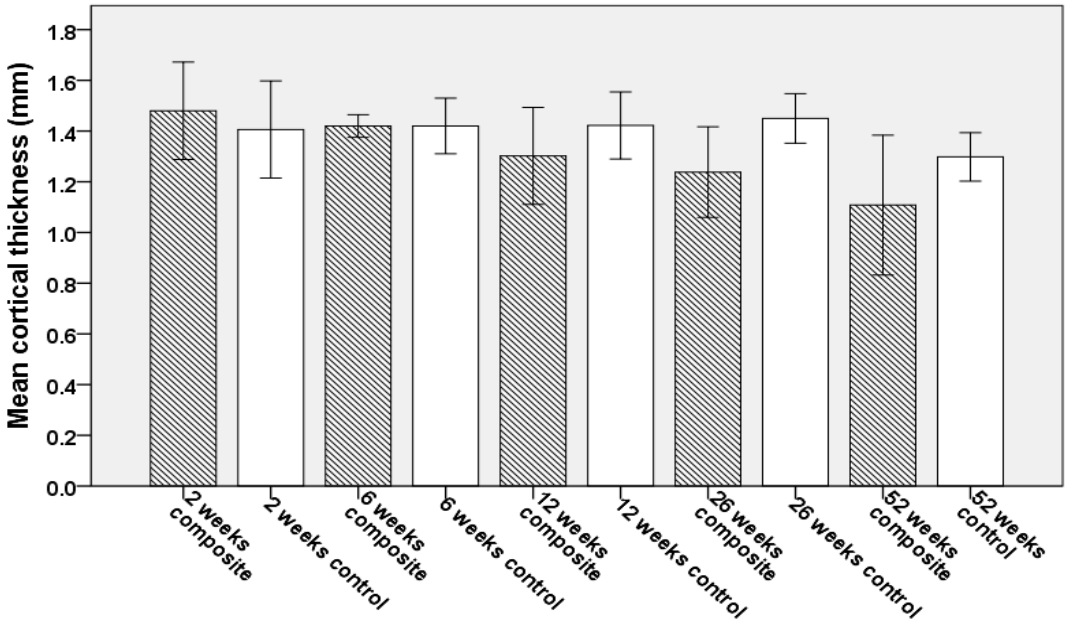


Figure 3.11 Bar chart of the radiographic measurements of mean composite and control bone cortical thickness at each of the time points (error bars = ±SD).

The mean normalised cortical thickness (NCT) in the metal plated bones decreased from 67.2% at 2 weeks to 31.1% at 26 weeks relative to the control bones (Table 3.3, Figure 3.12). In contrast, in the composite plated bones the mean NCT was 85.2% at 26 weeks. Although, the mid plate cortical thickness could not be measured in the 52 week samples, there was a progressive reduction in the cortical thickness in the metal plated bones at each successive time point.

Table 3.3 Radiographic measurements of mean cortical thickness in the mid plate section in the metal plated and respective control bones at each time points. *The normalised cortical thickness was calculated by expressing the plated cortical thickness as a percentage of the control cortical thickness.

Duration of implantation (weeks)	**Mean metal plated cortical thickness (mm) (±SD)**	**Mean control cortical thickness (mm) (±SD)**	***Mean Normalised Cortical Thickness (%) (±SD)**
2 weeks	0.8 ± 0.2	1.2 ± 0.1	67.2 ± 18.9
6 weeks	0.7 ± 0.2	1.4 ± 0.2	51.1 ± 13.4
12 weeks	0.7 ± 0.3	1.3 ± 0.2	58.3 ± 26.9
26 weeks	0.4 ± 0.3	1.4 ± 0.1	31.1 ± 23.9
52 weeks	unable to measure	1.4 ± 0.1	unable to measure

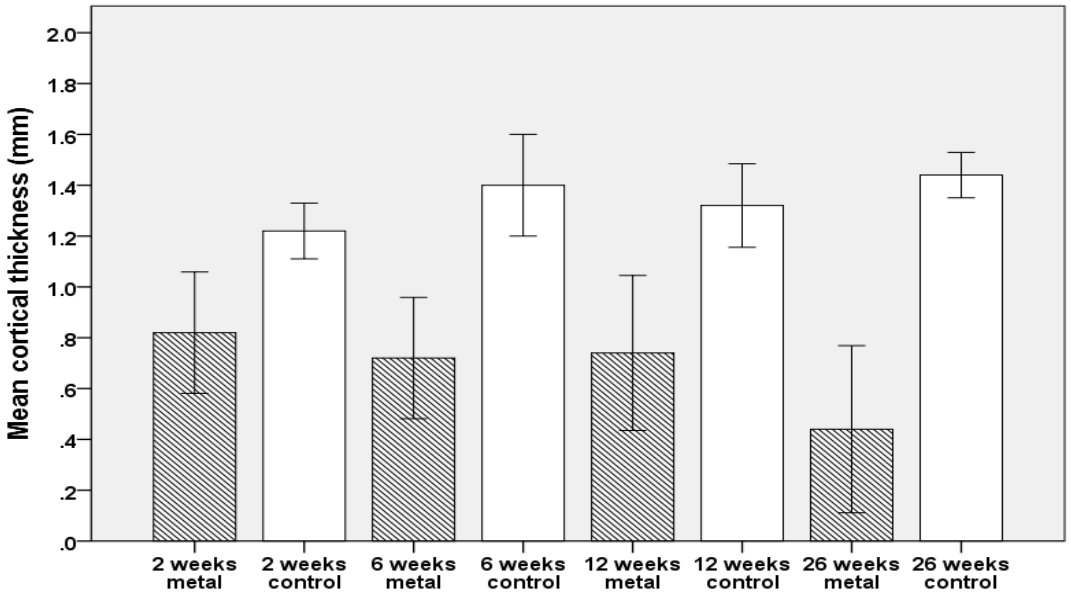


Figure 3.12 Bar chart of mean metal and control bone cortical thickness measured on radiographs at each of the time points from 2 to 26 weeks (error bars = ±SD).

A two way ANOVA test was undertaken to assess the influence of type of plate and duration of implantation on the normalised cortical thickness (NCT) as measured on plain radiographs. There were outliers greater than three box lengths from the edge of the box in boxplots of the residuals reflecting the limited sample size. The data was normally distributed as assessed by the Shapiro-Wilk test ($p>0.05$) and there was homogeneity of variances as assessed by Levene's test ($p=0.355$).

The interaction effect between the type of plate and duration of implantation on normalised cortical thickness on plain radiographs was not statistically significant, $F(3, 36) = 0.762$, $p=0.523$, partial $\eta 2 = 0.060$. Analysis of the main effects of type of plate and duration of implantation indicated that these main effects were statistically significant. Therefore, simple main effects and pairwise comparisons were run with a Bonferroni adjustment of the p values.

There was a statistically significant main effect of the type of plate ($p<0.001$) and there was a statistically significant main effect of the duration of implantation ($p=0.008$). Comparing the mean NCT between the two types of plate demonstrated a

statistically significant difference at the first four time points. Comparing the mean NCT between different time points for each type of plate demonstrated a statistically significant difference (p=0.013) between the NCT at 2 weeks (67.3+/-18.9) and 4 weeks (31.1+/- 23.9) in the metal plated group. There was no significant difference when comparing the NCT at different time points in the composite plated group. The statistical analysis indicated greater cortical thinning in the metal plated group compared with the composite plated group. In the metal plated group, this reduction was progressive whereas in the composite plated group no statistically significant trend could be demonstrated.

3.3.4 Micro Computed Tomography Imaging

3.3.4.1 Structural changes in the composite plate

The resolution of the obtained images permitted limited assessment of changes in the composite plate structure over time. There was no obvious change in the laminar architecture of the plate over time. Bands differentiating the glass fibre layers were clearly discernible up to 52 weeks. Due to the variation in the thickness of individual fibre and matrix rich layers between individual plates, it was difficult to detect any subtle structural changes occurring over time due to degradation. At 26 and 52 weeks there was some evidence of distortion of the outer aspect of the plate with visible fissures in some of the samples (see Figures 3.16 and 3.17). There was no clear evidence of fibre or matrix resorption at any of the surveyed time points.

3.3.4.2 Structural changes in composite plated bones

At 2 weeks there was obvious bone formation around the periphery of the plate and around the site of screw penetration in the opposite cortex (Figure 3.13) with a consequent increase in the cross-sectional area of the bone. The sides of the bone did not demonstrate new bone formation leading to a change in the cross sectional shape of the bone.

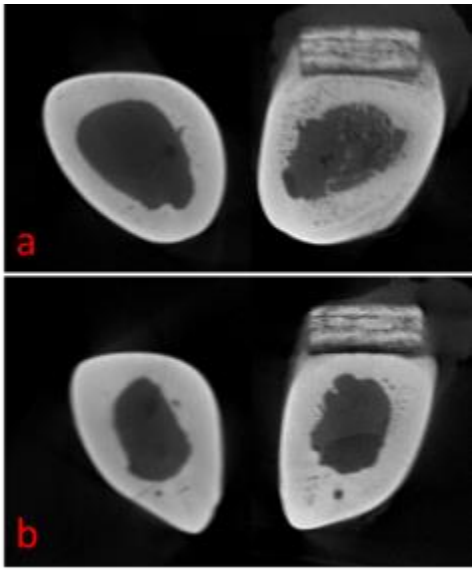


Figure 3.13 Micro CT axial images of composite plated bone (right) and control bone (left) at level 1 (a) and level 2 (b) retrieved at 2 weeks. There was an increase in the bone area in the plated bone due to bone formation around the plate and in the opposite cortex altering the cross sectional profile of the plated bone compared with the control. (Specimen 2C - 0.06mm voxel thickness)

At 6 weeks, the new bone around the plate periphery had matured creating a thickened cortex around the plate (Figure 3.14). The cortex beneath the plate was thicker compared with the opposite control bone. There was an increase in porosity in the cortex beneath the plate compared with the control bone.

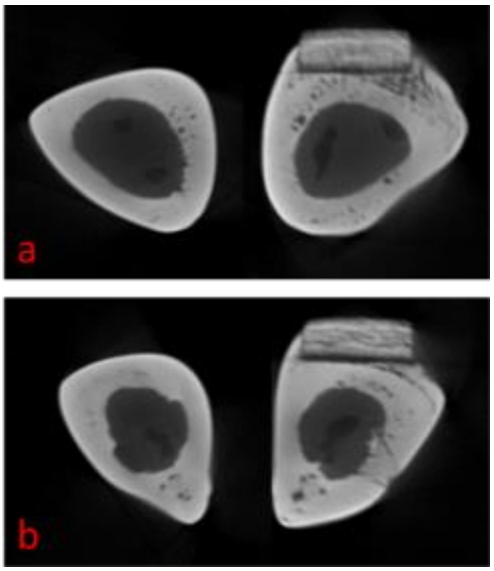


Figure 3.14 Micro CT axial images of composite plated bone (right) and control bone (left) at level 1 (a) and level 2 (b) retrieved at 6 weeks. The new bone surrounding the plate more closely resembles the pre-existing bone. There is porosity evident in the cortex beneath the plate compared with the control bone. (Specimen 6B - 0.06mm voxel thickness)

The 12 week samples demonstrated mature bone around the sides of the plate which was indistinguishable from the neighbouring cortical bone (Figure 3.15). In one specimen there was evidence of bone growth over the top of the plate (Figure 3.15a).

There was no obvious cortical thinning in the plated bones relative to the controls. The porosity beneath the plate seen at the preceding time point had decreased.

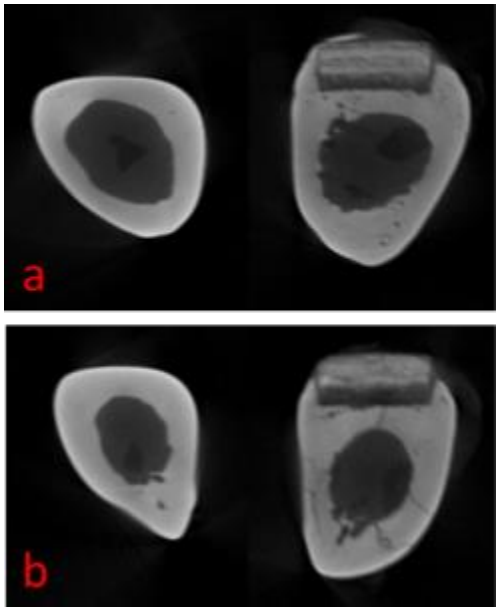


Figure 3.15 Micro CT axial images of composite plated bone (right) and control bone (left) at level 1 (a) and level 2 (b) retrieved at 12 weeks. There was some new bone formation over the top of the plate (a). The bone around the sides of the plate was indistinguishable from the cortical bone. (Specimen 12C - 0.06mm voxel thickness)

Structural bone changes occurred in the composite plated bones between 12 and 26 weeks. Two of the three specimens at 26 weeks demonstrated complete bone growth over the top of the plate (see Figure 3.16a, b). In the third sample there was evidence of bone growth over the top edges of the plate (see Figure 3.16c). This bone growth was accompanied by a reduction in the cortical thickness below the plate with the formation of large cavities. The specimens demonstrating greater bone growth over the top of the plate demonstrated greater cortical thinning beneath the plate. The cavities were mainly observed in the cortex surrounding the plate as well as in the opposite cortex.

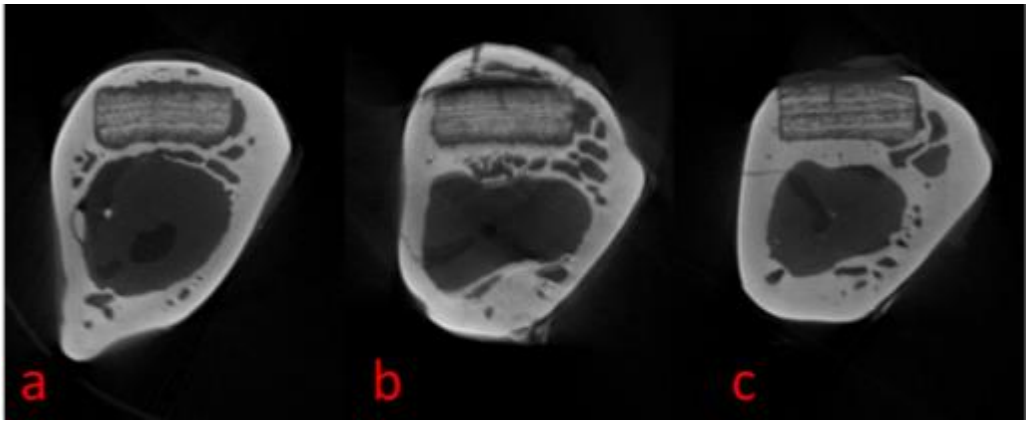


Figure 3.16 Micro CT axial images of composite plated bones retrieved at 26 weeks- (a) Specimen 26B, (b) Specimen 26C and (c) Specimen 26D (Level 2 - 0.06mm voxel thickness). There was marked bone resorption in the cortex beneath the plate with large cavities forming. In two specimens (a, b), there was bone growth over the top of the plate. Greater bone resorption was present in the specimens in which there was bone over the top of the plate (a, b) compared the specimen in which there was no bone growth over the plate (c).

In the 52 week samples, there were fewer cavities in the bone compared with the 26 week samples (Figure 3.17). There was thinning of the cortex beneath the plate in comparison with the cortex at the same level in the opposite control bone.

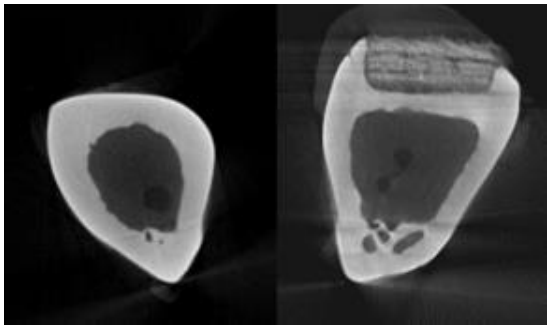


Figure 3.17 Micro CT axial images of composite plated bone (right) and control bone (left) at level 2 retrieved at 52 weeks. (Specimen 52B - 0.06mm voxel thickness). There were fewer cavities present in the bone with thinning of the cortex beneath the plate.

3.3.4.3 Micro CT cortical thickness measurements

Table 3.4 shows the mean absolute measurements of cortical thickness in the plated and control bones at each of the time points as well as the mean Normalised Cortical Thickness (NCT). Figure 3.18 displays the mean NCT for both levels at each time point as a bar chart.

Table 3.4 Mean cortical thickness and Normalised Cortical Thickness (NCT) measurements for composite plated bones and controls in the plate periphery (level 1) and plate mid-section (level 2) at each of the time points.

Duration of implantation	Mean Composite Level 1 cortical thickness (mm) (±SD)	Mean Control Level 1 cortical thickness (mm) (±SD)	Mean Level 1 NCT (%) (±SD)	Mean Composite Level 2 cortical thickness (mm) (±SD)	Mean Control Level 2 cortical thickness (mm) (±SD)	Mean Level 2 NCT (%) (±SD)
2 weeks	1.1 ± 0.2	1.1 ± 0	112.9 ± 10.5	1.1 ± 0.1	1.2 ± 0.2	98.9 ± 11.8
6 weeks	1.2 ± 0.1	1 ± 0.1	121.1 ± 7.8	1.1 ± 0.2	1.4 ± 0.2	79.8 ± 0.6
12 weeks	1.2 ± 0.2	1.2 ± 0.1	100.4 ± 14.3	1 ± 0.1	1.4 ± 0.1	70.3 ± 5
26 weeks	1 ± 0.2	1 ± 0	104.1 ± 22.3	0.7 ± 0.1	1.4 ± 0	52.5 ± 7.2
52 weeks	0.9 ± 0.1	1 ± 0.3	90.9 ± 30.7	0.7 ± 0.1	1.2 ± 0.1	57.3 ± 5.8

In the plate periphery (level 1), the mean NCT was greater than 100% at 2 and 6 weeks indicating a relatively thicker cortex in the plated bone compared with the same level in the control bone. The relative mean improvements were marginal – 12.9% at 2 weeks and 21.1% at 6 weeks. At 12 and 26 weeks, the mean NCT was close to 100% indicating near equivalence of cortical thickness in both plated and control bones. At 52 weeks, there was a small decrease with the plated bones demonstrating a mean cortical thickness 90.9% that of their respective control bones.

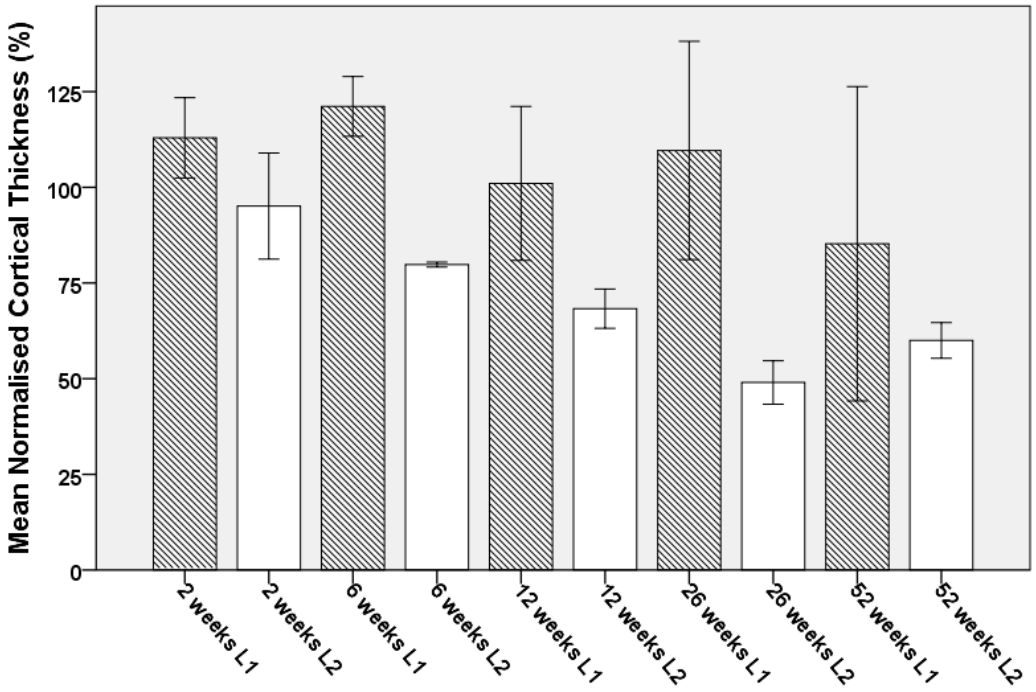


Figure 3.18 Bar chart of mean normalised cortical thickness (NCT) at level 1(L1- shaded bars) and level 2 (L2 - white bars) at each of the time points (error bars = ±SD).

In the level 2 section images, there was progressive reduction in the mean NCT suggesting progressive cortical thinning in the composite plated bones relative to the controls. The reduction in mean cortical thickness in the plated bones relative to the control bones was 1.1% at 2 weeks, 20.2% at 6 weeks, 29.7% at 12 weeks, 47.5% at 26 weeks and 42.7% at 52 weeks suggesting the reduction in cortical thickness at level 2 progressed up to 26 weeks.

A Two way ANOVA test was undertaken to investigate the influence of the plate sampling location (level 1 and 2) and the duration of implantation on the normalised cortical thickness (NCT). Boxplot analysis of residuals revealed outliers but the data sets were normally distributed as assessed by the Shapiro-Wilk test ($p>0.05$). The assumption of homogeneity of variances was violated (Levene's test, $p=0.009$). In view of the data sets being normally distributed and the ratio of the largest group variance to the smallest group variance equating to less than 3, the two way ANOVA for normalised cortical thickness was performed despite this violation. The ANOVA analysis did not reveal any statistically significant interaction effect between the two

variables of sampling location (level 1 or 2) and duration of implantation. Simple main effects and multiple pairwise comparisons were undertaken with a Bonferroni correction for statistical significance.

There was no significant difference when comparing the normalised cortical thickness (NCT) at level 1 (plate periphery) between different time points. Mean NCT was significantly lower at level 2 (plate mid-section) at 26 weeks (mean NCT = 52.5%, p=0.017) and 52 weeks (mean NCT = 57.3%, p=0.039) compared with the mean NCT at 2 weeks (mean NCT =98.9%). Comparing the NCT between Level 1 and 2 at each of the time points demonstrated a statistically significant difference at four out of five time points – 6 weeks (p=0.015), 12 weeks (p=0.027), 26 weeks (p=0.001) and 52 weeks (p=0.015). The statistical analysis supports a significant reduction in cortical thickness in the plate mid-section compared with the plate periphery at each time point. Cortical thickness did not change significantly at level 1 whereas at the later time points a statistically significant progressive reduction was observed at level 2.

3.3.4.4 Micro CT cortical area measurements

Table 3.5 shows the mean cortical area in the plated and control bones (2mm x 4mm rectangular region of interest) at each of the time points as well as the normalised cortical area (NCA). Figure 3.19 displays the mean NCA for both levels at each time point as a bar chart.

Table 3.5 Mean cortical area and normalised cortical area (NCA) measurements for composite plated bones and controls for levels 1 and 2 at each of the time points.

Duration of implantation	Mean Composite Level 1 cortical area (mm^2) (±SD)	Mean Control Level 1 cortical area (mm^2) (±SD)	Mean Level 1 NCA (%) (±SD)	Mean Composite Level 2 cortical area (mm^2) (±SD)	Mean Control Level 2 cortical area (mm^2) (±SD)	Mean Level 2 NCA (%) (±SD)
2 weeks	5.9 ± 0.6	6 ± 0.2	102.8 ± 13	6.4 ± 0.5	6.5 ± 0.4	97.6 ± 3
6 weeks	5.9 ± 0.1	5.2 ± 0.4	112 ± 8.8	5.5 ± 0.6	6.5 ± 0.6	83.7 ± 1.9
12 weeks	5.1 ± 1.5	5.9 ± 0.3	87.3 ± 24.3	5.3 ± 0.5	6.5 ± 0	81.2 ± 8.2
26 weeks	4 ± 0.8	5.5 ± 1	74.2 ± 16.5	3.1 ± 0.9	6.2 ± 0.2	50.3 ± 13.4
52 weeks	3.5 ± 0.4	5.1 ± 0.3	68 ± 8.9	3.4 ± 0.6	6 ± 0.5	56.7 ± 10.3

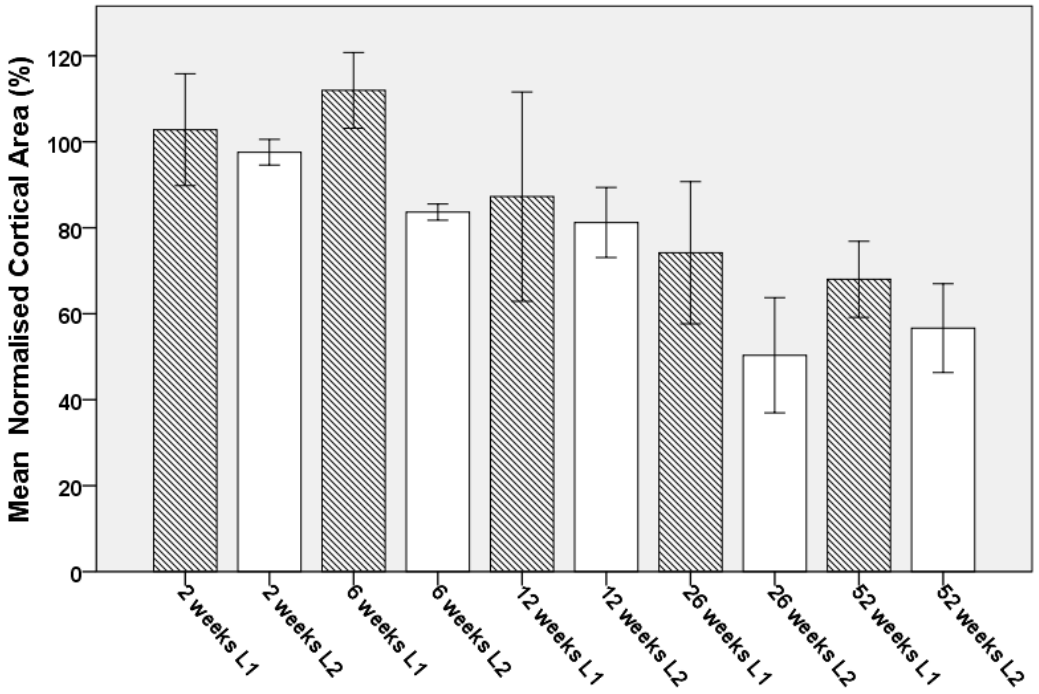


Figure 3.19 Bar chart of mean normalised cortical area (NCA) at level 1(L1-shaded bars) and level 2 (L2 - white bars) at each of the time points (error bars = ±SD).

The normalised cortical area (NCA) measurements demonstrated a similar trend to the cortical thickness measurements. At 2 and 6 weeks, the plated bones demonstrated a greater mean cortical area in the plate periphery (level 1) compared with their respective control bones. After 6 weeks, there was a progressive reduction in the mean cortical area in the plate periphery. The mean reduction in the NCA was 12.7% at 12 weeks, 25.8% at 26 weeks and 32% at 52 weeks. At level 2, there was a greater reduction in the mean cortical area when comparing the plated with the control bones. The reduction in mean cortical area was progressive up to 26 weeks at which time point the mean NCA in the plated bones was 50.3%.

A Two way ANOVA test was undertaken to investigate the influence of the plate sampling location (level 1 and 2) on the normalised cortical area (NCA) measured on Micro CT. Boxplot analysis of residuals did not reveal any outliers. The data sets were normally distributed except for the residuals for one cell in the analysis (Level 2 at 2 weeks, Shapiro-Wilk test p=0.026). There was homogeneity of variances as assessed by Levene's test (p=0.124). The two way ANOVA did not reveal any statistically significant interaction effect between the two variables of sampling location (level 1 or 2) and duration of implantation. Simple main effects and multiple pairwise comparisons were undertaken with a Bonferroni correction for statistical significance.

At level 1 (plate periphery), the mean normalised cortical area (NCA) was significantly lower at 52 weeks (NCA=68, p=0.017) compared with at 6 weeks (NBA=112). At level 2 (plate mid-section), the mean NCA was significantly lower at 26 weeks (NBA=50.3, p=0.003) and 52 weeks (NBA=56.7, p=0.013) compared with at 2 weeks (NCA=97.6). Comparing the mean NCA of levels 1 and 2 at each of the time points, demonstrated a statistically significant difference at two out of five time points (6 weeks and 26 weeks). At 6 weeks, the mean NCA was 83.7 at level 2 compared with 112 at level 1 (p=0.043). At 26 weeks the mean NCA was 50.3 at level 2 compared with 74.2 at level 1 (p=0.038). The results indicate a reduction in the cortical area by the final time point at both sampling locations with a greater reduction in the plate mid-section (level 2) compared to the periphery (level 1).

3.3.4.5 Micro CT bone area measurements

Table 3.6 shows the mean cross sectional bone area in the plated and control bones at each of the time points as well as the normalised bone area (NBA). Figure 3.20 displays the mean NBA for both levels at each time point as a bar chart.

Table 3.6 Mean cross sectional area and normalised bone area (NBA) measurements for composite plated bones and controls for levels 1 and 2 at each of the time points.

Duration of implantation	Mean Composite Level 1 cross sectional area (mm^2) (±SD)	Mean Control Level 1 cross sectional area (mm^2) (±SD)	Mean Level 1 NBA (%)(±SD)	Mean Composite Level 2 cross sectional area (mm^2) (±SD)	Mean Control Level 2 cross sectional area (mm^2) (±SD)	Mean Level 2 NBA (%)(±SD)
2 weeks	35.3 ± 2.8	27.3 ± 1.1	127 ± 18.3	35.1 ± 2.8	28.3 ± 1.9	124.5 ± 9
6 weeks	34.6 ± 8.3	28 ± 3.7	122.5 ± 13.4	33.4 ± 6.5	27.7 ± 5	120.4 ± 1.6
12 weeks	40.2 ± 3.6	30.7 ± 1.1	131 ± 8.5	35 ± 3.9	31.2 ± 1	112.2 ± 12.3
26 weeks	49.7 ± 8.6	31.4 ± 2.2	158.5 ± 27.2	45.8 ± 5.9	32.4 ± 2.5	141.4 ± 11.9
52 weeks	35.3 ± 2.1	26.8 ± 1.7	131.7 ± 10.5	29.2 ± 2.9	27.8 ± 3.5	106.3 ± 16.7

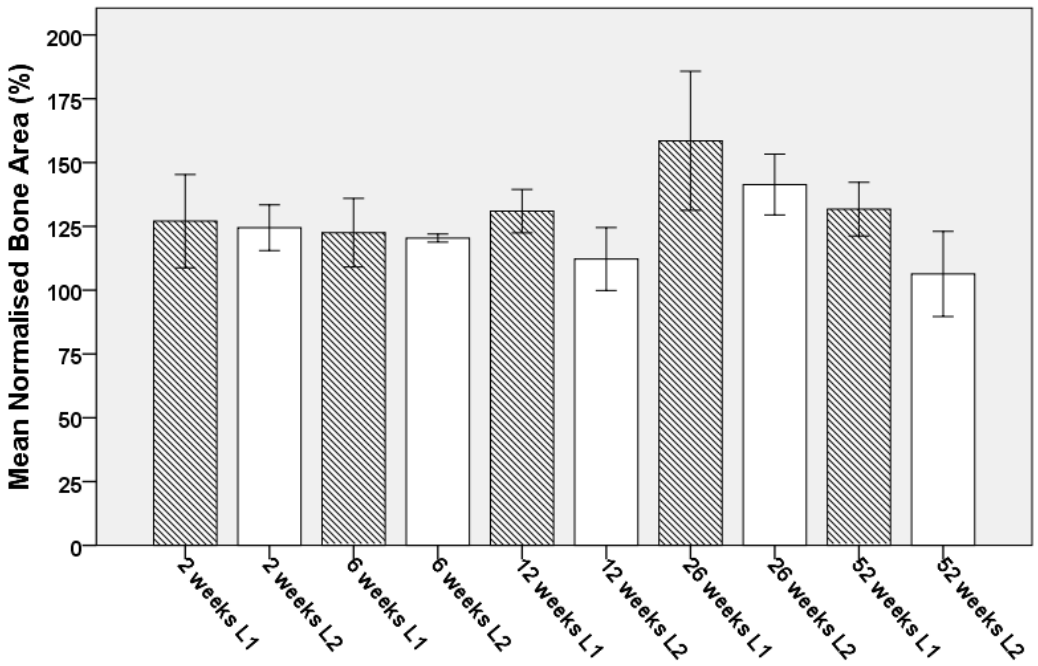


Figure 3.20 Bar chart of mean normalised bone area (NBA) at level 1(L1-shaded bars) and level 2 (L2 - white bars) at each of the time points (error bars = ±SD).

The mean NBA values demonstrated that the cross sectional bone area in the plated bones was greater than in the opposite control bones. At both levels 1 and 2, at each time point, the mean NBA was greater than 100. At level 1, the mean improvement in cross sectional bone area in the plated bones was 27% at 2 weeks, 22.5% at 6 weeks, 31% at 6 weeks, 58.5% at 26 weeks and 31.7% at 52 weeks relative to the control bones. A similar trend of an increase in mean bone area up to 26 weeks was also observed in the plate mid-section (level 2). However, the relative improvement in mean bone area in the plated bones relative to the control bones was less at level 2 compared with level 1 – 24.5% at 2 weeks, 20.4% at 6 weeks, 12.2% at 12 weeks, 41.4% at 26 weeks and 6.3% at 52 weeks. The results would suggest that there was a progressive increase in mean bone area up to 26 weeks after which the bone area decreased. This effect was greater in the plate periphery (level 1) compared with the plate mid-section (level 2).

Two way ANOVA testing was undertaken to investigate the influence of the plate sampling location (level 1 and 2) and the duration of implantation on the normalised bone area (NBA) measured on MicroCT. Boxplot analysis of residuals did not reveal any outliers and the data sets were normally distributed as assessed by the Shapiro-Wilk test ($p>0.05$). There was homogeneity of variances as assessed by Levene's test ($p=0.435$). The two way ANOVA did not reveal any statistically significant interaction effect between the two variables of sampling location (level 1 or 2) and duration of implantation. Simple main effects and multiple pairwise comparisons were undertaken with a Bonferroni correction for statistical significance.

There was no significant difference when comparing the normalised bone area (NBA) between different time points at each level. When comparing the NBA between the two sampling locations at each time point, there was a statistically significant difference in the normalised bone area at level 1 (NBA =131.7) compared with level 2 (NBA=106.3) at 52 weeks ($p=0.049$) but not at the other four time points.

Both the cortical thickness and cortical area in the plated bones reduced over time relative to the control bones. This relative bone loss was more apparent in the central

plate region (level 2) compared with the plate periphery (level 1). In contrast, the total cross sectional area in the plated bones demonstrated an improvement in the plated bones compared with the control bones at each time point. The relative improvement was greater in the plate periphery (level 1) compared with the central plate region (level 2). The changes in all three parameters were progressive up to 26 weeks with a comparatively smaller change between 26 and 52 weeks suggesting development of an equilibrium state between 26 and 52 weeks. This was supported by the axial image appearances which demonstrated large cavities at 26 weeks which were not present at 52 weeks.

3.4 Scanning electron microscopy of resin embedded sections

3.4.1 Reproducibility of bone blocks corresponding to the plate periphery and plate mid-section

The mean distance index (DI) measurement for the bone blocks corresponding to level 1 (plate periphery) in the plated bones was 28.9 ± 3.7% and in the control bones was 29.5 ± 3.6%. The mean DI measurement for the bone blocks corresponding to level 2 (plate mid-section) in the plated bones was 39.2 ± 3.5% and in the control bones was 38.9 ± 3.6%. These results are depicted as a bar chart in Figure 3.21 and demonstrate satisfactory reproducibility in sampling, evidenced by small standard deviations, and good concordance in the location of the two bone block levels in the plated and control bones.

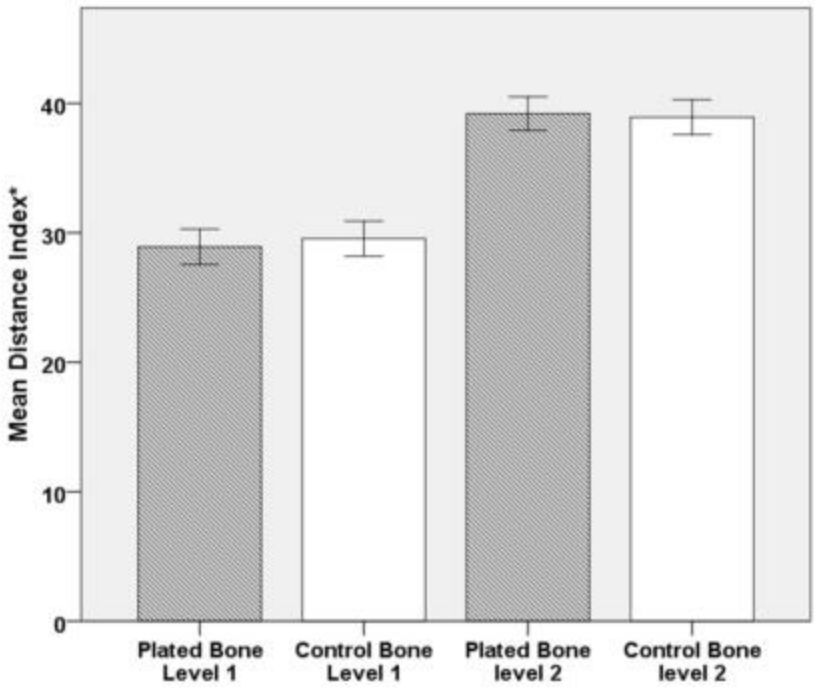


Figure 3.21 Bar chart showing mean distance index for level 1 and 2 bone blocks from composite and metal plated bones and their respective control bones (error bars = 1 standard deviation)

3.4.2 Structural bone changes in composite plated bones

At 2 weeks, there was evidence of new periosteal bone formation around the plate edges, on the inner aspect of the bone and on the outer aspect of the opposite cortex (Figure 3.22). There was comparatively less new bone formation around the sides of the bone (Figure 3.22g). This new bone formation was more obvious in the plate mid-section (level 2) compared with the plate periphery (level 1).

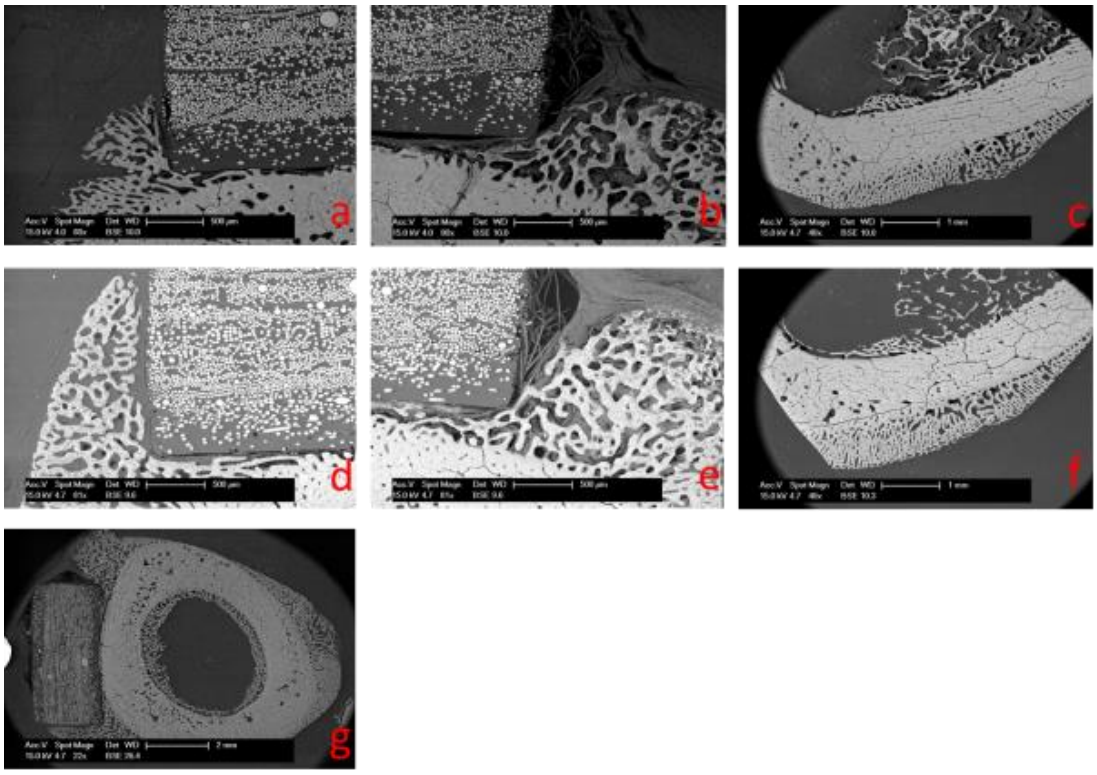


Figure 3.22 Specimen 2E retrieved at 2 weeks. Level 1(a-c, 80xmag) and level 2 images (d-f, 80xmag).(a)(b) New bone formation around the edges of the composite plate at level 1.The new bone is distinguished by its loose areolar structure compared to the compact cortical bone beneath the plate. (c) New bone formation on the endosteal and periosteal surface of the cortex opposite the plate. (d-f) New bone formation around the plate edges and opposite cortex at level 2 demonstrating greater area of new bone compared with level 1(a-c).(g) Cross section of bone and composite plate (level 2, 22xmag). New bone formation around the plate edges and opposite cortex.

At 6 weeks, the bone growth around the plate was more prominent (Figure 3.23) and had increased in density to more closely resemble the pre-existing cortical bone. The bone growth was more pronounced in the mid plate region (level 2, Figure 3.23d-f) compared with the peripheral plate region (level 1, Figure 3.23a-c).

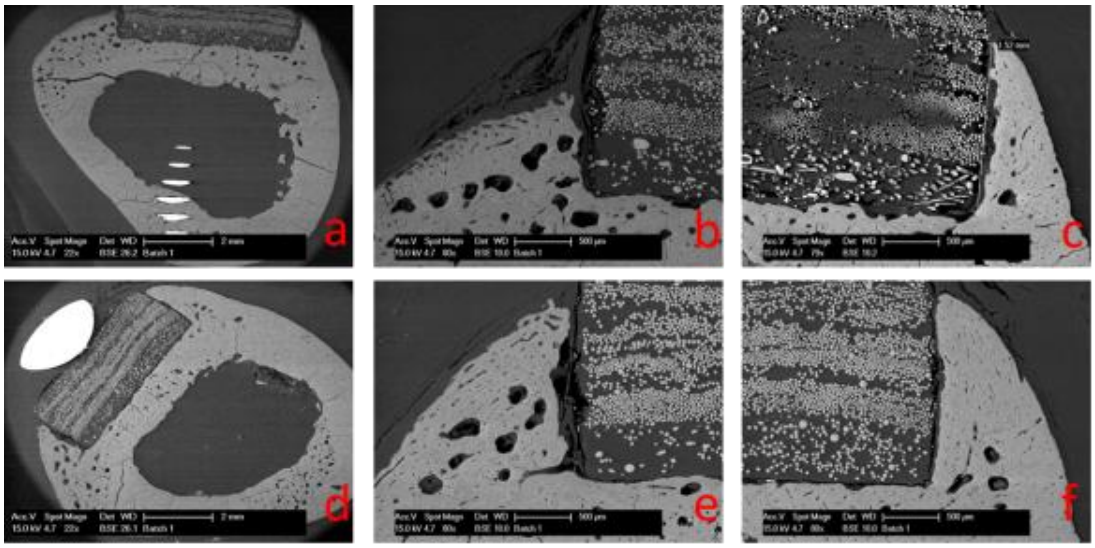


Figure 3.23 Specimen 6E retrieved at 6 weeks. Level 1 (a, 22xmag; b-c, 80xmag) and level 2 images (d, 22x mag; e-f, 80x mag). The bone around the plate edges resembles the cortical bone. At level 2 there is greater bone formation around the plate compared with level 1.

At 12 weeks, the bone growth around the plate had progressed with one sample (12E) demonstrating complete encapsulation of the plate (Figure 3.24a-c). Porosity was evident in the cortex beneath the plate in two out of three samples (12D and 12E), and in the opposite cortex in one out of three samples (12D) (Figure 3.24d-f).

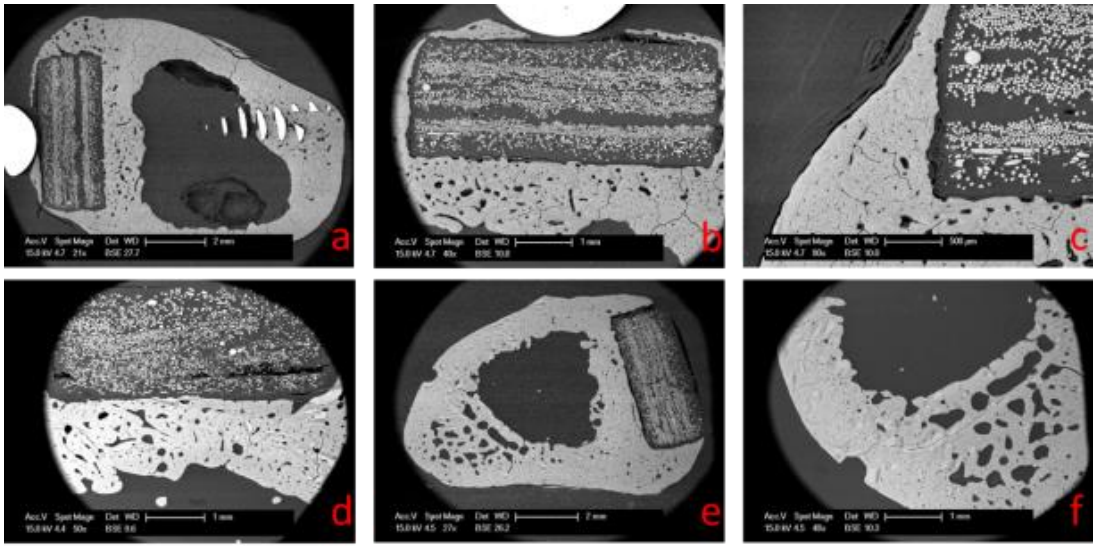


Figure 3.24 Specimen 12E (a-c) and 12D (d-f) retrieved at 12 weeks. (a) Cross section of bone and composite plate demonstrating complete bone growth around plate (21xmag). (b) Porosity in cortex beneath plate (40xmag). (c) Compact bone surrounding plate edges (80xmag). (d) Specimen 12D level 1 showing porosity beneath plate (50x mag). (e)Specimen 12D level 2 demonstrating porosity in opposite cortex (27x mag) and again at higher magnification (f, magx48).

At 26 weeks, bone was still present around the plate edges (Figure 3.25). However, large resorptive cavities were noted in the vicinity of the plate and in the underlying cortex. The cortical thickness beneath the plate was also significantly reduced in one of the specimens (26D) compared with the others.

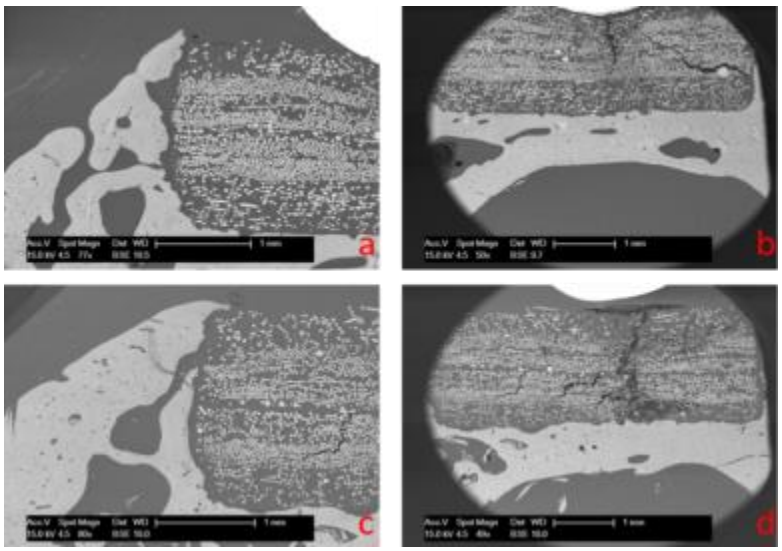


Figure 3.25 Specimen 26D level 1 (a, magx80; b, magx50) and level 2(c, magx80; d, magx50) retrieved at 26 weeks. Considerable porosity is evident in the bone at the plate edges and in the cortex beneath.

At 52 weeks, there were fewer resorptive cavities (Figure 3.26). There was a reduction in the cortical thickness beneath the centre of the plate (level 2). In two out of three specimens (52D and 52E), the plate was completely encapsulated with bone. Greater cortical thinning beneath the plate was noted in these specimens compared with the specimen without bone covering the plate.

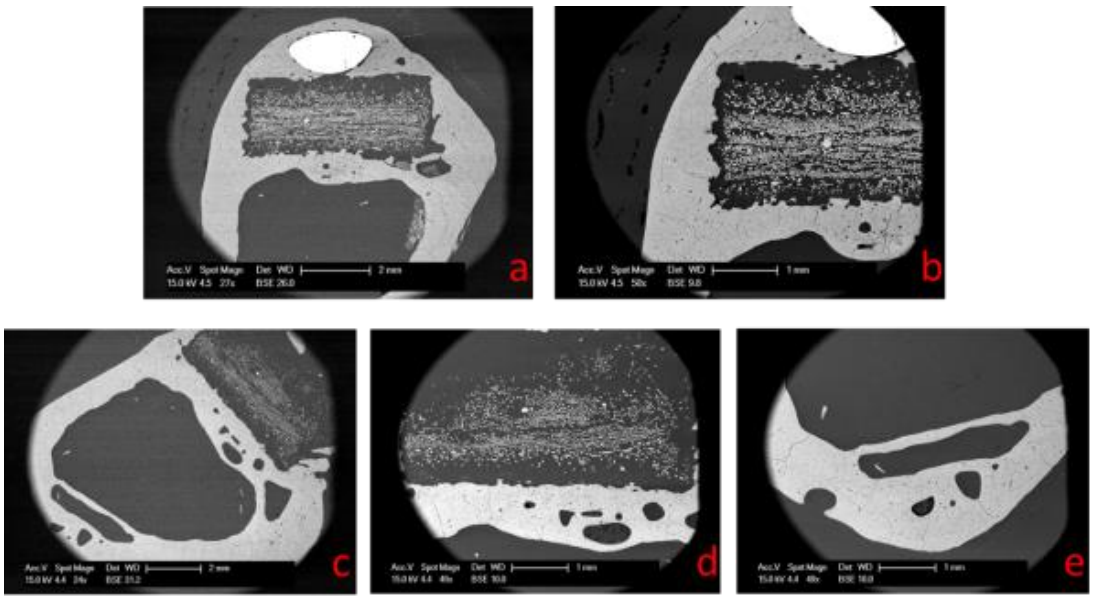


Figure 3.26 Specimens 52D (a, 27xmag; b, 50xmag) and 52E (c, 24xmag; d-e, 50xmag). There is persisting bone over the top of the plate (a-c). Resorptive cavities are present in the cortex beneath the plate and in the opposite cortex (c-e).

3.4.3 Structural changes in the composite plate over time

Assessment of the in vivo composite plate degradation at each time point was difficult due to damage caused to the plate cut surface during sample processing. Although macroscopic disruption of the plate was evident at each time point due to specimen processing, there were no obvious voids in the fibre rich regions of the plate suggesting glass fibre resorption (Figure 3.27). The glass fibre diameter, density and laminar distribution demonstrated marked heterogeneity between individual samples. There were no matrix voids around the fibres suggestive of fibre-matrix dissociation at the interface or outer fibre resorption causing fibre shrinkage.

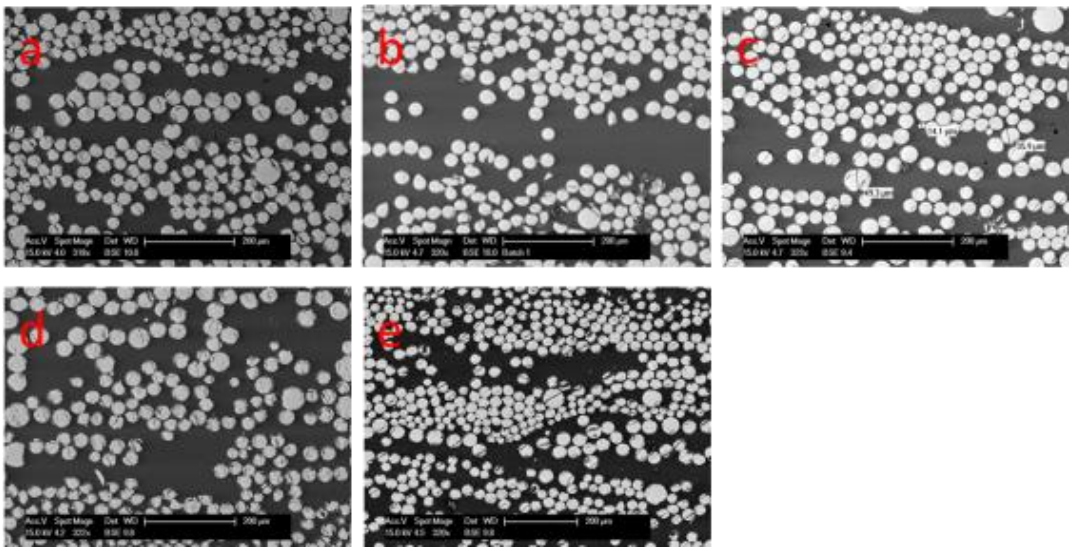


Figure 3.27 Cross sectional images of composite plate at each of the time points (a-2 weeks, b-6 weeks, c-12 weeks, d-26 weeks, e-52 weeks)(320xmag). The white circles are the cross sectional appearance of the glass fibres running longitudinally through the darker surrounding PLA matrix. There was no obvious change in the glass fibre size, density or distribution over time.

3.4.4 Structural bone changes in metal plated bones

At 2 weeks, there was new bone formation around the plate edges (Figure 3.28). The new bone demonstrated a more areolar structure which distinguished it from the adjacent cortical bone. Similar to the composite specimens, there was new bone formation in the endosteal surface as well as on the opposite cortex.

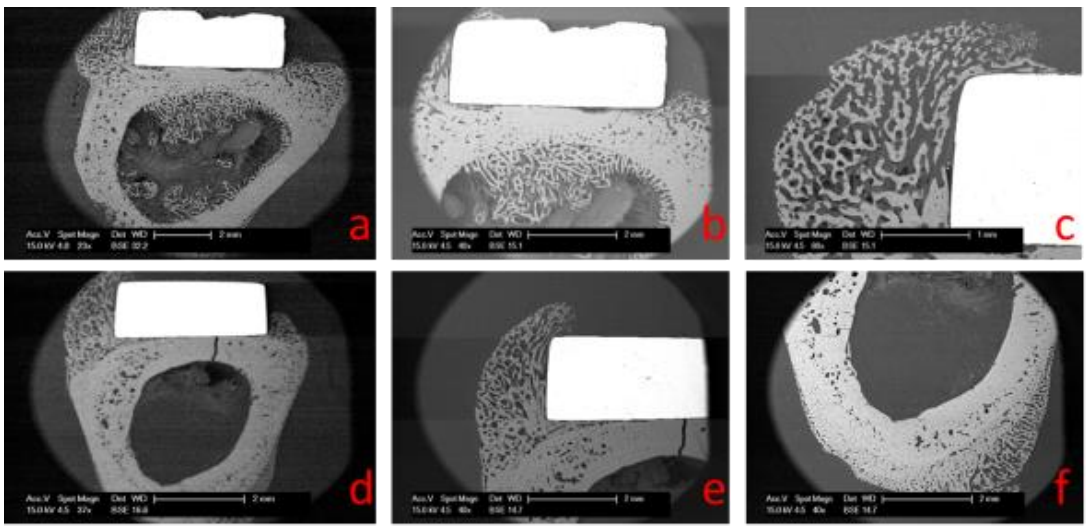


Figure 3.28 Specimen 2MC level 1 (a, 23xmag; b, 40xmag; c, 80xmag) and level 2 (d, 37xmag; e-f, 40xmag) demonstrating new bone formation around the plate edges and in the opposite cortex.

At 6 weeks, the new bone had increased in density and more closely resembled the adjacent cortical bone (Figure 3.29).

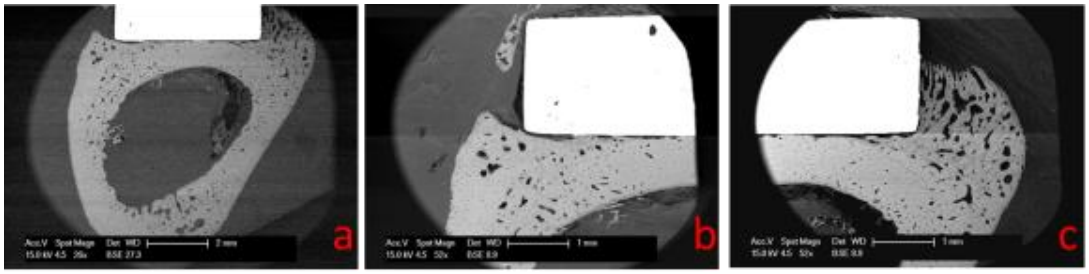


Figure 3.29 Specimen 6ME level 2 retrieved at 6 weeks (a, 26xmag; b-c, 52xmag). The new bone around the edge of the plate bears a closer morphological resemblance to the cortical bone compared with the 2 week retrieved samples.

In the 12 week samples, the plate was completely surrounded by bone in two out of three specimens (12MB and 12MD – Figure 3.30). There was also increased porosity evident beneath the plate. Comparison of the two levels demonstrated a difference in cortical thickness beneath the plate. The cortex was thinner at level 2 compared with level 1 (Figure 3.30).

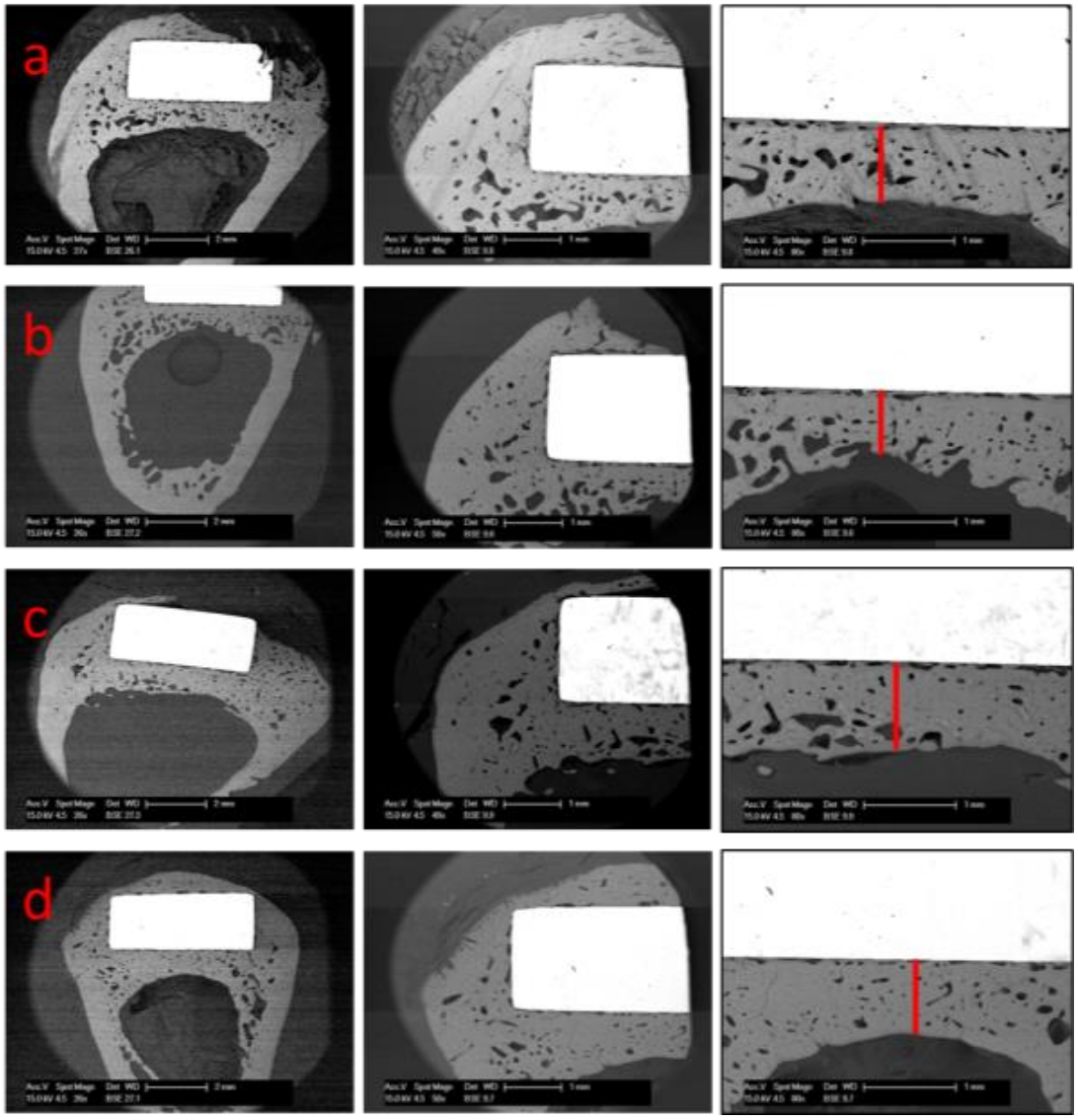


Figure 3.30 Specimens 12MB (a – level 1, b – level 2) and 12MD (a-level 1, b-level 2) retrieved at 12 weeks. There was complete bone growth around the plate. Comparing cortical thickness beneath the plate in level 2 (b and d) with the respective samples from level 1(a and c) demonstrated greater cortical thinning directly under the centre of the plate at level 2 (red line indicates cortical thickness)

In the 26 week samples, two out of three specimens demonstrating bone formation over the top of the plate (Figure 3.31). Large resorptive cavities had formed in the bone surrounding the plate. There was greater bone loss observed under the centre of the plate on the level 2 samples compared with the level 1samples. Conversely, there was greater bone formation over the top of the plate at level 2 compared with level 1.

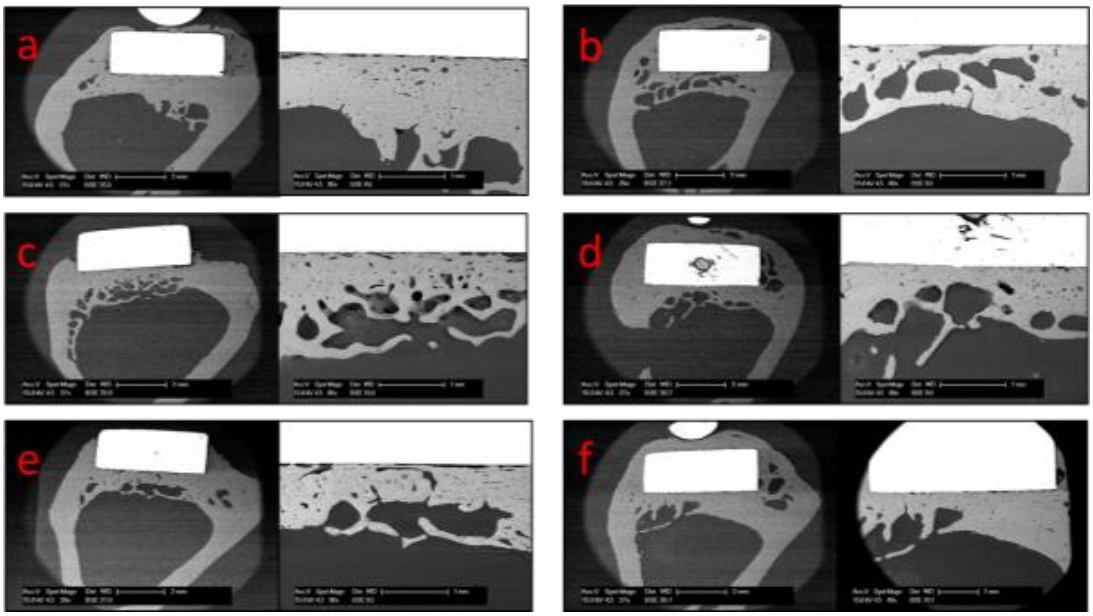


Figure 3.31 Metal plated bone specimens retrieved at 26 weeks (cross section overview -27x mag, plated cortex -80x mag). Specimen 26MB level 1(a) and level 2(b); specimen 26MC level 1(c) and level 2(d); specimen 26ME level 1(e) and level 2(f). There was greater bone loss beneath the centre of the plate at level 2 compared with level 1 in each of the three specimens.

In the 52 week retrievals, fewer larger cavities were evident. There was obvious cortical thinning beneath the plate. There was also a marked difference in the cortical thickness beneath the centre of the plate when comparing level 2 with level 1(Figure 3.32). This relative difference in cortical thinning was greater at 52 weeks compared with 26 weeks. The level 2 samples demonstrated greater bone formation over the top of the plate compared with the level 1 samples. Comparing the level 2 sections, there was greater bone formation over the top of the plate and increased bone loss beneath the plate in the 52MD specimen compared with 52ME (Figure 3.32). At 26 weeks and 52 weeks, the magnitude of bone loss under the plate demonstrated an inverse relationship with the magnitude of bone formation over the top of the plate.

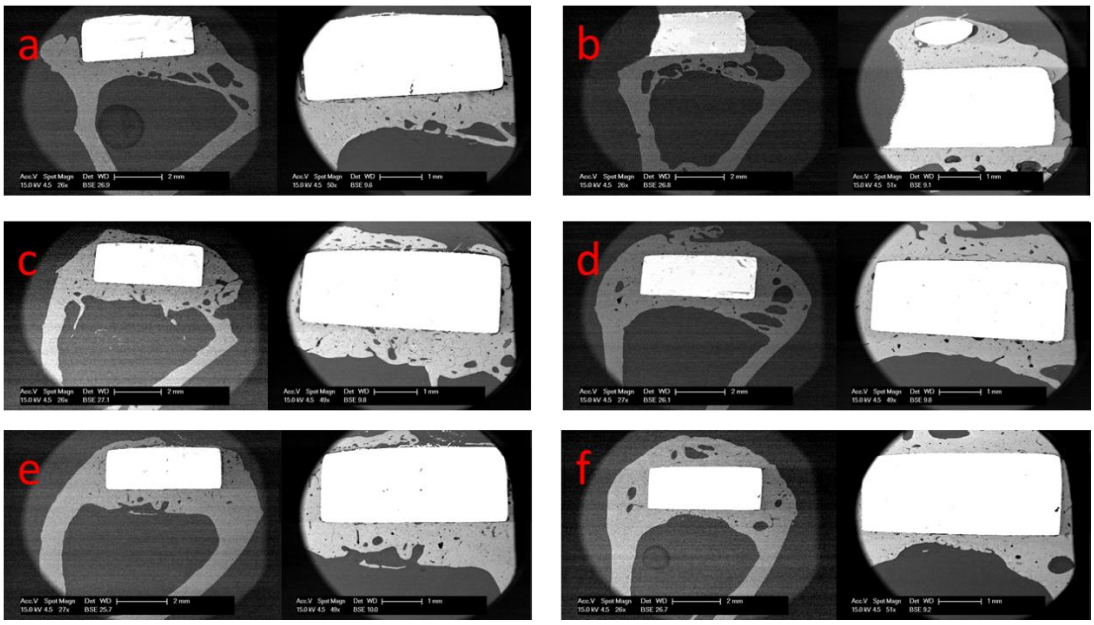


Figure 3.32 Metal plate bone specimens retrieved at 52 weeks (cross section overview -27x mag, plated cortex -80x mag). Specimen 52MB level 1(a) and level 2(b); specimen 52MD level 1(c) and level 2(d); specimen 52ME level 1(e) and level 2(f). There was greater cortical thinning beneath the centre of the plate in the level 2 sections (b, d, f) compared with the level 1 sections (a, c, e). The level 2 sections demonstrated greater bone formation over the top of the plate compared with the level 1 sections.

3.4.5 Cortical thickness and cross sectional bone area measurements

To improve the sample size to n=3 at each time point, following mechanical testing one pair of plated and control bones at each time point in both the composite plated and metal plated groups were used to generate bone blocks. Due to the fractures in the mechanically tested specimens and processing artefacts in others, thickness and area measurements were not possible in all of the samples. Cortical thickness measurements were not possible in two bone blocks in the composite plate group (26 weeks and 52 weeks) and two bone blocks in the metal plate group (6 weeks and 52 weeks). Cortical area measurements could not be performed in 4 bone blocks in the composite plated group (6 weeks - 1, 26 weeks - 1 and 52 weeks - 2) and 9 bone blocks in the metal plated group (6 weeks – 2, 12 weeks -1, 26 weeks – 3 and 52 weeks -3).

3.4.5.1 Cortical thickness measurements in composite and metal plated groups

The normalised cortical thickness (NCT) expressed the cortical thickness of the plated bone as a percentage of the same measurement in the respective control bone (Tables 3.7 and 3.8). The composite plated bones did not demonstrate any obvious changes in the NCT at each of the sampled levels as the duration of implantation increased (Table 3.7, Figures 3.33, 3.34). In the plate periphery (level 1), the mean NCT was greater than 100% in the composite plated bones at four out of five time points suggesting that the cortex in the plated bones was greater than the opposite control bones. At the plate mid-section (level 2), the mean NCT in the composite plated bones was less than 100% at all of the time points suggesting that the cortex was thinner compared with the opposite control bones. However, the magnitude of this relative reduction was small as the lowest mean NCT in the plate mid-section of the composite plated bones was 74.1% at 2 weeks.

Table 3.7 Mean cortical thickness and normalised cortical thickness (NCT*) measurements for composite plated bones and controls for levels 1 and 2 at each of the time points.

Duration of implantation	**Mean Composite Level 1 cortical thickness (µm)**	**Mean Control Level 1 cortical thickness (µm)**	**Mean Composite Level 1 NCT* (%)**	**Mean Composite Level 2 cortical thickness (µm)**	**Mean Control Level 2 cortical thickness (µm)**	**Mean Composite Level 2 NCT* (%)**
2 weeks	1156±191	1070±161	110.9±30.7	1017±131	1403±227	74.1±18.1
6 weeks	1095±159	1190±123	92.3±12.9	1150±252	1185±183	97.4±17.6
12 weeks	1125±227	1035±59	108.5±19.6	944±58	1185±183	80.7±10.5
26 weeks	1174±324	1001±179	121.4±42.8	1024±215	1180±113	79.1±21.9
52 weeks	1200±193	986±48	110.8±9.7	844±74	983±104	86.6±12.6

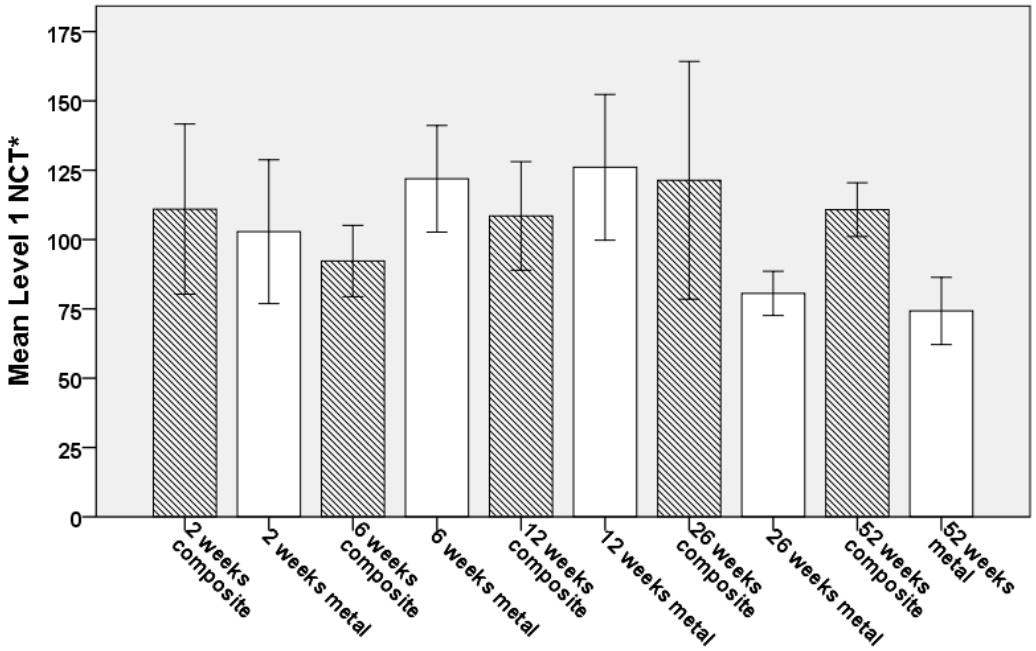


*Figure 3.33 Bar chart of mean level 1 normalised cortical thickness (*NCT) comparing composite plated and metal plated specimens at each of the time points(error bars = 1 standard deviation). At the later time points (26 and 52 weeks) the metal plated specimens demonstrated lower cortical thickness indices compared with the composite plated samples.*

In the metal plated bones, there was evidence of relative cortical thinning compared with the control bones which progressed with an increasing duration of implantation (Table 3.8, Figures 3.33, 3.34). At the plate periphery (level 1), although there was an initial increase in the mean NCT from 102.8% at 2 weeks to 126.1% at 12 weeks, there was a progressive reduction thereafter with the mean NCT falling to 74.3% at 52 weeks. In the plate mid-section (level 2), the improvement was of a lower magnitude with a peak in the mean NCT at 6 weeks of 108.9%. However, the reduction was more pronounced in this plate location with a mean NCT of 43.6% at 52 weeks suggesting that the cortical thickness in the metal plated bones was less than half of the opposite control bones.

Table 3.8. Mean cortical thickness and normalised cortical thickness (NCT*) measurements for metal plated bones and controls for levels 1 and 2 at each of the time points.

Duration of implantation	Mean Metal Level 1 cortical thickness (µm)	Mean Control Level 1 cortical thickness (µm)	Mean Metal Level 1 NCT* (%)	Mean Metal Level 2 cortical thickness (µm)	Mean Control Level 2 cortical thickness (µm)	Mean Metal Level 2 NCT* (%)
2 weeks	1051±195	1037±90	102.8±25.9	1011±149	1079±127	94±12.6
6 weeks	1233±289	1008±126	121.9±19.2	1242±549	1044±222	108.9±23.4
12 weeks	1160±330	914±99	126.1±26.3	895±362	1067±29	84.4±35.6
26 weeks	718±133	886±79	80.6±8	795±57	960±121	83.7±12.8
52 weeks	741±145	995±48	74.3±12.1	477±226	1155±35	43.6±28.6

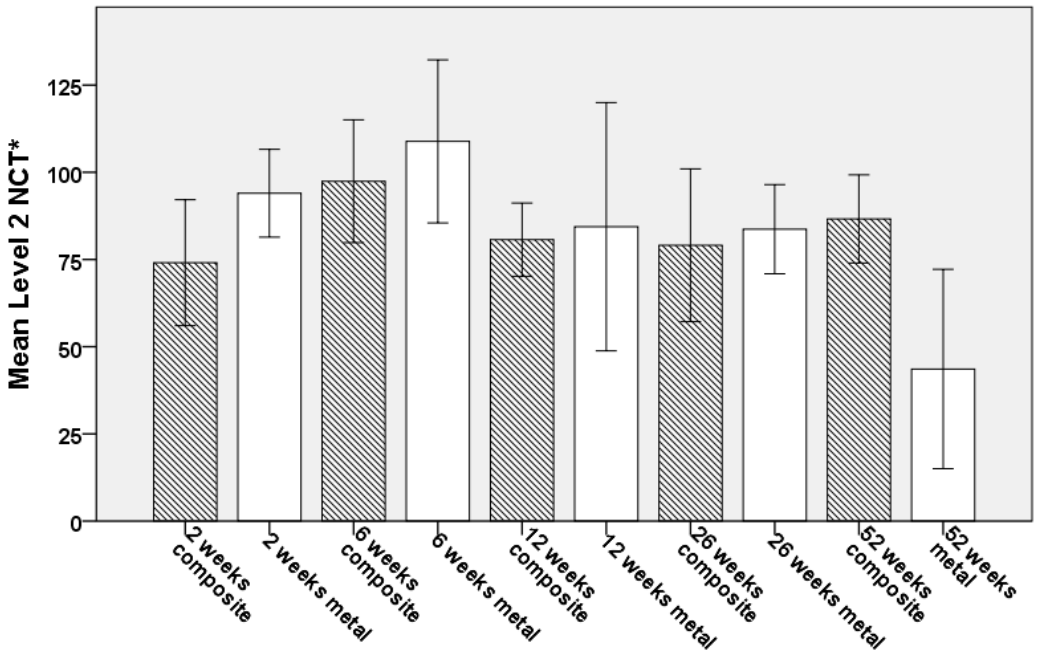


*Figure 3.34 Bar chart of mean level 2 normalised cortical thickness (*NCT) comparing composite plated and metal plated specimens at each of the time points (error bars = 1 standard deviation). The NCT is comparable for both types of plates from 2 weeks to 26 weeks. However, at 52 weeks there is a large difference with much greater cortical thinning in the metal plated sample compared to the difference observed at level 1.*

Three way ANOVA testing was undertaken to investigate the influence of the type of plate, plate sampling location (level 1 and 2) and the duration of implantation on the normalised cortical thickness (NCT). Boxplot analysis of residuals did not reveal any outliers and the data sets were normally distributed (Shapiro-Wilk test ,$p>0.05$) except for one cell out of twenty. The assumption of homogeneity of variances was violated (Levene's test, $p=0.033$). In view of the majority of the cells being normally distributed and the ratio of the largest group variance to the smallest group variance equating to less than 3, the three way ANOVA was performed despite this violation.

The three way ANOVA for the normalised cortical thickness did not reveal any statistically significant interaction effect between the three independent variables of type of plate, sampling location and duration of implantation. However, there was a significant two way interaction between the type of plate and the duration of implantation ($p=0.025$). Simple main effects and multiple pairwise comparisons were undertaken with a Bonferroni correction for statistical significance.

Multiple pairwise comparisons with respect to the type of plate demonstrated a significantly lower NCT in the metal plated samples compared with the composite plated samples at level 1 at 26 weeks (NCT= 80.6 vs 121.4, $p=0.029$) and level 2 at 52 weeks (NCT= 43.6 vs 86.6, $p=0.039$). Comparing the NCT between level 1 and level 2 in the composite plated samples demonstrated a significant difference at 2 weeks (NCT: level 1 110.9, level 2 74.1; $p=0.048$) and 26 weeks (NCT: level 1 121.4, level 2 79.1; $p=0.042$). In the metal plated samples, the mean NCT at level 2 was significantly less than at level 1 (84.4 vs 126.1, $p=0.026$) at 12 weeks. The results would suggest that as the duration of implantation increased, progressively greater cortical thinning was observed in the metal plated bones compared with the composite plated bones but this difference was not statistically significant. Greater bone loss was observed in both plate groups in the plate mid-section (level 2) compared to the periphery (level 1) and this finding was statistically significant.

Post hoc sample size calculation was undertaken to determine the appropriate sample size to observe the measured difference in mean normalised cortical thickness at

level 2 when comparing the composite (mean 86.6, sd 12.6, n=3) and metal (mean 43.6, sd 28.6, n=2) groups at 52 weeks. The calculation yielded a sample size of n=6 in each group with 80% power and 5% sensitivity which was double the actual sample size in the current study.

3.4.5.2 Cortical area measurements in composite and metal plated groups

The normalised cortical area (NCA) expressed the area of bone in a specified region of interest below the plate as a percentage of the same area in a similar region of interest in the opposite control bone (Tables 3.9 and 3.10). In the plate periphery (level 1) of the composite plated bones, the mean NCA was less than 100% after two weeks suggesting cortical thinning. However, the mean NCA remained greater than 90% indicating that the relative bone loss in the composite plated bones was less than 10% at 6, 12 and 26 weeks. This was not significant in view of the relatively large standard deviations (Figure 3.35). Although the mean NCA dropped further to 70.8% in the plate periphery at 52 weeks, sampling at this level at 52 weeks was restricted to a single pair of experimental bones. In the plate mid-section, the mean NCA was less than 100% at all but one time point (Figure 3.36). The mean NCA was lower in the plate mid-section at 12 weeks (86.9% vs 94.3%) and 26 weeks (72.09% vs 96.4%) compared with the plate periphery suggesting greater bone loss towards the centre of the plate. However, the reduction in mean NCA at level 2 at 52 weeks was relatively small compared with the magnitude of the standard deviation.

Table 3.9 Mean cortical area and normalised cortical area (NCA*) measurements for composite plated bones and controls for levels 1 and 2 at each of the time points.

Duration of implantation	Mean Composite Level 1 cortical area (mm^2)	Mean Control Level 1 cortical area (mm^2)	Mean Composite Level 1 NCA* (%)	Mean Composite Level 2 cortical area (mm^2)	Mean Control Level 2 cortical area (mm^2)	Mean Composite Level 2 NCA* (%)
2 weeks	4.7±0.8	4.3±0.7	110.8±24.2	5.4±0.9	5.8±0.1	92.8±17.4
6 weeks	4.2±0.2	4.9±1.2	90.5±20.6	5±1.3	5.2±0.6	101.6±15
12 weeks	4.6±0.5	4.9±0.4	94.3±17.7	4.8±0.2	5.5±0.4	87±7.4
26 weeks	4.6±0.7	4.8±0.6	96.4±21	4.3±0.9	5.3±0.2	72.1±7.7
52 weeks	4.7±1.4	4.4	70.8	4±1.8	4.6±0.4	88.6±48.2

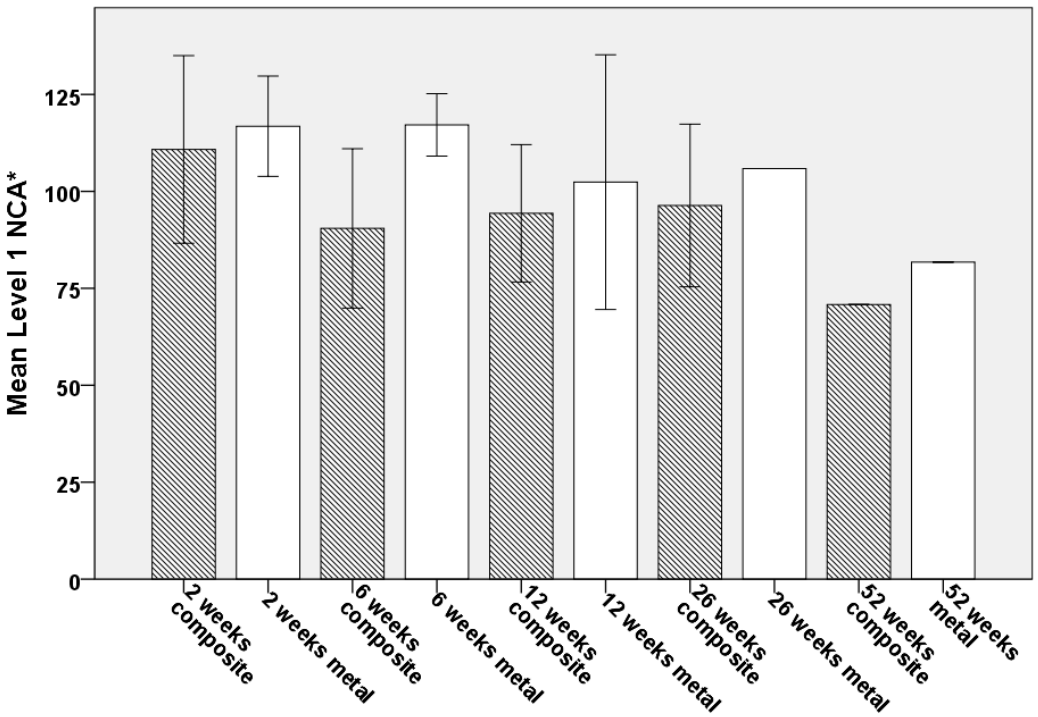


*Figure 3.35 Bar chart of mean level 1 normalised cortical area (*NCA) comparing composite plated and metal plated specimens at each of the time points (error bars = 1 standard deviation). Although the mean NCA is lower at 52 weeks in both plated groups, there is no obvious relationship with the duration of implantation.*

The cortical area measurements in the metal plated bones demonstrated a similar trend to the changes in cortical thickness (Table 3.10, Figures 3.35, 3.36). At the plate periphery, the mean NCA measurements suggested that the plated cortex was thicker at 2 weeks (116.8%) and 6 weeks (117.2%). At 12 weeks, the mean NCA indicated equivalence between the plated and control bones. There were a limited number of specimens at 26 weeks (n=1) and 52 weeks (n=1). These specimens demonstrated a reduction in the mean NCA to 81.8% at 52 weeks. In the plate mid-section, there was a progressive reduction in the mean NCA from 97.3% at 2 weeks to 53.5% at 52 weeks.

Table 3.10 Mean cortical area and normalised cortical area (NCA*) measurements for metal plated bones and controls for levels 1 and 2 at each of the time points.

Duration of implantation	**Mean Metal Level 1 cortical area (mm^2)**	**Mean Control Level 1 cortical area (mm^2)**	**Mean Metal Level 1 NCA* (%)**	**Mean Metal Level 2 cortical area (mm^2)**	**Mean Control Level 2 cortical area (mm^2)**	**Mean Metal Level 2 NCA* (%)**
2 weeks	4.8±0.7	4.1±0.1	116.8±12.9	4.8±0.4	5±0.3	97.3±7.6
6 weeks	5±1	4.2±0.9	117.2±8.1	5±1.2	4.2±0.5	92.9
12 weeks	4.1±1.4	4±0.1	102.4±32.9	3.6±0.2	4.3±0.1	82.7±7.6
26 weeks	3.9±0.8	4.5	105.9	3.5±0.5	4.6±0.7	70±2.7
52 weeks	3.3±0.1	4.2	81.8	2.4±0.4	4.5±0.3	53.5±9.4

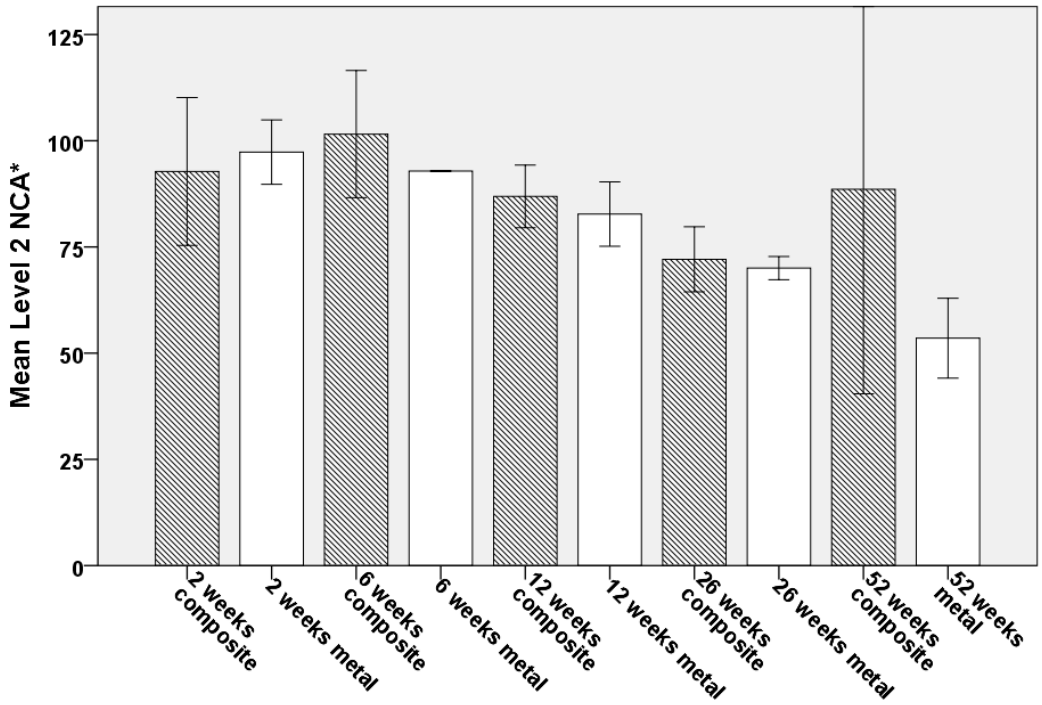


*Figure 3.36 Bar chart of mean level 2 normalised cortical area (*NCA) comparing composite plated and metal plated specimens at each of the time points (error bars = 1 standard deviation). In the metal plated group, there is a progressive reduction in the mean NCA at each successive time point.*

Three way ANOVA testing was undertaken to investigate the influence of the type of plate, plate sampling location (level 1 and 2) and the duration of implantation on the normalised cortical area (NCA). Boxplot analysis of residuals did not reveal any outliers. The data sets were normally distributed (Shapiro-Wilk test, $p>0.05$) except for two cells out of twenty. The assumption of homogeneity of variances was violated (Levene's test, $p=0.033$). In view of the majority of the cells being normally distributed and the ratio of the largest group variance to the smallest group variance equating to less than 3, the three way ANOVA was performed despite this violation.

The three way ANOVA for the normalised cortical area (NCA) did not reveal any significant three way or two way interaction effect between the three independent variables of type of plate, sampling location and duration of implantation. Analysis of main effects demonstrated the mean NCA to be significantly lower at level 2 compared with level 1 in the metal plated samples ($p=0.019$) irrespective of time

point. Multiple pairwise comparisons did not reveal any statistically significant differences when looking at the influence of each factor on the normalised cortical area reflecting limitations in the sample size. Although the mean NCA was significantly lower at 52 weeks in the metal group (53.5%) compared to the composite group (88.6%), this was not statistically significant due to the relatively large standard deviation in the composite group (48.2%).

Post hoc sample size calculation was undertaken to determine the appropriate sample size to observe the measured difference in mean normalised cortical area at level 2 when comparing the composite (mean 88.6, sd 48.2, n=3) and metal (mean 53.5, sd 9.4, n=2) groups at 52 weeks. The calculation yielded a sample size of n=19 in each group with 80% power and 5% sensitivity reflecting the large standard deviation in the composite group.

3.5 Mechanical testing of in vitro and in vivo specimens

3.5.1 In vitro testing of cadaveric bones and plates

Eight un-degraded composite plates were tested to failure. The fracture always occurred through one of the central two screw holes nearest the plate mid-section (Figure 3.37). In two specimens, the plate did not break into two pieces. In these samples, the fracture line extended mid-way through the plate before propagating through inter-laminar shear. This resulted in a crack extending through part of the plate with bending of the remaining intact layers (Figure 3.37c). The stress strain curve demonstrated a linear relationship up to the point of the failure (Figure 3.38a). In contrast, the degraded composite plates failed through ductile failure as demonstrated by extensive plastic deformation of the fractured ends (Figure 3.37c, d). The stress strain curve had a flatter profile demonstrating reduced stiffness due to the slope of the gradient and a lower ultimate load to failure (Figure 3.38a) compared to the un-degraded composite plates.

The PLA plates demonstrated failure with less deformation of the fractured ends compared with the composite plates. The stress strain curves were less steep for the degraded PLA plates compared with the un-degraded plates suggesting reduced stiffness with degradation. The metal plates demonstrated very little deformation during initial loading compared with the other plates (Figure 3.38e). When the metal plates failed there was significant bending due to deformation without fracture (Figure 3.37e, f). The bending occurred at the plate mid-section corresponding to the site of maximal three point bending.

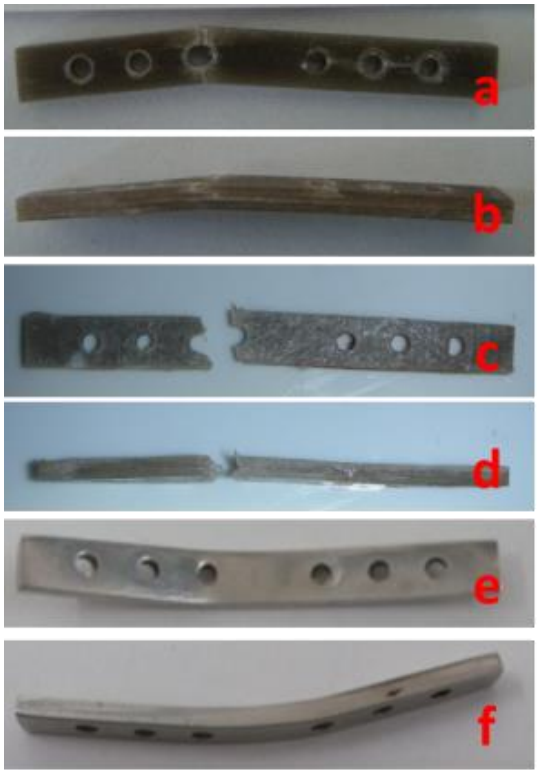


Figure 3.37 Photographs showing retrieved plate specimens following flexural testing. (a, b) Un-degraded composite plate demonstrating failure through third screw hole. The side view shows how the crack extends partially through the plate before propagating through inter-laminar shear leaving the lower layer intact (b). (c, d) Degraded composite plate demonstrating deformation of the fractured ends and a frayed appearance due to fibre shearing. (e, f) Metal plate demonstrating bending of the plate in the mid-section without fracture.

Stress strain curve analysis revealed the metal plates to have superior mechanical properties compared with the PLA and composite un-degraded plates (Table 3.11). The metal plates demonstrated a greater mean ultimate load to failure with a four to five-fold increase compared with the composite and PLA un-degraded plates respectively. The relative difference in flexural stiffness was greater with a fifteen-fold improvement compared with the composite plate and twenty-fold compared with the PLA plate. These results suggested significantly reduced deformation in the metal plates compared with the resorbable plates under the same loading conditions.

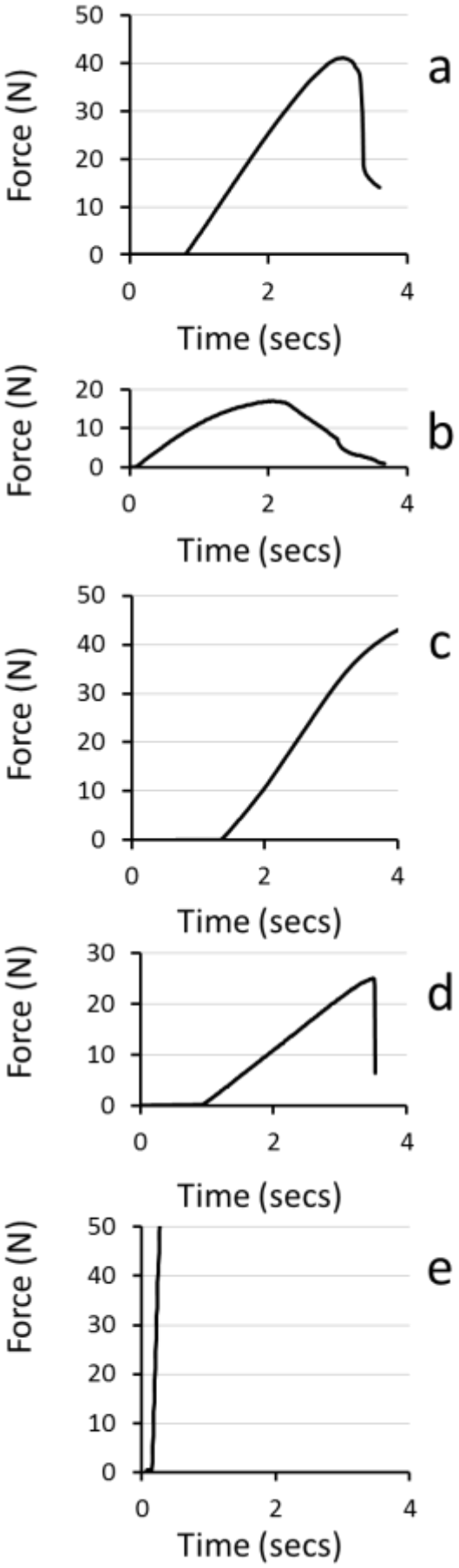


Figure 3.38 Stress strain curves derived from the mechanical testing of the plates. (a) Composite plate (un-degraded). (b) Composite plate (degraded). (c) PLA plate (un-degraded). (d) PLA plate (degraded). (e) Metal plate. To enable direct comparison between the curves, similar scales for force (y axis) and time (x axis) are shown.

Table 3.11 Mechanical testing results of in vitro experiments demonstrating mean ultimate load and flexural stiffness of tested specimens. Five types of plate were tested in addition to five groups of cadaveric rabbit bones.

Specimen	Number of samples	Mean Ultimate Load (N) ±SD	Mean Flexural Stiffness (N/mm) ±SD
Composite plate	8	56.9±12	29.7±9.6
Composite plate - degraded	3	13.2±4.8	16.4±6
PLA plate	3	45.9±0.3	19.7±0.3
PLA plate - degraded	3	23.9±3.1	9.3±1.3
Metal plate	3	200.4±20.8	422.1±40.5
Fibula	4	51.03	67.9
Bone	4	733.4±31	660±88
Bone + screw holes	3	492.6±38.1	490.7±23
Bone + composite plate	3	758.9±116.5	633.5±144.2
Bone + metal plate	3	862±54.9	863.9±57.6

The un-degraded composite plates demonstrated superior mechanical properties compared with the un-degraded PLA plates. Following degradation, both types of plates demonstrated a similar decrease in the flexural stiffness (Figure 3.40- Composite plate 47% decrease, PLA plate 55% decrease). However, the reduction in the mean ultimate load to failure was greater (77%) in the composite plates compared with the PLA plates (48%) (Figure 3.39). The results suggested a greater decrease in the strength of the composite plate following degradation compared with the PLA plate. The standard deviation in the mechanical outcomes was greater for the composite plates compared with the PLA plates suggesting greater inter-specimen variation in the mechanical properties of the degraded composite plates compared with the PLA plates.

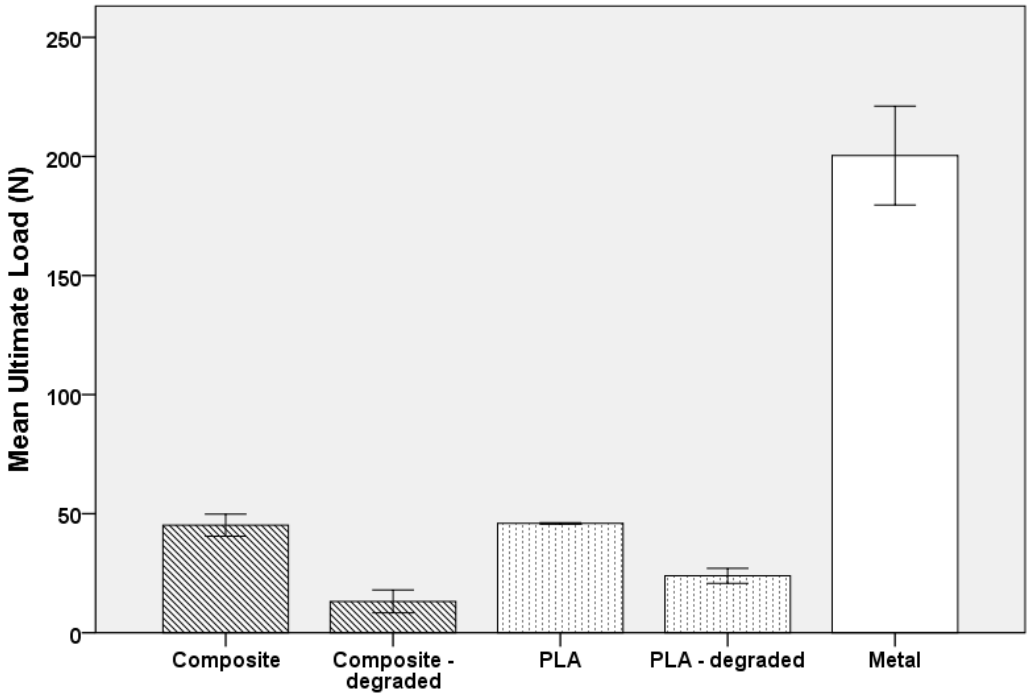


Figure 3.39 Bar chart of mean ultimate load to failure of the tested plate specimens (error bars = ±SD).

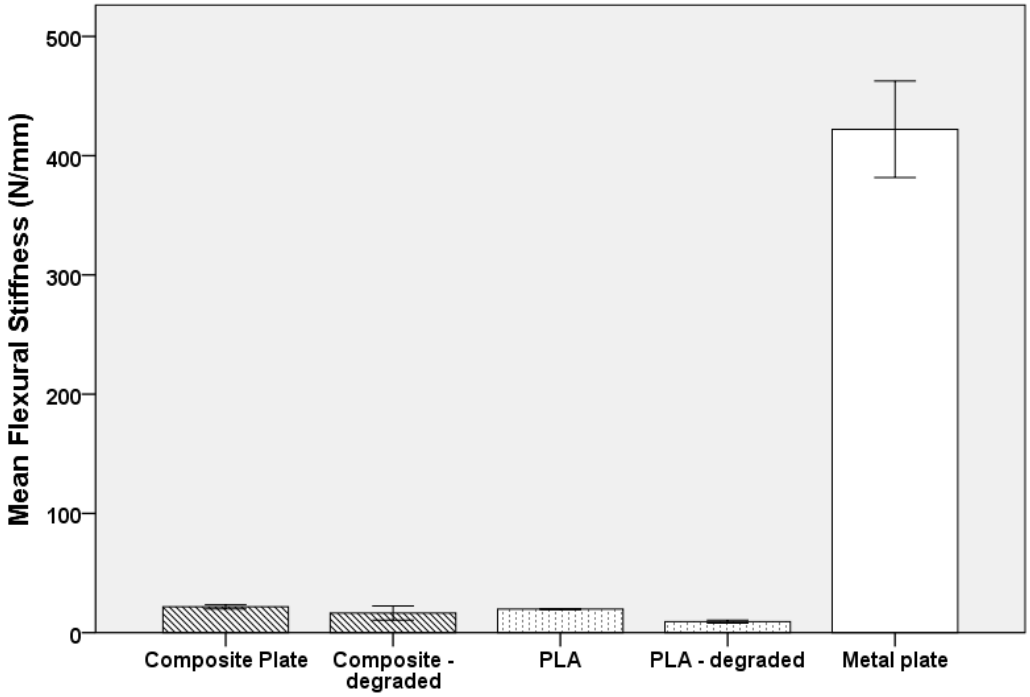


Figure 3.40 Bar chart of mean flexural stiffness of the tested plate specimens (error bars = ±SD).)

The fracture morphology of the tested bone specimens demonstrated common features (Figure 3.41). The un-plated tibiae demonstrated mainly transverse fracture patterns. The tibias with screws demonstrated failure through one of the central two screws with an oblique morphology. The fracture line always extended to either the screw head or the screw tip. In both types of plated specimens, failure occurred in the bone through an oblique fracture involving one of the central two screw holes. The composite plate demonstrated failure at the screw hole involved whilst the metal plate demonstrated bending without fracture in the plate mid-section.

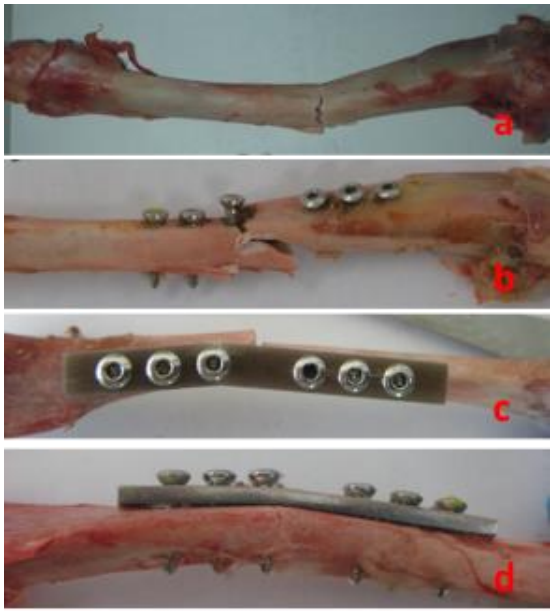


Figure 3.41 Photographs showing fractured specimens from cadaveric in vitro mechanical testing. (a) Unplated tibiae demonstrating transverse fracture. (b) Tibia with screws. Oblique fracture extending from 4th screw head to 3rd screw tip. (c) Composite plated bone demonstrating plate failure at 3rd screw hole. (d) Metal plated bone demonstrating plate bending with oblique fracture extending from 3rd screw head to 4th screw tip.

The fibula specimens demonstrated less than 10% of the mechanical properties of their respective tibias (Figures 3.42, 3.43). Comparing the results for the tibias with and without screws demonstrated reduced mechanical properties in the latter reflected by the fracture occurring through the screw holes. Comparing the composite plated cadaveric tibiae with the tibiae alone demonstrated similar mechanical properties with a higher mean ultimate load and a lower flexural stiffness in the composite plated bones. The metal plated bones demonstrated improved mechanical characteristics compared with both the tibiae alone and the composite plated bones. The standard deviations were larger for the composite plated bones compared with the metal plated bones and the tibiae alone suggesting inter-specimen variation in the mechanical properties of the composite plates.

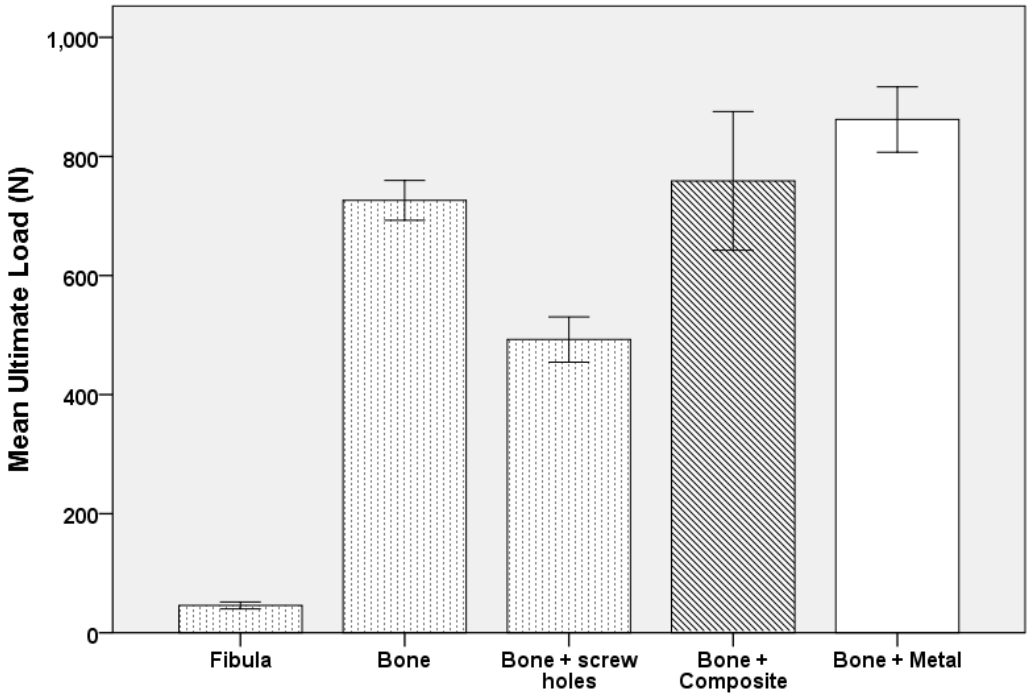


Figure 3.42 Bar chart of mean ultimate load to failure of the tested cadaveric bone specimens (error bars= ±SD).

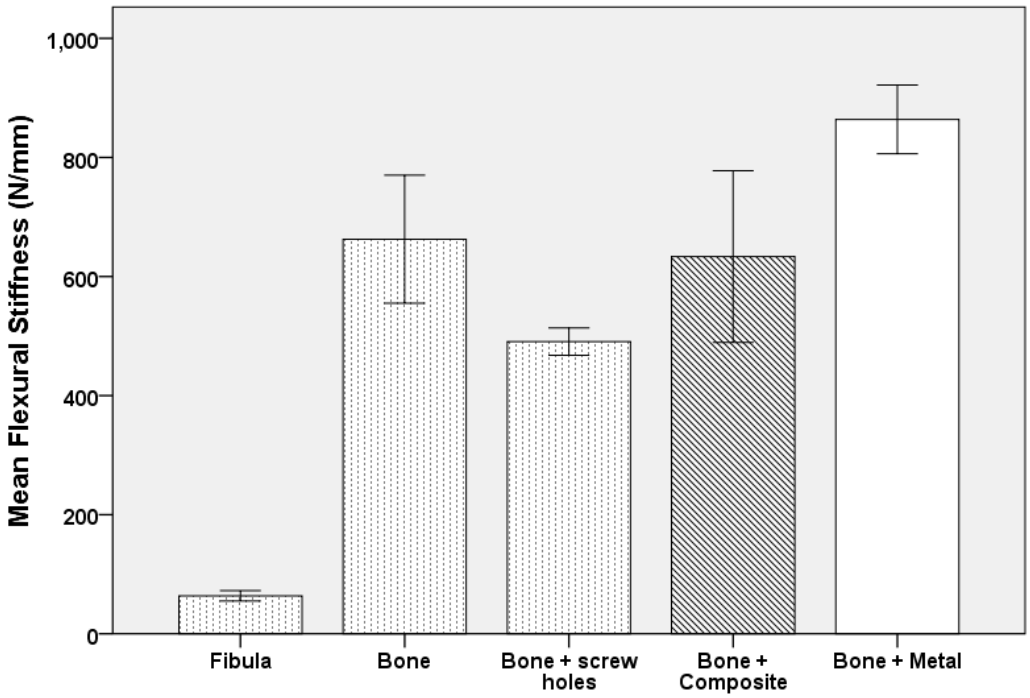


Figure 3.43 Bar chart of mean flexural stiffness of the tested cadaveric bone specimens (error bars= ±SD).

3.5.2 Fracture morphology of in vivo plated specimens and controls

The retrieved composite plated bones and their respective control bones from each time point (n=3 pairs per time point) were mechanically tested. The bone fracture morphology was similar to the cadaveric experiments with either a transverse or an oblique fracture pattern (Figure 3.44). In some specimens, no obvious fracture was visible macroscopically due to the absence of disruption in the overlying periosteum.

The mode of failure of the composite plate differed when comparing the earlier time points with the later time points. Up to 12 weeks, the plates demonstrated failure with a definable crack propagating across the laminar structure of the plate. In the 26 and 52 week specimens, it was noted that the plate fractured via a ductile mode of failure with bending and extensive deformation of the plate. The location of the plate failure in all 15 composite plated specimens was in the mid-plate region between the third and fourth screw holes. This corresponded to the position of the central roller during testing.

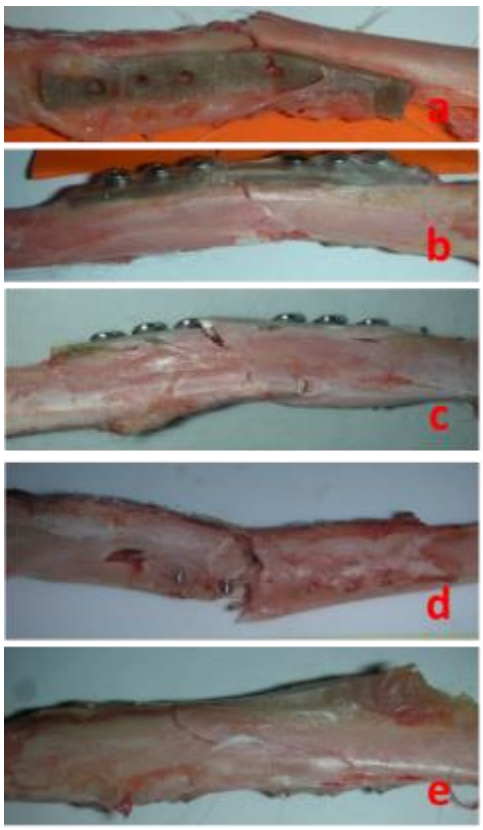


Figure 3.44 Photographs demonstrating fracture morphology in the composite plated bones at each of the time points – (a) 2 weeks, (b) 6 weeks, (c) 12 weeks, (d) 26 weeks and (e) 52 weeks. In most cases the failure occurred through an oblique fracture extending between the third and fourth screw holes.

Analogous to the composite plate group, the fifteen pairs of metal plated bones and their respective control bones retrieved at the five time points were tested to failure. The resulting fractures in the bones demonstrated transverse or short oblique fracture morphologies (see Figure 3.45). There was no difference in the fracture configuration when comparing time points. Similar to the composite plate group, the fracture always occurred in the region between the third and fourth screw holes. The mode of failure of the metal plate was always ductile with progressive plate bending. The fracture lines were less distinct in the metal plated group compared with the composite plated group. As the metal plate failed in bending rather than fracturing, this limited the displacement of the fractured bone ends compared to the composite plate group where the plate fractured leading to separation of the bone ends.

The control bones demonstrated consistent features in their fracture morphology. Twenty one out of thirty control bones failed in transverse fracture with the remaining nine demonstrating a short oblique fracture morphology. All fractures occurred within 7mm of the plate mid-section (mean 1.3mm, CI, range 0-6.9mm).

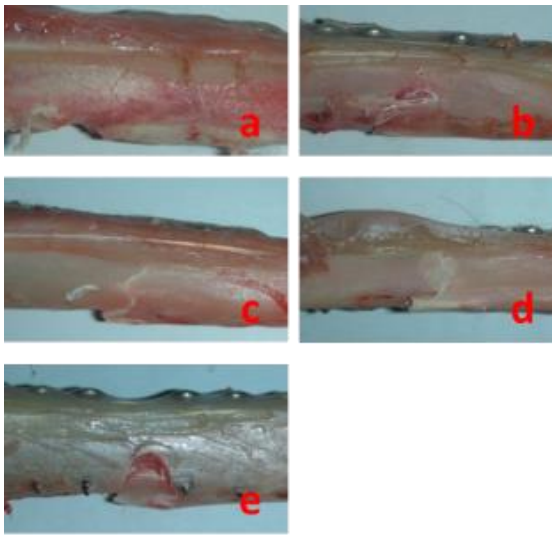


Figure 3.45 Photographs demonstrating fracture morphology in the metal plated bones at each of the time points – (a) 2 weeks, (b) 6 weeks, (c) 12 weeks, (d) 26 weeks and (e) 52 weeks. Compared to the composite plated bones, the fractures were minimally displaced.

3.5.3 Correlation between mechanical properties of control bones and host characteristics

To investigate the relationship between rabbit weight and tibia length on the mechanical properties of the control bones, correlation analysis was undertaken. The ultimate load and flexural stiffness of all 30 control bones from both plate groups retrieved at the five time points were correlated with the respective lengths of the control tibiae and the rabbit weights. Pearson's correlation coefficients were calculated (Table 3.12). There was a statistically significant correlation ($p<0.05$) for both variables. The p values were lower for the length of the control bone compared with the weight of the rabbit with respect to correlation with the mechanical testing outcomes. The scatter plots for the lengths of the control bones plotted against the ultimate load and flexural stiffness are shown in Figures 3.46 and 3.47.

Table 3.12 Pearson's correlation coefficients for correlation between results of mechanical testing and length of control bone and rabbit weight.

	Ultimate load	**Flexural stiffness**
Length of control bone	0.521 (p=0.003)	0.599 (p=0.000)
Rabbit weight	0.454 (p=0.012)	0.510 (p=0.004)

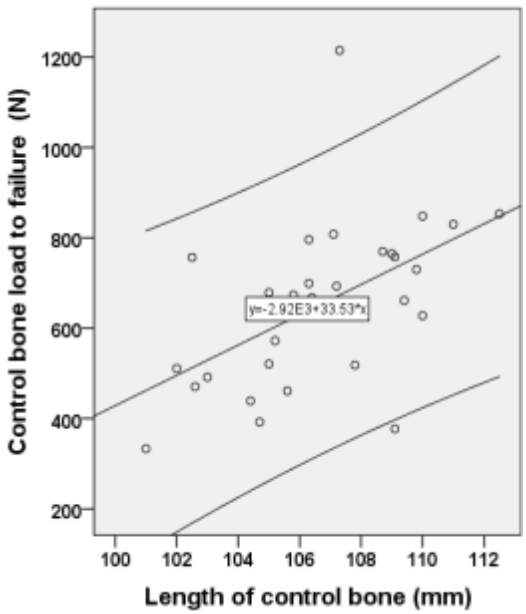


Figure 3.46. Scatter plot of length of control bone against load to failure demonstrating line of best fit with 95% confidence intervals

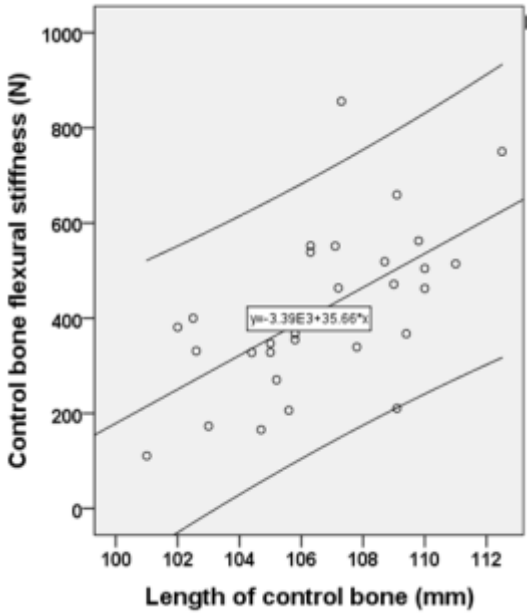


Figure 3.47. Scatter plot of length of control bone against flexural stiffness demonstrating line of best fit with 95% confidence intervals

3.5.4 Ultimate load of in vivo plated specimens

The mean ultimate load to failure in the control bones increased up to 12 weeks in the metal plated group and 26 weeks in the composite plated group before falling at 52 weeks (Tables 3.13 and 3.14). This suggested a period of growth up to a point between these two time points where there was a concurrent improvement in mechanical properties of the bone. The mean ultimate load in the composite plate – bone construct was greater than in the opposite control bone at each of the time

points (Table 3.13). This relative improvement remained fairly constant with the composite plated bones demonstrating a mean ultimate load between 172.2% and 179.4% relative to the control bones at all but one time point (Figure 3.48). There was a dip in the mean normalised ultimate load at 26 weeks where the composite plated bones demonstrated a mean ultimate load of 114.8% relative to the control bones.

Table 3.13 Table of mean ultimate load to failure of retrieved composite plated bones and their respective control bones at each of the five time points. The normalised ultimate load (NUL)* expresses the composite plated bone's ultimate load as a percentage of the respective control bone's ultimate load.

Duration of implantation (weeks)	Number of samples	Mean composite plate-bone ultimate load (N) [±SD]	Mean control bone ultimate load (N) [±SD]	Mean NUL* (%)[±SD]
2	3	912±59.9	507.6±8.5	179.4±16
6	3	829.9±20.7	516.8±105.6	174.2±58.4
12	3	945.3±43.7	622.1±126	172.2±87.6
26	3	1002±134	932.7±252.1	114.8±41.2
52	3	991.2±484.1	599.4±153.7	178.3±120.5

The metal plated bones demonstrated a greater augmentation in the mean normalised ultimate load (NUL)compared with the composite plated bones (Table 3.14, Figure 3.48). The improvement in the mean NUL in the metal plated bones was 286% at 2 weeks compared with 179.4% in the composite plated bones. However, this relative improvement decreased with the passage of time (Table 3.14). At 52 weeks, the improvement in the mean NUL in the metal plated bones (101.1%) was less than that of the composite plated bones (178.3%). Comparing the results of the two types of plated bones required consideration of the mechanical properties of the two types of plate. The metal plate demonstrated a significantly higher mean ultimate load compared with the composite plate in the in vitro tests. This suggested that there was a substantial deterioration in the mechanical properties of the metal plated bones at 52 weeks reflecting the bone loss beneath the plate.

Table 3.14 Table of mean ultimate load to failure of retrieved metal plated bones and their respective control bones at each of the five time points. The normalised ultimate load (NUL)* expresses the composite plated bone's ultimate load as a percentage of the respective control bone's ultimate load.

Duration of implantation (weeks)	Number of samples	Mean metal plate-bone ultimate load (N) [±SD]	Mean control bone ultimate load (N) [±SD]	Mean NUL* (%)[±SD]
2	3	1239.6±88	433±39.3	286±8.3
6	3	1735.8±411.3	687.5±63.4	250.9±46.4
12	3	1764.7±195.4	808.5±39.2	218.4±24.3
26	3	1389.2±244.8	719.7±95.6	192.5±14.3
52	3	686.2±185.6	688±65.4	101.1±31.4

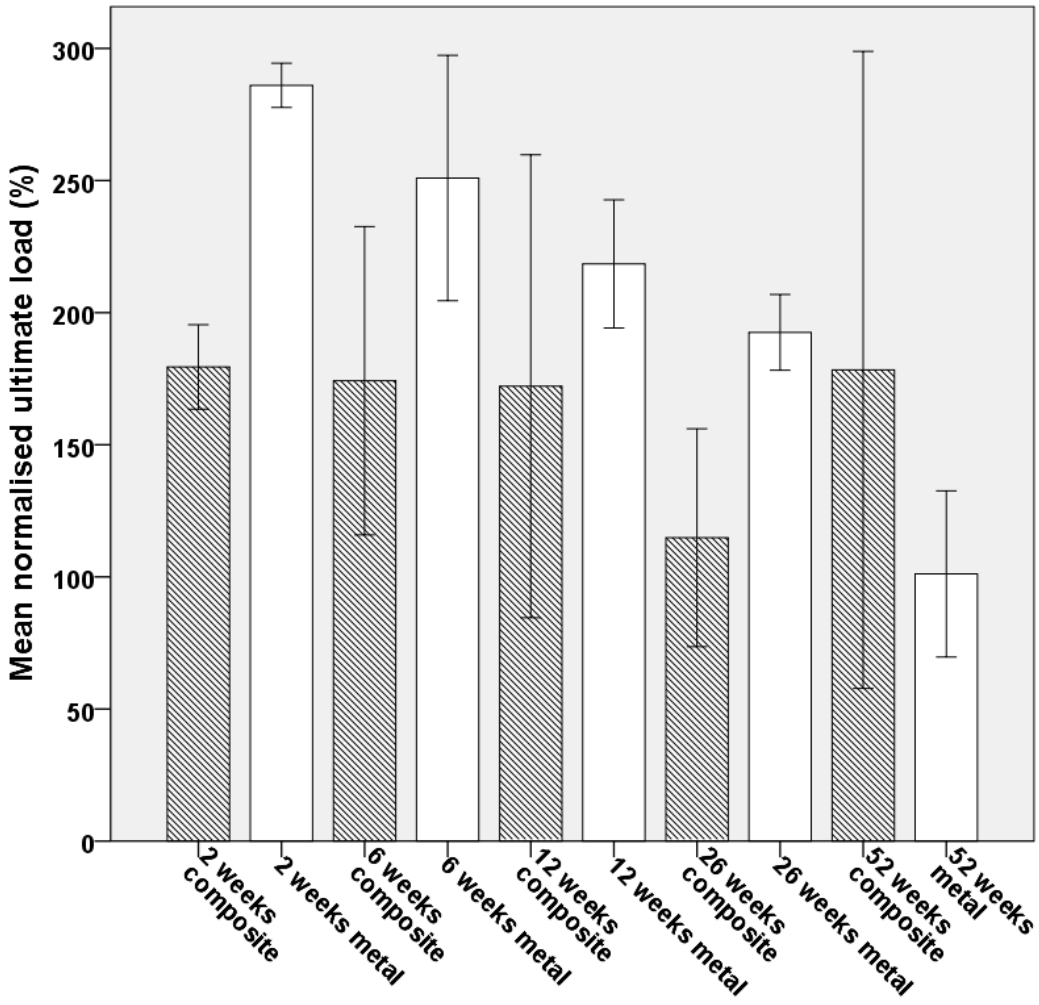


Figure 3.48 Bar chart of mean normalised ultimate load (%) of the composite and metal plated bones at each time point (error bars= ±SD).

A Two way ANOVA test was undertaken to assess the influence of type of plate and duration of implantation on the normalised ultimate load (NUL). There were no outliers greater than three box lengths from the edge of the box in boxplots. The data was not normally distributed in one out of the ten cells (composite plated samples at 2 weeks, p=0.039). The assumption of homogeneity of variances was violated (Levene's test, p=0.003) reflecting the limited sample sizes and large standard deviations. In view of the data sets being normally distributed and the ratio of the largest group variance to the smallest group variance equating to less than 3, the two way ANOVA was undertaken.

The two way test for the normalised ultimate load (NUL) did not reveal any significant two way interaction effect between the type of plate and the duration of implantation. The mean NUL was significantly lower in the composite plated samples (179.4%) compared with the metal plated samples (286%) at 2 weeks (p=0.031) but not at the subsequent time points. Comparing the Mean NUL at different time points did not reveal any significant difference in the composite plated samples. In the metal plated samples, the mean NUL was significantly lower at 52 weeks (101.1%) compared with at 2 weeks (286%, p=0.007) and 6 weeks (250.9%, p=0.039).

Post hoc sample size calculation was undertaken to determine the appropriate sample size to observe the measured difference in mean normalised ultimate load when comparing the composite (mean 178, sd 121, n=3) and metal (mean 101, sd 31, n=3) groups at 52 weeks. The calculation yielded a sample size of n=17 in each group with 80% power and 5% sensitivity reflecting the large standard deviations in both groups.

3.5.5 Flexural stiffness of in vivo plated specimens

The results of the mean flexural stiffness of the control bones demonstrated a similar trend to the mean ultimate load. The mean stiffness progressively increased up to 26 weeks in the composite plated group (Table 3.15) and 12 weeks in the metal plated group (Table 3.16) suggesting increases in stiffness relating to growth occurring up to this point. The mean flexural stiffness of the composite plated bones relative to the controls increased up to 317% at 6 weeks before falling to near equivalence at 109.9% at 26 weeks (Figure 3.49). A similar dip in the normalised ultimate load was observed in the composite plated bones at 26 weeks. The mean normalised flexural stiffness of the composite plated bones increased from 26 weeks to 52 weeks. The reduction in ultimate load and flexural stiffness up to 26 weeks followed by improvement suggested a progressive stress shielding response up to a time point between 26 and 52 weeks after which the stress shielding effect reduced allowing recovery of the mechanical properties of the composite plated bones.

Table 3.15 Table of mean flexural stiffness of retrieved composite plated bones and their respective control bones at each of the five time points. The normalised flexural stiffness (NFS)* expresses the composite plated bone's flexural stiffness as a percentage of the respective control bone's flexural stiffness.

Duration of implantation (weeks)	Number of samples	Mean composite plate-bone flexural stiffness (N/mm) [±SD]	Mean control bone flexural stiffness (N/mm) [±SD]	Mean NFS* (%) [±SD]
2	3	694.4±105.3	294±62.4	244.5±35.6
6	3	684.3±140.8	329.6±123.7	317.2±254
12	3	722.4±104	408.6±102.3	205.4±101.4
26	3	783.5±228.5	722.8±148.5	109.9±29.7
52	3	768.1±323.2	316.1±138.4	283±205.6

The metal plated bones demonstrated a greater augmentation in the mean flexural stiffness relative to the control bones compared with the composite plated bones at the earlier time points. At 2 weeks, the metal plated bones demonstrated a mean normalised flexural stiffness(NFS) of 465.6% compared with 244.5% in the composite plated bones. However, there was a progressive reduction in the mean NFS from 2 weeks onwards (Figure 3.49) similar to the reductions observed in the mean ultimate load. At 52 weeks, the mean NFS was 171.3% compared with 283% in the composite plated bones.

Table 3.16 Table of mean flexural stiffness of retrieved metal plated bones and their respective control bones at each of the five time points. The normalised flexural stiffness (NFS)* expresses the metal plated bone's flexural stiffness as a percentage of the respective control bone's flexural stiffness.

Duration of implantation (weeks)	**Number of samples**	**Mean metal plate-bone flexural stiffness (N/mm) [±SD]**	**Mean control bone flexural stiffness (N/mm) [±SD]**	**Mean NFS* (%)[±SD]**
2	3	1138.2±88.4	274.8±94.6	465.6±224.8
6	3	1611.3±669.3	374.1±23.3	434.3±196.2
12	3	1569.1±273.8	510.9±45	306.5±37.8
26	3	1409.1±178.9	430.4±75.7	330.5±39.9
52	3	791±66.5	503.5±156.2	171.3±70.7

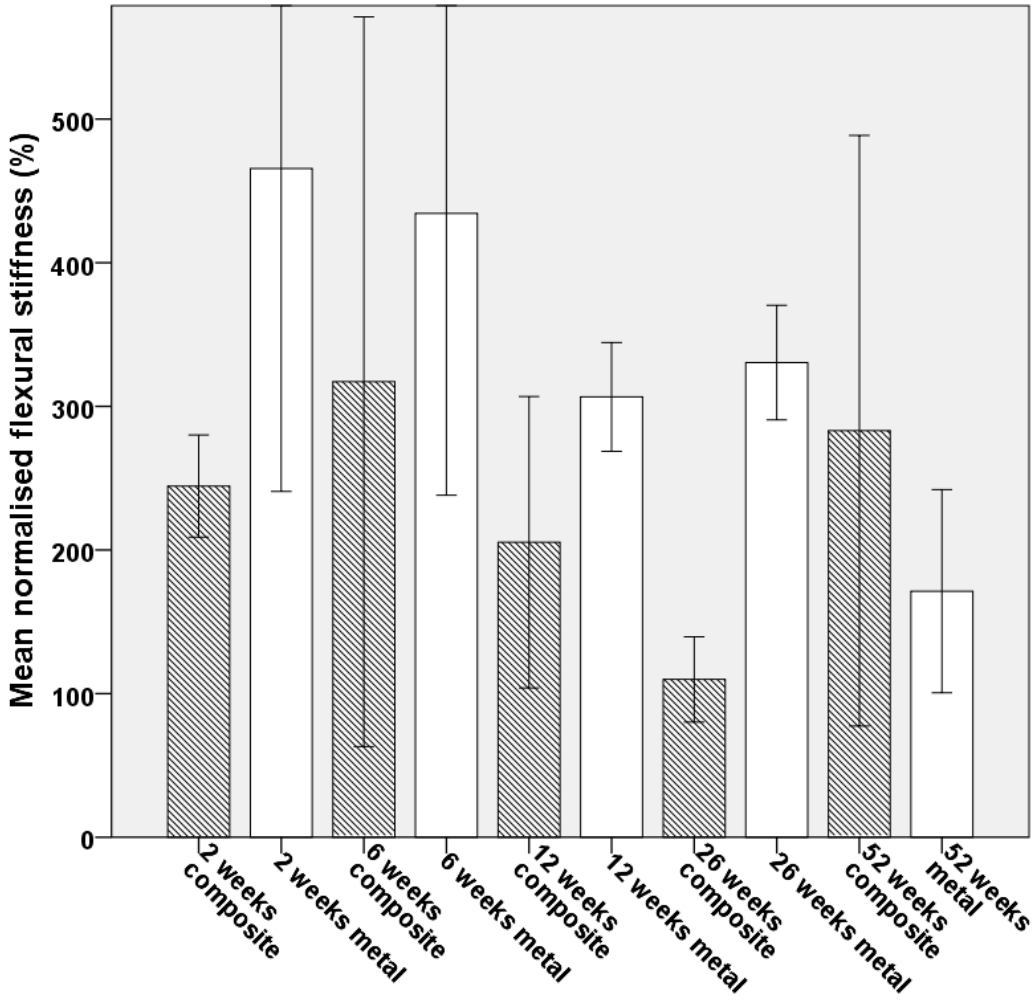


Figure 3.49 Bar chart of mean normalised flexural stiffness (%) of the composite and metal plated bones at each time point (error bars= ±SD).

Two way ANOVA testing was undertaken to assess the influence of type of plate and duration of implantation on the normalised flexural stiffness (NFS). There were no outliers greater than three box lengths from the edge of the box in boxplots. The data was normally distributed as assessed by the Shapiro-Wilk test ($p>0.05$). The assumption of homogeneity of variances was violated on conducting Levene's test ($p=0.01$) reflecting the limited sample sizes and large standard deviations. In view of the data sets being normally distributed and the ratio of the largest group variance to the smallest group variance equating to less than 3, the two way ANOVA was undertaken.

The two way ANOVA for the normalised flexural stiffness (NFS) did not reveal any significant two way interaction effect between the type of plate and the duration of implantation. Pairwise analysis did not demonstrate any significant difference when comparing the NFS for the two types of plate at each time point, or a significant difference between the mean NFS between different time points for each type of plate.

The results suggest that there was a greater attenuation in the bending mechanical properties of the metal plated bones compared with the composite plated bones as the duration of implantation increased. Although these changes were not statistically significant when assessing the flexural stiffness, there was a significant difference in the normalised ultimate load in the metal group at 52 weeks compared with the first two time points. Post hoc sample size calculation was undertaken to determine the appropriate sample size to observe the measured difference in mean normalised flexural stiffness when comparing the composite (mean 283, sd 205.6, n=3) and metal (mean 171.3, sd 70.7, n=3) groups at 52 weeks. The calculation yielded a sample size of n=26 in each group with 80% power and 5% sensitivity reflecting the relatively small difference between the two groups and the large standard deviations.

3.6 Results Paraffin embedded histology

3.6.1 Inflammatory response in Composite plated specimens and controls

The composite plated and respective control tibiae from three out of five rabbits from each time point were processed for paraffin histology. One block was taken from each composite plated tibia in the central plate region. The distance of the block from the top of the bone was used to generate a block at the same level in the respective control bone. The blocks were processed to generate representative slides which were stained with a Giemsa stain to detect inflammatory cells.

Table 3.17 shows the absolute numbers of macrophages and neutrophils found in the specific region of interest in each of the three slides per time point. No macrophages were observed in the control samples. In the composite plated samples, macrophages were detected on the composite plated slides at each time point (Figure 3.50). Macrophage activity was present on 2 slides at 2 weeks, 1 slide at 6 weeks, 2 slides at 12 weeks, 1 slide at 26 weeks and 2 slides at 52 weeks. The macrophage counts were low in all but one of these slides, generally numbering one or two. However, in one slide at 12 weeks, seven macrophages were noted. At each time point at least one out of three slides did not have any detectable macrophages. There did not appear to be any relationship between the duration of implantation and the number of macrophages detected in both the composite plated and control specimens.

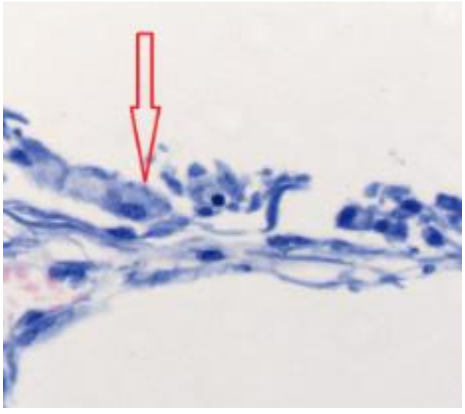


Figure 3.50 A photomicrograph demonstrating a cell with morphology resembling a macrophage (red arrow) in the interface tissue in a composite plated specimen at 12 weeks. [Giemsa stain, obj. x 40]

Table 3.17 Numbers of macrophages and neutrophils in composite plated specimens and their respective controls

Duration of implantation	Sample	Composite plate macrophages	Control macrophages	Composite plate neutrophils	Control neutrophils
2 weeks	2A	0	0	1	0
2 weeks	2B	2	0	8	0
2 weeks	2C	2	0	1	0
6 weeks	6A	0	0	0	0
6 weeks	6B	1	0	12	0
6 weeks	6C	0	0	0	0
12 weeks	12A	1	0	0	0
12 weeks	12B	0	0	0	0
12 weeks	12C	7	0	1	2
26 weeks	26A	1	0	16	0
26 weeks	26B	0	0	0	0
26 weeks	26C	0	0	1	0
52 weeks	52A	1	0	0	0
52 weeks	52B	2	0	0	0
52 weeks	52C	0	0	0	1

In the control specimens, neutrophils were only observed in two specimens- at 12 and 52 weeks. Both counts were less than two. In the composite plated specimens, neutrophils were observed at all time points in at least one slide except at 52 weeks (Figure 3.51). However, they were only observed on seven out of the total of 15 slides. Four slides at different time points demonstrated one neutrophil alone (two at 2 weeks, one at 12 weeks and one at 26 weeks). In the three remaining slides, higher counts were observed. The largest number was found at 26 weeks (n=16) followed by 6 weeks (n=12) and 2 weeks (n=8). There was no obvious relationship between the duration of implantation and the number of neutrophils observed in the composite plated samples when comparing the different time points.

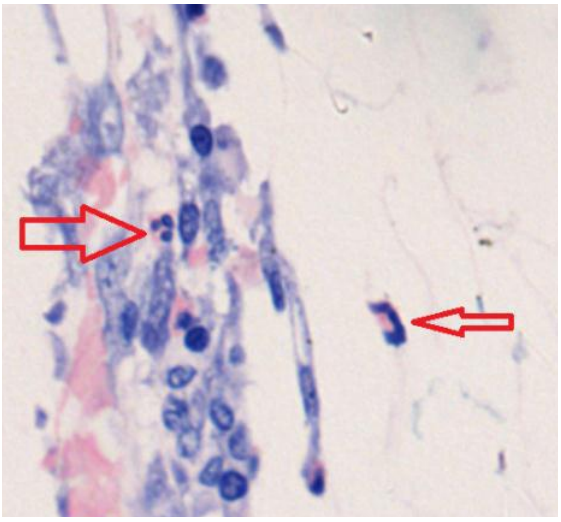


Figure 3.51 A photomicrograph showing neutrophils (red arrows) in the interface tissue in a composite plated sample retrieved at 2 weeks. [Giemsa stain, obj. x 4]

3.6.2 Inflammatory response in metal plated specimens and controls

The metal plated tibia and respective control from each of three rabbits from the first time points (2, 6 and 12 weeks) were used to generate slides corresponding to the central plate region. Difficulties were encountered in sectioning the metal slides due to the presence of metal debris. Consequently, at the 6 week time point slides could only be generated for two rabbits out of three (6A and 6B). A total of 8 slides were suitable for further processing and were stained with the Giemsa stain to detect neutrophils and macrophages. Table 3.18 shows the absolute numbers of neutrophil and macrophage counts in the pre-determined region of interest for the metal plated specimens and their respective controls. Macrophages were detected at each surveyed time point. A solitary macrophage was observed on each of these slides with the exception of one slide at 2 weeks where three macrophages were observed. No macrophages were observed in the control specimens. No neutrophils were observed on any of the metal plated or control slides.

Table 3.18 Numbers of macrophages and neutrophils in metal plated specimens and their respective controls.

Duration of implantation	Sample	Metal plate macrophages	Control macrophages	Metal plate neutrophils	Control neutrophils
2 weeks	2A	3	0	0	0
2 weeks	2B	1	0	0	0
2 weeks	2C	1	0	0	0
6 weeks	6A	0	0	0	0
6 weeks	6B	1	0	0	0
12 weeks	12A	1	0	0	0
12 weeks	12B	0	0	0	0
12 weeks	12C	1	0	0	0

The marked variation in the numbers of both cell types observed combined with the limited sample size did not permit statistical analysis to compare the metal plated and composite specimens. However, the macrophage cell counts were equivalent or lower at each time point in the metal plated samples compared with the composite plated samples. The presence of neutrophils at each comparable time point in the composite plated samples compared with the complete absence of this cell type in the metal plated samples suggested a difference in the inflammatory response to the two types of plate.

3.6.3 Structural bone changes in the plated bones

The TRAP stained slides demonstrated changes in the bone architecture at progressive time points in both groups. At 2 weeks there was evidence of new bone formation around the periphery of the plate and in the opposite cortex (Figure 3.52). The newly formed bone had a loose areolar structure which distinguished it from the pre-existing compact bone. The new bone demonstrated a specific distribution with formation around the sides of the plate and in the opposite cortex close to the screw tip. This corresponded with the sites of periosteal disruption during surgical

application of the plate and screws. This pattern of bone was observed in both metal and composite plated specimens at the 2 week time point. In comparison to the opposite control bone, the new bone significantly increased the cross sectional bone area.

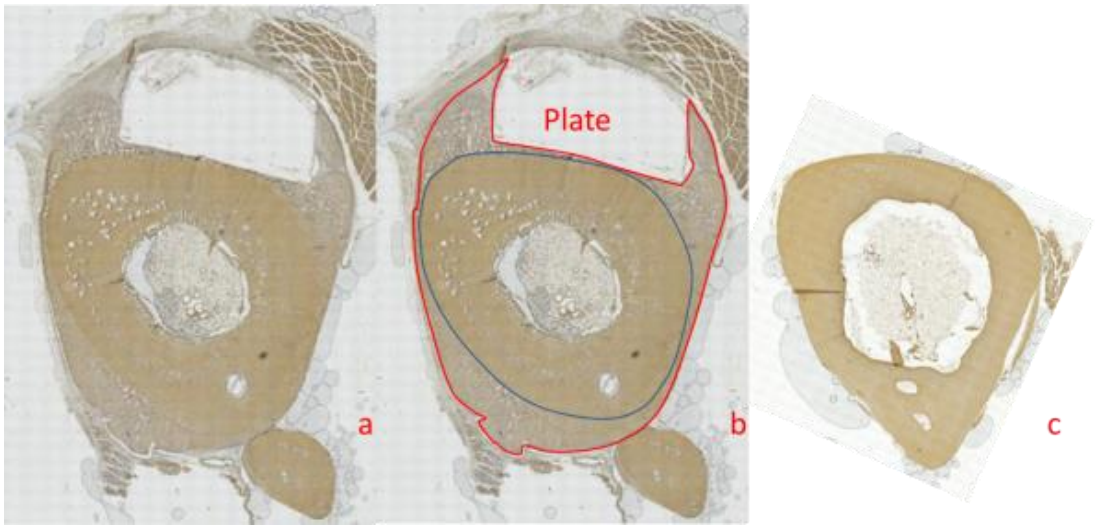


Figure 3.52 TRAP stained slides from a composite plated tibia (a), same image highlighting features (b) and respective control tibia (c) retrieved at 2 weeks. The image of the control tibia (c) has been flipped horizontally to allow direct comparison of the cortical outlines. (b) In the composite plated bone, the plate was chemically removed prior to embedding. The new bone around the plate and in the opposite cortex (red) was clearly distinguishable from the pre-existing cortical bone (blue) due to the former's less compact appearance. The new bone increased the cross sectional area of the composite plated bone compared with the control bone (c) [TRAP stain, objx5].

The bone which formed against the sides of the plate became progressively more compact with the passage of time (Figure 3.53). At 6 weeks, the bone had a denser appearance and at 26 weeks, the new bone was indistinguishable from the neighbouring pre-existing cortical bone. In some of the slides, there was bone formation over the top of the plate. The new bone around the plate endured up to 52 weeks. In contrast to this bone formation, bone loss was observed in the cortex beneath both types of plate (Figure 3.54). This was most apparent at the later time points of 26 and 52 weeks. This led to a change in the cross sectional area properties of the plated bones due to the selective bone formation and loss. These changes were progressive up to 52 weeks.

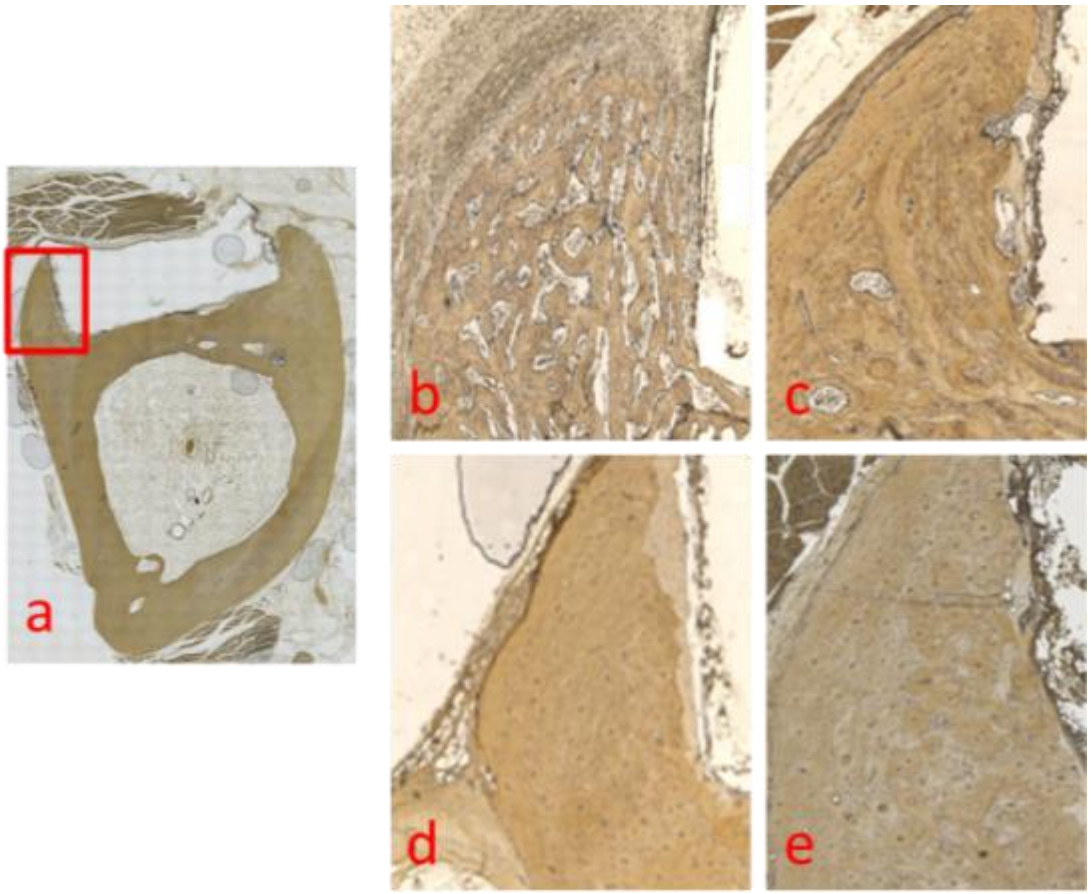


Figure 3.53. (a) TRAP stained slide of a composite plated specimen retrieved at 12 weeks demonstrating the region of interest shown in the slide images to the right. (b-e) Slide images demonstrating region of interest of bone formation around the side of the plate in composite plated specimens retrieved at (b) 2 weeks, (c) 6 weeks, (d) 26 weeks and (e) 52 weeks [TRAP stain, objx5].

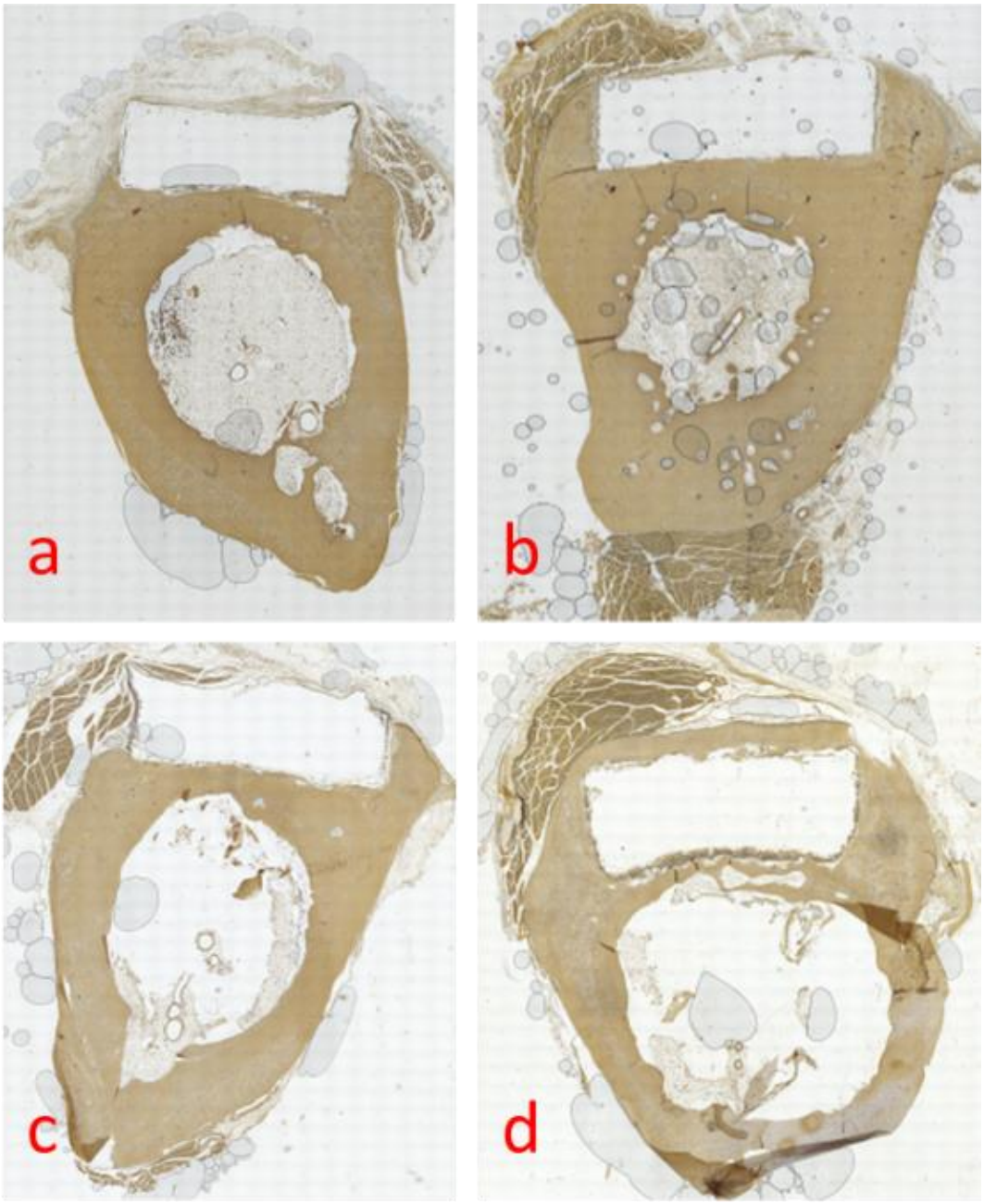


Figure 3.54 TRAP stained slides of composite plated tibiae retrieved at (a) 6 weeks, (b) 12 weeks, (c) 26 weeks and (d) 52 weeks. Bone formation occurred around the plate periphery with a complete bony envelope around the plate at 52 weeks (d). In contrast there was evidence of progressive cortical thinning beneath the plate. At 26 weeks (c) and 52 weeks (d), there was obvious cortical thinning beneath the plate [TRAP stain, objx5].

Histological evaluation of the cortex in the plated bones demonstrated that the new bone formation occurred through centripetal growth rather than centrifugal growth (Figure 3.55). In the 2 week sample, there was a clear line of distinction between the pre-existing cortex and the overlying new bone (Figure 3.55b). This new bone had a uniform appearance with a loose areolar structure compared with the underlying compact cortical bone. At 6, 12 and 26 weeks, the overlying new bone was still distinguishable from the cortical bone but had increased in thickness. However, the new bone did not demonstrate a uniform appearance (Figure 3.55c-e). The outermost new bone demonstrated a more compact appearance compared with the new bone closest to the pre-existing cortex. This suggested that the circumferential growth of the plated bones occurred through centripetal growth with new bone forming under the periosteum and being deposited on to the pre-existing cortex. Therefore, in the newly formed bone, the most compact mature bone was found outermost. At 52 weeks (Figure 3.55f) there was no obvious distinction between the pre-existing cortex and the new bone formation. However, the bone morphology demonstrated a denser architecture in the outer cortex compared with the inner cortex suggesting continued remodelling in the latter at this time point. This remodelling on the inner cortex was associated with cortical thinning beneath the plate at this final time point.

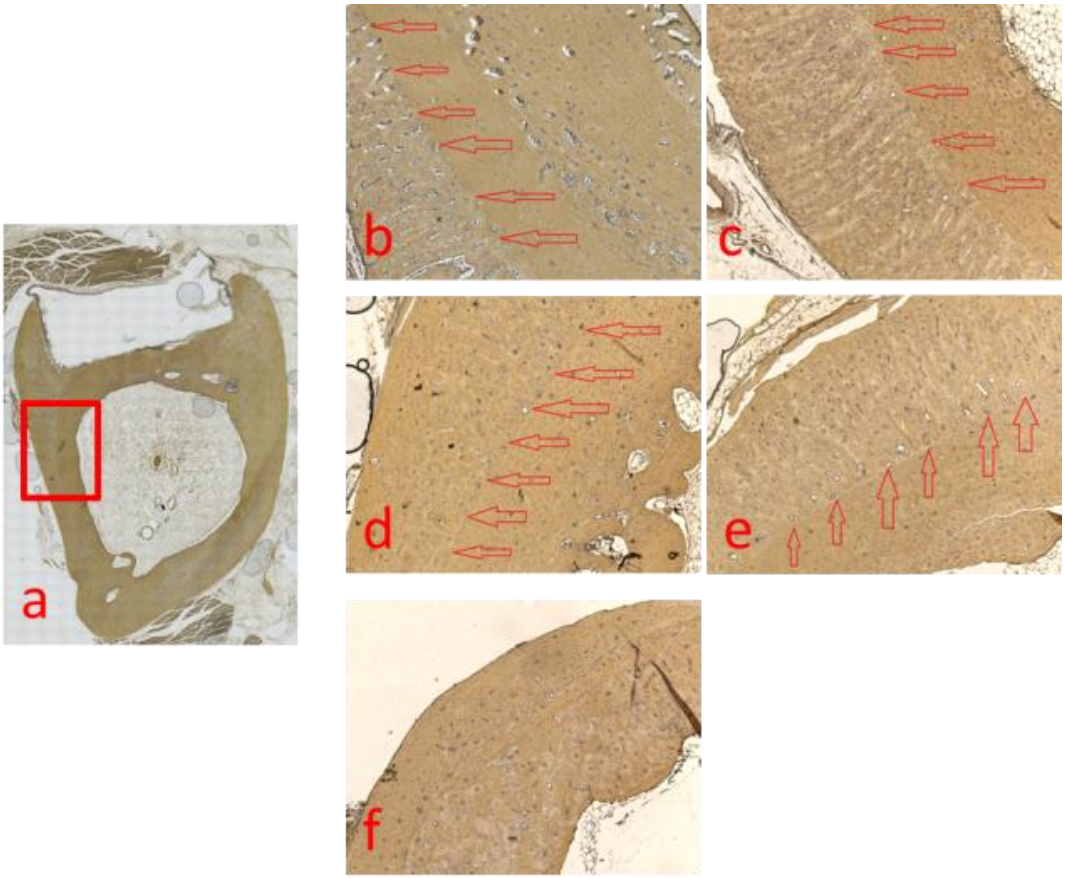


Figure 3.55 (a) TRAP stained slide of a composite plated specimen retrieved at 12 weeks demonstrating the region of interest shown in the photomicrographs to the right. (b-f) Photomicrographs depicting region of interest in the composite plated specimens retrieved at (b) 2 weeks, (c) 6 weeks, (d) 12 weeks, (e) 26 weeks and (f) 52 weeks [TRAP stain, objx5]. In the 2 and 6 week samples (b, c) the dense cortical bone was distinguishable from the overlying new bone (red arrows). In the specimens at 26 and 52 weeks (d, e) the distinction was still present. However, the new bone appeared less uniform with dense compact bone on the outer surface and less compact bone near the line of distinction suggesting a centripetal pattern of bone growth. At 52 weeks (f), there was no obvious distinction between the new bone and pre-existing cortex. However, the outer cortical bone was more compact compared with bone on the inner surface suggesting continued remodelling in the inner cortex [TRAP stain, objx5].

Chapter 4 Discussion

The aim of the current study was to evaluate the feasibility of using the current bioresorbable composite plate to fix an osteotomy in an in vivo animal model. The single experiment demonstrated early failure with analysis showing significant limitations in the composite plate design precluding further testing in an osteotomy model. Consequently, the study aims were redesigned to compare the in vivo effects of the composite plate in an intact bone model with a similarly dimensioned metal plate. The specific outcomes of interest were changes in the extent of bone loss observed beneath the plate in different regions, the mechanical properties of the plated bones and inflammatory response with an increasing duration of implantation. The aim was to determine if stress shielding induced changes induced by a metal plate could be attenuated through the use of a composite plate with mechanical properties closer to bone.

4.1 Structural changes in the plated bones

This study utilised different scientific techniques to characterise the influence of the two types of plate on structural changes in the underlying bone. These included cortical thickness from plain radiographs and bone area measurements from Micro CT and SEM images. Previous studies have thrown up conflicting findings regarding the structural changes in bone induced by application of different types of plate prompting speculation that the discordant findings may reflect differences in the animal models and sites of implantation studied[49, 59]. Thus, it was important in the current study to establish concurrent validity by measuring the same structural parameters utilising different analytical techniques.

4.1.1 Plain radiographic assessment

The plain radiographs were used to determine growth related changes in the bone and to compare cortical thickness measurements. The plain radiographs demonstrated an increase in the length of the plated tibias at sequential time points reflecting growth of the host. The maximum increase in the length of the plated tibia was less than 10% of the overall length and principally occurred during the first 12 weeks following implantation. Longitudinal growth of the tibia was accompanied by a change in the plate position relative to the bone. The magnitude of plate migration was comparable for different groups of animals in the two arms of the experiment adding validity to sampling based on referencing the plate's position in the Micro CT and scanning electron microscopy experiments.

The plain radiographs demonstrated structural changes in the plated bones with an increasing duration of implantation. Cortical thinning was observed in both types of plates but was greater in the metal plated bones. In comparison with the cortical thickness measurements on the Micro CT images, similar measurements on the plain radiographs overestimated the reduction in cortical thickness. The thickness of the visualised cortex on plain radiographs is dependent on the rotational alignment of the bone relative to the plane the radiograph is taken in. The cortical thickness on a radiograph is measured in the region of the cortex which is directly perpendicular to the direction of the x-ray beam. Therefore, differences in rotation alignment between different plated bones result in cortical thickness measurements from different regions of the bone reducing the reliability of measurement (see Figure 4.1). Rotational alignment also limits the use of radiographs in cortical thickness measurements in metal plated bones. If the metal plated bone is not rotationally aligned the cortex cannot be visualised beneath the plate producing errors in measurement (see Figure 4.1c).

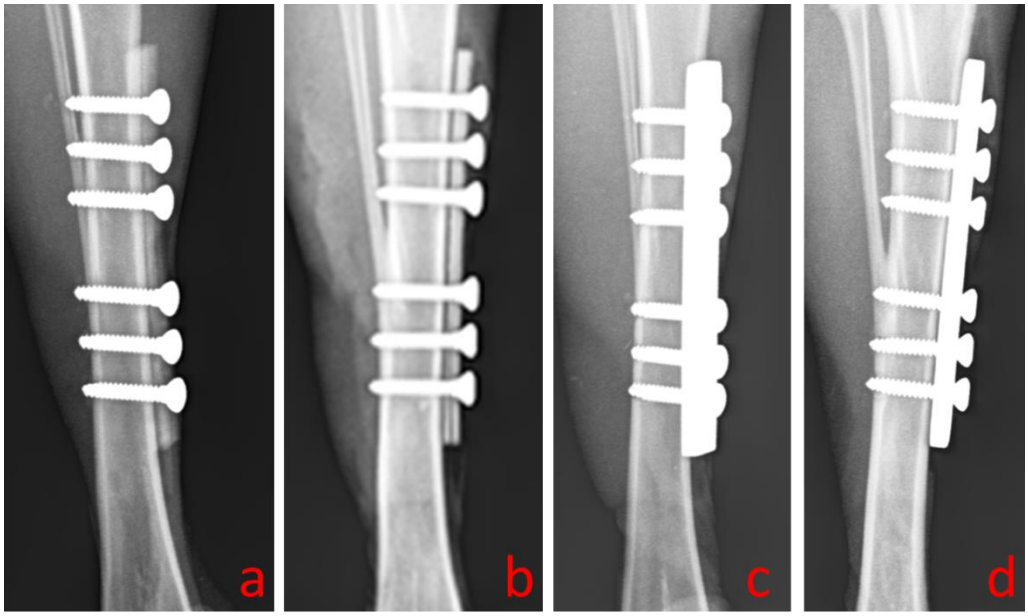


Figure 4.1 Radiographs showing differences in rotational alignment of the composite (a-b) and metal (c-d) metal plated tibias. Radiographs in the correct orthogonal plane show the edge of the plate "end on" (b,d). If the plated bone is slightly rotated an oblique profile of the plate is seen on the radiograph (a,c).

4.1.2 Cross sectional analysis using Micro CT and Scanning Electron Microscopy (SEM)

These techniques enabled measurement of (a) the cortical thickness beneath the plate; (b) the area of bone in a pre-determined region of interest beneath the plate; and (c) the total cross-sectional area of bone at a particular level (Micro CT only). Two levels were selected for evaluation corresponding to the mid-section of the plate and the plate periphery. These levels were selected to demonstrate potential differences in the bone loss beneath different regions of the plate[52, 89]. The plate mid-section (level 1) corresponded to the region of bone beneath the centre of the plate between the central two screws (3rd and 4th). The plate periphery (level 2) corresponded to the plate region between the 1st and 2nd screws at the proximal aspect of the plate. The normalised measurements expressed these geometric parameters in the plated bones as percentage functions of the same measurements in the respective control bones. These normalised outcomes enabled comparison of different sized rabbits from different time points in the two arms of the study.

In the composite plated bones, there was a marginal reduction in the cortical thickness in the plate periphery as the duration of implantation increased. In the Micro CT study, there was no significant difference when comparing the normalised cortical thickness (NCT) at level 1 in the composite plate group between different time points. In the scanning electron microscopy (SEM) study, there was no significant difference when comparing the NCT at level 1 between different time points. The results suggest that the composite plate did not induce significant bone loss at the plate periphery.

In the plate mid-section (level 2), cortical thickness decreased in the composite plate group as the duration of implantation increased. In the Micro CT study, the mean level 2 NCT was significantly lower in the composite plated samples at 26 weeks and 52 weeks compared with at 2 weeks. Comparing the NCT between the two levels at each time point in the composite plated group did show statistically significant differences in cortical thickness between the plate periphery and plate mid-section. In the Micro CT study, there was a statistically significant difference in NCT between the two levels in the composite plated bones at every time point except 2 weeks. In the SEM study, there was a statistically significant difference at two time points – 2 weeks and 26 weeks. The results suggest that there was a progressive reduction in cortical thickness at level 2 as the duration of implantation increased which was not observed in the plate periphery.

In the metal plated group, comparing the cortical thickness at both levels revealed a significant difference at only one time point. In the SEM study, the mean normalised cortical thickness (NCT) was significantly lower at level 2 compared with level 1 at 12 weeks. Although this was the only statistically significant result, analysis of the mean NCT at both levels demonstrated reduced cortical thickness at the plate mid-section compared with the plate periphery. The ANOVA testing enabled comparison of the two types of plate with respect to differences in the normalised cortical thickness at each time point. At the plate periphery, the NCT was significantly lower in the metal group compared with the composite group at 26 weeks. At the plate mid-section, the mean NCT was significantly lower in the metal group at 52 weeks. Multiple pairwise comparisons yielded few statistically significant differences between the two levels and the two types of plate reflecting the small sample size.

However, cumulative analysis of the statistically significant findings agree that (i) greater bone loss was observed in the plate mid-section than in the plate periphery; (ii) the bone loss was greater in the metal group compared with the composite group and (iii) the magnitude of bone loss was progressive with an increasing duration of implantation. Although the sample sizes in each experiment were small, the results of both types of experiment, Micro CT and scanning electron microscopy, support the same effects establishing concurrent validity.

The Micro CT and scanning electron microscopy (SEM) studies enabled determination of the cortical cross-sectional area in a defined area beneath the plate at the two levels. In the Micro CT study there were statistically significant differences in the normalised cortical area (NCA) between different time points in the composite plated samples. At the plate periphery, there was a significant reduction in the mean NCA at 52 weeks compared with at 6 weeks. At the plate mid-section, the mean NCA was significantly reduced at 26 weeks and 52 weeks compared with at 2 weeks. Comparing the area measurements between the two levels in the Micro CT study demonstrated a smaller normalised cortical area at the plate mid-section compared with the periphery at 6 weeks and 26 weeks. These findings suggest a time dependent reduction in the cortical area in the composite plated bones, which was greater at the plate mid-section compared with the plate periphery. This statistically significant effect was not observed when the same normalised NCA measurements were compared in the SEM study although a similar trend was observed. This likely reflects the greater sample size in the Micro CT experiments and the significant artefacts in the SEM study which restricted accurate area measurements.

Comparisons of cortical area measurements between the two plate groups were only feasible in the SEM study. Cortical area measurements in the metal plated samples demonstrated a statistically significant reduction in the cortical area at the plate mid-section compared with the plate periphery. Although the mean normalised cortical area was significantly less in the metal plated group compared with the composite group at each time point, this did not approach statistical significance due to the limited sample size and the large standard deviations in the composite group. Despite

the lack of statistical significance in this comparison, the area measurements agree with the comparison of cortical thickness between the two plate groups. Both sets of results support greater bone loss in the metal plated bones compared with the composite plated bones. In both types of plated bones, there was greater bone loss in the plate mid-section compared with the plate periphery, the magnitude of which increased with the duration of implantation.

These results support the mechanical basis of the stress shielding effect where the extent of bone loss beneath a plate is a function of the relative difference in mechanical characteristics between the plate and the bone[39]. The stronger the plate compared to the underlying bone, the greater the ability of the plate to mechanically insulate the bone and shield it from external mechanical forces. This stress protection alters the strain distribution in the bone underlying the plate. As the plate absorbs some of the load from applied external mechanical forces, there is reduced deformation or strain within the protected bone. The intrinsic homeostatic mechanisms within bone which preserve the normal strain distribution result in selective bone resorption until the optimum strain conditions are restored[20].

As the metal plate is relatively stiffer with respect to the underlying bone compared with the composite plate, it theoretically exerts a greater mechanical influence on the underlying bone. Although the in vitro tests demonstrated that the metal plate had a reduced mean ultimate load to failure compared with the tibia, the material properties of stainless steel are vastly greater. The elastic modulus of steel is 200GPa compared to an elastic modulus of 20GPa for cortical bone[159]. This equates to a ten-fold greater deformation in bone compared to steel when subjected to the same loading conditions. In vitro tests demonstrated that the metal plate was almost four times stronger than and at least ten times as stiff as the composite plate in its undegraded form. The magnitude of bone loss beneath the two plate types suggested there may be a dose response effect with respect to the plate's mechanical characteristics and changes in the underlying bone as has been suggested previously[50, 53, 207]. The relatively greater stiffness of the metal plate imparted a greater stress shielding response both in terms of the magnitude of bone loss beneath the plate but also the duration over which this bone loss progressed. In contrast, the

similar mechanical properties of the composite plate (flexural modulus 4-24GPa[195]) compared to the host bone induced less stress shielding and less bone resorption

Studies investigating changes in the cortical thickness beneath different types of plates have generated conflicting findings. Several studies have demonstrated a reduction in cortical thickness following plating of intact long bones[47 50, 51, 53, 55, 59]. In all but one study[47], bone resorption was related to the internal surface of the cortex as has been observed in the current study. However, one study failed to demonstrate a change in cortical thickness with plating [60] whilst another study demonstrated that changes in cortical thickness influenced the cortex adjacent to but not under the plate[53]. Comparative studies have sought to determine whether plates with different mechanical characteristics exert different effects on the underlying bone. Many of these studies reported no difference in the extent of porosity following application of plates of different stiffness[50, 51 52]or failed to demonstrate a difference in porosity in plated and unplated regions of the same bone[53-55]. In contrast, some studies demonstrated that similar sized plates with different mechanical properties exerted different magnitudes of structural changes in the underlying bone[50, 51, 53]. These studies demonstrated that comparatively stiffer plates induced greater bone loss in the underlying cortex. The three studies measured different outcomes including skeletal bone mass measured using photon absorptiometry[50, 53] and cortical thickness measured on calcified histological sections[51]. Few studies have established concurrent validity by using different techniques to measure the same phenomenon of interest as has been undertaken in the current study.

Mechanical theory can also explain the preferential bone loss observed beneath the plate mid- section compared with the plate periphery. Previous studies have demonstrated that structural changes induced by plating were most pronounced in the cortex underlying the plate compared with the opposite un-plated cortex or the diaphysis beyond the plate[47, 51, 52, 54, 83, 85]. Within the plated region of the bone, the stress shielding and resulting bone loss principally occurred beneath the plate mid-section. Mechanical theory predicts that the maximum stress shielding effect occurs between the points of mechanical coupling of the plate and bone[52] with external forces applied to the plated bone preferentially propagating along the metal plate rather than the bone. Applied forces are transmitted to the plate through mechanical

coupling at the bone screw interface causing bone hypertrophy at these points[52, 89]. Cross sections of both types of plated bone demonstrated endosteal bone formation around the screws supporting bone hypertrophy in response to stress transfer at these sites (see Figure 4.2).

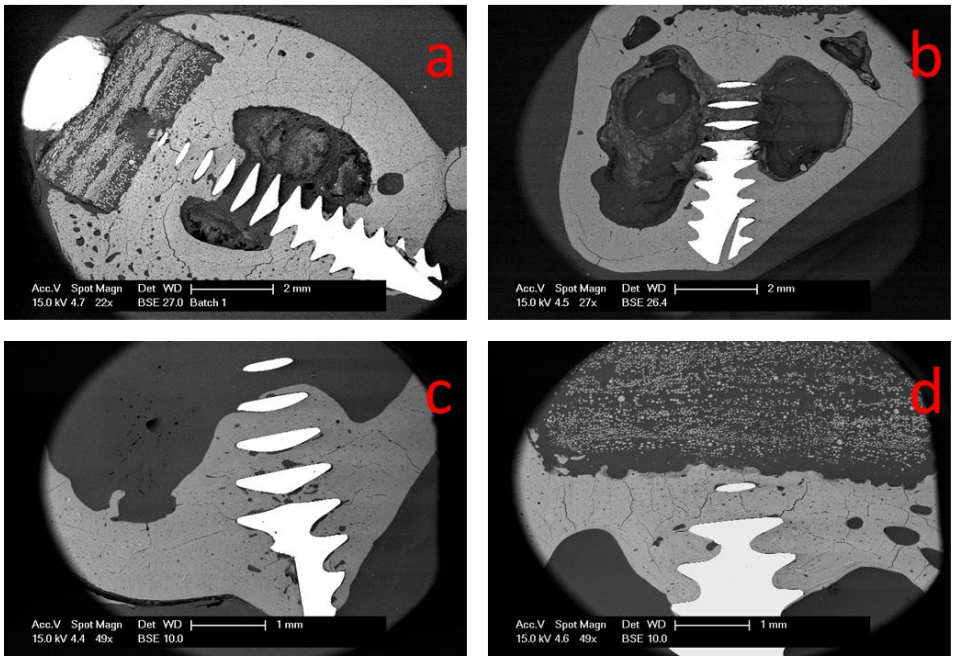


Figure 4.2 Scanning electron microscopy (SEM) images of composite plated specimens showing bone formation around the screws. Specimens retrieved at 6 (a) and 52 (b) weeks showing bone growth on the inner surface around the screw threads. (c) Composite plated specimen retrieved at 26 weeks showing bone growth around the screw in the cortex opposite the plate. (d) Composite plated sample retrieved at 52 weeks showing bone around the screw beneath the cortex. In all images the bone completely surrounds the screw threads.

As the stress is transferred from the bones to the plate via the screw coupling, the bone between the screws is shielded from stress. The current findings support this theory as greater bone loss was observed in the mid plate region compared with the plate periphery in both types of plate. This effect occurs as a continuum along the plate rather than in a step wise fashion in the plate mid-section (see Figure 4.3). Studies suggest that the outer most screws are chiefly responsible for the transmission of stress from plate to bone as evidenced by proximal and distal bone hypertrophy at these sites[52, 87, 88] whose magnitude was a function of the bone loss in the central plate region. The two levels analysed in the plated bones corresponded to

the plate periphery between screws 1 and 2 and the plate mid-section between the central two screws. Statistical analysis comparing the cortical thickness and area in these two regions demonstrated a larger difference for the composite group compared with the metal group. Analysis of the descriptive statistics demonstrated a greater reduction in cortical thickness in the plate periphery of the composite plated bones compared with the metal plated bones. This increased thickness may represent bone hypertrophy around the outer screws in the metal plated bones correlating with greater bone loss observed in the plate mid-section.

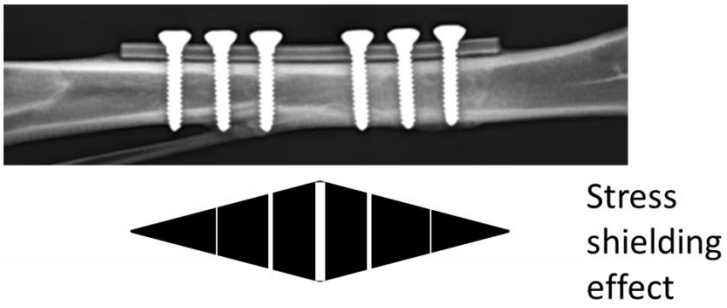


Figure 4.3 Schematic diagram depicting magnitude of stress shielding effect. The maximum stress shielding and consequent bone resorption occurs in the plate mid-section and the gradually reduces towards the ends of the plate.

The Micro CT study additionally enabled the assessment of total cross-sectional bone area at the two levels as the entire plated bone cross section could be quantitatively assessed on a single image. This did not suggest progressive bone loss as was observed when specifically looking at cortical thickness and cortical area in the region of interest beneath the plate. As the duration of implantation increased, there was an increase in the total cross-sectional area of the composite plated bones in the plate periphery relative to the control bones. In the plate mid-section, the total cross-sectional area was maintained at similar levels to the opposite control bone. There was no significant difference when comparing the normalised bone area between different time points for either of these regions. The results would suggest that the assessment of cortical changes beneath a plate alone do not sufficiently describe the complex structural changes induced by plating as have been reported in

the literature. Although progressive bone loss occurred beneath the composite plate as the duration of implantation increased, the overall cross-sectional bone area was maintained and even increased suggesting a net gain in bone following application of the composite plate. Unfortunately, the current study did not permit measurement of the total cross-sectional area of bone in the metal plated samples to determine if the greater stress shielding effect observed in the metal plated bones resulted in a progressive reduction in the total bone cross sectional area as the duration of implantation increased.

Scanning electron microscopy (SEM) and Micro CT images of both plated bones demonstrated evidence of new bone formation around the plate as early as two weeks. The new bone was easily distinguishable on the SEM images due to its porous appearance. This bone growth mainly occurred around the sides of the plate and in the opposite cortex at the site of screw penetration. The net effect in the composite plated bones was a redistribution of net bone volume bone as new bone formed around the plate whilst bone loss occurred beneath the plate mid-section. A previous *in vivo* study demonstrated similar structural changes in the cross sectional characteristics of the intact rabbit tibia after application of a metal plate[59]. They noted an increase in the outer diameter of the bone due to subperiosteal new bone formation but a reduction in the cortical thickness reflecting bone resorption from the inner cortex.

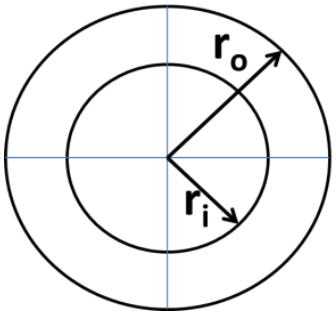
4.2 The effects of plating on the mechanical properties of the plated bones

Stress shielding describes the attenuation in the mechanical properties of a plated bone secondary to the loss of bone induced by plate application[20]. The current study demonstrated that although bone loss occurred beneath both types of plate, the magnitude of the loss was far greater in the metal plated bones. To establish whether this bone loss resulted in reduced mechanical properties, mechanical testing (three-point flexural tests) of the plated bones was undertaken.

In the composite plated bones, the strength and stiffness of the plated bones was greater than that of the opposite control bones at all time points. The augmentation in mechanical properties in the plated bones was of a constant magnitude. Comparing the mean normalised ultimate load for the composite group at different time points did not reveal any statistically significant differences. As progressive improvements in the mechanical properties of the control bones occurred up to 26 weeks, the relative improvement in mechanical properties in the respective composite plated bones decreased reflecting the cross sectional bone area changes. Thus, a net increase in the total bone area conferred improved mechanical characteristics despite evidence of progressive bone loss beneath the composite plate mid-section. The Micro CT and SEM images revealed how the new bone formation might exert this effect on the mechanical properties. Both the normalised ultimate load and flexural stiffness demonstrated an improvement at 52 weeks compared with 26 weeks in the composite plated group although this difference was not statistically significant given the small sample size and the large standard deviations. This suggests that the stress shielding response was maximal at 26 weeks and that there was some recovery of mechanical properties between 26 weeks and 52 weeks.

The second moment of area is a geometric parameter used to describe the quantitative distribution of the cross-sectional area relative to the neutral axis for a structure subjected to bending. The parameter is expressed quantitatively as an *I* value. The greater the *I* value, the greater the strength of the structure with respect to bending. Long bones such as the rabbit tibia can be likened to a cylindrical model.

For a given cylinder with outer radius (r_o) and inner radius (r_i), the second moment of area (*I* value) is calculated using the following formula (Figure 4.4).



$$I = \frac{\pi}{2}(r_o^4 - r_i^4)$$

Figure 4.4 Schematic representation of a cylindrical cross section of outer radius (r_o) and inner radius (r_i) and formula for calculating the second moment of area (I).

For a constant cross-sectional area, the formula predicts an increased *I* value and greater strength gains by increasing the outer radius rather than reducing the inner radius. In the context of a cylindrical bone, peripheral bone formation increasing the outer radius improves mechanical properties to a greater degree compared with bone formation on the inner cortex leading to a reduction in the inner radius. In the composite plated bones, bone growth was observed around the edges and the upper surface of the plates increasing the *I* value of the plated bone. The bone resorption preferentially occurred beneath the plate on the inner surface of the cortex leading to an increase in the inner radius but crucially preserving the outer radius. Several studies have demonstrated that the reduction in cortical thickness induced by plating principally involves the internal surface of the cortex as was observed in the current study [50, 51, 53, 55, 59, 208]. These changes may explain the augmentation in the mechanical characteristics of the composite plated bones relative to the controls.

In vitro testing demonstrated the metal plated intact bone to have only marginally improved mechanical properties when compared with the intact bone alone. However, two weeks following implantation the metal plated bone constructs demonstrated three times the flexural strength and almost four times the flexural stiffness compared to the opposite control bones. The disparity between these *in vitro* and *in vivo* findings may be explained by the presence of new bone around the plate which was observed on the Micro CT and SEM images as early as 2 weeks.

The new bone formation could account for the improved mechanical characteristics of the metal plated bones up to 12 weeks. However, after 12 weeks there was a progressive decline in the mechanical properties of the metal plated bones. At one year, the strength of the metal plated bones was similar to that of the opposite control bones. The mean normalised ultimate load was significantly lower at 52 weeks (101.1%) compared with at 2 weeks (286%) and 6 weeks (250.9%). A similar downward trend in the normalised flexural stiffness as the duration of implantation increased was observed although the differences between time points were not statistically significant. The results would suggest that if the metal plate was removed from the plated bone, the bone's mechanical characteristics would be significantly inferior to that of the control bone suggesting that stress shielding had occurred.

Previous studies have demonstrated reductions in the ultimate load to failure in metal plated bones compared with bones plated with more flexible plate designs[51, 53]. Studies comparing the mechanical properties of plated bones with their opposite controls have demonstrated reduced mechanical properties in the plated bones[49, 54, 63, 71, 72]. The stress shielding effect observed in the results of mechanical testing of the metal plated bones agree with the finding of a significantly greater reduction in the cortical thickness and bone area beneath the plate in the metal plated bones compared with the composite plated bones. In the composite plated bones, the localised loss of bone beneath the plate was offset by greater bone formation around the plate edges leading to a net increase in bone cross sectional area and a persistent augmentation in the mechanical characteristics at each time point. The results of mechanical testing suggested a converse phenomenon in the metal plated bones where progressive bone loss from 12 weeks onwards was not offset by new bone growth leading to a progressive attenuation in mechanical characteristics.

Mechanical testing of plated bones must take in to account the effect of screw holes in the plated bone. The presence of screw holes reduces a bone's mechanical properties as observed in the *in vitro* cadaveric experiments. However, this attenuation is not static as the bone responds by forming bone around the screw threads as observed in the SEM study (see Figure 4.2). A previous in vivo study in rabbit femoral bones investigated the effects of screw holes and found that recovery

of strength occurred within 8 weeks due to new bone growth around the screw[86]. Improvements in mechanical characteristics in both types of plated bones in the first 8 weeks likely reflected contributions from the new bone formation around the screws as well as around the plate.

4.3 The time dependent effects of plate application

The use of five progressive time points for retrieval enabled evaluation of the temporal relationship between the duration of implantation and the observed structural and mechanical changes in the two types of plated bone. It is important to note that the rabbits were skeletally immature at the time of surgery. Therefore, the effects of plate application cannot be determined independent of concurrent growth of the animal with the passage of time during the experiments.

The plain radiographs demonstrated progressive longitudinal growth of the plated tibias up to the 12 weeks' time point. The Micro CT study demonstrated very little change in the cross-sectional area of the control bones at the two levels when comparing successive time points. However, with an increasing duration of implantation, the mechanical properties of the control bones improved up to 26 weeks with a fall thereafter to the levels at 12 weeks. This improvement in mechanical properties likely reflected the effects of growth which were concurrent with the progressive increases in the length of the plated bones. This is supported by the derived linear relationship between both tibia length and rabbit weight, when plotted against the outcomes of mechanical testing as has been demonstrated in a previous study[70]. These correlations would suggest that improvements in the mechanical properties of the control bones represented a change in bone dimensions rather than material properties. However, the current analysis cannot disprove a concurrent change in material properties. Previous studies have suggested different mechanical properties between immature and adult bone with immature bone demonstrating reduced stiffness and strength characteristics compared to adult bone[209, 210]. The relatively greater gains observed in mechanical properties between 12 and 26 weeks may represent the transition from immature bone to more compact adult bone. The drop in mechanical properties after 26 weeks suggests that there may be a peak age of bone mechanical properties in this animal model occurring close to the 26 week time point.

In both types of plated bones, growth effects are likely to have impacted on the structural and mechanical changes observed. Remaining growth potential in the

plated bones up to the 12 week time point may explain the transitions in structural and mechanical outcomes observed around this time point. In the scanning electron microscopy study, the reduction in cortical thickness and bone area beneath the composite plate compared to the control bones remained fairly static after 12 weeks. In the Micro CT study, the relative reduction in cortical thickness beneath the composite plate principally occurred before 26 weeks and was unchanged thereafter. Cumulatively, these results suggest that much of the structural changes observed occurred at a time point either before or between 12 and 26 weeks. The results of mechanical testing demonstrated a diminishing improvement in the mechanical properties of the composite plated bones relative to the control bones up to the 26 week time point. An equilibrium point may have existed in the composite plated bones between 12 and 26 weeks with respect to changes in bone structure and mechanical properties. This equilibrium may represent progressive attenuation of the stress shielding response in the bone; the cessation of structural bone changes once growth is complete or a complex interplay of the two suggested phenomena.

In the metal plated bones, the 12 week time point also assumed importance with respect to transitions in the observed outcomes. In the plate periphery, the cortical thickness and bone area beneath the plate progressively increased relative to the control bones up to the 12 week time point coinciding with the theorised period of remaining growth. However, beyond 12 weeks the normalised cortical thickness and bone area progressively decreased. In the plate mid-section, profound reductions in these structural parameters occurred after 12 weeks. The flexural strength and stiffness of the metal plated bones improved relative to the control bones up to the 12 week time point after which they deteriorated to equivalence with the opposite control bones. The deterioration in structural and mechanical properties of the metal plated bones was progressive up to the final time point of 1 year. It is unknown whether continuation of the experiments beyond this time point would have demonstrated further loss of bone beneath the metal plate or whether equilibrium had been achieved between 6 months and 1 year after which little change occurred.

Previous animal studies have demonstrated progressive structural changes and reductions in the mechanical properties of plated bones as the duration of implantation increased. Studies of metal plated dog bones have demonstrated

progressive changes up to nine months[50] and twelve months[51]. Three in vivo rabbit studies have investigated the effects of the duration of implantation and have demonstrated conflicting findings[49, 63, 71]. The dimensions of the steel plates and the chosen time points differed between the studies. The key features and findings of these studies are summarised in Table 4.1. Terjesen and Benum[49] found a progressive reduction in the bone mineral content and relative strength of the plated bones up to 12 weeks with little change between 12 and 18 weeks. At each time point they noted cortical thinning beneath the plate which remained constant as the duration of implantation increased. The study by Paavolainen *et al*[63] demonstrated an improvement in the maximum torsional load to failure up to 12 weeks with a progressive decrease thereafter to 36 weeks. The progressive reduction in mechanical properties was ascribed to increasing porosity and reduced thickness in the cortex induced by stress shielding[59]. Laftman et al[71] demonstrated a progressive reduction in the maximum torque capacity of the plated bones of 25% relative to the control bones by 6 weeks which progressed to 53% by 12 weeks.

Compared to the current study, these studies demonstrated substantial differences in the plates used, the type of controls used to eliminate the influence of varied bone sizes, and the durations of implantation investigated. However, the current study outcomes do agree with some of their findings. In contrast to the other studies[49, 71], Paavolainen et al[59, 63] demonstrated improvements in the plated bones up to 12 weeks. The findings from this study were reported in two publications which reported structural[59] and mechanical[196] outcomes respectively. The structural study[59] noted the presence of subperiosteal bone formation around the plate which may have led to attempts to preserve this bone prior to mechanical testing. In all three studies, the metal plates were removed from the bones prior to mechanical testing. The current study findings demonstrated progressive subperiosteal bone formation around the plate contributing to its mechanical properties. In order to remove the plate, a significant amount of overlying new bone would have to be removed. This may explain why two of the studies reported a progressive attenuation in mechanical properties before twelve weeks. The contribution of the new bone to the bone geometric parameters is likely to have been excluded as one of the two studies reported no change in the outer dimensions of the plated bones[49]. In this study,

cortical diameter was measured on the retrieved bones following mechanical testing after the plate and the overlying bone had been removed.

Two of the three studies investigated durations of implantation beyond 12 weeks[49, 59, 63]. Terjesen's study demonstrated progression towards an equilibrium state at 12 weeks in the metal plated bone after which no further loss occurred[49]. In the current metal plated experiments, progressive attenuation in structural and mechanical testing results was observed up to the 52 weeks' time point. The steel plate in the current study had similar dimensions but double the thickness of the plate in Terjesen's study. Doubling the thickness of a metal plate increases its second moment of area and flexural mechanical properties by a factor of eight. This relative increase in stiffness could explain why the current study demonstrated progressive stress shielding in the metal plated bones beyond 12 weeks. The Paavolainen study similarly demonstrated progressive stress shielding effects up to 36 weeks which has been theorised to relate to a thicker plate compared with Terjesen's study[49]. Although the mechanical properties of the steel plate were not reported by Paavolainen et al[59, 63], it is likely that it had similar mechanical characteristics to the steel plate used in the current study.

Table 4.1 Table summarising study characteristics and outcomes of three previous in vivo studies investigating the effects of metal plate application on intact rabbit tibia.*plate dimensions were not provided in this study.

Author, year published	Number of rabbits	Weight	Experimental tibia	Control Tibia	Plate location	Time points	Failure rate	Outcomes in experimental tibiae
Paavolainen[63], 1978 Slatis[59], 1978	40 adult	2400-3850g	4 hole dynamic compression plate with compression*	4 hole dynamic compression plate without compression	Anterolateral	1 day, 3 days, 1, 3, 6, 12, 18, 24 and 36 weeks	7/40 (1 infection, 6 fracture)	Subperiosteal bone growth around the plate. Improved mechanical properties up to 12 weeks. Cortical thinning beneath the plate after 12 weeks. Progressive reductions in mechanical properties up to 36 weeks.
Laftman[71], 1980	87 adult land breed	3000-5000g	4 hole steel plate (35 x 6 x 2 mm)	Plate removed, screws reinserted	Anterolateral	6, 8, 10 and 12 weeks	22/87	Progressive reduction in mechanical properties up to 12 weeks
Terjesen[49], 1983	18 Chinchilla	2425-3785g	6 hole steel plate (45 x 5 x 1 mm)	Plate removed, screws reinserted	Anterolateral	6, 12 and 18 weeks	0/18	Progressive reduction in mechanical properties up to 12 weeks. Reduction in cortical thickness which remained unchanged

4.4 The influence of remaining growth on structural bone changes in plated bones

Both types of plate induced the formation of new bone around the plate as had been observed in previous studies[56, 59, 63]. The growth and maturation of this new bone coincided with the period during which longitudinal growth of the plated bones occurred. The new bone was present at 2 weeks suggesting surgical exposure and periosteal elevation as a precipitant. This was supported by the new bone appearing at the edges of the plate and in the opposite cortex at the site of screw penetration. The new bone was easily distinguishable from the pre-existing cortical bone due to its porous woven architecture compared to the compact lamellar arrangement of the pre-existing cortex. Over time, the new bone matured and became more compact. The pattern of maturation of the new bone suggested centripetal growth as the outer new bone became compact first. This appositional growth increased the diameter of the plated bones. Although this phenomenon was not observed in the control bones, it may represent an accentuation of the normal growth process occurring during the period of normal longitudinal growth of the bone induced by localised periosteal elevation.

At the earlier time points in the composite plate experiments, new bone growth predominated secondary to the inherent growth potential and the surgical stimulus. The progressive increase in the bone cross sectional area altered the strain distribution within the bone. To maintain the optimum strain conditions, localised bone resorption occurred in the bone beneath the plate as predicted by stress shielding theory. Once new bone growth and consequent bone resorption had ceased, an equilibrium state predominated with the net effect of an increased cross-sectional area despite bone loss beneath the plate.

In the metal plated bones, new bone growth also predominated at the earlier time points. In the first 12 weeks, the new bone induced by the surgical stimulus and inherent growth potential was greater than the bone loss due to stress shielding. The net effect was increased bone at the plate periphery and maintenance of bone at the

plate mid-section where the stress shielding effect was greater. However, once the growth potential had ceased, the stress shielding influence of the metal plate predominated leading to the progressive bone loss and attenuation in mechanical characteristics observed beyond 12 weeks.

The current study suggests that the new bone formation stimulated by periosteal disruption and remaining growth potential may have offset the stress shielding effects of fixation during the first 12 weeks. Previous studies investigating the effects of plating in an in vivo rabbit model[49, 62, 63, 71] have not commented on the influence of growth during their experiments despite performing the experiments on rabbits in a weight range indicative of remaining growth potential. The lack of structural assessment of bone changes in these studies permits limited conclusions regarding the influence of growth on the observed outcomes.

4.5 Transitional mechanical properties of the composite plate

Although cessation of growth and attenuation in the stress shielding response may explain progress to an equilibrium state in the composite plated bones, the influence of the transitional mechanical properties of the composite plate require consideration. The *in vitro* tests demonstrated a significant reduction in the mechanical properties of the composite plate following *in vitro* degradation with a fourfold reduction in strength. The current study does not offer comparisons between the *in vivo* degradation observed and the *in vitro* degradation experiments. However, the scanning electron microscopy (SEM) analysis demonstrated microscopic disruption of the composite plates at each time point. The principle observation was fissuring of the PLA matrix. It is likely that these cracks represented processing artefact as there were no obvious voids in the matrix or fibre rich regions suggestive of fibre or matrix resorption. The Micro CT images of the composite plated bones similarly did not demonstrate any obvious matrix voids or selective fibre resorption. Although the Micro CT and SEM images did not demonstrate obvious implant degradation, retrieval of the *in vivo* composite plated bones at 52 weeks demonstrated a change in the composite plate's appearance, colour and surface hardness. The results of *in vitro* mechanical testing on degraded composite plate specimens demonstrated reduced mechanical properties despite the overall structural integrity of the plate being retained.

The mechanical testing results, macroscopic appearance and SEM analysis would suggest that although there was no obvious bulk degradation, hydration of the polymer matrix regions is likely to have impaired the mechanical characteristics of the plate. Potential mechanisms include altered fibre-matrix interaction leading to reduced pull out strength, increased inter-laminar shear stresses at the interface between matrix and fibre rich regions and a reduction in the matrix mechanical properties secondary to hydration. Unfortunately, the implanted composite plates could not be retrieved intact at the later time points to permit flexural testing and comparison of the mechanical testing outcomes of *in vivo* degradation with i*n vitro* degradation in phosphate based saline. The suggested *in vivo* deterioration in mechanical properties would have resulted in significantly reduced stress shielding

effects and reduced bone loss beneath the plate with the passage of time. This is the theorised advantage of bio-resorbable plating technologies which enable the favourable transmission of forces to the bone due to the time dependent loss of mechanical properties. It is likely that the progressive stress transfer from the plate to bone caused by plate degradation will have contributed towards achievement of an equilibrium state after 12 weeks in the composite plated bones.

4.6 Non-mechanical effects of plating on bone structural changes

Previous studies have suggested that the bone resorption occurring beneath plates may represent a vascular insult to the bone due to compression of the periosteal blood supply[57, 58]. Studies have demonstrated early transient porosity beneath plates distinct from the later bone loss observed in relation to stress shielding[208]. The current study did not specifically assess porosity in the cortex beneath the plate although there was evidence of this at the earlier time points from the Micro CT and scanning electron microscopy images (see Figure 4.5). The results of mechanical testing suggested that if present, this transient vascular insult did not significantly affect the mechanical properties of the plated bones.

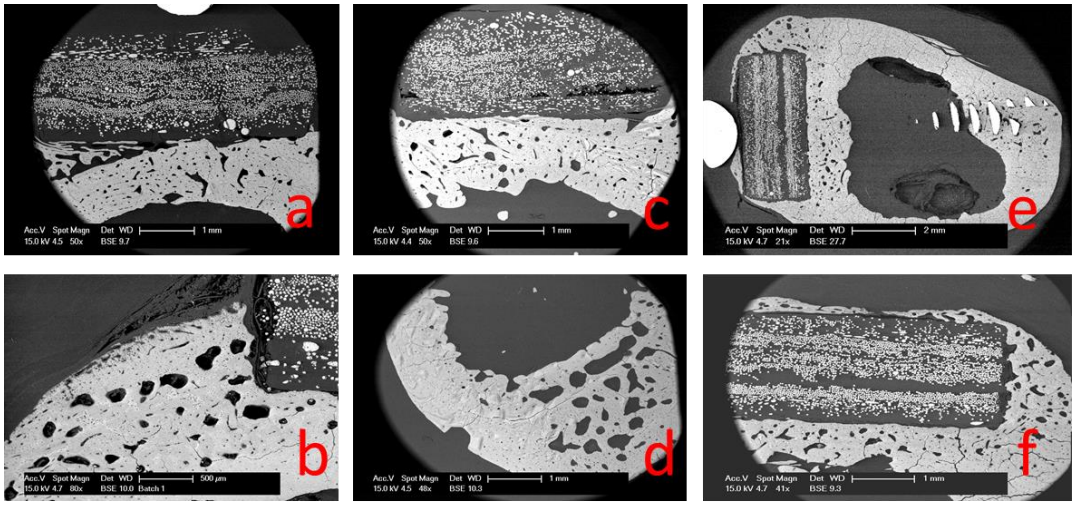


Figure 4.5 Scanning electron microscopy (SEM) images of composite plated samples retrieved at 6 weeks (a, b) and 12 weeks (c-f). The porosity was evident in the cortex beneath the plate (a, c, e, f), the new bone around the sides of the plate (b, e, f) and in the cortex opposite the plate (d, e).

Intra-osseous placement of bioresorbable implants has been associated with surrounding bone resorption secondary to the acidic by-products of polymeric degradation[103]. The SEM and Micro CT images did not demonstrate any evidence of polymer bulk degradation. This finding is in agreement with the histological

assessment of inflammation in the interface tissue between the plate and bone. Quantitative analysis demonstrated very low numbers of inflammatory cells in both types of plated bone at all time points. It is therefore unlikely that the structural bone changes observed in the sampled regions represent bone resorption secondary to inflammation caused by polymeric bulk degradation.

The degradation kinetics of implants manufactured from bioresorbable polymers are dependent on a multitude of factors and are difficult to predict[118, 120]. Important host factors include the choice of animal model, the site of implantation and the host immune response. The composite plate matrix phase was composed of polylactic acid which starts degrading within weeks but may take several years to completely degrade *in vitro*[106-108] . A previous *in vivo* study investigated the plating of rabbit tibia osteotomies using a bioresorbable plate manufactured from a carbon fibre reinforced PGA-PLA composite[211]. They reported loss of reduction and non-healing of the osteotomy site in three out of six animals at 6 months post implantation. In these three cases, the polymer plate had completely resorbed at this time point.

In the current study the composite plate was applied to intact bone and did not demonstrate significant resorption at 1 year. The differences in imposed forces when comparing an *in vivo* osteotomy model with an intact bone are likely to account for the faster resorption seen in the above mentioned study. In that study, the three of the six rabbit tibia osteotomies which healed demonstrated significant angulation indicating significant mechanical stresses being imparted to the carbon fibre PLA-PGA composite. Fracture biology represents a less favourable chemical environment with respect to bioresorbable implant degradation compared with the plating of intact bone. The first stage of fracture healing involves the formation of a haematoma at the fracture site and accompanying inflammation. Hydration from the haematoma favours matrix degradation in bioresorbable composites. Fracture healing is also associated with formation of greater vascular channels around the fracture site and implant. This environment favours the continual recruitment of inflammatory cells while facilitating transport of the hydrolysed products of plate degradation away from the site, in turn, increasing the kinetics of degradation. The combined effects of mechanical insults due to bone discontinuity and fracture induced inflammation and increased blood flow are likely to favour faster

degradation in an osteotomy model compared with plating in intact bone. Conversely, plating intact bone creates a more stable environment where degradation may take place more slowly. The formation of a fibrous capsule[126] around the composite plate and surrounding new bone formation may have acted as a barrier to the ingress of water and consequent hydrolysis of the matrix polymer. Unfortunately, the current study in the osteotomised rabbit tibia model did not permit comparison of the two different plating experimental conditions of intact versus osteotomised bone.

4.7 Critical analysis of experimental design

4.7.1 Selection of animal model

In vivo animal model experimentation is an essential intermediary step between the *in vitro* testing of novel clinical devices and clinical application in humans. The species, age, site of implantation, as well as the selection and timing of proposed outcomes all assume importance in the choice of an appropriate animal model. The rabbit animal model was selected on the basis of its popularity in assessing the structural changes in plated bones in previous studies[49, 63, 71]. Due to its relative size and anatomical accessibility, the rabbit tibia has been used extensively to investigate the influence of plating on fracture healing[76, 197] and on intact bone[49, 59, 63, 71]. Further advantages included previous studies suggesting plate geometries with external validity to human fracture fixation plates[85] and methodologies for creating reproducible fractures[199] and mechanical testing conditions[49, 70, 85]. Previous studies have also established the relationship between rabbit tibia structural and mechanical properties[70] as well as the use of a bioresorbable plate in this model[211].

In humans, the tibia and the fibula develop as distinct long bones with separate growth plates at each end of these paired bones. However, in the rabbit, the distal tibia and fibula develop as one tissue mass with a single growth plate[212]. This difference in anatomy has a bearing on the fracture mechanics of the two types of bone during mechanical testing which was not investigated in the current study.

Previously, canine[47, 50-53] and sheep models[60, 68] have been used to investigate the effects of plating with one study suggesting that canine bone approximates the mechanical properties of human bone to a greater degree than rabbit bone[213]. Practical limitations in the manufacture and achievement of the requisite mechanical properties of the composite plate for application in these larger animal models restricted choice to smaller animals. Although, plating of rat femur[214] and tibia[215] have been described, there are greater differences in the biochemical and mechanical properties when compared with human bone[198].

The New Zealand White is the commonest rabbit strain used in *in vivo* orthopaedic research[216] and demonstrates favourable cost, handling, and husbandry characteristics[198]. Exclusively female rabbits were used to enable group housing and reduce costs. In keeping with previous studies, the rabbits were 14 weeks old at the time of surgery equating to a weight of 2.5 to 3kg[49, 59, 63, 71]. At the time of surgery, the growth plates were open and radiographic measurements demonstrated longitudinal growth up to 12 weeks following surgery with radiographic evidence of growth plate fusion between 12 to 26 weeks. This agrees with previous longitudinal studies of the growth of this rabbit strain which have shown that by 16 weeks, 91% of mature adult body length and 94% of adult tibia length was achieved with fusion of the distal growth plate[212, 217]. A limitation to these studies is that measurements were gained from radiographs without the use of anaesthesia using a specially designed restrainer. The experience from the current study is that appropriate orthogonal views to permit accurate measurements of tibial length are hard to obtain without the use of anaesthesia.

The current study commented on the potential influences of remaining growth potential of the rabbit on the measured outcomes. The previous rabbit plating studies reported the exclusive use of adult rabbits despite a reported weight range suggestive of the inclusion of immature rabbits[59, 63, 70, 71] (Table 4.1). The current study suggested that residual growth has an important bearing on changes in the plated bones. The previous studies may have included immature as well as adult rabbits which may explain some of the discordancy in their findings. The current study based the rabbit weights on the previous literature. The use of skeletally mature rabbits aged greater than 16 weeks would have enabled improved characterisation of the changes in plated bones by removing the confounding influence of residual growth on new bone formation induced by plate application. In the current study the rabbits could only be acquired at 12 weeks of age. Due to the husbandry and housing costs of delaying the experiments until the rabbits were of 16 years of age, the experiments were conducted soon after acquisition to ensure the project budget was not exceeded.

4.7.2 Selection of plate location and reproducible placement

In the current study we applied the plate to the medial aspect of the tibia as has been described in previous studies[18, 211]. Previous studies investigating plating in intact rabbit tibia applied the plate to the lateral aspect of the tibia[49, 59, 63, 71]. A lateral placement was considered technically more challenging due to the proximity of the fibula near the upper part of the bone and the thicker soft tissue envelope over the lateral cortex. Lateral plating has biomechanical advantages due to the plate lying on the tension side of the bone and the tendency of tibial osteotomies to undergo progressive varus displacement[211]. It is unknown whether medial or lateral plate placement affects the strain distribution in the underlying bone or the magnitude of sub-periosteal bone formation in this animal model.

Preliminary cadaveric experiments were conducted to develop a reproducible technique of plating the rabbit tibia. Based on previous studies, the tibiofibular junction served as a landmark for the positioning of the midpoint of the plate[49, 63]. Cadaveric analysis demonstrated that positioning the plate so that the plate tip was at the level of the inferior aspect of the tibial tuberosity reproduced this plate localisation. Radiographic measurements demonstrated reproducibility of plate location when comparing different animals which minimised variations in the relative location of the sampled plated regions in bones from different animals.

4.7.3 Selection of plate geometry

The current study used a plate design based on a previous study. This study compared the *in vitro* characteristics of plated human and rabbit tibiae to determine the geometry of a stainless steel plate in a rabbit tibia model which would exert the same effect on the bending stiffness when compared with a standard human tibia fracture fixation plate[85]. However, this plate design was 1 mm thick and it was felt that the composite plate would have to be at least twice as thick to improve the mechanical properties to enable application in an osteotomy model. Therefore, we used 2mm thick composite plates. The failure of the composite plate in the

osteotomy experiments demonstrated the poor retention of mechanical characteristics of this plate design *in vivo*. Due to the time scale of experimentation, further development of the plate to improve its mechanical characteristics to enable a second trial in an osteotomy model was not feasible. Further experimentation comparing the composite plate with the metal plate used the current design and geometry. Direct comparisons of this plate geometry for either type of plate with the previous literature was difficult due to the variety of plate dimensions previously used in this animal model (see Table 4.1). Only two studies provided plate dimensions[49, 71] while in the remaining studies, the plate dimensions were not reported[59, 63].

Further improvements in the method of plate manufacture and geometry to improve its mechanical characteristics and their retention *in vivo* would likely lead to the development of a plate with very different geometric and mechanical properties compared to the current design. It would be difficult to extrapolate the findings from the current study investigating the stress shielding effects of the current plate design on bone to model the *in vivo* behaviour of any future plate design. Further *in vivo* experiments would need to be conducted to assess the stress shielding response of the new plate design on intact bone. By using the same animal model, the current experiments would serve as a useful comparator of the stress shielding effects of the new plate with the current composite and metal plates.

4.7.4 Selection of time points

The current study demonstrated that the composite plated bones structural and mechanical characteristics progressed towards an equilibrium state before the final time point of 1 year. In contrast, the metal plated bones demonstrated structural and mechanical changes which were progressive up to this final time point. Two previous studies[59, 63] investigating a maximum duration of implantation of 36 weeks, demonstrated progressive structural changes up to this time point (Table 4.1). The current study demonstrated that metal plate application induced bone changes which progressed beyond 36 weeks this time point. However, it is unknown whether the changes in the metal plated bones would continue to progress or maintain an

equilibrium state beyond 1 year. In contrast to the *in vitro* studies, there was limited evidence of composite plate degradation at the final time point. Longer term studies would be required to investigate the *in vivo* degradation of the composite plate as well as the effects of the metal plate beyond 1 year.

4.7.5 Selection of controls, sample size and statistics

One of the principle limitations in research involving animal models is the need to restrict the sample size to the minimum required to achieve the stated aims[218]. In experiments investigating novel phenomenon, it is difficult to determine an appropriate sample size when the magnitude and direction of the effect of interest are unknown. Sample size determination must also consider the influence of variation in the population characteristics when comparing groups of animals from different experiments. The current study investigated different groups of rabbits based on two independent variables – the type of plate and the duration of implantation. Although the gender and species were constant factors, there was considerable variation in the weights of different animals. Rabbit weight correlates with the mechanical properties of retrieved tibias as has been demonstrated in this study and previously[70]. Varying rabbit and bone sizes introduces a further variable influencing the structural and mechanical testing outcomes when comparing different groups of rabbits. A sufficiently large study population can negate this influence through the use of parametric statistics to compare groups but this approach is difficult to achieve in animal studies.

Some previous study designs have sought to find ways to limit the influence of variation in size between different animals when comparing small groups. One study correlated the results of mechanical testing with the weight of the animal to create a correction factor to reduce the influence of varying rabbit size[63, 70] on outcomes. Several studies have demonstrated symmetrical mechanical properties and mineral content in paired bones in the same animal[53, 62, 69-71] justifying the use of one of the bone as a control bone. Measured outcomes in the experimentally plated bone can then be expressed as a function of the same parameter in the opposite control bone to

negate the influence of size variation when comparing outcomes from different sized animals[49, 52, 71, 219]. This approach was employed in the present study to enable normalisation of the plated bones relative to the controls to enable comparison of groups of rabbits with respect to the two types of plate and the different durations of implantation. Further transformation of the data sets to enable use of different statistical models, was discussed with the statistician. It was felt that this would introduce further distortion of measured effect sizes in limited sample sets and therefore lacked empirical and statistical justification.

The use of a paired study design eliminates the need for a separate group of normal control animals. The use of the contralateral bone in the same animal as a normal control assumes that there are no indirect effects of plating on the opposite untreated limb. However, the structural and mechanical properties of plated and control bones in the same animal are a function of their shared mechanical environment. Alterations in gait induced by surgery to one limb may lead to disparities in the mechanical environments between the paired bones and thus influence outcomes[216]. A previous study demonstrated that sham surgery on the canine tibia did not affect the rate of bone formation in the femur.[50] In contrast to this, one study reported abnormalities in the knee of a rabbit following transection of a stabilising ligament in the opposite knee[220]. The extent of gait deviation and mechanical asymmetry in the paired tibiae following plating of the intact rabbit tibia on one side is unknown. Previous studies comparing plates with different mechanical properties have applied plates to both paired bones in the same animal to determine the effects of each plate relative to each other[50, 51, 53, 59, 63]. However, the absence of a normal control from which to reference outcomes makes it difficult to determine the absolute rather than the relative magnitude of the phenomenon under investigation.

In the current study, the opposite control bone was left undisturbed. Previous studies have sought to eliminate the influence of screws by applying the plate on the control bone and then removing the plate and reinserting the screws[49, 71, 219]. This has been justified on the basis of examining the effects of the plate alone[49]. This approach was not favoured in the current study as it was felt that this dichotomisation of the fixation construct lacked empirical justification on the basis that plates cannot be

applied to bone in the absence of screws. Potential stress shielding effects arising from a plate's mechanical characteristics require mechanical coupling between plate and bone provided by screws. The presence of screws in the control bone introduces another variable susceptible to unintended experimental manipulation.

The current study compared groups of five rabbits for each time point for the two types of plate. Difficulties arose as not all outcomes could be assessed in the same animal due to the destructive nature of some experimental techniques limiting the use of the bones in further experiments. The rabbits destined for histological evaluation required perfusion fixation with formaldehyde at the time of sacrifice. Formaldehyde fixation alters the mechanical properties of bones[201] and could not be undertaken in the rabbits destined for mechanical testing. To achieve a sample size of three for each of these experiments, the plated and control bones from one rabbit were retrieved following mechanical testing and post fixed in formaldehyde for subsequent histological analysis. The fractures in these specimens made it difficult to assess structural parameters in some of these samples on scanning electron microscopy. The ideal experimental technique is one that is non-destructive to the bone specimen and enables the application of further analytical techniques. In this respect, Micro CT offers satisfactory evaluation of the cross-sectional properties of both the plate and bone without introducing physical effects restricting their use in further experiments. However, the technique could not be applied to the metal plated samples due to significant artefact from the metal plate obscuring the neighbouring bone (Figure 4.6).

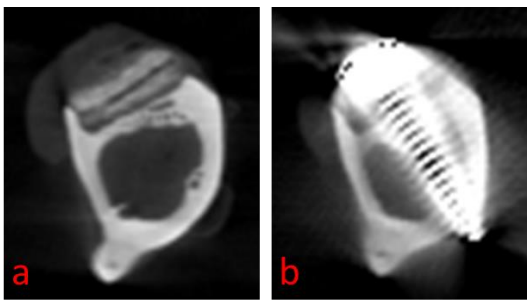


Figure 4.6. Micro CT images (voxel thickness 0.213mm) of composite plated bone showing the cortical bone beneath the plate (a) and in a neighbouring axial slice at the level of the screw (b) demonstrating the extensive artefact obscuring the cortical bone beneath the plate.

A theoretical advantage of non-invasive techniques such as Micro CT is that outcomes at sequential time points can be evaluated in the same group of animals. This approach offers two key advantages. The confounding influence of rabbit size variation on comparing outcomes between different groups of animals is negated enabling improved evaluation of the magnitude of the effect size with a smaller number of animals. Additionally, as the outcome instrument is non-destructive, it does not limit the use of the animals in further experiments following sacrifice. Modern *in vivo* cross sectional imaging combined with the systemic administration of radiolabelled tracers linked to bone activity enables detailed evaluation of bone remodelling changes in response to different medical treatments and surgical procedures[221]. A longitudinal study design could investigate the *in vivo* structural changes in plated bones as well as concurrently assessing the physiological bone remodelling response at each time point. A suggested study design could use cross sectional imaging techniques to assess bone structural changes in a single large group of animals with an increasing duration of plate implantation as the imaging could be conducted at the scheduled time points under anaesthesia without the need to sacrifice the animals.

The current study design did not permit determination of an effect size with respect to the normalised outcome measures in the composite group due to the lack of any previous studies investigating this plate design in an animal model. Sample size was based on the use of resource equations. Post hoc sample size calculations were undertaken to determine the minimum sample size required to detect the observed differences in the outcomes between the two types of plate. The current experiments looked at several different outcomes relating to the structural and mechanical properties of the plated bones. Four normalised outcomes comparing the two types of plate were used in power calculations to determine the appropriate sample size to detect the observed difference between the two groups at the final time point of 52 weeks. The means, standard deviations and group sizes from the current study are shown alongside the sample size calculations to yield 80% power and 5% sensitivity in Table 4.2.

Table 4.2. Table showing sample size calculations to detect observed differences in normalised outcomes comparing the two plate groups at 52 weeks. Sample size based on 80% power and 5% sensitivity (sd = standard deviation, SEM = scanning electron microscopy).

Outcome measure (experiment)	Mean value Composite Group +/- sd (sample size)	Mean value Metal Group +/- sd (sample size)	Predicted sample size each group
Normalised cortical thickness-52 weeks (SEM)	86.6±12.6 (n=3)	43.6±28.6 (n=2)	n=6
Normalised cortical area-52 weeks (SEM)	88.6±48.2 (n=3)	53.5±9.4 (n=2)	n=19
Normalised ultimate load-52 weeks (mechanical testing)	178.3±120.5 (n=3)	101.1±31.4 (n=3)	n=17
Normalised flexural stiffness-52 weeks (mechanical testing)	283±205.6 (n=3)	171.3±70.7 (n=3)	n=26

Comparison of the mean normalised outcome values for the two plate groups demonstrated a large difference. However, the effect size of each of these comparisons for the four outcomes was offset by both the limited sample size in each group and the large standard deviations. By convention, the power of detecting a significant difference is set at 80% and sensitivity at 5% as has been done in the current analysis. Given these constants, sample size is then determined by the magnitude of the effect size, or difference between the two groups; the sample size in each group; and the standard deviation or variance of each outcome in the two groups. The sample size calculation for normalised cortical thickness demonstrated a much smaller sample size (n=6) due to the large difference between the groups and the smaller standard deviation relative to this difference. Conversely, the sample size calculation for the other three outcomes, despite having a large difference between the means of both groups, predicted much larger group sizes due to the standard deviations in the composite group exceeding the mean difference between the groups. As the magnitude of variance increases and the size of each group becomes smaller, the sample calculation becomes less reliable. Biological variables in a large population typically assume a normal bell-shaped distribution. As the sample size

increases, accuracy in the estimation of the population mean improves and the magnitude of the standard deviation reduces. A larger sample size in each plate group in the current analysis would permit sample size calculations with improved validity.

The current study constraints in terms of animal resources did not permit the use of sample sizes predicted from the above calculations. Due to the parallel nature of the study design involving sacrificing different groups of animals at each time point, a predicted sample size of n=19 in each group at each of five time points, would require 95 animals in each arm of the study. Such a study would require sufficient funding and resources but would satisfy the home office refinement ethos that the smallest possible sample size was used to answer the intended research question. The current study sought to maximise the gains from the sample size in each group by using concurrent validity to bolster confidence in the findings through using different experiments and outcome measures to compare the two plate groups. Although statistical significance was not achieved in many of the inferential statistical comparisons, the descriptive statistical outcomes of different experiments demonstrated similar trends in the structural and mechanical properties of the plated bones in both plated groups. Concurrent validity should not replace statistical validity. However, when practical constraints limit the establishment of the latter, concordance in outcomes between different experiments investigating the same phenomenon of interest improves the overall validity of the study findings.

Statistical analysis in the current study compared normalised outcomes with respect to the type of plate, the duration of implantation and, additionally, the level of sampling in the SEM and Micro CT experiments. Analysis of variance (ANOVA) testing was used to determine if an interaction effect existed between these independent variables. The analysis was limited by the sample size of each cell in each ANOVA analysis. Consequently, the ANOVA tests did not demonstrate significant interaction effects although certain simple main effects were statistically significant. ANOVA testing of the normalised cortical thickness in both the plain radiography and scanning electron microscopy experiments demonstrated a significant interaction between the type of plate and the duration of implantation. Multiple pairwise comparisons were undertaken in each ANOVA test and

demonstrated some significant findings. The use of an ANOVA model and Bonferroni corrections of significant results on multiple pairwise analysis provided statistical validity to the results in comparison to isolated statistically significant comparisons on arbitrary multiple testing. In several instances, the assumptions of the ANOVA test were violated with respect to the presence of outliers, normality of distributions and the homogeneity of variances. However, on the recommendation of the statistician, these violations were noted and the tests were still conducted as ANOVA testing of the current experimental outcomes was considered robust to these violations[205, 206].

4.7.6 Surgical complications

There were no surgical complications in the 50 rabbits in the current study. Three rabbits were excluded due to fractures in the post-operative period and were replaced in the study. In two of these, the fracture propagated from the most distal screw hole which may reflect technical error in screw placement. Alternatively, failure may have occurred due to the most distal screw hole being located in the narrowest region of the bone. The third fracture occurred in the pelvis on the operated side in one of the composite plated rabbits. This may have been caused by an abnormal weight bearing profile following surgery. The current failure rate of 3 out of 53 is relatively low compared to previous studies (Table 4.1). In one study, 22 out of 87 rabbits were excluded due to complications arising from anaesthesia, infection and technical failings[71]. The current lack of anaesthetic and infection complications may reflect advances in anaesthetics, surgical standards and housing arrangements in the intervening decades from when these studies were published. Previous studies did not report the routine administration of antibiotics at the time of surgery[49, 59, 63, 71]. There were significantly less fractures and technical failures in the current study compared with previous studies. This may reflect the relative sizes of the screws and drills, the use of a custom made jig for attaching the composite plate in the current experiments and previous surgical training of the experimenter.

4.7.7 Selection of screws

The current study used conventional stainless steel screws to fix both types of plate. The combined plate screw construct in the composite group was not resorbable in contrast to a previous study[211]. Bioresorbable screws constructed from the same composite were not available during the study. The introduction of differences in the fixation stiffness by using two different types of screws would further complicate analysis when comparing the mechanical effects of the two types of plate. The size, number, positioning and applied torque of screws have a bearing on the results of mechanical testing[52]. The stress shielding response in plated bones exists as a function of the extent of coupling between the plate and bone. Loosening all of the screws in a plate by half a turn has been shown to completely eliminate the augmentation in mechanical characteristics when comparing the flexural rigidity of the combined bone-plate construct compared with the bone alone[52]. Previous studies have used torque screw drivers to reduce differences in screw tightness by applying the same torque during application[50, 53]. However, these studies investigated plating in dog femora where large screws enabled the use of torque limiting screw drivers. In the current study, 2mm screws were used and screw torque was judged manually as in previous rabbit studies[49, 63, 71].

4.7.8 Mechanical testing conditions

Currently, there are no established standards for the mechanical testing of whole bones. Previous studies removed the plate prior to mechanical testing to determine the mechanical properties of the bone alone[49, 52, 63, 71, 207]. Our study demonstrated that this was not feasible without removing the sub-periosteal new bone covering the plate. In the composite plated bones, the theoretical risk of re-fracture of the bone following plate removal did not require investigation as the plate was designed not to remain *in situ*. The practical limitations in removing a potentially degraded composite plate at the later time points also favoured the choice of testing the entire bone plate construct.

Previous studies utilised two main types of loading profile when testing whole bones – bending[49] and torsion[63, 70, 71]. Flexural testing favours elucidation of mechanical properties in specific regions of interest rather than the whole bone. Cortical changes were most pronounced beneath the centre of the plate and this was the intended site of force application in order to highlight the mechanical differences between the two types of plated bone. The aim was to compare these outcomes in intact bones with the study comparing the two types of plate in an osteotomised rabbit tibia model. Four-point bending tests are more appropriate in the evaluation of fracture models[101, 208]. However, preliminary four-point bending experiments demonstrated unacceptable specimen rotation during testing due to the varied cross section of the rabbit tibia and its asymmetric centroidal axis. The varied rotation influenced the slope of the load deformation curves and derived strength and stiffness indices. A previous study using three point bending, filed the bone ends to produce flat surfaces to prevent rotation during force application[49]. Alterations to the bone's geometry or constraining the bone ends during testing may create an additional variable influencing outcomes and were thus not used. Preliminary testing on cadaveric specimens using three point bending, a roller span width equal to the plate length and a previously reported displacement rate[49] produced the most reproducible results.

The orientation of the bone during a bending test influences the results of mechanical testing. The flexural strength of a bone is a function of the second moment of area which varies for a fixed cross sectional area depending on the direction of the flexural stress. The choice was made to orientate the bone plate construct based on the plate's position with the plate resting on the inferior rollers. During testing, the plate and the medial side of the bone were stressed in tension and the lateral aspect was stressed in compression. This is the opposite loading profile to what occurs in *in vivo* where the medial aspect is stressed in compression[211]. However, this orientation generated the most reproducible results as the plate was always stressed perpendicular to its long axis and never obliquely. Thus, the plate mechanical characteristics were kept constant during the mechanical testing placing emphasis on any difference in outcomes observed on structural bone changes rather than variation introduced by orientation of the bone-plate construct.

4.7.9 Selection of outcome measures

The current study utilised different experimental techniques to measure similar structural outcomes. Plain radiographs, scanning electron microscopy and Micro CT were used to measure cortical thickness beneath the plate and the cross sectional area of bone. Agreement between these different techniques measuring the same outcomes provided concurrent validity of the study design. Establishing concurrent validity is important for many reasons. There are significant controversies in the previous literature regarding the time dependent effects of plating on intact bone. Although this may reflect differences in experimental design, the nature of animal studies limits study numbers. Small study numbers introduce significant variance in measured outcomes and large standard deviations were observed in the current study. Consequently, statistical validity was only demonstrated in some of the ANOVA models and frequently on the multiple pairwise analysis. Although some statistically significant results were observed, the use of different measurement techniques to establish concurrent validity improved confidence in the observed differences in outcomes when comparing the two types of plated bone. This is particularly important where the sample sizes in individual experiments are not large enough to permit hypothesis testing to determine differences of effect with statistical significance.

Previous studies investigating changes in the structure and material properties of plated bones used different outcomes compared to the current study. Investigation of bone material properties included assessment of bone mass using photon absorptiometry[49, 53] as well as histomorphometric measurement of tetracycline labelling in different regions of the plated bone[50, 51, 59]. Various techniques have been used to obtain structural measurements including measurements from plain radiographs[208, 222], optical measurements of magnified specimens[51] and calliper measurements of retrieved specimens following mechanical testing[49]. Micro-radiographs of plated bone cross sections have been used to derive area and porosity measurements[49, 52, 59, 222].

Bone mass analysis has been used as an outcome in previous studies. However, this may not differentiate between varying structural changes in the cross sectional characteristics of a plated bone. For example, bone mass may remain constant as bone loss beneath the plate may be offset by new bone formation around the plate. Micro CT can be used to measure bone density. However, accurate quantification of bone density using Micro CT required the concurrent imaging of phantoms of known density to accurately calibrate measurements. These were not available during the study which limited the inclusion of these outcomes.

The current study has demonstrated that the effects of plating on intact bone are complex and cannot be simplified to specific structural parameters such as cortical thickness or bone area beneath the plate. In the current study, although cortical thickness decreased beneath the composite plate mid-section, there was a progressive increase in the total cross-sectional area and mechanical properties. Histo-morphometric measurements of specific microscopic regions of the plated bone may not characterise the overall structural changes due to sampling bias dependent on the region of interest. Macroscopic measurements such as cortical thickness also introduce complexity. The scanning electron microscopy images demonstrated that the cortical thickness beneath the plate was not uniform in cross section. Bone area measurements beneath the plate are probably more representative of bone loss beneath the plate but ignore the effects of new bone formation around the plate. Outcome measures must therefore focus on changes in the overall cross-sectional characteristics of plated bones to fully characterise the structural changes in plated bones.

4.7.10 Sampling errors

Concurrent validity is important to establish if some techniques may be influenced by sampling or measurement errors. Sampling errors may arise from excluding the region of interest from analysis or attrition in sample numbers during processing. Measurement errors may arise due to artefacts arising from processing. Only two

regions of the plated and control bones were sampled - the plate mid-section and plate periphery. These were selected to investigate variation in the stress shielding effects along the length of the plate. However, the plate periphery region was only sampled in the top half of the plate. Consequently, structural changes in the other half of the plated region or beyond the plate were not investigated. Although, the sampling was limited to these two levels, the inter-sample variation when comparing the location of these bone blocks from different animals demonstrated satisfactory reproducibility.

Inflammatory cell analysis was restricted to the bone plate interface region in a single level in each of the plated and control bones. Reduced sampling introduces significant error when generalising the findings to the entire plated bone. However, the finding of low numbers of inflammatory cells in both types of plated specimens mirrored the absence of macroscopic inflammation in the retrieved plated bones. Although inflammatory cell analysis was only undertaken up to the 12 week time point in the metal plated samples, the absence of inflammation suggested that these findings would be unchanged at later time points. The influence of sampling bias may be further confounded by poor reproducibility in experimental technique. The current study demonstrated satisfactory reproducibility of plate location during surgery, experimental conditions during mechanical testing and sampling of the two pre-determined levels thereby improving the internal validity of the study.

4.7.11 Processing artefacts

The paraffin embedded histological slides demonstrated significant anatomical distortion restricting their use to qualitative analysis of structural bone changes rather than quantitative analysis (see Figure 4.7a). Sawing the metal plated specimens into blocks created significant metal debris which was difficult to section using a microtome (see Figure 4.7c, 4.7d). Consequently, many of these paraffin blocks were melted down to remove the metal plates and re-processed into paraffin blocks. Removal of the metal plates required removal of the overlying sub-periosteal new

bone formation (see Figure 4.7b). The metal plated paraffin specimens were principally used to assess the presence of inflammatory cells in the interface tissue. Although the undecalcified specimens processed for scanning electron microscopy analysis demonstrated significant cracks, this did not interfere with thickness or area measurements. The Micro CT image sequences in some specimens demonstrated poor resolution (see Figure 4.8). As the images were taken before further processing, these image sequences could not be repeated with optimised resolution. Consequently, the low resolution images yielded poor images when thresholded which may have introduced errors in thickness and area measurement.

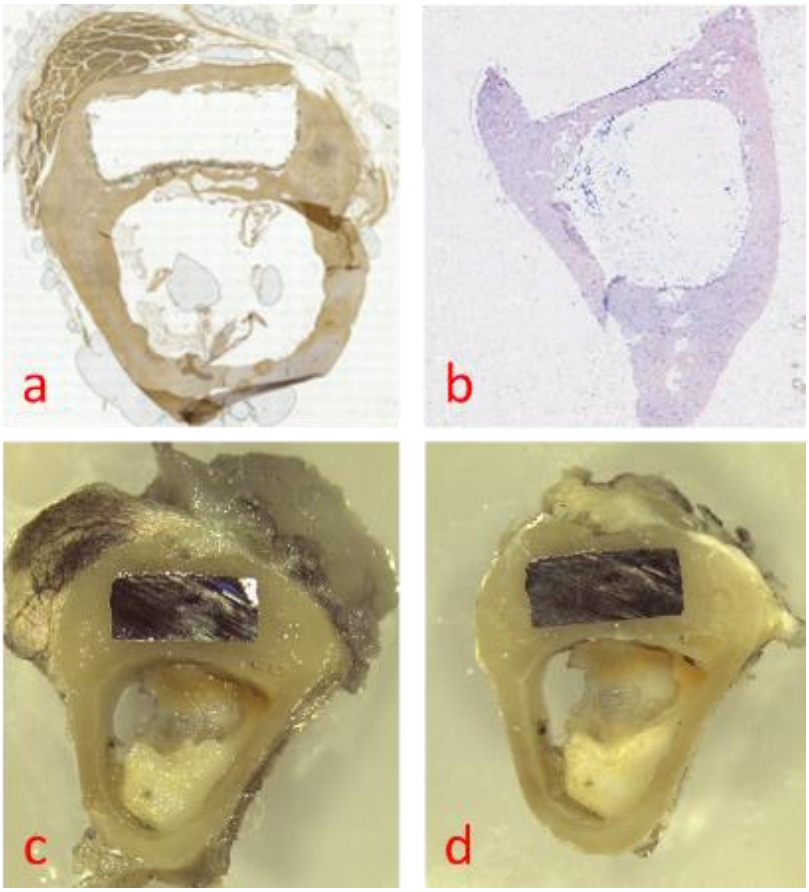


Figure 4.7 Images demonstrating different processing artefacts. (a) TRAP stained slide of composite plated tibia retrieved at 26 weeks demonstrating warping and overlap of cortex. (b) Giemsa stained slide of metal plated specimen retrieved at 12 weeks demonstrating removal of subperiosteal bone covering the plate. (c) Block corresponding to plate mid-section from a metal plated tibia retrieved at 52 weeks. There is abundant bone formation around the plate but metallic debris staining of the overlying soft tissues after cutting the block. (d) Same specimen where the soft tissue have been removed but ingrained metal debris still remains.

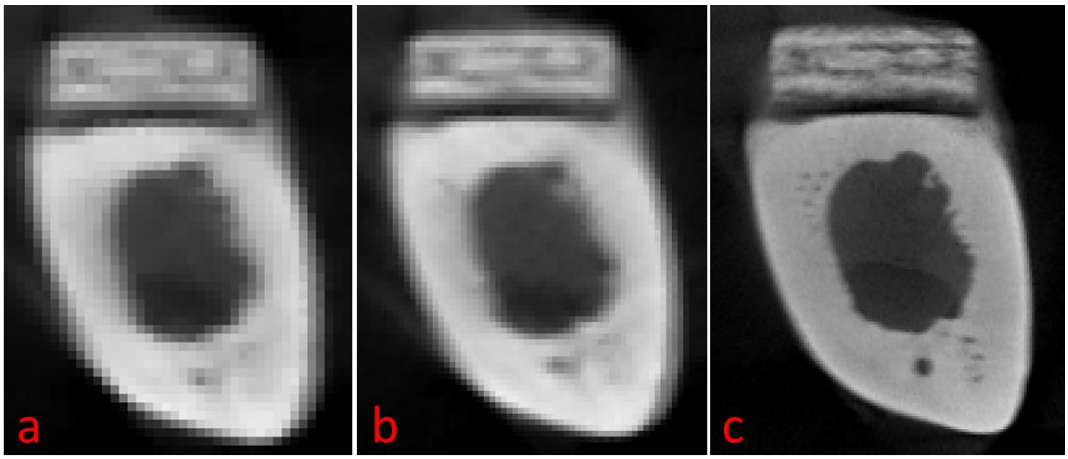


Figure 4.8 Comparative Micro CT axial images of a composite plated bone retrieved at 2 weeks taken from sequences using three different voxel thicknesses – (a) 0.213mm, (b) 0.140mm and (c) 0.06mm. The detail and accuracy of measurements were greater in the images with lower voxel thicknesses due to the improved resolution.

4.7.12 Observer bias

The use of instrumentation to record the results of mechanical testing and computer programs to measure cortical area and thickness helped to limit the influence of observer bias. However, expectancy effects can supervene when the observer directly measures phenomenon of interest such as the characterisation and quantification of inflammatory cells in the interface tissue between bone and plate.

Observer bias can be reduced through repeated measurements by the same observer at different times or two separate observers undertaking independent measurements to determine the intra- and inter-observer reliability respectively. This was not feasible during the current study. Blinding could be employed to limit expectancy effects if the observer is unaware if he is taking measurements from a composite plated specimen or a metal plated specimen. However, this was difficult due to obvious differences between the two types of plated bones during the experiments.

4.8 Creating a model to explain the structural and mechanical behaviour of plated bones

An elusive goal of *in vivo* studies investigating the effects of plating on intact bone has been the development of a unifying model, which can amalgamate all of the proposed mechanisms of bone loss and formation to predict the effects of specific types of fixation. Investigation of these mechanisms in *in vivo* models has not yielded agreement when comparing the results of individual studies. Large scale studies involving animals exert financial as well as ethical constraints. Numerical simulation using finite element models has been put forward as an efficient way to model the behaviour of metal and composite plated constructs. Previous simulation studies have demonstrated that stress shielding can be successfully reduced when a composite plate is used to fix a fractured tibia[94, 223]. Finite element modelling of the mechanical behaviour of plated bones engenders significant complexity. The geometry of the bone and spacial arrangement of cortical and trabecula bone have to be considered. In addition to the plate characteristics, a multitude of contact interfaces have to be modelled including cortical/trabecular, bone/screw, plate/screw, bone/plate and bone/mechanical testing device[224]. Chakladar et al investigated the outcomes of a flexural test for finite models of metal and composite plated bones compared with similar outcomes in experimental plated bones[224]. Their findings demonstrated that predicted failure modes and sites from the finite element model agreed well with the experimental data. Furthermore, the estimated stiffness and strength values of the two types of plated construct were generally within 10% of the experimental values.

The current study could have utilised finite element modelling to predict the stress shielding response in the composite plated bones. However, a significant limitation of the above finite element study is that the reference standard of experimental data with which the finite element model was compared related to experiments on cadaveric plated bones. *In vivo* bone models demonstrate adaptive changes in response to plating which vary with the duration of implantation. The use of finite element models to predict the stress shielding response in response to bioresorbable plate application requires appropriate modelling of the structural and mechanical

changes occurring in both plate and bone as the duration of implantation increases. Simulated models will also have to include predictions of changes in each of the mechanical interfaces as the duration of time increases. The complexity of these predictions based on current experimental data and the lack of a unifying model including all proposed mechanisms of bone formation and loss in plated bone limits the current inclusion of finite element models in predicting the *in vivo* stress shielding response in composite plated bones. The results of the current study have investigated the *in vivo* structural bone changes occurring in the composite plated bone providing an evidence base for devising future numerical models to predict the stress shielding effects of the composite plate. However, the failure of this plate to fix an osteotomy suggests that significant changes would have to be made in any future plate design to achieve the required mechanical properties. Therefore, the current study findings could not be used to create a numerical model of future plate designs without further *in vivo* studies.

The current study has demonstrated several theorised mechanisms dictating bone formation and bone loss. These are represented schematically in Figure 4.9 below. The effect size of each mechanism assumes analogue characteristics in two dimensions. These pertain to the magnitude of the effect (depicted in Figure 4.9 along the y axis) and the temporal duration over which the effect occurs (depicted in Figure 4.9 along the x axis). The relative magnitudes and temporal durations of these effects are difficult to characterise in studies due to them occurring concurrently and being difficult to study in isolation. It is also unknown whether the individual mechanisms dictating bone formation or bone loss have an additive effect or summative effect when occurring concurrently. For example, we do not know if the superimposition of residual growth on new bone formation induced by periosteal elevation induces a greater rate of bone formation compared with these two phenomena occurring independently.

An important question is whether these mechanisms can be modified by changing the conditions of plating to yield beneficial effects. Previous studies have suggested that the extent of sub-periosteal new bone formation is determined by the space created by periosteal elevation[56]. Theoretically, altering the plate dimensions and

geometry may increase the extent of new bone formation. The bone loss and structural weakening induced by screw holes have been extensively studied[86] and likely exert a limited influence during the early period following plate application. The current study did not quantitatively assess the extent of early porosity beneath either type of plate suggestive of transient necrosis induced by periosteal vascular disruption as has been done in previous studies[57, 208, 225]. However, Micro CT and SEM analysis did reveal some early porosity in both types of plated bones which may represent this phenomenon.

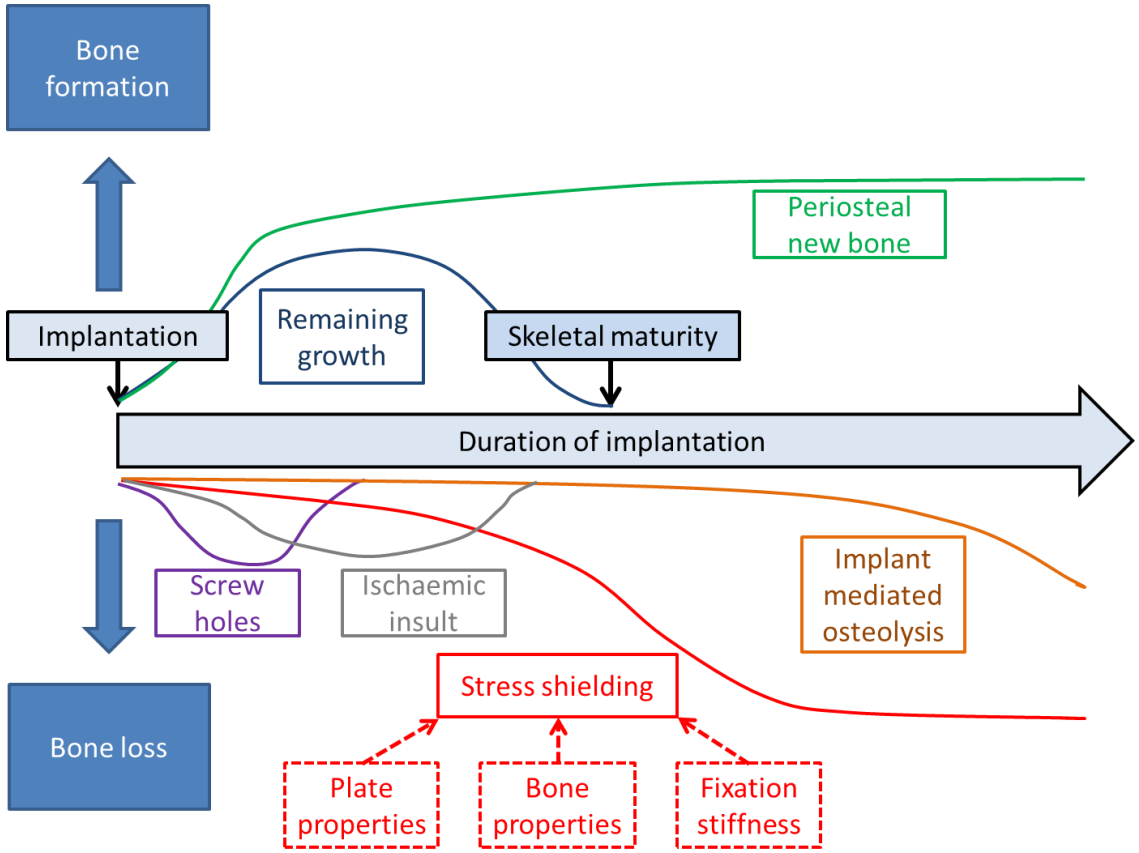


Figure 4.9 A theorised model encompassing different mechanisms of bone formation and bone loss (y axis) occurring over an increasing duration of plate application (x axis). The individual coloured curves for each mechanism suggest the relative magnitudes of the bone changes and the relative durations over which these occur. The stress shielding mechanism of bone loss (red curve) has three key determinants – the bone properties, the plate properties and the stiffness of fixation.

The stress shielding response induced by differences in the mechanical properties of the composite plate and the metal plate with respect to bone assumes a complex function with many determinants. In the current study, the bone loss beneath the metal plates progressed as the duration of implantation increased up the final timepoint. However, in the composite plated bones, the bone loss beneath the plate eventually tailed off to achieve an equilibrium state. In the metal plated bones, the magnitude of bone loss was greater and was progressive up to the final time point. These findings suggested that increasing the plate stiffness led to an increase in both the magnitude and duration of the stress shielding response. Eventually an equilibrium state is achieved[49]. Although the plate mechanical properties are probably the most important determinant of the stress shielding function[54, 59, 60], the bone properties and fixation characteristics also assume importance. Differences in the effects of plating different bones in different animal models likely represent differences in the normal physiological mechanical environments of these bones. The stress shielding response is critically dependent on the transmission of the plate's mechanical properties to the bone through the screws. Previous studies have demonstrated that reductions in contact between the plate and bone and screw loosening exert significant effects on the extent of bone loss beneath the plate[52]. Therefore, the persistence of a stress shielding effect requires a constant fixation stiffness over time. However, such ideal interface conditions may not be achievable *in vivo* with current plate designs suggesting that the degree of stress shielding may be significantly less than previously thought[226]. Therefore, the stress shielding influence may itself degrade over time due to loss of fixation stiffness resulting in the eventual restitution of normal bone anatomy as has been suggested in some studies[82, 83].

Bioresorbable plates further complicate the prediction of stress shielding induced bone changes. Plate degradation is advantageous due to the consequent reduction in the plate's mechanical properties over time gradually transferring more stress to the healed bone thereby reducing the stress shielding effect. Stress shielding could be further reduced by using bioresorbable screws for plate fixation which would degrade over time reducing the fixation stiffness of the construct. Tailoring the mechanical and degradation properties of the bioresorbable plate would ensure

adequate plate strength and fixation stiffness was retained while the fracture healed. Degradation of the plate and screws causing a reduction in the plate's mechanical properties and reduced fixation stiffness due to screw degradation following fracture healing would prevent bone resorption due to stress shielding.

Bioresorbable plates can cause bone loss through mechanisms other than stress shielding. Inflammation induced by the acidic by-products of polymeric degradation can cause bone resorption around implants as they degrade[103, 152]. However, this was not observed in the current series of composite plate experiments. The results of the current study suggest that although the hydration characteristics of the polymer matrix may have altered there was no obvious bulk degradation stimulating inflammation. Longer term studies are required to adequately assess complete degradation of the current composite plate and effects of this process on the underlying bone.

A theoretical advantage of phosphate glass fibre reinforced composites is that as the glass fibres degrade through hydrolysis, they release calcium and phosphate ions. Similarities in the chemical formulation of the glass fibres and the mineral content of bone[194] may enable released calcium and phosphate ions to exert bioactive effects favouring bone formation. Calcium phosphate ceramics are used in clinical practice to stimulate bone union in unhealed fractures by a similar mode of action[227]. In the current *in vivo* study, we did not observe evidence of glass fibre degradation which could have had a contributory influence on bone formation around the composite plate. This reflected insufficient degradation of the composite plate at the final time point. Further long term studies are required to investigate the influence of bioactive ion release on bone formation following composite plate degradation.

4.9 Extrapolating the current findings to human studies

In the single experiment undertaken in an osteotomy model, the composite plate was unsuccessful in stabilising an osteotomy of the rabbit tibia to permit fracture healing. This plate geometry was double the thickness of a metal plate suggested as being comparable to clinical plates in humans[85]. It was difficult to extrapolate the composite plate dimensions which would provide the requisite mechanical properties to enable adequate load bearing function in humans but current evidence would suggest that such a composite plate would be considerably oversized compared to a conventional metal plate. Previous plating studies of osteotomies in the rabbit tibia have reported varied failure rates ranging from relatively low[18, 197, 199, 228-231] to as high as 15 out of 35 rabbits[196]. One study reported no fractures having placed the rabbits in a retention appliance for 3 weeks following plating of the osteotomised tibia[230]. Key differences in fracture fixation principles in humans are that functional loads can be minimised through restricted weight bearing and fracture stabilisation can be supplemented by cast application to aid fracture healing. These measures are not practical in animal models which may have contributed to the higher failure rates observed.

The *in vivo* force profile in the tibia of quadrupeds such as rabbits is likely to significantly differ compared with humans who have a bipedal gait pattern. Variations in the normal mechanical environment of the tibia in these two species are likely to translate into different bone strain distributions and tolerances. The normal strain distribution within a bone influences the stress shielding phenomenon and varies according to the anatomical location of the bone[232]. Although a previous study demonstrated a rabbit plate design exerting similar *in vitro* effects on the rabbit tibia compared with a conventional plate in humans[85], this approach ignores differences in the *in vivo* strain distribution between these bones. In addition to physiological differences, studies looking at bone composition have shown substantial interspecies variations in collagen and mineral content[213, 233]. A previous study investigated the bone fracture and mineralisation properties of femoral specimens from five different species including humans and rabbits[213]. Although, both the fracture toughness and bone mineral density of human bone were similar to that of rabbit bone, they

exhibited different osteonal architectures. Studies have suggested that the number and size of osteons have an effect on the mechanical properties of bone[234, 235]. These differences may impact on the transduction mechanisms by which mechanical forces induce structural adaptations in bone which may distance the rabbit tibia model further from its human counterpart.

4.10 Bioresorbable composites as fracture fixation devices – current limitations and future developments

4.10.1 Theorised effects of the composite plate on soft tissue inflammation and infection

The *in vivo* biocompatibility of bioresorbable implants has been extensively investigated in various animal models. These studies, like the current study, have demonstrated that macroscopic inflammatory foreign body reactions to bioresorbable implants are conspicuously absent in animal models[106, 135]. Conversely, clinical use of such implants has been associated with a risk of developing local soft tissue inflammatory reactions with a reported incidence ranging from 2% to 46.7%[131]. This disparity between animal and human studies remains a significant limitation in the pre-clinical evaluation of bioresorbable implants using animal models. Two large clinical series have not demonstrated a difference in the rate of soft tissue reactions related to the volume of the implant[136, 146]. However, a previous study demonstrated large bioresorbable plates to have a soft tissue reaction incidence of 47.4%[144]. These clinical studies investigated implants manufactured from polymers of aliphatic esters. Large volume polymer implants have a risk of bulk degradation causing inflammation associated with polymeric debris[144]. The current composite plate is composed of a PLA polymer matrix reinforced with phosphate glass fibres which reduces the volume of polymer. The addition of phosphate glass fibres may have several favourable effects on degradation. The separation of the polymer matrix by interspersed phosphate glass fibres may limit the extent of bulk degradation by various mechanisms. Hydrolysis of the fibres could form channels within the implant enabling the controlled egress of acidic products of polymer degradation away from the host tissue to prevent their build up. This is in contrast to the scenario in polymeric implants, where progressive degradation causes liquification of the centre of the polymeric implant which eventually bursts discharging large volumes of debris overwhelming the local tissue bed capacity for metabolism and transport[131]. Additionally, as the phosphate glass fibres resorb, they release calcium and phosphate ions which could theoretically buffer the acidic products of polymer degradation thereby lessening the induced inflammatory response. These benefits

could enable the use of large volume composite plates with sufficient mechanical properties for fracture fixation in long bone fractures where traditional large volume resorbable devices have demonstrated inflammatory complications. The intended clinical application for the composite plate was as a wrist fracture fixation plate which could be feasible with further studies optimizing the mechanical properties and degradation characteristics.

A study has suggested a correlation between polymer volume and the frequency of secondary bacterial infection[145] which raises concerns regarding potential large volume implants used for fracture fixation. It is unknown whether the composite structure of a bioresorbable implant increases the risk of infection. Based on previous successful animal studies[207, 236, 237], a carbon fibre composite plate was designed for use in humans on the basis of its reduced stiffness causing reduced stress shielding associated bone loss. A clinical trial investigating outcomes of patients with tibial fractures treated with this composite plate demonstrated an unacceptably high rate of deep infection which restricted further clinical use of the implant[238]. It is unknown whether the composite structure of the current composite plate would increase host susceptibility to infection. An important distinction between polymer composites and fibre reinforced composites is that the latter demonstrate a greater potential for tailoring characteristics through modifications in the fibre chemistry. The composition of the phosphate based glass fibres can be modified to include silver ions with antibacterial properties which could make them superior to metal plates in terms of infection risk[194].

4.10.2 Bone forming potential of phosphate glass fibre composites

An interesting finding from the current study was the characterization of the sub-periosteal new bone formation around both types of plate. Cross sectional area measurements demonstrated that there was an overall increase in bone area in the composite plated bones suggesting that reduced stiffness plates induce a net gain in bone mass. A similar phenomenon has been observed by researchers attempting the

in vivo engineering of bone tissue in the same animal model[239]. The approach was based on the manipulation of an experimentally created space beneath the periosteum in the tibia of New Zealand White rabbits using hydraulic elevation. This "*in vivo* bioreactor" was maintained by filling the space with a biocompatible alginate gel which successfully reconstituted into functional bone over a 12 week period. They demonstrated that this bone could be harvested to fill a large defect in the opposite tibia. The choice of gel filler was based on the premise that the presence of calcium within the matrix would favor bone formation. This was supported by the experimental observation that in the absence of these calcium ions, substantially less bone formation was seen.

The "bone reactor" study shares findings observed in the current series of experiments where mechanically maintained elevation of the periosteum favored bone growth around the plate. However, the "bone reactor" study was conducted in adult rabbits suggesting that this phenomenon occurred independent of remaining growth potential in skeletally immature rabbits. Theoretically a bioresorbable plate could serve a similar function as a resorbable subperiosteal spacer enabling progressive substitution with new bone. Plates have been designed for subperiosteal insertion with minimal overlying soft tissue stripping[240, 241] supporting the feasibility of a plate in creating and maintaining this subperiosteal space. The previous study noted that the space created was limited by the compressive forces acting on the alginate gel filled space leading to a slightly reduced volume of bone compared to the volume of injected gel. The plate mechanical characteristics could theoretically generate a greater volume of new bone by better resisting these compressive forces. A theoretical advantage of the composite plate is that the contained phosphate glass fibres have a chemical composition close to that of normal bone[192]. Future trials of a phosphate glass fibre rich plate with a low volume of polymer matrix may demonstrate superior bone formation due to the progressive liberation of ions theoretically exerting greater osteoinductive effects.

Free bone graft is required in many treatments to aid healing in un-united fractures and in surgically created osteotomies to correct deformities[242]. Although, bone graft may be harvested from the same patient at a site remote from surgery this can confer some morbidity with post-operative discomfort at the harvest site[243]. In certain

situations, there is a surplus in demand in the amount of bone required for a procedure and retrieved bone from another donor may be required. This allograft bone typically has to be sterilized using gamma irradiation to avoid the transmission of infection between the donor and recipient[244]. Irradiation of bone has been shown to affect the mechanical and bioactive properties of allograft bone[245]. Although synthetic calcium phosphate based substitutes are available[246], fresh bone graft remains the gold standard of bone union as the primary outcome[242]. Phosphate glass fibre composites in *in vivo* bone bioreactor technologies may enable the potential to create bone within patients for planned surgery where the use of bone graft is required. Ideally, the bone could be created at the surgical site to avoid separate donor site morbidity.

4.10.3 Stress shielding and bioresorbable composite fixation devices

The ideal fracture fixation device should have excellent biocompatibility, be fully resorbable, have adequate initial mechanical properties to sustain the mechanical stresses during early fracture healing followed by a gradual decline in mechanical properties to enable transfer of stress to the healing bone[187, 247]. Implant resorbtion causing minimisation of the stress shielding response is the principal theorised advantage of resorbable fracture fixation devices compared to metallic devices. The permanence of metals *in vivo* increases the possibility of long term complications such as wear, migration, late foreign body reactions and obscuring underlying bone on radiographs[248]. The desirability of bioresorbable implants in this regard is offset by the inherent poor mechanical properties of conventional bioresorbable polymers. Bioresorbable composites offer the potential of improving mechanical properties by mechanically reinforcing the low modulus polymer matrix phase with a high modulus fibre phase while retaining biodegradability. The improvement in mechanical properties occurs through transfer of externally applied stresses through the matrix to the high modulus fibre phase via the fibre-matrix interface. Thus, the mechanical properties of bioresorbable composites are determined by the properties of the matrix, the fibres, their relative volumes and geometric arrangement and the

fibre-matrix interface. The retention of mechanical properties with degradation is of vital importance to prevent early implant failure during fracture healing with authors suggesting that fracture fixation devices should retain at least 80% of their mechanical properties after 6 to 8 weeks degradation[249].

4.10.4 Composite plate failure following fixation of in vivo osteotomy

The single in vivo osteotomy experiment resulted in early failure due to loss of structural integrity of the composite plate. Microscopic analysis of the retrieved plate specimen demonstrated failure to occur though inter laminar shearing between layers of the composite implant. Analysis of the failure mechanism of the composite implant should be used to determine potential improvements in the composite design for *in vitro* testing prior to further *in vivo* osteotomy experiments.

Phosphate glass fibres (PGF) were used as the reinforcement phase in the composite plates used in the current experiments. The theorised advantages of these fibres is their high modulus and ability to degrade to release ions with potential osteoinductive effects. Phosphate glass fibres are typically produced using a melt drawn technique and collected over a rotating drum. Glass fibre diameter is controlled by altering the glass melt viscosity, hydrostatic pressure and drum speed[248]. Fibre diameters of 20µm produce a high fibre length to diameter ratio which optimises the surface area enabling maximum stress transfer from the matrix to fibres. Scanning electron microscopy of the composite plate in the retrieved specimens demonstrated significant variation in the diameter of the glass fibres (Figure 4.10). The majority of fibres were greater than 20µm leading to a greater fibre aspect ratio and impaired composite mechanical properties. Deficiencies in fibre-matrix bonding may have further attenuated the mechanical properties of the composite plate.

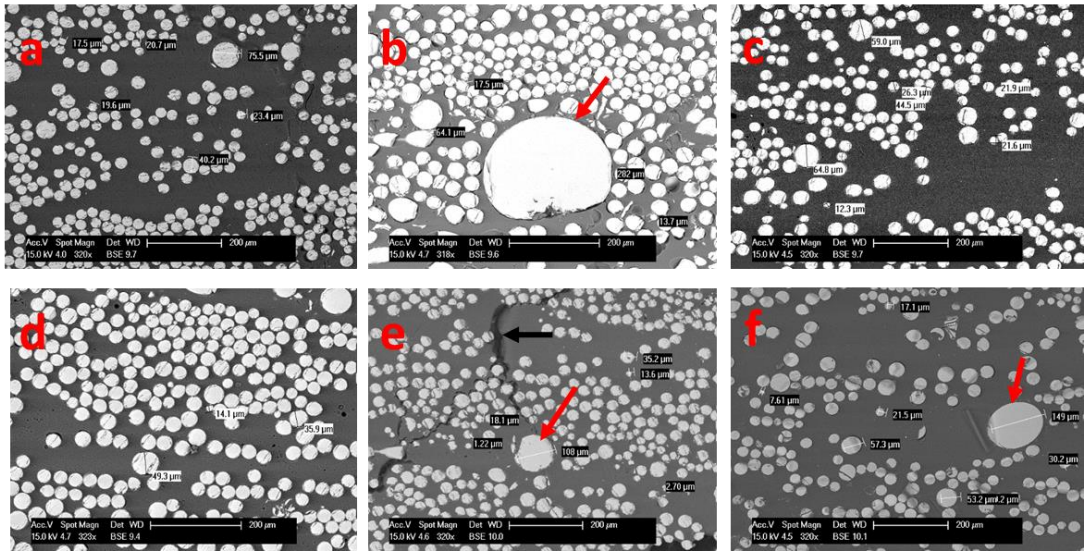


Figure 4.10. Scanning electron microscopy (SEM) images (obj x320) of composite plate from the in vivo study at 2 weeks(a,b), 6 weeks (c), 12 weeks (d) and 26 weeks (e,f). The arrows (b,e and f) highlight glass fibres greater than 150µm in diameter. There was quite a large variation in glass fibre size and distribution amongst the retrieved composite plates with sampled regions showing fibre rich regions(b, d) and matrix rich regions (a,c,f). There is a large crack visible in one of the samples (e) which may represent an inherent defect or artefact produced during processing.

Composites are defined as materials composed of at least two physically or chemically different constituent phases separated by a distinct interface[250, 251]. Most phosphate glass fibre (PGF) reinforced composites for fracture fixation systems have used polylactic acid (PLA) as the matrix phase due to its improved mechanical properties and slower degradation kinetics compared with other polymers. In the current study, the composite was manufactured using a manual layup film stacking process where polymer sheets were stacked alternately between layers of fibre lamina and compression moulded. The fibre lamina were constructed as pre-coated fibre impregnated sheets (pre-pregs) to enhance matrix infiltration and improve the quality of the fibre-matrix interface. Previous studies[194] have compared the effects of different composite fibre architectures, fibre volume fractions and lamina stacking on composite mechanical properties and their retention following in vitro degradation in phosphate buffered saline. Stacking of eight pre-preg mats improved the mechanical characteristics of the composite plate compared to a single fibre lamina during compression moulding due to increased polymer infiltration[195]. Improved mechanical characteristics were observed with higher fibre volume

fractions and in the unidirectional fibre composites compared with the random mat composites[194, 195]. Thus, the current plate design consisted of eight layers of alternating unidirectional fibre pre-pegs and PLA to optimise mechanical properties.

Microscopy of the retrieved plate specimen following the failed osteotomy experiment demonstrated failure at the screw hole nearest the osteotomy site. At the screw hole the cross-sectional area of the plate reduced from $10mm^2$ to $6mm^2$. The microscopy images demonstrated failure of the laminar interface in the central region of the plate with fibre pull-out. The theorised failure mechanism was axial loading along the length of the plate resulting in shear forces in the fibre matrix interface in regions of poor wet out during the manufacturing process. Composite mechanical behaviour would favour ductile failure rather than brittle failure due to progressive deformation secondary to internal shear between different layers of the composite. Stiffness is a crucial mechanical property in high load bearing applications as it dictates the extent of deformation under loading. A plate with lower stiffness will bend to a greater degree when a load is applied. If the loads are substantially lower than the ultimate flexural strength, the implant may not fail but the resulting deformation may result in the fracture healing in a displaced position[184]. Bending of the implant creates further problems as the stiffness of the entire bone-plate construct is reduced. The osteonal architecture of long bones is primarily designed to resist longitudinal compressive forces when weight bearing. A transverse fracture or osteotomy has a stable configuration as imposed longitudinal forces will favour compression at the osteotomy site rather than displacement of the broken bone ends (see Figure 4.11a). In this way, the forces are shared between the plate and bone which lessens the demand on the mechanical properties of the bone while the osteotomy is healing.

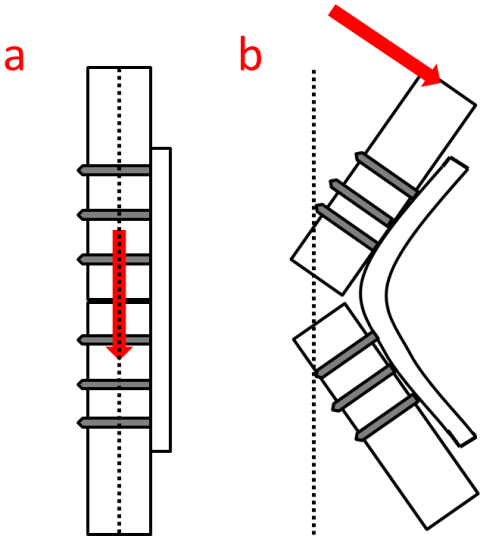


Figure 4.11 (a) Free body diagram of an osteotomy of a long bone fixed with a plate. The longitudinal force on weight bearing (red arrow) is directed through the neutral axis (dash line) of the bone plate construct favouring compression at the osteotomy site. (b) Free body diagram of an osteotomy of a long bone fixed with a plate in which the plate has deformed over time causing separation of the bone ends. The longitudinal force (red arrow) now acts away from the neutral axis (dash line) to cause a bending moment, the magnitude of which is a function of the distance of the applied force from the neutral axis. As the plate bends, the bending moment is increased. The osteotomised bone offers no resistance to these imposed forces and the plate eventually fails.

If a plate bends under loading, the loading environment changes due to loss of contact between the two bone ends at the osteotomy site (see Figure 4.11b). Once this occurs, the plate is the sole recipient of all imposed forces along the bone. Forces acting on the bone are no longer longitudinal and compressive but act as moments to cause angulation at the osteotomy site. The force applied is now amplified by the magnitude of the lever arm secondary to the extent of bending. Plate deformation resulting from low plate stiffness predisposes such plates to failure as has been observed in a previous study of bioresorbable plate fixation of rabbit tibia osteotomies[211]. This is the likely mechanism of failure in the single experiment where the composite plate was used to stabilise an osteotomy

The *in vitro* tests demonstrated significant deterioration in the mechanical properties of the composite plate which had been degraded over 6 weeks in phosphate based saline. Although the un-degraded composite plate was stronger and stiffer compared to the PLA polymer plate, the ultimate load to failure and stiffness of the degraded composite plate was inferior compared with the degraded PLA polymer plate. The *in vitro* testing demonstrated increased ductility of the composites compared with the PLA plates with greater standard deviations indicative of greater intra-sample

variation in mechanical properties. Due to practical difficulties in retrieving the composite plates in the *in vivo* mechanically tested composite plated bones, scanning electron microscopy analysis of the failure mode was not feasible. Inter-laminar stresses are a recognised failure mechanism of composite materials where shear forces induced by bending of the implant cause separation of the laminar structure of the composite plate. Analysis of all composite plate fractured specimens from the *in vitro* experiments as well as the mechanical testing of the *in vivo* bone-composite plate constructs revealed characteristic laminar separation causing plate failure (Figure 4.12).

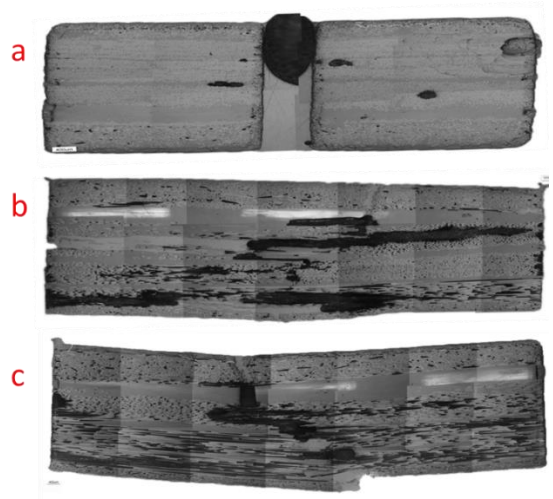


Figure 4.12 SEM images of entire composite plate cross section before mechanical testing (a) and after mechanical testing (b,c). Cracks can be seen running through the composite plate between different layers suggestive of failure at the inter-laminar interface.

Subsequent mechanical testing on larger composite plates revealed that the failure occurred in regions with high fibre concentration (see Figure 4.13) adjacent to matrix rich regions. In some specimens, continuous cracks occurred across the full width of the composite plate. Micro cracks were also observed in the polymer rich regions which were attributed to differential shrinkage during the manufacturing process. It was hypothesised that the micro-cracks could provide slippage planes for crack propagation causing fatigue failure at considerably lower loads than the ultimate flexural strength. These experiments demonstrated that thicker composite plates were more susceptible to this failure due to the greater number of laminar planes along which shear could occur.

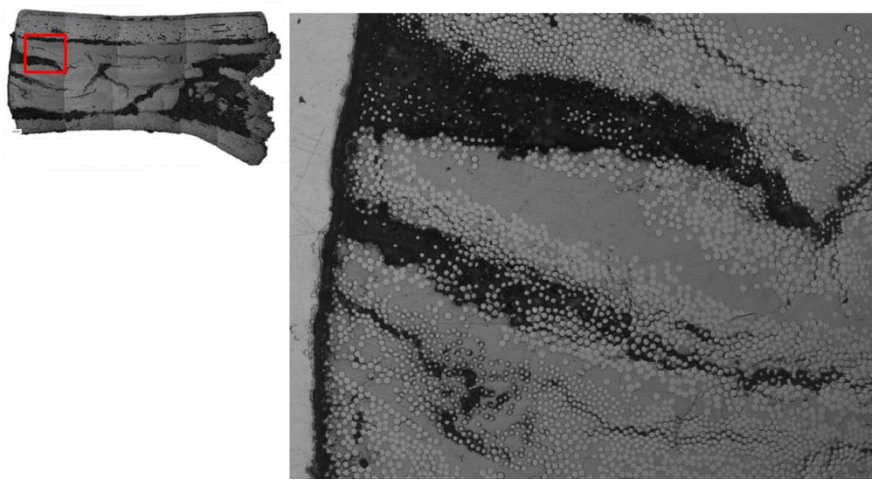


Figure 4.13 Magnified view of composite plate cross section on SEM demonstrating laminar failure occurring at the edge of the plate and propagating inwards. The cracks occurred in areas with the highest fibre concentration.

4.10.5 Future developments in composite plate design

Improvement in the mechanical properties of composite materials compared to their individual components reflects the strength of adhesion or interface bonding between the matrix and reinforcing phases. Failure analysis of the current composite plate suggested poor fibre-matrix interaction which can occur due to several mechanisms. Degradation studies in saline have demonstrated a rapid attenuation in mechanical properties of phosphate glass fibre (PGF) composites[194]. Ingress of water into PGF composites causes dissolution of the glass fibres by hydrolysis. Theoretically, this may occur more readily in unidirectional fibre composites where water can easily wick along the continuously aligned fibres compared to more random fibre arrangements[194]. Phosphate glass fibre dissolution causes a fall in the local pH due to the formation of phosphoric acid which can promote auto-catalysis of the polymer matrix[248]. Neither of these phenomena were observed in the current *in vivo* experiments in intact bone. At 52 weeks, there was no evidence of fibre resorption on the scanning electron microscopy images. As failure occurred in the osteotomy model within a few hours, it is unlikely that fibre dissolution was contributory.

Composite hydration has physical effects on the matrix as well as the glass fibres. Hydration induces plasticisation of the matrix which reduces crystallinity favouring ductile transformation with reduced stiffness[248]. This effect would be most marked in polymer rich regions as fibre reinforcement of the matrix may act to restrict localised plastic deformation of the matrix. The presence of polymer rich regions with poor wet out of the central longitudinal fibres suggests limitations in the manufacturing process in achieving equivalent mechanical properties throughout the composite plate. The current composite plate was manufactured using a laminate stacking and hot press moulding technique. Due to the high viscosity of the molten polymer, laminate stacking frequently results in areas of sub-optimal matrix impregnation and wet out of the fibre surface resulting in poor fibre-matrix adhesion[182]. The scanning electron microscopy studies of the composite plate did not demonstrate any obvious voids from fibre resorption, matrix

voids due to insufficient wet out of the central fibres or generalised separation at the fibre-matrix interface. Where disruptions in the matrix were observed, this may have reflected artefact introduced from processing the cut plate surface for electron microscopy. However, analysis of composite plate fibre arrangement did reveal matrix rich zones and this was the theorised site of failure in the current study. Surface damage to the composite from machining the laminate stacked composites into plates and drilling of the screw holes are likely to have produced surface defects. Crack propagation from these defects may have contributed to shear between the different composite layers causing eventual failure.

Since the completion of the study, refinements in the manufacturing process of phosphate glass fibre (PGF) composites have seen the introduction of in-situ polymerisation techniques to improve fibre-matrix adhesion[252]. Instead of using polymer resin as the matrix, a mixture of monomer and catalyst is injected into a mould and polymerised in situ to form the matrix around the fibres directly. As the viscosity of the monomer is lower than the polymer melt, it results in improved fibre impregnation and increased interfacial bond strength. A recent study has compared PGF composites produced by laminate stacking and in-situ polymerisation manufacturing techniques[252]. In-situ polymerisation generated composites with improved mechanical properties. The retention profile for mechanical properties was also significantly improved. Scanning electron microscopy analysis of freeze fractured specimens of the laminate stacked composite demonstrated dry fibre bundles and polymer rich zones as has been observed in the current experiments (Figure 4.14 a,b). In the in situ polymerised composites there was a more even distribution of fibres throughout the matrix with improved fibre-matrix adhesion (Figure 4.14 c,d). The profile of the stress strain curves of the laminate stacked composite demonstrated a more ductile failure mechanism suggesting progressive fibre pull-out. In contrast, the in situ polymerised composites demonstrated a brittle failure mode and reduced hydration following immersion due to improved fibre-matrix adhesion. Improved interface properties can limit the presence of channels or voids permitting the ingress of water. Importantly, the in situ polymerised composites

demonstrated retention of mechanical properties within the range of the flexural properties of cortical bone. Studies are currently underway to introduce textile fibre layers rather than manual fibre mat layup with in situ polymerisation manufacturing techniques to create bioresorbable composites with improved mechanical properties and degradation characteristics[252]. Optimisation of mechanical properties must necessarily supersede expected *in vivo* demands due to the expected early loss of strength following implantation due to degradation[131].

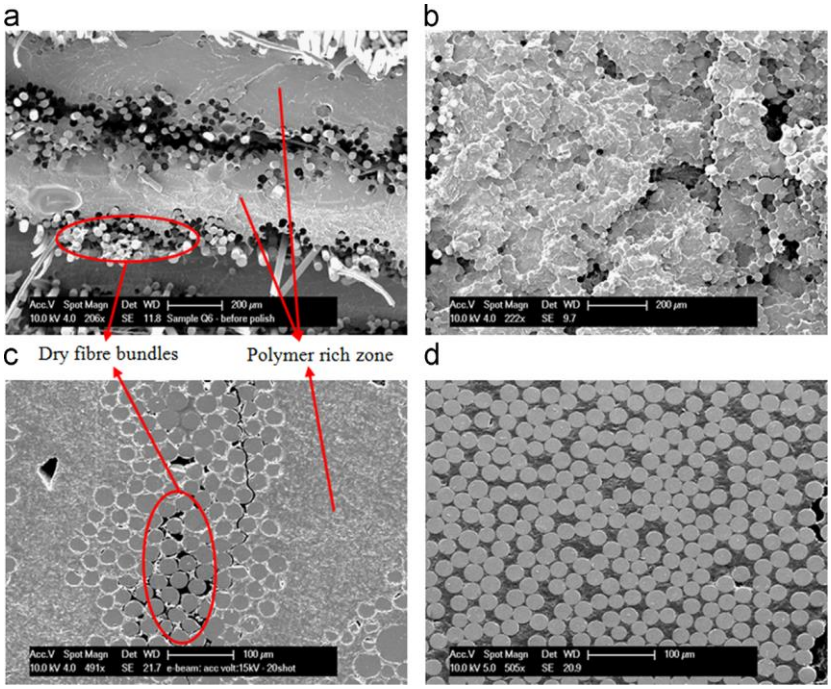


Figure 4.14. SEM micrographs of freeze fractured laminate stacked (a,b) and in situ-polymerisation (c,d) composites demonstrating dry fibre bundles and polymer rich zones in the former (reproduced from Chen et al[252], 2016).

An additional advantage of in situ polymerisation techniques is the ability to manufacture contoured fracture fixation devices as closed moulds with complex cavity shapes can be manufactured[252]. Geometries are thus not restricted to a standard plate design used in the current study. In the current study, stainless steel screws were used to fix the plate to bone due to the practical difficulties in manufacturing small screws from laminate stacked composite materials. Development of compatible bioresorbable screws

is required before the bioresorbable composite plate can be classed as a bioresorbable fracture fixation system. In situ polymerisation using closed moulds may permit the manufacture of bioresorbable composite screws.

4.11 Conclusion

The current study has demonstrated that the composite plate lacks sufficient mechanical properties to fix an experimentally created osteotomy in an animal model which negates its potential as a future fracture fixation device. Limited conclusions can be drawn from the single failed experiment but it is likely that the primary cause of failure was poor interface bonding between the matrix and reinforcing fibre phases of the composite. Further refinements in the material properties would be required to improve matrix fibre bonding before consideration of *in vitro* biomechanical testing in an osteotomy model. These advances would need to occur in parallel with the development of compatible bioresorbable screws to enable studies of the composite plate as a feasible bioresorbable fracture fixation system.

The current study has demonstrated the superior outcomes in terms of bone preservation when comparing the composite plate with a steel plate in an intact bone model. Although these findings have limited applicability in view of the composite plate's failure as a fracture fixation device, they support the basis of stress shielding theory and have provided further insight into the structural bone changes occurring in this animal model in response to implants with different mechanical properties with an increasing duration of implantation. The composite plate did not induce any significant difference in inflammation when compared with the metal plate establishing a basis of biocompatibility for phosphate glass fibre-PLA composites enabling their further evaluation in future studies.

References

1. Muller ME, Allgower M, Schneider R, Willenegger H. Manual of internal fixation: techniques recommended by the AO-ASIF group. Berlin: Springer-Verlag; 1991.
2. Pead MJ, Lanyon LE. The adaptation of bone architecture to mechanical function. In: Sumner-smith G, editor. Bone in clinical orthopedics. 2nd ed: AO publishing; 2002.
3. Summerlee AJS. Bone formation and development. In: Sumner-smith G, editor. Bone in clinical orthopedics. 2nd ed. Stuttgart: AO publishing; 2002.
4. Wolff JJ. Das Gestez der transformation der Knochen. Berlin: Verlag August Hirschwald; 1892.
5. Currey JD. MECHANICAL-PROPERTIES OF BONE TISSUES WITH GREATLY DIFFERING FUNCTIONS. J Biomech. 1979;12(4):313-9.
6. Lanyon LE. EXPERIMENTAL SUPPORT FOR TRAJECTORIAL THEORY OF BONE-STRUCTURE. J Bone Joint Surg-Br Vol. 1974;B 56(1):160-6.
7. Wolff JJ. Ueber dieinnere Architecktur der Knochen und ihre Bedeutung fur die frage vom knochenwachstum. Virchow's Arch. 1870;50:389.
8. Roux W. Beitrage zur morphologie der funktionellen anpassung. 3. Beschreibung und Erlauterung einer knochernen Kniegelenksankylose. Arch Anat Physiol. 1885.
9. Culmann C. Die Graphische Statik. 2nd ed. Zurich: Meyer and Zeller; 1875.
10. Schaffler MB, Radin EL, Burr DB. MECHANICAL AND MORPHOLOGICAL EFFECTS OF STRAIN RATE ON FATIGUE OF COMPACT-BONE. Bone. 1989;10(3):207-14.
11. Burr DB, Martin RB, Schaffler MB, Radin EL. BONE REMODELING IN RESPONSE TO INVIVO FATIGUE MICRODAMAGE. J Biomech. 1985;18(3):189-&.
12. Ralis ZA, Ralis HM, Randall M, Watkins G, Blake PD. CHANGES IN SHAPE, OSSIFICATION AND QUALITY OF BONES IN CHILDREN WITH SPINA-BIFIDA. Dev Med Child Neurol. 1976;18(6):29-41.
13. Garland DE, Stewart CA, Adkins RH, Hu SS, Rosen C, Liotta FJ, et al. OSTEOPOROSIS AFTER SPINAL-CORD INJURY. Journal of Orthopaedic Research. 1992;10(3):371-8.
14. Vaananen HK. PATHOGENESIS OF OSTEOPOROSIS. Calcif Tissue Int. 1991;49:S11-S4.
15. Jaworski ZFG, Uhthoff HK. REVERSIBILITY OF NONTRAUMATIC DISUSE OSTEOPOROSIS DURING ITS ACTIVE PHASE. Bone. 1986;7(6):431-9.
16. Oconnor JA, Lanyon LE, Macfie H. THE INFLUENCE OF STRAIN RATE ON ADAPTIVE BONE REMODELING. J Biomech. 1982;15(10):767-81.
17. Rahn BA. Bone healing: histological and physiological concepts. In: Sumner-smith G, editor. Bone in clinical orthopedics. 2nd ed. Stuttgart: AO publishing; 2002.
18. Rahn BA, Gallinar.P, Baltensp.A, Perren SM. PRIMARY BONE HEALING - EXPERIMENTAL STUDY IN RABBIT. J Bone Joint Surg-Am Vol. 1971;A 53(4):783-&.
19. Goodship AE, Kenwright J. THE INFLUENCE OF INDUCED MICROMOVEMENT UPON THE HEALING OF EXPERIMENTAL TIBIAL FRACTURES. J Bone Joint Surg-Br Vol. 1985;67(4):650-5.
20. Ruedi TP, Buckley RE, Moran CG. Biology and biomechanics in bone healing. Davos: AO publishing; 2007.
21. Perren SM, Cordey J. TISSUE DIFFERENCES IN FRACTURE HEALING. Unfallheilkunde-Traumatology. 1977;80(5):161-4.

22. Perren SM. Evolution of the internal fixation of long bone fractures - The scientific basis of biological internal fixation: Choosing a new balance between stability and biology. J Bone Joint Surg-Br Vol. 2002;84B(8):1093-110.
23. Perren SM, Ganz R, Ruter A. Oberflachliche Knochenresorption um Implantate. Med orthop Tech. 1975;95:6-10.
24. Perren SM. PHYSICAL AND BIOLOGICAL ASPECTS OF FRACTURE-HEALING WITH SPECIAL REFERENCE TO INTERNAL-FIXATION. Clinical orthopaedics and related research. 1979(138):175-96.
25. EK GIR. Biomechanics in Applications. In: V K, editor.2011.
26. Sophia Fox AJ, Bedi A, Rodeo SA. The basic science of articular cartilage: structure, composition, and function. Sports health. 2009;1(6):461-8.
27. Vanwanseele B, Lucchinetti E, Stussi E. The effects of immobilization on the characteristics of articular cartilage: current concepts and future directions. Osteoarthritis and Cartilage. 2002;10(5):408-19.
28. Bohler L. Technik der Knochenbruchbehandlung. Wien: Maudrich; 1938.
29. Latta LL, Sarmiento A, Tarr RR. THE RATIONALE OF FUNCTIONAL BRACING OF FRACTURES. Clinical orthopaedics and related research. 1980(146):28-36.
30. Sarmiento A, Sobol PA, Hoy ALS, Ross SDK, Racette WL, Tarr RR. PREFABRICATED FUNCTIONAL BRACES FOR THE TREATMENT OF FRACTURES OF THE TIBIAL DIAPHYSIS. J Bone Joint Surg-Am Vol. 1984;66A(9):1328-39.
31. Creditor MC. HAZARDS OF HOSPITALIZATION OF THE ELDERLY. Annals of Internal Medicine. 1993;118(3):219-23.
32. Baratz ME, Jardins JDD, Anderson DD, Imbriglia JE. Displaced intra-articular fractures of the distal radius: The effect of fracture displacement on contact stresses in a cadaver model. J Hand Surg-Am Vol. 1996;21A(2):183-8.
33. Perren SM. THE BIOMECHANICS AND BIOLOGY OF INTERNAL-FIXATION USING PLATES AND NAILS. Orthopedics. 1989;12(1):21-34.
34. Ruedi TP, Buckley RE, Moran CG. AO philosophy and basic principles. Davos: AO publishing; 2007.
35. Bynum D, Jr., Allen GF, Ray DR, Ledbetter WB. In vitro performance of installed internal fixation plates in compression. Journal of biomedical materials research. 1971;5(4):389-405.
36. J GL. Looking at bone plates and screws. Engineering in Medicine. 1971;1(1):17-8.
37. H HJ. The Fixation of Fracture using Plates. Engineering in Medicine. 1973;2:60-3.
38. Lindahl O. RIGIDITY OF FRACTURE IMMOBILIZATION WITH PLATES. Acta Orthop Scand. 1967;38(1):101-&.
39. Cornell CN, Lane JM. NEWEST FACTORS IN FRACTURE-HEALING. Clinical orthopaedics and related research. 1992(277):297-311.
40. K S. Tibial fractures treated according to the AO method. Injury. 1974;4:213-20.
41. F RALJS. Les refractures apres osteosynthese par plaque a compression. Helv chir Acta 1967;43:49-64.
42. Dietschi C, Zenker H. REFRACTURES AND NEW FRACTURES OF TIBIA AFTER AO PLATE AND SCREW OSTEOSYNTHESIS. Arch Orthop Trauma Surg. 1973;76(1):54-64.
43. Schenk R, Willenegger H. ON THE HISTOLOGY OF PRIMARY BONE HEALING. Langenbecks Archiv fur klinische Chirurgie vereinigt mit Deutsche Zeitschrift fur Chirurgie. 1964;308:440-52.
44. Refior HJ, Meister P, Matzen K. MICROSTRUCTURAL EXAMINATIONS OF BEHAVIOR OF HUMAN CORTICAL BONE AFTER COMPRESSION OSTEOSYNTHESIS. Arch Orthop Trauma Surg. 1975;81(1):45-56.

45. Akeson WH, Woo SLY, Coutts RD, Matthews JV, Gonsalves M, Amiel D. QUANTITATIVE HISTOLOGICAL EVALUATION OF EARLY FRACTURE HEALING OF CORTICAL BONES IMMOBILIZED BY STAINLESS-STEEL AND COMPOSITE PLATES. Calcified Tissue Research. 1975;19(1):27-37.
46. Olerud S, Danckwardt-Lilliestrom G. Fracture healing in compression osteosynthesis in the dog. The Journal of bone and joint surgery British volume. 1968;50(4):844-51.
47. Uhthoff HK, Dubuc FL. Bone structure changes in the dog under rigid internal fixation. Clinical orthopaedics and related research. 1971;81:165-70.
48. Uhthoff HK, Lavigne P. INFLUENCE OF RIGID METAL PLATES ON INTACT DIAPHYSES - EXPERIMENTAL STUDY. Union Medicale Du Canada. 1972;101(9):1772-&.
49. Terjesen T, Benum P. THE STRESS-PROTECTING EFFECT OF METAL PLATES ON THE INTACT RABBIT TIBIA. Acta Orthop Scand. 1983;54(6):810-8.
50. Moyen BJL, Lahey PJ, Weinberg EH, Harris WH. EFFECTS ON INTACT FEMORA OF DOGS OF APPLICATION AND REMOVAL OF METAL PLATES - METABOLIC AND STRUCTURAL STUDY COMPARING STIFFER AND MORE FLEXIBLE PLATES. J Bone Joint Surg-Am Vol. 1978;60(7):940-7.
51. Akeson WH, Woo SLY, Rutherford L, Coutts RD, Gonsalves M, Amiel D. EFFECTS OF RIGIDITY OF INTERNAL-FIXATION PLATES ON LONG BONE REMODELING - BIOMECHANICAL AND QUANTITATIVE HISTOLOGICAL STUDY. Acta Orthop Scand. 1976;47(3):241-9.
52. Carter DR, Shimaoka EE, Harris WH, Gates EI, Caler WE, McCarthy JC. CHANGES IN LONG-BONE STRUCTURAL PROPERTIES DURING THE FIRST 8 WEEKS OF PLATE IMPLANTATION. Journal of Orthopaedic Research. 1984;2(1):80-9.
53. Tonino AJ, Davidson CL, Klopper PJ, Linclau LA. PROTECTION FROM STRESS IN BONE AND ITS EFFECTS - EXPERIMENTS WITH STAINLESS-STEEL AND PLASTIC PLATES IN DOGS. J Bone Joint Surg-Br Vol. 1976;58(1):107-13.
54. Claes L, Kinzl L, Neugebauer R. EXPERIMENTAL STUDIES ON THE INFLUENCE OF PLATE MATERIAL ON STRESS-RELIEF AND ATROPHY OF THE BONE BENEATH OSTEOSYNTHESIS PLATES. Biomed Tech. 1981;26(4):66-71.
55. Stromberg L, Dalen N. ATROPHY OF CORTICAL BONE CAUSED BY RIGID INTERNAL-FIXATION PLATES - EXPERIMENTAL-STUDY IN DOG. Acta Orthop Scand. 1978;49(5):448-56.
56. Klaue K, Fengels I, Perren SM. Long-term effects of plate osteosynthesis: Comparison of four different plates. Injury-Int J Care Inj. 2000;31:51-62.
57. Gunst MA, Suter C, Rahn BA. BLOOD-SUPPLY TO BONES AFTER PLATE OSTEOSYNTHESIS - VITAL STAINING OF THE INTACT RABBIT TIBIA WITH DISULFINE BLUE. Helvetica Chirurgica Acta. 1979;46(1-2):171-5.
58. Gautier E, Perren SM. THE LIMITED CONTACT DYNAMIC COMPRESSION PLATE (LC-DCP) - BIOMECHANICAL RESEARCH AS A BASIS FOR THE MODIFIED PLATE DESIGN. Orthopade. 1992;21(1):11-23.
59. Slatis P, Karaharju E, Holmstrom T, Ahonen J, Paavolainen P. STRUCTURAL-CHANGES IN INTACT TUBULAR BONE AFTER APPLICATION OF RIGID PLATES WITH AND WITHOUT COMPRESSION. J Bone Joint Surg-Am Vol. 1978;60(4):516-22.
60. Baggott DG, Goodship AE, Lanyon LE. A QUANTITATIVE ASSESSMENT OF COMPRESSION PLATE FIXATION INVIVO - AN EXPERIMENTAL-STUDY USING THE SHEEP RADIUS. J Biomech. 1981;14(10):701-11.
61. Terjesen T, Nordby A, Arnulf V. BONE ATROPHY AFTER PLATE FIXATION - COMPUTED-TOMOGRAPHY OF FEMORAL-SHAFT FRACTURES. Acta Orthop Scand. 1985;56(5):416-8.
62. Terjesen T, Benum P. STRESS-PROTECTION AFTER EXTERNAL FIXATION ON THE INTACT RABBIT TIBIA. Acta Orthop Scand. 1983;54(4):648-54.

63. Paavolainen P, Slatis P, Karaharju E, Holmstrom T. STUDIES ON MECHANICAL STRENGTH OF BONE .2. TORSIONAL STRENGTH OF CORTICAL BONE AFTER RIGID PLATE FIXATION WITH AND WITHOUT COMPRESSION. Acta Orthop Scand. 1978;49(6):506-11.
64. Currey JD. MECHANICAL CONSEQUENCES OF VARIATION IN MINERAL CONTENT OF BONE. J Biomech. 1969;2(1):1-&.
65. Brennwal.J, Perren SM. INVIVO MEASUREMENT OF STRESS-DEPENDENT BONE EXPANSION. Helvetica Chirurgica Acta. 1974;41(4):455-7.
66. J B, Perren SM. Bestimmung der Knochen-dehnung in vitro und in vivo nach Plattenosteosynthese. Langenbecks Archiv fur klinische Chirurgie vereinigt mit Deutsche Zeitschrift fur Chirurgie. 1972;Supplement.
67. Cochran GVB. IMPLANTATION OF STRAIN GAGES ON BONE IN-VIVO. J Biomech. 1972;5(1):119-&.
68. Gautier E, Perren SM, Cordey J. Strain distribution in plated and unplated sheep tibia an in vivo experiment. Injury. 2000;31 Suppl 3:C37-44.
69. White AA, Panjabi MM, Hardy RJ. ANALYSIS OF MECHANICAL SYMMETRY IN RABBIT LONG BONES. Acta Orthop Scand. 1974;45(3):328-36.
70. Paavolainen P. STUDIES ON MECHANICAL STRENGTH OF BONE .1. TORSIONAL STRENGTH OF NORMAL RABBIT TIBIO-FIBULAR BONE. Acta Orthop Scand. 1978;49(6):497-505.
71. Laftman P, Sigurdsson F, Stromberg L. RECOVERY OF DIAPHYSEAL BONE STRENGTH AFTER RIGID INTERNAL PLATE FIXATION - AN EXPERIMENTAL-STUDY IN THE RABBIT. Acta Orthop Scand. 1980;51(2):215-22.
72. Stromberg L, Dalen N. INFLUENCE OF A RIGID PLATE FOR INTERNAL-FIXATION ON MAXIMUM TORQUE CAPACITY OF LONG BONES. Acta Chirurgica Scandinavica. 1976;142(2):115-22.
73. Slatis P, Paavolainen P, Karaharju E, Holmstrom T. STRUCTURAL AND BIOMECHANICAL CHANGES IN BONE AFTER RIGID PLATE FIXATION. Can J Surg. 1980;23(3):247-50.
74. M L-K, HK U. Radiologic and histologic determination of optimal time for the removal of titanium alloy plates in beagle dogs - results of early removal.: Springer-Verlag; 1980.
75. WC H, SS S, DM N, RB H, GW M, S S, et al. Mechanical properties of healing fractures treated with compression plate fixation. . Proceedings of the Second International Symposium on Internal Fixation of Fractures. Lyon1982. p. 81-4.
76. Terjesen T, Apalset K. THE INFLUENCE OF DIFFERENT DEGREES OF STIFFNESS OF FIXATION PLATES ON EXPERIMENTAL BONE HEALING. Journal of Orthopaedic Research. 1988;6(2):293-9.
77. Hidaka S, Gustilo RB. REFRACTURE OF BONES OF THE FOREARM AFTER PLATE REMOVAL. J Bone Joint Surg-Am Vol. 1984;66A(8):1241-3.
78. Richards RH, Palmer JD, Clarke NMP. OBSERVATIONS ON REMOVAL OF METAL IMPLANTS. Injury-Int J Care Inj. 1992;23(1):25-8.
79. Muller M. Technique of Internal Fixation of Fractures. In: Muller, Allgower, Willenegger, editors. New York: Springer-Verlag; 1965. p. 8.
80. Hesketh KT. RIGID FIXATION OF FRACTURES BY COMPRESSION PLATING - A PILOT STUDY. Proceedings of the Royal Society of Medicine-London. 1968;61(10):983-&.
81. Vattolo M. Der Einfluss von Rillen in Osteosyntheseplatten auf den Umbau der Kortikalis. Berne1987.
82. Gautier E, Rahn B, Perren S. Effect of different plates on internal and external remodelling of intact long bones. Ann Orthop Res Soc. 1986;32:322.
83. Matter P, Brennwal.J, Perren SM. BIOLOGICAL REACTION OF BONE TO OSTEOSYNTHESIS PLATES. Helvetica Chirurgica Acta. 1974:1-&.

84. Pilliar RM, Cameron HU, Binnington AG, Szivek J, Macnab I. BONE INGROWTH AND STRESS SHIELDING WITH A POROUS SURFACE COATED FRACTURE FIXATION PLATE. Journal of biomedical materials research. 1979;13(5):799-810.
85. Terjesen T, Benum P. MECHANICAL EFFECTS OF METAL PLATE FIXATION - INVITRO INVESTIGATION ON INTACT AND OSTEOTOMIZED HUMAN AND RABBIT TIBIAE. Acta Orthop Scand. 1983;54(2):256-62.
86. Burstein AH, Currey J, Frankel VH, Heiple KG, Lunseth P, Vessely JC. BONE STRENGTH THE EFFECT OF SCREW HOLES. Journal of Bone and Joint Surgery American Volume. 1972;54-A(6):1143-56.
87. Cheal EJ, Hayes WC, White AA, Perren SM. STRESS-ANALYSIS OF A SIMPLIFIED COMPRESSION PLATE FIXATION SYSTEM FOR FRACTURED BONES. Comput Struct. 1983;17(5-6):845-55.
88. Simon BR, Woo SLY, Stanley GM, Olmstead SR, McCarty MP, Jemmott GF, et al. EVALUATION OF 1 2 AND 3 DIMENSIONAL FINITE ELEMENT AND EXPERIMENTAL MODELS OF INTERNAL FIXATION PLATES. J Biomech. 1977;10(2):79-86.
89. Haase K, Rouhi G. A discussion on plating factors that affect stress shielding using finite element analysis. Journal of Biomechanical Science and Engineering. 2010;5(2):129-41.
90. Szivek JA, Weatherly GC, Pilliar RM, Cameron HU. A STUDY OF BONE REMODELING USING METAL-POLYMER LAMINATES. Journal of biomedical materials research. 1981;15(6):853-65.
91. Anderson LD. COMPRESSION PLATE FIXATION AND EFFECT OF DIFFERENT TYPES OF INTERNAL FIXATION ON FRACTURE HEALING. J Bone Joint Surg-Am Vol. 1965;A 47(1):191-&.
92. Yamagishi M, Yoshimura Y. THE BIOMECHANICS OF FRACTURE HEALING. J Bone Joint Surg-Am Vol. 1955;37(5):1035-68.
93. Zhang XL, Bao K, Dai KR. Stress-relaxation plates and the remodeling of callus and cortex under the plate in rabbits. Chin Med J. 2000;113(9):805-9.
94. Ganesh VK, Ramakrishna K, Ghista DN. Biomechanics of bone-fracture fixation by stiffness-graded plates in comparison with stainless-steel plates. Biomedical engineering online. 2005;4:46.
95. Richon A, Livio JJ, Saegesse.F. LES REFRACTURES APRES OSTEOSYNTHESE PAR PLAQUE A COMPRESSION. Helvetica Chirurgica Acta. 1967;34(1-2):49-&.
96. Muller ME, Allgower M, Willenegger H. Manual of Internal Fixation. Berlin: Springer-Verlag; 1970.
97. Muller ME, Allgower M, Schneider R, Willenegger H. Manual of internal fixation: techniques recommended by the AO group. 2nd ed. Berlin: Springer-Verlag; 1979.
98. Woo SLY, Lothringer KS, Akeson WH, Coutts RD, Woo YK, Simon BR, et al. LESS RIGID INTERNAL FIXATION PLATES HISTORICAL PERSPECTIVES AND NEW CONCEPTS. Journal of Orthopaedic Research. 1984;1(4):431-49.
99. Bostman O, Pihlajamaki H. Clinical biocompatibility of biodegradable orthopaedic implants for internal fixation: a review. Biomaterials. 2000;21(24):2615-21.
100. Burg KJL, Orr DE. An overview of bioresorbable materials. Degradation Rate of Bioresorbable Materials: Prediction and Evaluation. 2008:3-18.
101. An YH, Woolf SK, Friedman RJ. Pre-clinical in vivo evaluation of orthopaedic bioabsorbable devices. Biomaterials. 2000;21(24):2635-52.
102. Braun J, Bollow M, Remlinger G, Eggens U, Rudwaleit M, Distler A, et al. Prevalence of spondylarthropathies in HLA-B27 positive and negative blood donors. Arthritis Rheum. 1998;41(1):58-67.

103. Bostman OM. OSTEOLYTIC CHANGES ACCOMPANYING DEGRADATION OF ABSORBABLE FRACTURE FIXATION IMPLANTS. J Bone Joint Surg-Br Vol. 1991;73(4):679-82.
104. Heller J, Sparer RV, Zenter GM. Polyorthoesters. In: Langer R, Chasin M, editors. Biodegradable polymers as drug delivery systems. New York: Marcel Dekker; 1990. p. 121-61.
105. Middleton JC, Tipton AJ. Synthetic biodegradable polymers as orthopedic devices. Biomaterials. 2000;21(23):2335-46.
106. Bostman O, Paivarinta U, Partio E, Vasenius J, Manninen M, Rokkanen P. DEGRADATION AND TISSUE REPLACEMENT OF AN ABSORBABLE POLYGLYCOLIDE SCREW IN THE FIXATION OF RABBIT FEMORAL OSTEOTOMIES. J Bone Joint Surg-Am Vol. 1992;74A(7):1021-31.
107. Bostman OM. ABSORBABLE IMPLANTS FOR THE FIXATION OF FRACTURES. J Bone Joint Surg-Am Vol. 1991;73A(1):148-53.
108. Bergsma JE, Debruijn WC, Rozema FR, Bos RRM, Boering G. LATE DEGRADATION TISSUE-RESPONSE TO POLY(L-LACTIDE) BONE PLATES AND SCREWS. Biomaterials. 1995;16(1):25-31.
109. Kontakis GM, Pagkalos JE, Tosounidis TI, Melissas J, Katonis P. Bioabsorbable materials in orthopaedics. Acta Orthopaedica Belgica. 2007;73(2):159-69.
110. Vasenius J, Vainionpaa S, Vihtonen K, Makela A, Rokkanen P, Mero M, et al. COMPARISON OF INVITRO HYDROLYSIS, SUBCUTANEOUS AND INTRAMEDULLARY IMPLANTATION TO EVALUATE THE STRENGTH RETENTION OF ABSORBABLE OSTEOSYNTHESIS IMPLANTS. Biomaterials. 1990;11(7):501-4.
111. Paivarinta U, Bostman O, Majola A, Toivonen T, Tormala P, Rokkanen P. INTRAOSSEOUS CELLULAR-RESPONSE TO BIODEGRADABLE FRACTURE FIXATION SCREWS MADE OF POLYGLYCOLIDE OR POLYLACTIDE. Arch Orthop Trauma Surg. 1993;112(2):71-4.
112. Rokkanen PU. Bioabsorbable fixation devices in orthopaedics and traumatology. Annales Chirurgiae Et Gynaecologiae. 1998;87(1):13-20.
113. Ashammakhi N, Suuronen R, Tiainen J, Tormala P, Waris T. Spotlight on naturally absorbable osteofixation devices. Journal of Craniofacial Surgery. 2003;14(2):247-59.
114. Suuronen R, Pohjonen T, Hietanen J, Lindquist C. A 5-year in vitro and in vivo study of the biodegradation of polylactide plates. J Oral Maxillofac Surg. 1998;56(5):604-14.
115. Waris E, Ashammakhi N, Kaarela O, Raatikainen T, Vasenius J. Use of bioabsorbable osteofixation devices in the hand. J Hand Surg-Br Eur Vol. 2004;29B(6):590-8.
116. Majola A, Vainionpaa S, Rokkanen P, Mikkola HM, Tormala P. ABSORBABLE SELF-REINFORCED POLYLACTIDE (SR-PLA) COMPOSITE RODS FOR FRACTURE FIXATION - STRENGTH AND STRENGTH RETENTION IN THE BONE AND SUBCUTANEOUS TISSUE OF RABBITS. J Mater Sci-Mater Med. 1992;3(1):43-7.
117. Degradation Rate of Bioresorbable Materials: Prediction and Evaluation. Buchanan FJ, editor2008. 1-410 p.
118. Bhatia S, Shalaby SW, Powers DL, Lancaster RL, Ferguson RL. THE EFFECT OF SITE OF IMPLANTATION AND ANIMAL AGE ON PROPERTIES OF POLYDIOXANONE PINS. J Biomater Sci-Polym Ed. 1994;6(5):435-46.
119. Daniels AU, Chang MKO, Andriano KP, Heller J. MECHANICAL-PROPERTIES OF BIODEGRADABLE POLYMERS AND COMPOSITES PROPOSED FOR INTERNAL-FIXATION OF BONE. J Appl Biomater. 1990;1(1):57-78.
120. Vert M, Li S, Garreau H. NEW INSIGHTS ON THE DEGRADATION OF BIORESORBABLE POLYMERIC DEVICES BASED ON LACTIC AND GLYCOLIC ACIDS. Clinical Materials. 1992;10(1-2):3-8.
121. International A. ASTM F1635-11, Standard Test Method for in vitro Degradation Testing of Hydrolytically Degradable Polymer Resins and Fabricated Forms for Surgical Implants. 2011.

122. Williams DF. Some observations on the role of cellular enzymes in the in vivo degradation of polymers. Spech Tech Publ. 1979;684:61-75.
123. Williams DF. MECHANISMS OF BIODEGRADATION OF IMPLANTABLE POLYMERS. Clinical Materials. 1992;10(1-2):9-12.
124. Therin M, Christel P, Li SM, Garreau H, Vert M. INVIVO DEGRADATION OF MASSIVE POLY(ALPHA-HYDROXY ACIDS) - VALIDATION OF INVITRO FINDINGS. Biomaterials. 1992;13(9):594-600.
125. Li S. In vitro physicochemical test methods to evaluate bioresorbability. Degradation Rate of Bioresorbable Materials: Prediction and Evaluation. 2008:117-44.
126. Lickorish D, Zebardast N, Davies JE. The biological environment for bioresorbable materials. Buchanan FJ, editor2008. 19-40 p.
127. Khouw I, van Wachem PB, de Leij L, van Luyn MJA. Inhibition of the tissue reaction to a biodegradable biomaterial by monoclonal antibodies to IFN-gamma. Journal of biomedical materials research. 1998;41(2):202-10.
128. Furukawa T, Matsusue Y, Yasunaga T, Shikinami Y, Okuno M, Nakamura T. Biodegradation behavior of ultra-high-strength hydroxyapatite/poly (L-lactide) composite rods for internal fixation of bone fractures. Biomaterials. 2000;21(9):889-98.
129. Bos RRM, Rozema FR, Boering G, Nijenhuis AJ, Pennings AJ, Jansen HWB. BONE-PLATES AND SCREWS OF BIOABSORBABLE POLY (L-LACTIDE) - AN ANIMAL PILOT-STUDY. British Journal of Oral & Maxillofacial Surgery. 1989;27(6):467-76.
130. Buchanan F, Leonard D. Influence of processing, sterilisation and storage on bioresorbability. Degradation Rate of Bioresorbable Materials: Prediction and Evaluation. 2008:209-33.
131. Rokkanen PU, Bostman O, Hirvensalo E, Makela EA, Partio EK, Patiala H, et al. Bioabsorbable fixation in orthopaedic surgery and traumatology. Biomaterials. 2000;21(24):2607-13.
132. Nakamura T, Shimizu Y, Okumura N, Matsui T, Hyon SH, Shimamoto T. TUMORIGENICITY OF POLY-L-LACTIDE (PLLA) PLATES COMPARED WITH MEDICAL-GRADE POLYETHYLENE. Journal of biomedical materials research. 1994;28(1):17-25.
133. Campbell JH, Edsberg L, Meyer AE. POLYLACTIDE INHIBITION OF CARCINOMA CELL-GROWTH IN-VITRO. J Oral Maxillofac Surg. 1994;52(1):49-51.
134. Tegnander A, Engebretsen L, Bergh K, Eide E, Holen KJ, Iversen OJ. Activation of the complement system and adverse effects of biodegradable pins of polylactic acid (Biofix) in osteochondritis dissecans. Acta Orthop Scand. 1994;65(4):472-5.
135. Weiler A, Helling HJ, Kirch U, Zirbes TK, Rehm KE. Foreign-body reaction and the course of osteolysis after polyglycolide implants for fracture fixation - Experimental study in sheep. J Bone Joint Surg-Br Vol. 1996;78B(3):369-76.
136. Bostman O, Hirvensalo E, Makinen J, Rokkanen P. FOREIGN-BODY REACTIONS TO FRACTURE FIXATION IMPLANTS OF BIODEGRADABLE SYNTHETIC-POLYMERS. J Bone Joint Surg-Br Vol. 1990;72(4):592-6.
137. Bostman OM. INTENSE GRANULOMATOUS INFLAMMATORY LESIONS ASSOCIATED WITH ABSORBABLE INTERNAL-FIXATION DEVICES MADE OF POLYGLYCOLIDE IN ANKLE FRACTURES. Clinical orthopaedics and related research. 1992(278):193-9.
138. Casteleyn PP, Handelberg F, Haentjens P. BIODEGRADABLE RODS VERSUS KIRSCHNER WIRE FIXATION OF WRIST FRACTURES - A RANDOMIZED TRIAL. J Bone Joint Surg-Br Vol. 1992;74(6):858-61.
139. Hovis WD, Bucholz RW. Polyglycolide bioabsorbable screws in the treatment of ankle fractures. Foot Ankle Int. 1997;18(3):128-31.

140. Barfod G, Svendsen RN. SYNOVITIS OF THE KNEE AFTER INTRAARTICULAR FRACTURE FIXATION WITH BIOFIX(R) - REPORT OF 2 CASES. Acta Orthop Scand. 1992;63(6):680-1.
141. Hoffmann R, Weiler A, Helling HJ, Krettek C, Rehm KE. Local foreign-body reactions to biodegradable implants - A classification system. Unfallchirurg. 1997;100(8):658-66.
142. Pihlajamaki H, Bostman O, Hirvensalo E, Tormala P, Rokkanen P. ABSORBABLE PINS OF SELF-REINFORCED POLY-L-LACTIC ACID FOR FIXATION OF FRACTURES AND OSTEOTOMIES. J Bone Joint Surg-Br Vol. 1992;74(6):853-7.
143. Pelto-Vasenius K. Reliability of fixation of fractures and osteotomies with absorbable implants. A clinical study. Helsinki: Helsinki University; 1998.
144. Eitenmuller J, David A, Pommer A, Muhr G. Internal fixation of ankle fractures with biodegradable poly-L-lactide-screws and plates. Chirurg. 1996;67(4):413-8.
145. Sinisaari I, Patiala H, Bostman O, Makela A, Partio E, Hirvensalo E, et al. Effect of totally absorbable implant volume on wound infection rate: study of 2500 operated fractures, osteotomies, and ligament injuries. J Orthop Sci. 1997;2:88-92.
146. Bostman OM, Pihlajamaki HK. Adverse tissue reactions to bioabsorbable fixation devices. Clinical orthopaedics and related research. 2000(371):216-27.
147. Partio EK, Bostman O, Hirvensalo E, Vainionpaa S, Vihtonen K, Patiala H, et al. Self-reinforced absorbable screws in the fixation of displaced ankle fractures: a prospective clinical study of 152 patients. J Orthop Trauma. 1992;6(2):209-15.
148. Bostman OM, Pihlajamaki HK. Late foreign-body reaction to an intraosseous bioabsorbable polylactic acid screw - A case report. J Bone Joint Surg-Am Vol. 1998;80A(12):1791-4.
149. Dervin GF, Keene GCR, Chissell HR. Biodegradable rods in adult osteochondritis dissecans of the knee. Clinical orthopaedics and related research. 1998(356):213-21.
150. Friden T, Rydholm U. SEVERE ASEPTIC SYNOVITIS OF THE KNEE AFTER BIODEGRADABLE INTERNAL-FIXATION - A CASE-REPORT. Acta Orthop Scand. 1992;63(1):94-7.
151. Takizawa T, Akizuki S, Horiuchi H, Yasukawa Y. Foreign body gonitis caused by a broken poly-L-lactic acid screw. Arthroscopy. 1998;14(3):329-30.
152. Fraser RK, Cole WG. OSTEOLYSIS AFTER BIODEGRADABLE PIN FIXATION OF FRACTURES IN CHILDREN. J Bone Joint Surg-Br Vol. 1992;74(6):929-30.
153. Bostman OM. Osteoarthritis of the ankle after foreign-body reaction to absorbable pins and screws - A three- to nine-year follow-up study. J Bone Joint Surg-Br Vol. 1998;80B(2):333-8.
154. Rikli DA, Regazzoni P, Perren SM. Is there a need for resorbable implants or bone substitutes? Injury-Int J Care Inj. 2002;33:2-3.
155. Christel P, Chabot F, Leray JL, Morin C, Vert M. Advances in Biomaterials. Winter DG, D.F. G, J.J. P, editors. New York: Wiley; 1980. 271-80 p.
156. Tormala P, Vainionpaa S, Kilpikari J, Rokkanen P. THE EFFECTS OF FIBER REINFORCEMENT AND GOLD PLATING ON THE FLEXURAL AND TENSILE-STRENGTH OF PGA PLA COPOLYMER MATERIALS INVITRO. Biomaterials. 1987;8(1):42-5.
157. Carter DR, Hayes WC. COMPRESSIVE BEHAVIOR OF BONE AS A 2-PHASE POROUS STRUCTURE. J Bone Joint Surg-Am Vol. 1977;59(7):954-62.
158. Turner CH, Cowin SC, Rho JY, Ashman RB, Rice JC. THE FABRIC DEPENDENCE OF THE ORTHOTROPIC ELASTIC-CONSTANTS OF CANCELLOUS BONE. J Biomech. 1990;23(6):549-61.
159. Reilly DT, Burstein AH. ELASTIC AND ULTIMATE PROPERTIES OF COMPACT BONE TISSUE. J Biomech. 1975;8(6):393-&.
160. Tormala P. BIODEGRADABLE SELF-REINFORCED COMPOSITE MATERIALS MANUFACTURING STRUCTURE AND MECHANICAL PROPERTIES. Clinical Materials. 1992;10(1-2):29-34.

161. Tormala P, Pohjonen T, Rokkanen P. Bioabsorbable polymers: Materials technology and surgical applications. Proc Inst Mech Eng Part H-J Eng Med. 1998;212(H2):101-11.
162. Claes LE. MECHANICAL CHARACTERIZATION OF BIODEGRADABLE IMPLANTS. Clinical Materials. 1992;10(1-2):41-6.
163. Hara Y, Tagawa M, Ejima H, Orima H, Sugiyama M, Shikinami Y, et al. Clinical evaluation of uniaxially oriented poly-L-lactide rod for fixation of experimental femoral diaphyseal fracture in immature cats. Journal of Veterinary Medical Science. 1994;56(6):1041-5.
164. Manninen MJ, Pohjonen T. Intramedullary nailing of the cortical bone osteotomies in rabbits with self-reinforced poly-L-lactide rods manufactured by the fibrillation method. Biomaterials. 1993;14(4):305-12.
165. Miettinen H, Makela EA, Rokkanen P, Tormala P. Fixation of femoral shaft osteotomy with intramedullary metallic or absorbable rod: An experimental study on growing dogs. Journal of Biomaterials Science Polymer Edition. 1992;4(2):135-43.
166. Hofmann GO. BIODEGRADABLE IMPLANTS IN ORTHOPAEDIC SURGERY A REVIEW ON THE STATE-OF-THE-ART. Clinical Materials. 1992;10(1-2):75-80.
167. Kankare J. Tibial condylar fractures fixed with totally absorbable, self-reinforced polyglycolide screws - A preliminary report. Arch Orthop Trauma Surg. 1997;116(3):133-6.
168. Kankare J. Operative treatment of displaced intra-articular fractures of the calcaneus using absorbable internal fixation: A prospective study of twenty-five fractures. J Orthop Trauma. 1998;12(6):413-9.
169. Kankare J, Rokkanen P. Dislocated fractures of the talus treated with biodegradable internal fixation. Arch Orthop Trauma Surg. 1998;117(1-2):62-4.
170. Partio EK. Absorbable screws in the fixation of cancellous bone fractures and arthrodeses. A clinical study of 318 patients. Helsinki: Helsinki University; 1992.
171. Jahn R, Diederichs D, Friedrich B. ABSORBABLE IMPLANTS AND THEIR APPLICATION ILLUSTRATED EXEMPLARILY ON RADIAL HEAD FRACTURES. Aktuelle Traumatologie. 1989;19(6):281-6.
172. Kumta SM, Leung PC. The technique and indications for the use of biodegradable implants in fractures of the hand. Tech Orthop. 1998;13:160-3.
173. Haas HG. POLYDIOXANON SPLINTS IN FRACTURE TREATMENT. Handchirurgie Mikrochirurgie Plastische Chirurgie. 1986;18(5):295-7.
174. Kujala S, Raatikainen T, Kaarela O, Ashammakhi N, Ryhanen J. Successful treatment of scaphoid fractures and nonunions using bioabsorbable screws: Report of six cases. J Hand Surg-Am Vol. 2004;29A(1):68-73.
175. Pihlajamaki H, Bostman O, Rokkanen P. A BIODEGRADABLE EXPANSION PLUG FOR FIXATION OF THE CORACOID BONE BLOCK IN THE BRISTOW-LATARJET OPERATION. Int Orthop. 1994;18(2):66-71.
176. Albrecht-Olsen P, Kristensen G, Tormala P. Meniscus bucket-handle fixation with an absorbable Biofix tack: development of a new technique. Knee surgery, sports traumatology, arthroscopy : official journal of the ESSKA. 1993;1(2):104-6.
177. Manninen MJ, Paivarinta U, Taurio R, Tormala P, Suuronen R, Raiha J, et al. POLYLACTIDE SCREWS IN THE FIXATION OF OLECRANON OSTEOTOMIES A MECHANICAL STUDY IN SHEEP. Acta Orthop Scand. 1992;63(4):437-42.
178. Bucholz RW, Henry S, Henley MB. FIXATION WITH BIOABSORBABLE SCREWS FOR THE TREATMENT OF FRACTURES OF THE ANKLE. J Bone Joint Surg-Am Vol. 1994;76A(3):319-24.
179. Bostman O, Vainionpaa S, Hirvensalo E, Makela A, Vihtonen K, Tormala P, et al. BIODEGRADABLE INTERNAL-FIXATION FOR MALLEOLAR FRACTURES - A PROSPECTIVE RANDOMIZED TRIAL. J Bone Joint Surg-Br Vol. 1987;69(4):615-9.

180. Rangdal S, Singh D, Joshi N, Soni A, Sament R. Functional outcome of ankle fracture patients treated with biodegradable implants. Foot and ankle surgery. 2011.
181. Joukainen A, Partio EK, Waris P, Joukainen J, Kroger H, Tormala P, et al. Bioabsorbable screw fixation for the treatment of ankle fractures. J Orthop Sci. 2007;12(1):28-34.
182. Ahl T, Dalen N, Lundberg A, Wykman A. BIODEGRADABLE FIXATION OF ANKLE FRACTURES - A ROENTGEN STEREOPHOTOGRAMMETRIC STUDY OF 32 CASES. Acta Orthop Scand. 1994;65(2):166-70.
183. Klos K, Rausch S, Loffler M, Frober R, Hofmeier K, Lenz M, et al. A Biomechanical Comparison of a Biodegradable Volar Locked Plate With Two Titanium Volar Locked Plates in a Distal Radius Fracture Model. J Trauma-Injury Infect Crit Care. 2010;68(4):984-91.
184. Gangopadhyay S, Ravi K, Packer G. Dorsal plating of unstable distal radius fractures using a bio-absorbable plating system and bone substitute. J Hand Surg-Br Eur Vol. 2006;31B(1):93-100.
185. van Manen CJ, Dekker ML, van Eerten PV, Rhemrev SJ, van Olden GDJ, van der Elst M. Bio-resorbable versus metal implants in wrist fractures: a randomised trial. Arch Orthop Trauma Surg. 2008;128(12):1413-7.
186. Navarro M, Ginebra MP, Planell JA, Barrias CC, Barbosa MA. In vitro degradation behavior of a novel bioresorbable composite material based on PLA and a soluble CaP glass. Acta Biomater. 2005;1(4):411-9.
187. Huttunen M, Tormala P, Godinho P, Kellomaki M. Fiber-reinforced bioactive and bioabsorbable hybrid composites. Biomed Mater. 2008;3(3).
188. Russias J, Saiz E, Nalla RK, Gryn K, Ritchie RO, Tomsia AP. Fabrication and mechanical properties of PLA/HA composites: A study of in vitro degradation. Mater Sci Eng C-Biomimetic Supramol Syst. 2006;26(8):1289-95.
189. Barbon F, Locardi B, Verita M, Gabbi C, Grispigni C, Leali PT, et al. BIOCOMPATIBILITY AND OSTEOGENETIC CHARACTERISTICS OF NEW BIOCOMPATIBLE GLASSES. Biomaterials. 1991;12(6):565-8.
190. Ahmed I, Cronin PS, Abou Neel EA, Parsons AJ, Knowles JC, Rudd CD. Retention of Mechanical Properties and Cytocompatibility of a Phosphate-Based Glass Fiber/Polylactic Acid Composite. J Biomed Mater Res Part B. 2009;89B(1):18-27.
191. Ahmed I, Parsons A, Jones A, Walker G, Scotchford C, Rudd C. Cytocompatibility and Effect of Increasing MgO Content in a Range of Quaternary Invert Phosphate-based Glasses. J Biomater Appl. 2010;24(6):555-75.
192. Ahmed I, Lewis M, Olsen I, Knowles JC. Phosphate glasses for tissue engineering: Part 1. Processing and characterisation of a ternary-based P(2)O(5)-CaO-Na(2)O glass system. Biomaterials. 2004;25(3):491-9.
193. Felfel RM, Ahmed I, Parsons AJ, Haque P, Walker G, Rudd C. Investigation of crystallinity, molecular weight change, and mechanical properties of PLA/PBG bioresorbable composites as bone fracture fixation plates. J Biomater Appl. 2010.
194. Ahmed I, Jones IA, Parsons AJ, Bernard J, Farmer J, Scotchford CA, et al. Composites for bone repair: phosphate glass fibre reinforced PLA with varying fibre architecture. J Mater Sci-Mater Med. 2011;22(8):1825-34.
195. Han N, Ahmed I, Parsons AJ, Harper L, Scotchford CA, Scammell BE, et al. Influence of screw holes and gamma sterilization on properties of phosphate glass fiber-reinforced composite bone plates. J Biomater Appl. 2013;27(8):990-1002.
196. Paavolainen P, Slatis P, Karaharju E, Holmstrom T. HEALING OF EXPERIMENTAL FRACTURES BY COMPRESSION OSTEOSYNTHESIS .1. TORSIONAL STRENGTH. Acta Orthop Scand. 1979;50(4):369-74.

197. Laftman P, Nilsson OS, Brosjo O, Stromberg L. STRESS SHIELDING BY RIGID FIXATION STUDIED IN OSTEOTOMIZED RABBIT TIBIAE. Acta Orthop Scand. 1989;60(6):718-22.
198. Nunamaker DM. Experimental models of fracture repair. Clinical orthopaedics and related research. 1998;355S:S56-65.
199. Ashhurst DE, Hogg J. A method for making reproducible experimental fractures of the rabbit tibia. Injury.14(3):236-42.
200. Festing MFW. Design and statistical methods in studies using animal models of development. Ilar Journal. 2006;47(1):5-14.
201. Currey JD, Brear K, Zioupos P, Reilly GC. EFFECT OF FORMALDEHYDE FIXATION ON SOME MECHANICAL-PROPERTIES OF BOVINE BONE. Biomaterials. 1995;16(16):1267-71.
202. Fukui K, Kominami R, Kaneuji A, Matsumoto T, Shinohara H. A new method of perfusion fixation for the rabbit femur. Okajimas Folia Anatomica Japonica. 2004;81(4):57-62.
203. Schneider CA, Rasband WS, Eliceiri KW. NIH Image to ImageJ: 25 years of image analysis. Nature Methods. 2012;9(7):671-5.
204. Doube M, Klosowski MM, Arganda-Carreras I, Cordelieres FP, Dougherty RP, Jackson JS, et al. BoneJ Free and extensible bone image analysis in ImageJ. Bone. 2010;47(6):1076-9.
205. Maxwell SD, HD. Designing experiments and analyzing data: A model comparison perspective. 2nd ed. New York, NY: Psychology Press; 2004.
206. Jaccard J. Interaction effects in factorial analysis of variance. Thousand Oaks, CA.: Sage Publications, Inc.; 1998.
207. Woo SLY, Akeson WH, Coutts RD, Rutherford L, Doty D, Jemmott GF, et al. COMPARISON OF CORTICAL BONE ATROPHY SECONDARY TO FIXATION WITH PLATES WITH LARGE DIFFERENCES IN BENDING STIFFNESS. J Bone Joint Surg-Am Vol. 1976;58(2):190-5.
208. Uhthoff HK, Foux A, Yeadon A, McAuley J, Black RC. 2 PROCESSES OF BONE REMODELING IN PLATED INTACT FEMORA - AN EXPERIMENTAL-STUDY IN DOGS. Journal of Orthopaedic Research. 1993;11(1):78-91.
209. Currey JD, Butler G. The mechanical properties of bone tissue in children. The Journal of bone and joint surgery American volume. 1975;57(6):810-4.
210. Hirsch C, Evans FG. STUDIES ON SOME PHYSICAL PROPERTIES OF INFANT COMPACT BONE. Acta Orthop Scand. 1965;35(4):300-&.
211. Vainionpaa S, Vihtonen K, Mero M, Patiala H, Rokkanen P, Kilpikari J, et al. BIODEGRADABLE FIXATION OF RABBIT OSTEOTOMIES. Acta Orthop Scand. 1986;57(3):237-9.
212. Masoud I, Shapiro F, Moses A. Tibial epiphyseal development: a cross-sectional histologic and histomorphometric study in the New Zealand white rabbit. J Orthop Res. 1986;4(2):212-20.
213. Wang XD, Mabrey JD, Agrawal CM. An interspecies comparison of bone fracture properties. Bio-Medical Materials and Engineering. 1998;8(1):1-9.
214. Conflitti J, Graves M, Russell G, Tucci M, Benghuzzi H. Plating of rat femoral shaft osteotomies: Report of a technique and preliminary results. In: Benghuzzi H, Tucci M, editors. Biomedical Sciences Instrumentation, Vol 39. Biomedical Sciences Instrumentation. 392003. p. 278-83.
215. Savaridas T, Wallace RJ, Muir AY, Salter DM, Simpson AHRW. The development of a novel model of direct fracture healing in the rat. Bone & Joint Research. 2012;1(11):289-96.
216. An YH, Friedman RJ. In: An YH, Friedman RJ, editors. Animal Models in Orthopaedic Research. Boca Raton: CRC Press; 1999.
217. Masoud I, Shapiro F, Kent R, Moses A. A longitudinal study of the growth of the New Zealand white rabbit: cumulative and biweekly incremental growth rates for body length, body weight, femoral length, and tibial length. J Orthop Res. 1986;4(2):221-31.

218. Richmond J. Refinement, reduction, and replacement of animal use for regulatory testing: future improvements and implementation within the regulatory framework. ILAR journal / National Research Council, Institute of Laboratory Animal Resources. 2002;43 Suppl:S63-8.
219. Stromberg NE. Diaphyseal bone in rigid internal plate fixation. Experimental study of the weakening of canine long bone. Acta chirurgica Scandinavica Supplementum. 1975;456:1-34.
220. Frank CB, Loitz B, Bray R, Chimich D, King G, Shrive N. ABNORMALITY OF THE CONTRALATERAL LIGAMENT AFTER INJURIES OF THE MEDIAL COLLATERAL LIGAMENT - AN EXPERIMENTAL-STUDY IN RABBITS. J Bone Joint Surg-Am Vol. 1994;76A(3):403-12.
221. Lienemann PS, Metzger S, Kivelioe A, Blanc A, Papageorgiou P, Cinelli P, et al. Non-invasive Longitudinal Evaluation of Bone Regeneration by Hybrid SPECT/Micro-CT Imaging for Tissue Engineering. Tissue Engineering Part A. 2015;21:S388-S.
222. Claes L. THE MECHANICAL AND MORPHOLOGICAL PROPERTIES OF BONE BENEATH INTERNAL-FIXATION PLATES OF DIFFERING RIGIDITY. Journal of Orthopaedic Research. 1989;7(2):170-7.
223. Bagheri ZS, El Sawi I, Bougherara H, Zdero R. Biomechanical fatigue analysis of an advanced new carbon fiber/flax/epoxy plate for bone fracture repair using conventional fatigue tests and thermography. Journal of the Mechanical Behavior of Biomedical Materials. 2014;35:27-38.
224. Chakladar ND, Harper LT, Parsons AJ. Optimisation of composite bone plates for ulnar transverse fractures. Journal of the Mechanical Behavior of Biomedical Materials. 2016;57:334-46.
225. Perren SM, Cordey J, Rahn BA, Gautier E, Schneider E. EARLY TEMPORARY POROSIS OF BONE INDUCED BY INTERNAL-FIXATION IMPLANTS - A REACTION TO NECROSIS, NOT TO STRESS PROTECTION. Clinical orthopaedics and related research. 1988(232):139-51.
226. Carter DR, Vasu R, Harris WH. THE PLATED FEMUR - RELATIONSHIPS BETWEEN THE CHANGES IN BONE STRESSES AND BONE LOSS. Acta Orthop Scand. 1981;52(3):241-8.
227. Yuan HP, Kurashina K, de Bruijn JD, Li YB, de Groot K, Zhang XD. A preliminary study on osteoinduction of two kinds of calcium phosphate ceramics. Biomaterials. 1999;20(19):1799-806.
228. Greiff J. BONE HEALING IN RABBITS AFTER COMPRESSION OSTEOSYNTHESIS, STUDIED BY TC-99M(SN)POLYPHOSPHATE SCINTIMETRY AND AUTORADIOGRAPHY. Journal of Nuclear Medicine. 1981;22(8):693-8.
229. Terjesen T, Svenningsen S, Apalset K, Johnson E. COMPARISON BETWEEN 4 DIFFERENT METHODS OF TREATMENT IN EXPERIMENTAL FRACTURE-HEALING. Acta Orthop Scand. 1988;59(1):107-8.
230. Sumitomo N, Noritake K, Hattori T, Morikawa K, Niwa S, Sato K, et al. Experiment study on fracture fixation with low rigidity titanium alloy. J Mater Sci-Mater Med. 2008;19(4):1581-6.
231. Fan Y, Xiu K, Duan H, Zhang M. Biomechanical and histological evaluation of the application of biodegradable poly-L-lactic cushion to the plate internal fixation for bone fracture healing. Clinical Biomechanics. 2008;23:S7-S16.
232. Cristofolini L, Conti G, Juszczyk M, Cremonini S, Jan SVS, Viceconti M. Structural behaviour and strain distribution of the long bones of the human lower limbs. J Biomech. 2010;43(5):826-35.
233. Aerssens J, Boonen S, Lowet G, Dequeker J. Interspecies differences in bone composition, density, and quality: Potential implications for in vivo bone research. Endocrinology. 1998;139(2):663-70.

234. Barth RW, Williams JL, Kaplan FS. OSTEON MORPHOMETRY IN FEMALES WITH FEMORAL-NECK FRACTURES. Clinical orthopaedics and related research. 1992(283):178-86.
235. Corondan G, Haworth WL. A FRACTOGRAPHIC STUDY OF HUMAN LONG-BONE. J Biomech. 1986;19(3):207-18.
236. Woo SLY, Akeson WH, Levenetz B, Coutts RD, Matthews JV, Amiel D. POTENTIAL APPLICATION OF GRAPHITE FIBER AND METHYL-METHACRYLATE RESIN COMPOSITES AS INTERNAL-FIXATION PLATES. Journal of biomedical materials research. 1974;8(5):321-38.
237. Woo SLY, Simon BR, Akeson WH, McCarty MP. INTERDISCIPLINARY APPROACH TO EVALUATE EFFECT OF INTERNAL-FIXATION PLATE ON LONG BONE REMODELING. J Biomech. 1977;10(2):87-&.
238. Tayton K, Johnsonnurse C, McKibbin B, Bradley J, Hastings G. THE USE OF SEMIRIGID CARBON-FIBER-REINFORCED PLASTIC PLATES FOR FIXATION OF HUMAN FRACTURES - RESULTS OF PRELIMINARY TRIALS. J Bone Joint Surg-Br Vol. 1982;64(1):105-11.
239. Stevens MM, Marini RP, Schaefer D, Aronson J, Langer R, Shastri VP. In vivo engineering of organs: The bone bioreactor. Proceedings of the National Academy of Sciences of the United States of America. 2005;102(32):11450-5.
240. Frigg R, Appenzeller A, Christensen R, Frenk A, Gilbert S, Schavan R. The development of the distal femur Less Invasive Stabilization System (LISS). Injury-Int J Care Inj. 2001;32:24-31.
241. Helfet DL, Shonnard PY, Levine D, Borrelli J, Jr. Minimally invasive plate osteosynthesis of distal fractures of the tibia. Injury. 1997;28 Suppl 1:A42-7; discussion A7-8.
242. Calori GM, Mazza E, Colombo M, Ripamonti C. The use of bone-graft substitutes in large bone defects: Any specific needs? Injury-Int J Care Inj. 2011;42:S56-S63.
243. Banwart JC, Asher MA, Hassanein RS. ILIAC CREST BONE-GRAFT HARVEST DONOR SITE MORBIDITY - A STATISTICAL EVALUATION. Spine. 1995;20(9):1055-60.
244. Tomford WW. TRANSMISSION OF DISEASE THROUGH TRANSPLANTATION OF MUSCULOSKELETAL ALLOGRAFTS. J Bone Joint Surg-Am Vol. 1995;77A(11):1742-54.
245. Nguyen H, Morgan DAF, Sly LI, Benkovich M, Cull S, Forwood MR. Validation of 15 kGy as a radiation sterilisation dose for bone allografts manufactured at the Queensland Bone Bank: application of the VD(max) 15 method. Cell and Tissue Banking. 2008;9(2):139-47.
246. Greenwald AS, Boden SD, Goldberg VM, Khan Y, Laurencin CT, Rosier RN, et al. Bone-graft substitutes: Facts, fictions, and applications. J Bone Joint Surg-Am Vol. 2001;83A:98-103.
247. Parsons AJ, Ahmed I, Haque P, Fitzpatrick B, Niazi MIK, Walker GS, et al. Phosphate Glass Fibre Composites for Bone Repair. J Bionic Eng. 2009;6(4):318-23.
248. Colquhoun R, Tanner KE. Mechanical behaviour of degradable phosphate glass fibres and composites-a review. Biomed Mater. 2016;11(1):18.
249. Pietrzak WS, Eppley BL. Resorbable polymer fixation for craniomaxillofacial surgery: Development and engineering paradigms. Journal of Craniofacial Surgery. 2000;11(6):575-85.
250. Thomas SJ, K.; Malhotra, S.K.; Goda, K; Sreekala, S. Polymer composites, Macro- and Microcomposites. Weinheim: Wiley; 2012.
251. Balasubramanian M. Composite Materials and Processing Illustrated ed. Boca Raton, FL.: CRC Press; 2013.
252. Chen MH, Parsons AJ, Felfel RM, Rudd CD, Irvine DJ, Ahmed I. In-situ polymerisation of fully bioresorbable polycaprolactone/phosphate glass fibre composites: In vitro degradation and mechanical properties. Journal of the Mechanical Behavior of Biomedical Materials. 2016;59:78-89.